UNIVERSITAT POLITÈCNICA DE VALÈNCIA

Multidisciplinary study of the role of calcium in plant *in vitro* embryogenesis

Antonio Calabuig Serna

Supervisors:
José María Seguí Simarro
Rosa Porcel Roldán
Ricardo Mir Moreno

April 2023

Abstract

Ca^{2+} is an essential cation that plays fundamental roles in all living organisms. From a functional point of view, Ca^{2+} acts as a second messenger that regulates different cellular processes. Previous works point to the fact that Ca^{2+} signaling may be involved in the early stages of induction of *in vitro* plant embryogenesis, but the actual role of Ca^{2+} in this process remained unveiled. Thus, the main goal of the present Thesis is to study the role of Ca^{2+} in *in vitro* embryogenesis using two *in vitro* systems: somatic embryogenesis and microspore embryogenesis. Chemical treatments and detection of Ca^{2+} with fluorescent probes and genetically-encoded *cameleon* sensors imaged by fluorescence and confocal microscopy were performed to determine the importance of Ca^{2+} homeostasis for induction of embryogenesis and the dynamics of Ca^{2+} levels during the induction and establishment of somatic and microspore-derived embryos. We observed that Ca^{2+} increase is an early marker of induction of *in vitro* embryogenesis and Ca^{2+} levels during *in vitro* embryogenesis are dynamic in all the systems we studied. Moreover, Ca^{2+} oscillations might be related to the differentiation processes that take place in the induced cells upon binding to calmodulin. We showed that Ca^{2+} increase within a defined range has system-specific positive effects in embryo yield, being more sensitive those systems using isolated cell suspensions rather than those using tissues as explants. Finally, we studied the role of callose during somatic embryogenesis, and we observed that inhibiting callose deposition prevents embryo development, which suggests a relationship between the formation of a callose barrier and the establishment of embryo identity in somatic cells.

Resum

El Ca^{2+} és un catió essencial que juga un paper fonamental en tots els organismes vius. Des del punt de vista funcional, el Ca^{2+} actua com a un segon missatger que regula diferents processos cel·lulars. Treballs anteriors indiquen que la senyalització mitjançant el Ca^{2+} podria estar implicada en les primeres etapes de la inducció de l'embriogènesi *in vitro* de les plantes, però el paper real del Ca^{2+} en aquest procés encara és desconegut. Per això, el principal objectiu de la present Tesi és l'estudi del paper del Ca^{2+} en l'embriogènesi *in vitro* mitjançant dos sistemes *in vitro*: l'embriogènesi somàtica i l'embriogènesi de micròspores. Per tal de determinar la importància de l'homeòstasi del Ca^{2+} en la inducció de l'embriogènesi i les dinàmiques dels nivells de Ca^{2+} durant la inducció i l'establiment d'embrions somàtics i derivats de micròspores, es van utilitzar tractaments químics i es van detectar els nivells de Ca^{2+} mitjançant sondes fluorescents i sensors de *cameleon* codificats genèticament, visualitzats amb microscòpia fluorescent i confocal. Vam observar que l'augment de Ca^{2+} és un marcador primerenc en la inducció de l'embriogènesi *in vitro* i que els nivells de Ca^{2+} durant l'embriogènesi *in vitro* són dinàmics en tots els sistemes estudiats. A més, les oscil·lacions en els nivells de Ca^{2+} podrien estar relacionades amb els processos de diferenciació que tenen lloc en les cèl·lules induïdes una vegada uneix el Ca^{2+} a la calmodulina. Vam mostrar que un augment de Ca^{2+} dins d'un rang definit de concentració té un efecte positiu, depenent del sistema, en la producció d'embrions, essent més sensibles aquells sistemes basats en suspensions de cèl·lules aïllades que aquells que usen teixits com a explants. Finalment, vam estudiar el paper de la cal·losa durant l'embriogènesi somàtica, i vam observar que la inhibició de la deposició de cal·losa impedeix el desenvolupament embrionari, la qual cosa suggereix una relació entre la formació d'una barrera de cal·losa i l'establiment de la identitat embrionària en les cèl·lules somàtiques.

Resumen

El Ca^{2+} es un catión esencial que juega un papel fundamental en todos los organismos vivos. Desde el punto de vista funcional, el Ca^{2+} actúa como un segundo mensajero que regula distintos procesos celulares. Trabajos anteriores indican que la señalización mediante Ca^{2+} podría estar implicada en las primeras etapas de la inducción de la embriogénesis *in vitro* de las plantas, pero el verdadero papel del Ca^{2+} en este proceso es aún desconocido. Por eso, el principal objetivo de la presente Tesis es el estudio del papel del Ca^{2+} en la embriogénesis *in vitro* mediante dos sistemas *in vitro*: la embriogénesis somática y la embriogénesis de microsporas. Para determinar la importancia de la homeostasis del Ca^{2+} en la inducción de la embriogénesis y las dinámicas de los niveles de Ca^{2+} durante la inducción y el establecimiento de embriones somáticos y derivados de microsporas, se utilizaron tratamientos químicos y se detectaron los niveles de Ca^{2+} mediante sondas fluorescentes y sensores *cameleon* codificados genéticamente, visualizados con microscopía fluorescente y confocal. Observamos que el aumento de Ca^{2+} es un marcador temprano en la inducción de la embriogénesis *in vitro* y que los niveles de Ca^{2+} durante la embriogénesis *in vitro* son dinámicos en todos los sistemas estudiados. Además, las oscilaciones en los niveles de Ca^{2+} podrían estar relacionadas con los procesos de diferenciación que ocurren en las células inducidas una vez une el Ca^{2+} a la calmodulina. Mostramos que un aumento de Ca^{2+} dentro de un rango definido de concentración tiene un efecto positivo, dependiendo del sistema, en la producción de embriones, siendo más sensibles aquellos sistemas basados en suspensiones de células aisladas que aquellos que usan tejidos como explantes. Finalmente, estudiamos el papel de la calosa durante la embriogénesis somática, observando que la inhibición de la deposición de calosa impide el desarrollo embrionario, lo que sugiere una relación entre la formación de una barrera de calosa y el establecimiento de la identidad embrionaria en las células somáticas.

Index

Abbreviations

2,4-D	2,4-dichlorophenoxyacetic acid
AM	Acetoxymethyl ester
BAP	6-cenzylaminopurine
BAPTA-AM	1,2-Bis(2-aminophenoxy)ethane-N,N,N',N'-tetraacetic acid tetrakis acetoxymethyl ester
Ca^{2+}	Calcium
CaM	Calmodulin
CC	Compact callus
CCM	Co-cultivation medium
CFP	Cyan fluorescent protein
CIM	Callus induction medium
CPA	Cyclopiazonic acid
CPZ	Chlorpromazine hydrochloride
DH	Doubled haploid
DMSO	Dimethyl sulfoxide
EE	Exine-enclosed
EGTA	Ethylene glycol-bis(β-aminoethyl ether)-N,N,N′,N′-tetraacetic acid
EIM	Embryogenesis Induction Medium
EISM	Embryogenesis Induction Selective Medium
ER	Endoplasmic reticulum
FRET	Fluorescence resonance energy transfer
GM	Germination medium
HS	Heat shock
IAA	Indole-3-acetic acid
$InsP_3$	Inositol 1,4,5-trisphosphate
IZE	Immature zygotic embryo
LBS	Loose bicellular structure
LC	Loose callus
LSD	Least Significance Difference
MS	Murashige and Skoog
NAA	1-naphthaleneacetic acid
ROI	Region of interest
RRM	Root regeneration medium
SE	Somatic embryogenesis
SM	Selection medium

SOM	Shoot outgrowth medium
SRM	Shoot regeneration medium
SUS	Suspensor-bearing embryo
TDZ	Thidiazuron
WUS	*Wuschel*
W-7	N-(6-Aminohexyl)-5-chloro-1-naphthalenesulfonamide hydrochloride
YFP	Yellow fluorescent protein

1. Introduction

The first agricultural communities were established more than 10,000 years ago. Since then, humans have tried to increase crop yield and quality. At first, plant selection was carried out in an intuitive, observational way through mass selection, which means selecting individuals exhibiting the best agronomical traits. Although this method allowed fixing interesting characters in populations, the overall progress in terms of cultivar production along time was poor. With the rediscovery of Mendel's work and the setting of the modern genetic principles, the basis of genetics-based plant breeding were established at the beginning of the 20th century (Qaim 2020).

Plant breeding is the scientific field that aims to improve agronomical traits through genetic manipulation, either by conventional methods or by genetic engineering techniques (Masters 2004). Traditionally, conventional plant breeding comprised methods to improve the phenotypic traits of crops mainly through sexual crossings and hybridizations among sexually compatible materials (Hallauer and Darrah 1985). With the irruption of the first molecular advances, plant breeding integrated tools such as mutagenesis or molecular markers for early genotyping and selection, which greatly accelerated the protocols and made them much more efficient (Moeinizade et al. 2020). Among the biotechnological tools available for crop improvement, plant *in vitro* tissue culture is one of the most interesting due to its large number of applications. Plant tissue culture is possible because of the totipotency of plant cells. Plant cells have the ability of dedifferentiate and develop new individuals through organogenesis, i.e by the regeneration of vegetative organs, or through embryogenesis, i.e. by the induction of a fully functional embryo (Reinert and Backs 1968; Phillips and Garda 2019). These processes can be induced either in somatic cells (somatic embryogenesis, SE) or in cells of the germ line such as the male or female gametophytes or their precursors. When embryogenesis is induced from microspores, the precursors of male gametophytes, the process is known as microspore embryogenesis (Niazian and Shariatpanahi 2020; Elhiti and Stasolla 2022).

Recent reports state that plant breeding is currently an essential tool for human survival and development, mainly due to the agricultural challenge that supposes both persistent growth of world's population and climate change (Xiong et al. 2022). Biotechnological approaches are pivotal tools in order to face environmental challenges. In this sense, broadening the basic knowledge of these biotechnological processes at cellular and molecular levels would provide new opportunities to enhance their efficiency and increase their usefulness regarding the development of improved cultivars. Among others, calcium (Ca^{2+}) signaling and dynamics have been reported as relevant factors at the molecular level in both somatic and microspore embryogenesis.

1.1.Ca^{2+} signaling and dynamics in plants

Ca^{2+} is an essential micronutrient that plays fundamental roles, both structurally and functionally, in all living organisms. In plant cells, Ca^{2+} is mainly present in three ways: freely solubilized in cytosol, forming covalent bonds with macromolecules (crystalline forms) and stored in cellular components (loosely-bound) such as the cell wall, cell organelles or associated with proteins (Ge et al.

2007). From a structural point of view, Ca^{2+} confers stability to the cell wall by cross-linking with pectin and to the plasma membrane by interacting with phospholipids. Moreover, free Ca^{2+} acts as a second messenger that regulates different cellular processes (Thor 2019). In the cytosol Ca^{2+} concentration is around 0.1 μM (Thor 2019), and higher concentrations can be toxic for plant cells, due to its ability to bind with phosphate and precipitate. This is the reason why cells have developed finely tuned mechanisms to control Ca^{2+} cellular concentrations (Pittman 2011). Nevertheless, transient Ca^{2+} oscillations are thought to be responsible for encoding and decoding specific signals that lead to cellular and molecular changes in response to various stimuli, such as abiotic and biotic stresses or developmental changes, among others (Tian et al. 2020). These Ca^{2+} oscillations/peaks occur thanks to an intricate network of channels, pumps and exporters that allow the influx and efflux of the ion through membranes. Ca^{2+} enters the cell through channel proteins and it is externalized to the apoplast or mobilized to the intracellular stores by the action of H^+/Ca^{2+} antiporters and Ca^{2+}-ATPases (Thor 2019). Within cells, Ca^{2+} acts by binding to several Ca^{2+} sensors that, upon Ca^{2+} perception, trigger a specific signaling cascade. An example of these Ca^{2+}-binding proteins is calmodulin (CaM), a conserved protein with two globular domains containing EF-hand motifs. These two domains are separated by a linker, which undergoes conformational changes upon Ca^{2+} binding to the globular domains. The change in conformation induces the activation of calmodulin and, in turn, the Ca^{2+}-calmodulin complex activates kinases involved in multiple processes, such as transcriptional regulation and phosphorylation of other proteins (Bredow and Monaghan 2022). Additional examples of Ca^{2+} protein sensors that articulate the response to Ca^{2+} signals are calmodulin-like proteins (CMLs), Ca^{2+}-dependent protein kinases (CDPKs), calcineurin B-like proteins (CBLs) or CBL-interacting protein kinases (CIPKs) (Tang et al. 2020).

The role of Ca^{2+} in plant development is quite diverse, as it is involved on numerous processes such as cell wall growth (Lopez-Hernandez et al. 2020), root development (Leitão et al. 2019), plasma membrane permeability regulation, cell polarized growth (Hepler 2005), and determination of the identity of the shoot apical meristem (Li et al. 2019). Due to the importance of Ca^{2+} in such a wide range of processes, some molecular tools have been developed to track Ca^{2+} oscillations in plant cells (Sadoine et al. 2021). Among others, *cameleon* sensors are widely acknowledged tools to determine Ca^{2+} distribution *in vivo* at the cellular level (Fig. 1).

The mechanism of *cameleon* Ca^{2+} sensors is based on the energetic transfer that takes place when two fluorophores, an acceptor and a donor, are physically close (Miyawaki et al. 1997). The distance between the two fluorophores depends on the conformation of the protein that interconnects them, which in the case of *cameleon* sensors is the Ca^{2+}-binding protein calmodulin. Thus, when Ca^{2+} binds calmodulin, the conformational change in the protein allows the interaction between the two fluorophores and fluorescence resonance energy transfer (FRET) occurs from the donor to the acceptor. This way, excitation of the donor exclusively with its excitation wavelength induces emission in the acceptor. The higher the Ca^{2+} accumulation, the higher number of *cameleon* molecules change their conformation and the recorded FRET signal will be higher. This fact makes this sensor ideal for Ca^{2+} quantification and monitoring Ca^{2+} oscillations *in vivo*.

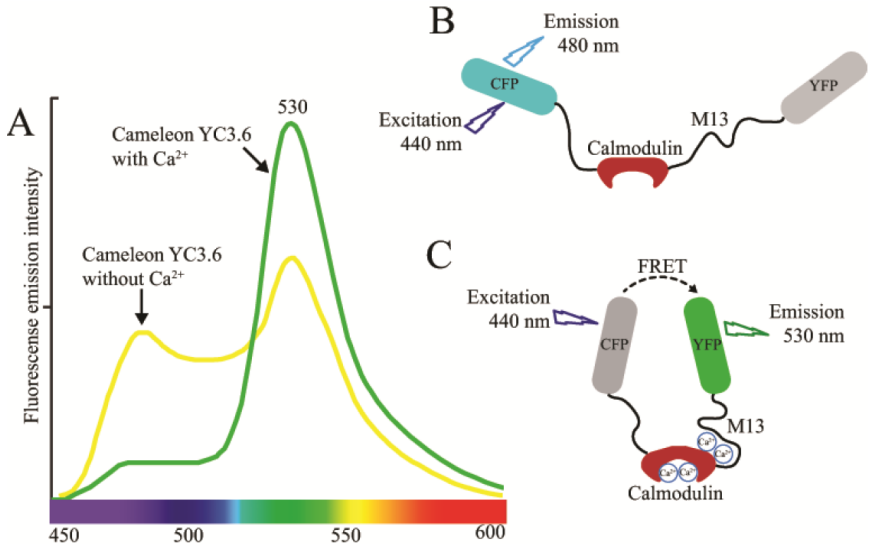

Fig. 1. ***Cameleon* working mechanism scheme**. A: emission spectrums of *cameleon* in the presence and in the absence of Ca^{2+}. B: conformation of *cameleon* in the absence of Ca^{2+}. C: *cameleon* conformation in the presence of Ca^{2+} (Kanchiswamy et al. 2014).

Among other developmental processes, Ca^{2+} plays an important role in plant embryogenesis. The first evidence of Ca^{2+} oscillations during fertilization was reported by Digonnet et al. (1997), who observed, by histochemical methods, an increase in cytosolic Ca^{2+} levels following gamete fusion in maize. A Ca^{2+} increase was described in rice zygotes within 9 and 12 hours after pollination, and following the first zygotic division Ca^{2+} levels decreased to the initial values except in the nucleolus and the cell wall, where Ca^{2+} signal stayed high (Zhao et al. 2002). Further works confirmed that Ca^{2+} influx is involved in egg cell activation following the sperm cell entrance, and a second, more prolonged peak of cellular Ca^{2+} is produced after gamete fusion (Dresselhaus and Jürgens 2021). Despite its importance, the effect of Ca^{2+} during zygotic embryogenesis has not been extensively studied, other than the cited works. This is due to the technical requirements associated with this biological system, mainly related to the difficulties for isolation of zygotic embryos and the requirement of efficient *in vitro* fertilization protocols, which is greatly limited by the reduced viability of plant gametes *in vitro*. In this context, alternative systems to zygote embryogenesis have emerged as tools to study embryo development. These systems include somatic embryogenesis and microspore embryogenesis, which have been used in several species, and whose regulation and progress resembles that of zygotic embryogenesis (Méndez-Hernández et al. 2019; Corral-Martínez et al. 2021; Sivanesan et al. 2022).

1.2.Somatic embryogenesis

Somatic embryogenesis (SE) is the process through which a differentiated somatic cell reprograms its gene expression patterns and develops as a bipolar structure, becoming a fully developed embryo (Elhiti and Stasolla 2022). SE can occur *in vivo* in few species grown under stress conditions, mainly heat shock or drought (Elhiti and Stasolla 2022). This is the case of *Kalanchoë* species, which are able to develop somatic embryos on leaves (Garcês and Sinha 2009), or lemon (*Citrus limon*), which can induce SE in nucellar cells (Spinoso-Castillo and

Bello-Bello 2022). However, under certain *in vitro* culture conditions, the activation of SE can be induced at a higher frequency and in a wider range of species, including crops. For this reason, in plant breeding research, *in vitro* SE methods have mostly been used as biotechnological tools rather than *in vivo* methods. The main inductive signals that lead to this genetic reprogramming towards SE are plant growth regulators and stress conditions (temperature, water or osmotic stress) (Elhiti and Stasolla 2022). In addition, factors such as the genotype, the explant type, the culture medium and the *in vitro* culture conditions are known to affect the embryogenic competence of plant cells (Bidabadi and Jain 2020).

There are several criteria to classify *in vitro* SE systems. The first criterion is based on the origin of the embryogenic development, which can occur through the differentiation of a single somatic cell into an embryo, or through the organization of groups of cells into meristematic regions, which will eventually develop into new individuals (Fehér 2019). The second criterion distinguishes between direct and indirect embryogenesis (Fig. 2).

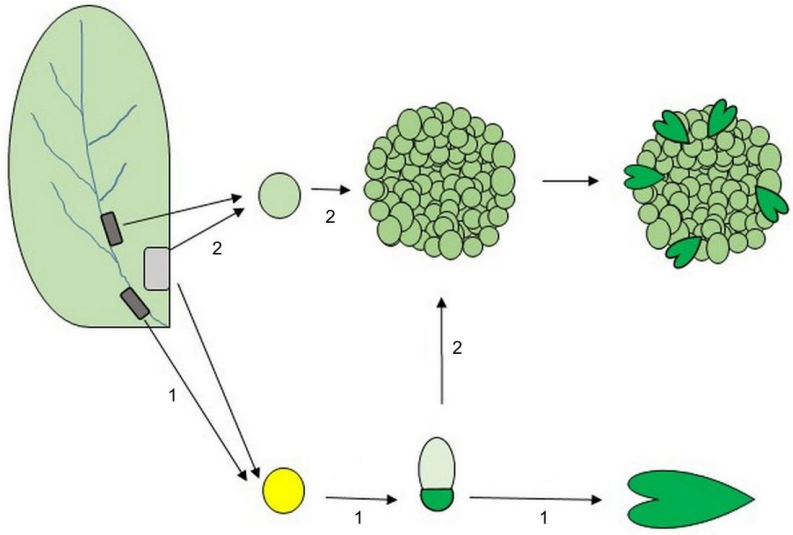

Fig. 2. **Scheme of direct (1) and indirect (2) SE from a leaf explant**. SE may be induced in differentiated somatic cells (light grey) or in pericycle-like stem cells (dark gray). Route 1 happens when the first asymmetrical division is followed by the regeneration of a complete embryo. Route 2 takes place when the induced cell proliferates into an embryogenic *calli* from which embryos will develop. Adapted from Fehér (2019).

Direct embryogenesis happens when embryos develop without an intermediate *calli* phase, as is the case of carrot (*Daucus carota* L.) (Reinert 1958; Steward et al. 1958) or tobacco (*Nicotiana tabacum* L.) (Stolarz et al. 1991). Alternatively, if explant tissue starts proliferating and this intermediate *callus* phase occurs, then the process is known as indirect embryogenesis (Raghavan 1986), as it happens in saffron (*Crocus sativus* L.) (Taheri-Dehkordi et al. 2020). In addition, there are species for which both indirect and direct SE have been reported, such as coffee (*Coffea arabica* L.) (Quiroz-Figueroa et al. 2002), *Camellia oleifera* Abel (Zhang et al. 2021) or *Arabidopsis thaliana* (Gaj 2001; Wu et al. 1992).

Besides its utility as a system to study embryogenic development, SE has many biotechnological applications. Traditionally, SE has been used as a method for micropropagation of genotypes with agronomic interest. Nowadays, thanks to the implementation of bioreactor technology, it is possible to automatize and scale-up SE-based systems to achieve massive micropropagation (Egertsdotter et al. 2019). In this context, micropropagation allows to clone hybrid genotypes, overcoming the requirement for parental pure lines. This, combined with artificial seed technology, has been used to optimize clonal plant propagation in different crop and forest species (Ghanbarali et al. 2016; Iqbal and Mollers 2019; Kitto and Janick 1982; Fiegert et al. 2000; Fujii et al. 1989). For this reason, understanding the basic mechanisms that controls SE would allow us to develop new protocols to increase the efficiency, or even to be applied in recalcitrant species.

1.2.1. Methods for induction of somatic embryogenesis

In vitro SE induction methods vary with the genotype and the explant type. Conversely, solid, semi-solid and liquid culture media have been used to induce embryogenesis in different species (Phillips and Garda 2019). For example, in tobacco and alfalfa (*Medicago sativa*), embryogenesis is achieved by culturing leaf explants in solid medium (Pathi et al. 2013; Tichá et al. 2020), while in carrot and some conifers, embryogenesis is induced in liquid suspensions (Baranski and Lukasiewicz 2019; Egertsdotter et al. 2019). In the case of carrot, considered as a model species for SE, solid and semi-solid medium-based protocols have also been developed (Von Arnold et al. 2002; Gonzalez-Calquin and Stange 2020), and different types of explants such as root sections, hypocotyls, epicotyls, cotyledons or leaves, have been used to induce SE (Baranski and Lukasiewicz 2019). On the other hand, *Arabidopsis thaliana* immature zygotic embryos are used as explants for SE in solid medium (Gaj 2011), and some attempts have been developed in order, to obtain liquid suspensions (Sello et al. 2017).

1.2.2. Factors affecting somatic embryogenesis

Great efforts have been made to increase SE efficiency by modifications of *in vitro* culture media and the use of molecular tools. Besides the use of high auxin levels, some species require to induce SE the application of other stresses such as wounding the explant tissue, changing the nitrogen source or the medium pH, exposing cells to heat-shock or treating explants with polyethylene glycol (Méndez-Hernández et al. 2019). It is also possible to induce somatic embryos by overexpressing certain embryogenesis-related genes and transcription factors (Sivanesan et al. 2022) such as *Somatic embryogenesis receptor kinase 1* (*SERK1*) (Hecht et al. 2001), *Leafy cotyledon* (*LEC*) (Lotan et al. 1998), *Baby boom* (*BBM)* (Boutilier et al. 2002), *Wound-responsive gene 1* (*WIND1)* (Iwase et al. 2011) or *Wuschel* (*WUS)* (Frugis et al. 1999). These approaches have proven helpful to increase SE efficiency and to better understand the mechanisms underlying the activation of embryo development from a differentiated somatic cell. Nevertheless, these mechanisms are still far from being fully understood.

Although Ca^{2+} signaling has not been studied in detail during zygotic embryo development, multiple works performed on somatic embryos support the idea that Ca^{2+} and Ca^{2+}-related proteins take a pivotal role in this process (Winnicki 2020).

Microscopy techniques using chemical staining and pharmacological approaches, consisting on the direct application of Ca^{2+} and Ca^{2+} modulators to the embryogenic cultures, have helped to infer the role that Ca^{2+} plays during induction of SE in plants. In carrot, maintaining a minimum level of Ca^{2+} is necessary for the embryogenic response, and inhibition of Ca^{2+}-channels affected SE negatively (Overvoorde and Grimes 1994). In sandalwood (*Santalum album*) SE, when cultures were treated with the Ca^{2+} ionophore A23187, an ion channel that allows the free entrance of Ca^{2+} in cells, embryogenesis was negatively affected (Anil and Rao 2000). However, in other species such as wheat (*Triticum aestivum*) or *Coffea canephora*, exogenous Ca^{2+} influxes induced by the addition of ionophore A23187 promoted SE (Mahalakshmi et al. 2007; Ramakrishna et al. 2011), indicating that the effect of these chemical modulators may vary among embryogenic systems. On the other hand, the direct observation of Ca^{2+} by staining with the fluorescent dye fura-2AM in sandalwood revealed that Ca^{2+} signal increased when cells were differentiating into embryos (Anil and Rao 2000), and ionophore A23187-treated cells in *Coffea canephora* also exhibited higher fluorescence. In light of these previous works, some discrepancies regarding Ca^{2+} regulation are observed among species and even within the same species. Thus, unveiling the role of Ca^{2+} in different SE systems would improve the general knowledge about its involvement as a second messenger in SE.

1.3.Doubled haploids

Haploid plants are sporophytic individuals with the same number of chromosomes than the gametes of their species. Upon duplication of their whole genome, either naturally or induced, they become doubled haploid (DH), which means homozygous for all their genetic *loci* (Seguí-Simarro et al. 2021a). Haploids and DHs can be developed *in vitro* by inducing embryogenesis from the precursors of both male and female gametophytes, or *in vivo* by crossings with *haploid inducer lines* (Seguí-Simarro et al. 2021a). Thus, fully homozygous individuals are obtained from heterozygous parental gametes in a single generation (Niazian and Shariatpanahi 2020).

Most importantly, DHs are very convenient tools for a variety of plant breeding techniques (Weyen 2021). DHs can be used as pure lines for hybrid seed production (Bourke et al. 2021), and to explore the genetic variability in hybrid-derived lines (Ferrie and Möllers 2011). This technology develops pure, 100% homozygous lines for plant breeding programs with notable advantages in terms of time and cost reductions, and. Besides hybrid seed production, DHs may be useful resources in various basic research areas. In genetics, DHs populations have been used to perform gene mapping, linkage studies, estimations of recombination frequencies, detection of recessive mutations, estimation of additive values and specific combining abilities, and to develop synthetic populations (Snape 1989; Seguí-Simarro 2010; Niazian and Shariatpanahi 2020). DHs may also reduce the time needed to obtain homozygous transgenic plants from hemizygous transformants (Thomas et al. 2020).

Embryogenesis can be induced *in vitro* from the male and female gametophytes or their precursors. In the case of inducing embryogenesis from the gametophyte precursor cells, the newly developed individuals will be DHs if they

duplicate their genome. However, sometimes duplication does not occur and it is necessary to apply specific treatments to induce the duplication of the haploid genome, being colchicine treatment the main used in the last decades. Colchicine is a chemical compound that inhibits the polymerization of the microtubules in the mitotic spindle, preventing the correct separation of chromosomes and generating a genome-duplicated cell (Hooghvorst and Nogués 2021). *Gynogenesis* is the process in which a haploid individual is obtained from the non-fertilized female gametophyte (San Noeum 1979). This embryogenic pathway has been successfully applied in sugar beet, onion and several *Cucurbita* species (Seguí-Simarro 2021a). To induce embryogenesis, immature ovules from the embryo sac are cultured in vitro and develop into haploid individuals. These individuals usually come from the egg cell, but sometimes the embryo develops from the antipodal or the synergid cells (Seguí-Simarro et al. 2021a). Gynogenesis may also be induced through non-functional mentor pollen, which triggers gynogenic development without fertilization (Marin-Montes et al. 2022).

The male gametophyte can also be deviated from its original gametophytic developmental route to develop into a complete embryo through induction of *androgenesis*. At present, there are almost 400 species with published protocols for DHs production (Seguí-Simarro et al. 2021b). This process may take place through three different ways (Fig. 3): inactivation of female nucleus in a zygote after fertilization (Route 1), regeneration of embryos or calli from vacuolated microspores or young bicellular pollen (Route 2), or induction of calli from meiocytes, and the regeneration of entire plants through organogenesis (Route 3).

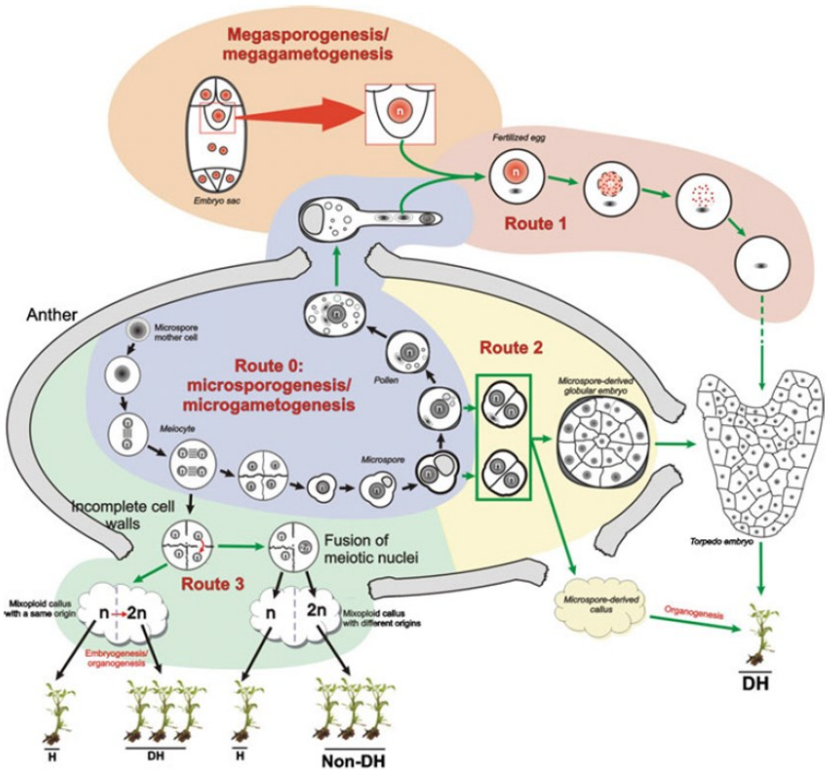

Fig. 3. **Different reprogramming routes of microspores from their original gametophytic development (Microsporogenesis/microgametogenesis; Route 0) towards embryogenesis**. Route 1 implies the deactivation of the maternal genome once fertilization occurs. Route 2 illustrates embryogenesis or callogenesis from vacuolated microspores or young bicellular pollen. Route 3 shows the formation of DHs through organogenesis from meiocyte-derived calli (Seguí-Simarro 2010).

Route 1 was the first reported, as it happens spontaneously in nature in some species, very few actually. Route 3 can be induced in vitro and it was first described in *A. thaliana* (Gresshoff and Doy 1972). Routes 1 and 3 are highly infrequent and, thus, are less studied and documented. Route 2 is by far the most studied of all and it is known as microspore embryogenesis. Typically, this androgenic route is induced by applying stress treatments to *in vitro* cultured microspores, which induces cellular, molecular and genetic changes that deviate microspores from the gametophytic pathway and switch them up into embryogenesis (Seguí-Simarro 2010).

1.3.1. Methods for induction of microspore embryogenesis

Induction of microspore embryogenesis may be achieved mainly through two techniques: anther culture and isolated microspore culture (Seguí-Simarro et al. 2021a). Anther culture is the simplest approach (Guha and Maheshwari 1964), and consists on the excision of buds from donor plants, the selection of buds containing a majority of microspores at the inducible developmental stages, and the extraction and *in vitro* culture of anthers on solid medium. This method implies some advantages: during the first stages of microspore development towards the embryogenic route, anther tissues provide substances that favor their growth. Besides, the technical complexity of anther culture is lower than in the other methods (Seguí-Simarro et al. 2021a). However, anther culture also presents drawbacks. Some structures may regenerate from the somatic tissues of anthers and molecular analysis should be performed in order to differentiate these individuals from DHs regenerated from microspores (Seguí-Simarro 2016).

The alternative method to overcome anther culture limitations is the isolated microspore culture. It is based on the extraction of microspores from the anthers and their culture in liquid media (Corral-Martínez et al. 2020). This technique requires more expertise than anther culture but it allows a higher control of culture media, as the effect of anther tissue in microspore development is avoided (Ferrie and Caswell 2011; Calabuig-Serna et al. 2021). In species where isolated microspore culture protocols are available the efficiency of the embryogenic response is higher than in anther culture (Seguí-Simarro 2010).

1.3.2. Factors affecting induction of microspore embryogenesis

There are several factors affecting the efficiency of induction of microspore embryogenesis, being the genotype the most relevant one, as it happens in many other *in vitro* culture techniques. The genetic background of the individual determines the degree of recalcitrance of the androgenic response. Indeed, the *Brassica napus* line DH4079 is considered a model species for the study of this experimental process (Custers et al. 2001) due to its high embryogenic response, whereas the DH12075 line, also from *Brassica napus*, is known to show a very low response to induction of microspore embryogenesis (Corral-Martínez et al. 2021). The age of the donor plants, their growth conditions and the developmental stage of microspores also affect to the response (Seguí-Simarro 2010; Rivas-Sendra et al. 2020). In general, the inducible stage of microspore development is the transition between vacuolated microspore and young bicellular pollen (Seguí-Simarro 2010). Other factors that influence microspore

embryogenesis are the composition of culture medium, including macronutrients, micronutrients and phytohormones (Calabuig-Serna et al. 2022; Juzoń-Sikora et al. 2022), and the conditions used for *in vitro* culture (Camacho-Fernández et al. 2018), including the stress treatment applied to induce the embryogenic development (Seguí-Simarro 2010; Shariatpanahi et al. 2006; Islam and Tuteja 2012). The different embryogenesis-inducing stress treatments comprehend centrifugation, changes in temperature, changes in media pH and osmotic stress among others (Asif et al. 2014; Shariatpanahi et al. 2006).

1.3.3. Changes associated to induction of microspore embryogenesis

What makes a microspore switch towards embryogenic development is still far from being fully understood. On the one hand, hormonal regulation is thought to have a prominent role in this process. In rapeseed, microspore embryogenesis is induced after a heat-shock stress treatment in the absence of hormones in culture media (Corral-Martínez et al. 2021), which indicates that, at least in some cases, the haploid or DH embryo is autonomous to suffice its own hormonal needs. However, recalcitrant species such as eggplant, pepper or cucumber require the presence of hormones in order to induce the embryogenic response (Calabuig-Serna et al. 2022; Asadi and Seguí-Simarro 2021; Albiñana Palacios and Seguí-Simarro 2021; Calabuig-Serna et al. 2021). Furthermore, epigenetic modifications introduced by histone deacetylases have been reported to be critical in determining the totipotency or recalcitrance of microspores. In this sense, treatments with the histone deacetylase inhibitor Trichostatin A have shown to enhance response in rapeseed, *Brassica rapa* and wheat microspore embryogenesis (Li et al. 2014; Zhang et al. 2016; Castillo et al. 2020).

Regarding the cellular changes accompanying cell reprogramming, several features have been described during rapeseed microspore embryogenesis. Indeed, the reprogramming of cell fate includes massive processes of macroautophagy and excretion of the digested material to the cell wall (Corral-Martínez et al. 2013), followed by the formation of a subintinal layer, an additional callose-rich layer extending below the intine (Parra-Vega et al. 2015). The putative role of this layer is to provide insulating conditions, which allow microspores to change their cellular identity and to start developing as embryogenic structures (Rivas-Sendra et al. 2019; Corral-Martinez et al. 2020). Finally, in rapeseed embryogenic microspores, callose deposition is preceded by a specific nuclear-cytosolic Ca^{2+} signal (Rivas-Sendra et al. 2019) and, probably, altering these Ca^{2+} accumulation peaks would interfere in microspore embryogenesis response. Although all these findings suggest that Ca^{2+} plays a crucial role in the embryogenic response, as it seems to be the case for zygotic and somatic embryogenesis, the actual role of Ca^{2+} in these processes remains unveiled.

2. Objectives

It is likely that Ca^{2+} signaling plays an important role during *in vitro* embryogenesis, and possible *in vivo* too. The main goal of the present Thesis is to study the role of Ca^{2+} in *in vitro* embryogenesis using two *in vitro* systems: somatic embryogenesis and microspore embryogenesis. Somatic embryogenesis has been studied in three different species: the model organism *Arabidopsis thaliana*, carrot (*Daucus carota* L.) as model species for SE, and tobacco (*Nicotiana tabacum* L.), where transgenic lines expressing nuclear *cameleon* Ca^{2+}-markers are available. SE in Arabidopsis and tobacco is initiated from explants (immature zygotic embryos and leaves, respectively), whereas in carrot embryogenesis is induced in cell suspensions. On the other hand, the high-response line DH4079 of rapeseed (*Brassica napus* L.) has been used for microspore embryogenesis. Chemical treatments and microscopy detection of Ca^{2+} with *cameleon* sensors and fluorescent probes have been performed to determine (1) the importance of Ca^{2+} homeostasis for induction of embryogenesis, both somatic and microspore-derived, and (2) the pattern of Ca^{2+} accumulation during the induction and establishment of somatic and microspore-derived embryos. Thus, the study of these systems will provide an overview of the role of Ca^{2+} in plant *in vitro* embryogenesis.

To achieve the main goal, the following specific objectives will be developed:

- To observe Ca^{2+} dynamics in somatic embryogenesis from *Arabidopsis thaliana* immature zygotic embryos and to evaluate the effect of Ca^{2+} modulation on the embryogenic response.
- To obtain transgenic lines in *D. carota* expressing *cameleon* Ca^{2+}-marker.
- To visualize Ca^{2+} dynamics through FRET system in *D. carota* somatic embryogenesis using *cameleon* transgenic lines and to study the effect of Ca^{2+} modulation.
- To monitor Ca^{2+} oscillations in the nucleus during somatic embryogenesis induction and embryogenic development using *N. tabacum cameleon* transgenic lines.
- To develop transgenic lines in *B. napus* high-response cultivar DH4079 expressing *cameleon* Ca^{2+}-marker.
- To assess the effect of modulation of Ca^{2+} homeostasis and to observe Ca^{2+} distribution in *B. napus* microspore embryogenesis.

3. Chapter 1: Calcium dynamics, *WUSCHEL* expression and callose deposition during somatic embryogenesis in *Arabidopsis thaliana* immature zygotic embryos

Antonio Calabuig-Serna, Ricardo Mir, Jose María Seguí-Simarro.

Cell Biology Group - COMAV Institute, Universitat Politècnica de València, 46022 Valencia, Spain.

Keywords: 2-deoxy-D-glucose; chlorpromazine; EGTA; FRET; *in vitro* culture; inositol 1,4,5- trisphosphate; ionophore A23187; W-7

This article has been published as: Calabuig-Serna *et al*. (2023) Calcium Dynamics, WUSCHEL Expression and Callose Deposition during Somatic Embryogenesis in *Arabidopsis thaliana* Immature Zygotic Embryos. *Plants*, 12(5), 1021.

In this research work, Antonio Calabuig-Serna contributed in the processes of investigation, methodology, data curation, formal analysis, and writing, reviewing and editing the draft.

Abstract

In this work, we studied the induction of somatic embryogenesis in *Arabidopsis* using IZEs as explants. We characterized the process at the light and scanning electron microscope level and studied several specific aspects such as WUS expression, callose deposition, and principally Ca^{2+} dynamics during the first stages of the process of embryogenesis induction, by confocal FRET analysis with an *Arabidopsis* line expressing a *cameleon* calcium sensor. We also performed a pharmacological study with a series of chemicals know to alter calcium homeostasis ($CaCl_2$, inositol 1,4,5-trisphosphate, ionophore A23187, EGTA), the calcium–calmodulin interaction (chlorpromazine, W-7), and callose deposition (2-deoxy-D-glucose). We showed that, after determination of the cotiledonary protrusions as embryogenic regions, a finger-like appendix may emerge from the shoot apical region and somatic embryos are produced from the WUS-expressing cells of the appendix tip. Ca^{2+} levels increase and callose is deposited in the cells of the regions where somatic embryos will be formed, thereby constituting early markers of the embryogenic regions. We also found that Ca^{2+} homeostasis in this system is strictly maintained and cannot be altered to modulate embryo production, as shown for other systems. Together, these results contribute to a better knowledge and understanding of the process of induction of somatic embryos in this system.

3.1.Introduction

Plant embryos are biological structures that aim to give rise to a new individual. Zygotic embryos are formed upon double fertilization and further zygote development, but this is not the only way to produce plant embryos. Embryos can also be produced artificially from immature male gametophytes, female gametes, or from vegetative (somatic) cells under certain in vitro conditions (Elhiti and Stasolla 2022; Seguí-Simarro et al. 2021). Somatic embryogenesis (the production of embryos from somatic cells) has been established as a model to study plant embryogenesis (Elhiti and Stasolla 2022). The first reports on somatic embryogenesis in *Daucus carota* date from 1958 (Steward et al. 1958; Reinert 1958). More than 60 years since then, the number of available protocols for different species, from herbaceous crops to woody trees, has increased notably (Loyola-Vargas and Ochoa-Alejo 2016), and this process nowadays has a wide range of applications in plant biotechnology and breeding (Horstman et al. 2017). Therefore, the study of the mechanisms that regulate somatic embryogenesis will help give a better understanding of this process, and to generate improved protocols to further exploit its benefits.

Somatic embryos are produced either directly from the explant or indirectly through an intermediate callus phase. In *Arabidopsis thaliana,* somatic embryogenesis can be in vitro induced from protoplasts (O'Neill and Mathias 1995), root explants (Zuo et al. 2002), shoot apical tip and floral bud explants (Ikeda-Iwai et al. 2003), shoot apex explants of young seedlings (Kadokura et al. 2018), or germinating embryos from mature seeds (Kobayashi et al. 2010). However, the best-known and studied system of somatic embryogenesis in *Arabidopsis* uses immature zygotic embryos (IZEs) at the late cotyledonary stage as explants (Wu et al. 1992). It was described that, when in vitro cultured on

auxin-containing medium, IZEs directly develop somatic embryos on the adaxial proximal ends of cotyledons within two weeks of culture (Kurczynska et al. 2007; Gaj 2011). Longer culture time results in the formation, on the cotyledon abaxial side, and of a callus-like structure that generates somatic embryos through indirect embryogenesis (Kurczynska et al. 2007). All other embryo regions were described as non-embryogenic (Kurczynska et al. 2007; Godel-Jedrychowska et al. 2020). Histological analysis showed that somatic embryos arise from protodermal and subprotodermal cell layers (Kurczynska et al. 2007). The establishment of totipotency in these cells and their reprogramming towards embryogenesis was reported to be mediated by a decrease of auxin signaling and their symplasmic isolation from the non-embryogenic neighboring cells by callose deposition at plasmodesmata (Godel-Jedrychowska et al. 2020). At the genetic level, somatic cell dedifferentiation and activation of the embryogenic pathway is a complex process that implies alterations of the transcriptional activity, turning off the expression of some specific genes and activating several others, principally embryo identity genes (Steward et al. 1958; de Silva et al. 2022). Specific master regulators involved in the activation of somatic embryogenesis have been identified (Mahdavi-Darvari et al. 2015; Jha et al. 2020). Specifically, overexpression of *WUSCHEL (WUS)*, a homeodomain protein characterized by its role in the shoot apical meristem maintenance, promotes the occurrence of somatic embryogenesis (Zuo et al. 2002; Su et al. 2009). The expression of *WUS* (Su et al. 2009), and of several other embryo marker genes such as *BABYBOOM* (Kulinska-Lukaszek et al. 2012), *LEC2* (Kurczynska et al. 2007), *SERK* (Schmidt et al. 1997), and *WOX2* (a *WUS*-related homeobox gene), has been used to determine the spatio-temporal patterns of this process. Although the last decade has witnessed significant advances in the elucidation of the genetic networks and the epigenetic mechanisms operating for the formation of somatic embryos (Steward et al. 1958; Mahdavi-Darvari et al. 2015), the intracellular signal that triggers somatic embryogenesis is not clearly determined. Ca^{2+} is one of the most important secondary messengers in plant cell signal transduction processes, controlling gene expression upon binding to calmodulin (CaM) or other Ca^{2+}-sensing proteins (Mohanta et al. 2019), and further interaction with transcription factors. The concentration of free resting cytosolic Ca^{2+} in plant cells is usually kept very low, within the range of 50–100 nM, being higher in the different cell compartments considered as Ca^{2+} reservoirs, namely the vacuole, the ER, and the apoplast (Pirayesh et al. 2021; Stael et al. 2011). Due to its cellular toxicity even at low concentrations, the role of Ca^{2+} as a secondary messenger is based on the generation of concentration gradients and transient increases of cytosolic concentrations (Tian et al. 2020). Thus, a possible scenario for induction of somatic embryogenesis could be cytosolic auxin-mediated Ca^{2+} that increases acting as a rapid activator of embryo identity genes. Indeed, a number of studies in different species, such as *Musa* (Marimuthu et al. 2019), *Cocos nucifera* (Rivera-Solís et al. 2018), *Hevea brasiliensis* (Etienne et al. 1997), and *Daucus carota* (Takeda et al. 2003), among others, support the notion that direct Ca^{2+} supplementation of in vitro media enhances somatic embryogenesis, therefore pointing to an important role of this secondary signal as inducer of somatic embryogenesis. Other studies, however, suggest that increased Ca^{2+} levels are not positive to increase production of somatic embryos (Overvoorde and Grimes 1994; Anil and Rao 2000; Malabadi and van Staden 2006; Ramakrishna et al. 2011). For this reason, the study of Ca^{2+}

dynamics during the first stages of this morphogenic process would give us valuable information about the factors governing the induction of somatic embryogenesis and, in particular, to decipher the role of Ca^{2+} in this process.

Due to the universal role of Ca^{2+} as a molecular signal, some tools have been developed to monitor Ca^{2+} levels in a broad range of biological systems. In *Arabidopsis*, the study of Ca^{2+} dynamics can be greatly facilitated by the use of *cameleon* lines. *Cameleon* constructs are based on the principle of fluorescence resonance energy transfer (FRET) that occurs between two fluorophores when they become spatially closer. This happens when the linker protein, usually CaM in the case of *cameleons*, binds to Ca^{2+} and undergoes a conformational change that approaches the donor fluorophore to the acceptor. Hence, when the donor is excited, it transfers a certain amount of energy to the acceptor, which becomes excited itself, emitting fluorescence. Krebs et al. (2012) developed a collection of *Arabidopsis* lines that express the *cameleon* construct specifically in certain cell regions, such as the cytoplasm or the plasma membrane, using cyan fluorescent protein (CFP) as a donor fluorophore and yellow fluorescent protein (YFP) as an acceptor. They are therefore excellent Ca^{2+} sensors. However, these lines have not yet been used to study Ca^{2+} dynamics during somatic embryogenesis.

Despite the importance of *Arabidopsis* as a model to study somatic embryogenesis (Elhiti and Stasolla 2022) and the role of Ca^{2+} in this process, it is surprising that, to the best of our knowledge, no studies of Ca^{2+} distribution or chemical modulation during somatic embryogenesis have been published in *Arabidopsis*. In this work, we studied Ca^{2+} dynamics during somatic embryogenesis from *Arabidopsis* IZEs. Using wild type, *WUS-reporter* and *cameleon*-transformed lines, we performed a multidisciplinary study including a characterization of the different stages through scanning electron microscopy (SEM), confocal microscopy for *WUS-reporter* expression and FRET-based Ca^{2+} imaging in *cameleon* lines, and a pharmacological study where different chemicals known to interfere with Ca^{2+} homeostasis and signaling were applied to embryogenic cultures. Our results shed light on the different origins of the IZE-derived somatic embryos, the embryogenic nature of the newly proliferating tissues, the distribution of Ca^{2+} during the initial stages of embryogenesis induction, and the role of Ca^{2+} and CaM modulation in this process.

3.2.Materials and methods

3.2.1. Plant material

We used *Arabidopsis thaliana* (Col-0) wild type and transgenic lines for expressing the YC3.6-Bar *cameleon* construct (Krebs et al. 2012) carrying a signal for cytoplasm targeting, kindly provided by Prof. Jörg Kudla (Münster University, Münster, Germany). To analyze the spatial distribution of *WUS* expression, we used the *A. thaliana* transgenic line pCLV3:GFP-ER_pWUS:DsRED-N7 (NASC ID: N23895), kindly provided by Dr. Cristina Ferrándiz (IBMCP-CSIC, Valencia, Spain). This *WUS*-reporter line expresses the DsRED fluorescent protein under the control of the *WUS* promoter.

3.2.2. Induction of Somatic Embryogenesis

Eight week-old silique-producing *Arabidopsis* plants were used as donors of explants. Siliques were harvested and surface-sterilized for 30 s in 70% ethanol and 20 min in 10% commercial bleach, followed by three rinses in sterile distilled water. Under a binocular microscope, siliques were dissected to isolate the immature seeds. IZEs with fully developed, bent, and green cotyledons were used as explants. They were rescued by carefully removing the seed coat and the endosperm, and in vitro cultured as previously described (Gaj 2011). IZEs were transferred to culture dishes with induction medium (Table 1). Dishes were kept at a 25 ◦C, 16/8 photoperiod for 15 days. Then, the induced somatic embryos were excised from the explant and transferred to germination medium (Table 1). Germinated plantlets were transferred to soil and acclimated at 25 ◦C in a 16/8 photoperiod.

Table 1. Composition of the in vitro culture media used for induction of somatic embryogenesis. GB5: Gamborg basal medium + B5 vitamins (Gamborg et al. 1968). MS: Murashige and Skoog basal medium + MS vitamins (Murashige and Skoog 1962). For all cases, pH was adjusted to 5.8 and media were autoclaved for 20 min at 121 ◦C. All basal media and other medium components were purchased from Duchefa (Netherlands).

	Induction	**Germination**
GB5 (g/L)	3.16	
MS (g/L)		4.6
Sucrose (%)	2	2
2,4-D (mg/L)	1.1	
Plant agar (%)	0.8	0.8

3.2.3. Scanning Electron Microscopy

For scanning electron microscopy, we processed samples of *Arabidopsis* IZEs cultured in vitro during 3, 5, 7, and 14 days in solid E5 medium. Samples were fixed in Karnovsky fixative as previously described (Satpute et al. 2005) for 5 h at room temperature under vacuum conditions, rinsed three times (30 min each) in 0.025 M cacodylate buffer, and kept in 0.025 M cacodylate buffer at 4 °C. Then, samples were dehydrated in an ascending series of ethanol dilutions in water as follows: 30% (4 h), 50% (4 h), 70% (overnight), 90% (2 h), and 100% (1 h). Once dehydrated, samples were dried in a Leica EM CPD300 automated critical point dryer, coated with platinum for 30 s in a Leica EM MED020 sputter coater, and mounted and observed in a ZEISS Ultra-55 scanning electron microscope operating at 2.0 kV.

3.2.4. Confocal Microscopy and FRET

Callose staining and *cameleon* and *WUS*-reporter lines were observed in a Zeiss 780 Axio Observer (Zeiss, Oberkochen, Germany) confocal laser scanning microscope. First, IZEs were cultured in solid E5 medium for five days. For callose staining, samples were then stained with 0.1% aniline blue in phosphate buffer for 1 h (Godel-Jedrychowska et al. 2020) and observed exciting at 405 nm and recording the 422–577 nm emission. For observation of *cameleon* and *WUS*-reporter lines, cultured IZEs were transferred to a microscope slide and mounted

in 50 µL of 1.5% liquid low melting point agarose (SeaPlaque, Duchefa, Haarlem, Netherlands). Samples were immediately covered with a cover glass, solidified at room temperature, and observed. For dsRED visualization of *WUS*-reporter lines, samples were excited at 561 nm and the 563–618 nm emission was recorded. For FRET visualization of *cameleon* lines, samples were excited at 405 nm and emission was recorded between 490–570 nm. CFP was excited at 405 nm and emission was recorded between 440–488 nm. YFP was excited at 514 nm and emission was recorded between 518–570 nm. Image treatment and calculation of fluorescence emission ratios were performed as previously described (Rizza et al. 2019). For imaging, the FRET (YFP/CFP) ratio was defined as the ratio between YFP and CFP emissions (480/535 nm).

For all cases, Ca^{2+} levels were defined as very low, low, moderate, high, or very high according to the colorimetric scale based on the FRET ratio images. Very low Ca^{2+} levels corresponded to dark blue colors, low levels to light blue, moderate to green–yellow, high to orange–red, and very high levels to white color. Image analysis was performed using the FIJI software v 1.53t (Schindelin et al. 2012).

3.2.5. Ca^{2+} Modulators and Callose Inhibitor

To modulate the intracellular Ca^{2+} levels, we used $CaCl_2$, the Ca^{2+} ionophore A23187, inositol 1,4,5-trisphosphate ($InsP_3$), ethylene glycol-bis(β-aminoethyl ether)-N,N,N′,N′- tetraacetic acid (EGTA), chlorpromazine, and N-(6-Aminohexyl)-5-chloro-1-naphthalenesul- fonamide hydrochloride (W-7). To inhibit callose deposition, 2-deoxy-D-glucose was used. Stocks of $CaCl_2$, $InsP_3$, EGTA, chlorpromazine, and 2-deoxy-D-glucose were prepared in sterile water. Stocks of ionophore A23187 and W-7 were prepared in DMSO following manufacturer instructions. Different concentrations of each compound were applied to IZE in vitro cultures, as described in Results. Control plates were prepared with the corresponding solvent concentration. Fifteen days after initiation, the percentage of embryogenic IZEs out of the total was calculated by field counting IZEs in microscopic images of culture dishes (Camacho-Fernández et al. 2018).

3.2.6. Statistical Analysis

Statistical analysis was performed using StatGraphics. The results of Ca^{2+} chemical modulation were analyzed performing an ANOVA and LSD test ($p \leq 0.05$). For non- homoscedastic samples, data were transformed with the arcsine transformation or the square root of the arcsine transformation to stabilize variance.

3.3.Results

3.3.1. Induction of Somatic Embryogenesis from IZEs of *Arabidopsis Cameleon* Lines

We used *Arabidopsis* seeds transformed with the *cameleon* YC3.6-Bar construct to isolate and in vitro culture IZEs at the cotyledonary stage (Fig. 1A). First, we checked the embryogenic response of the *cameleon* lines, comparing it

with Col-0 wild type plants. The embryogenic response of the two lines was not statistically different (Supplementary Figure S1), thus confirming the validity of these *cameleon* lines to study somatic embryogenesis under our experimental conditions. Four days after isolation, IZEs enlarged in general, but principally in the proximal region of the cotyledons, which induced their separation (Fig. 1B). Following that, visible embryogenic protrusions developed from the cotyledon nodes at the proximal adaxial region (Fig. 1C). Occasionally, embryogenesis was directly induced from the surface of the cotyledon (arrows in Fig. 1D,E). However, the most frequent scenario was the growth of embryogenic protrusions in the form of a cell mass (Fig. 1E, arrowhead). From these cell masses, clusters of embryos were formed after 14 days of culture (Fig. 1F, arrow). Upon excision of these clusters from the explant, by day 21 of culture they turned an intense green, continued elongating, and developed radicles (Fig. 1G). Their cotyledons, however, did not develop as much as those of the IZEs used as explants. Individualization of somatic embryos allowed for their germination into a rooted, regenerated plantlet (Fig. 1H) which, upon transference to soil and acclimatization, became a complete *Arabidopsis* plant in 15 days (Fig. 1I).

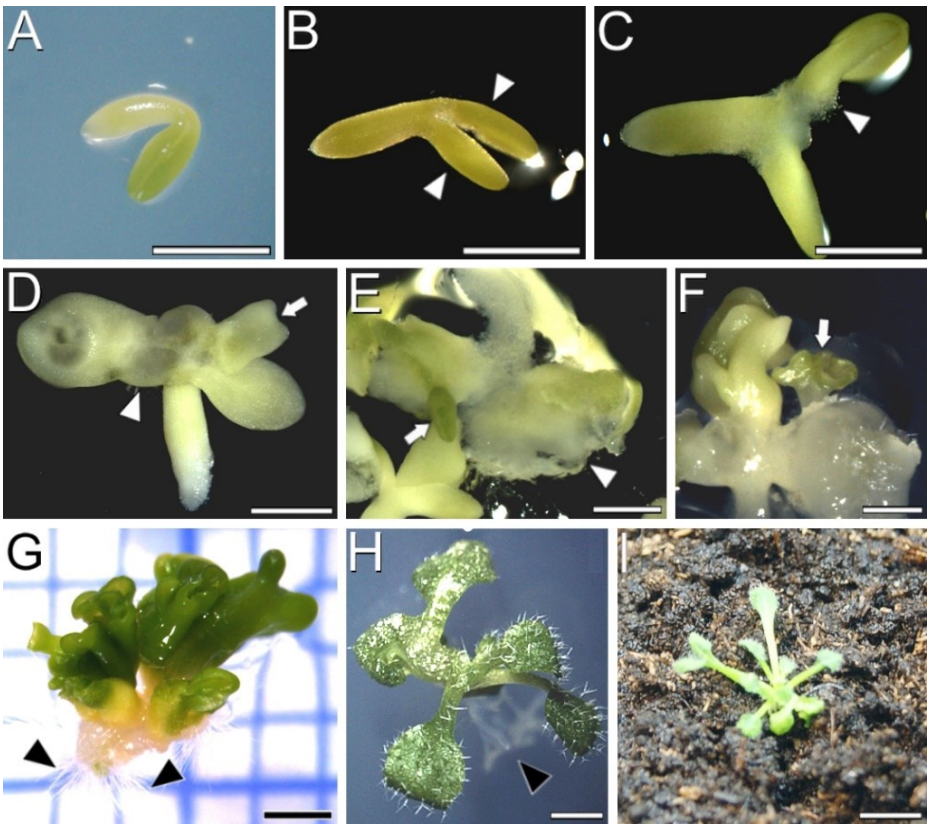

Fig. 1. **Induction of somatic embryogenesis from YC3.6-Bar *cameleon Arabidopsis* IZEs**. (**A**) Freshly isolated immature cotyledonary embryo. (**B**) Four-day-old cultured IZE with thickened cotyledons (white arrowheads). (**C**) Formation of protrusions (white arrowhead) in the adaxial side of cotyledons. (**D**) Formation of a protrusion (white arrowhead) in the adaxial side of the **left** cotyledon, and early emergence of a somatic embryo from the adaxial side of the **right** cotyledon (arrow). (**E**) Development of a callus mass from a cotyledonary protrusion (white arrowhead) and of a direct somatic embryo (arrow). (**F**) Somatic embryos (arrow) developed from a callus mass derived from a protrusion after 14 days of culture. (**G**) Cluster of somatic embryos excised from the explant after 21 days of culture. Black arrowheads point to the radicles formed at the basal pole of the cluster. (**H**) Germinated in vitro plantlet from an individualized somatic embryo. Black arrowhead points to roots. (**I**) *Arabidopsis* plant transferred to soil and acclimatized. Bars: (**A**–**F**) 500 µm; (**G**,**H**) 1 mm; (**I**) 5 mm.

3.3.2. Scanning Electron Microscopy of Somatic Embryogenesis from *Arabidopsis* IZEs

In order to have a closer view of the process of embryogenesis induction, we processed samples of IZEs at different stages during SE for analysis with FESEM. After three days of *in vitro* culture (Fig. 2A), no remarkable changes with respect to in vivo IZEs were observed. After 5 days, growth from inner cells of the apical region of the hypocotyl and principally the adaxial proximal region of the cotyledons was evident, and small protrusions arose (Fig. 2B, arrowhead), in some cases producing ruptures of the protodermis. Later (around day 7), the massive growth of the protrusions forced the rupture of the covering protodermal layer (Fig. 2C) and the emergence of a mass of proliferating cells (Fig. 2D). Further growth of the cell masses from both cotyledons may fuse into a single mass that frequently covers both cotyledons (Fig. 2E,F). In these cell masses, differentiation of some organs such as root-like structures could be distinguished (Fig. 2E arrowheads). Some of these structures continued their growth on the surface of the cell mass, becoming differentiated embryos (Fig. 2G). Elongated, cotyledonary-like embryos were clearly visible emerging on the surface of the cell masses after 14 days of culture (Fig. 2H). These embryos, however, frequently showed short cotyledons closely apposed or even fused by their margins, forming trumpet-shaped structures (Fig. 2I).

In addition to the formation of protrusions at the adaxial proximal regions of cotyledons, we also observed the occasional formation of protrusions at the cotyledon abaxial regions (Fig. 3A) and, more frequently, at the shoot apical meristem region, where a finger-like appendix emerged (Fig. 3B) after activation of growth at the cotyledon adaxial regions. In some IZEs, these protrusions elongated (Fig. 3C) and, after some days of culture, transformed into secondary somatic embryos (Fig. 3D–F) similar to those formed from the cotyledon adaxial regions, occurring at a lower frequency.

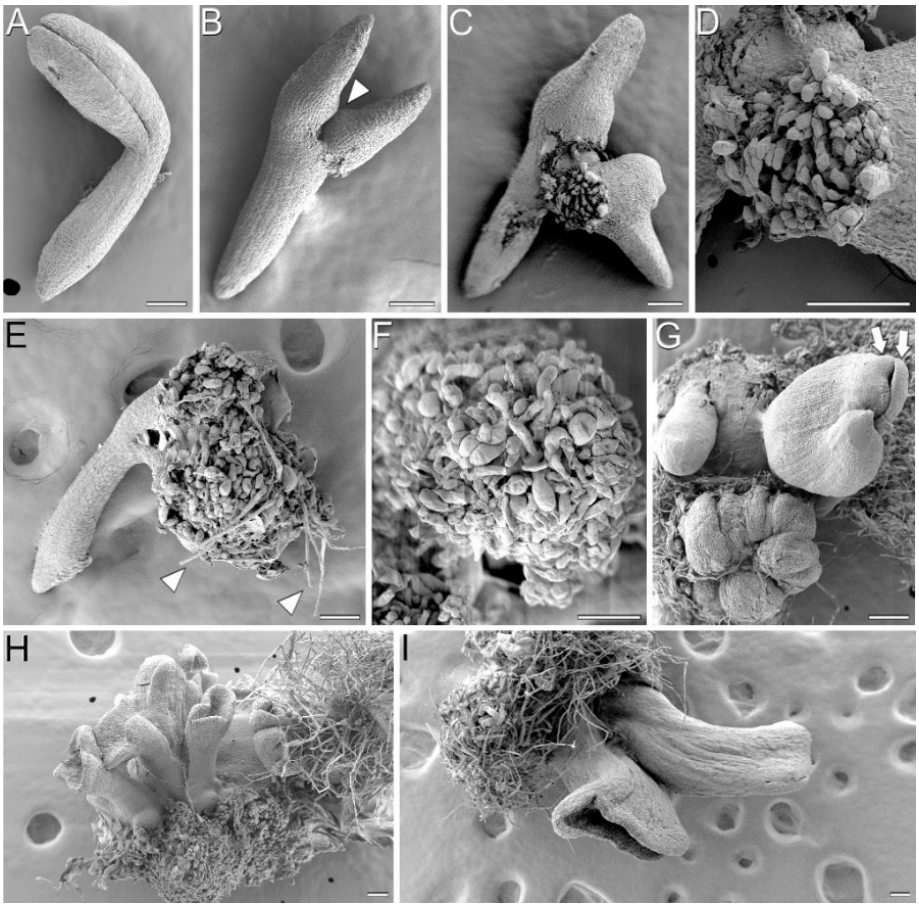

Fig. 2. SEM analysis of somatic embryogenesis from YC3.6-Bar *cameleon Arabidopsis* IZEs. (**A**) Isolated immature cotyledonary embryo after three days of culture. (**B**) Five-day-old cultured IZE with embryogenic protrusions (white arrowhead) in the adaxial proximal region of cotyledons. (**C**,**D**) Mass of proliferating cells emerged from the protrusion upon burst of the cotyledon epidermis at day 7 of culture. (**E**,**F**) Growth of the cell masses from both protrusions into a single mass that covers both cotyledons. Note the occurrence of the first radicles (arrows). (**G**) Development of somatic embryos at different developmental stages from the surface of the callus mass. Arrows point to the two cotyledons, still closed, of a bent torpedo embryo. (**H**) Cluster of somatic embryos excised from the explant after 14 days of culture. (**I**) Detail of two trumpet-shaped, elongated cotyledonary embryos. Bars: 100 µm.

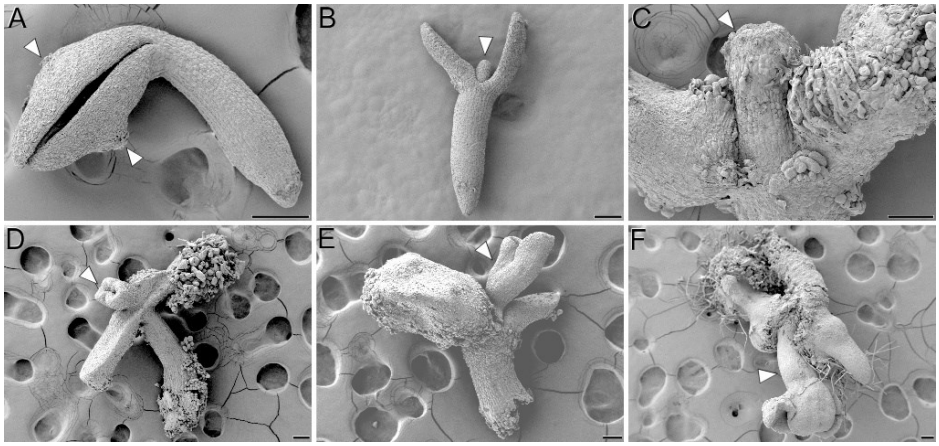

Fig. 3. SEM analysis of somatic embryogenesis from YC3.6-Bar *cameleon Arabidopsis* IZEs. (**A**) Cultured IZE after 3 days of culture. Note the occurrence of protrusions at the abaxial sides of both cotyledons (arrowheads). (**B**) Cultured IZE with a finger-like protrusion at the shoot apical meristem (arrowhead). (**C**) 14-day-old IZE with an elongating finger-like protrusion at the shoot apical meristem (arrowhead). (**D**–**F**) 14-day-old IZEs developing a secondary somatic embryo (arrowhead) from the shoot apical meristem. Bars: 100 µm.

3.3.3. Expression of the *WUS*-Reporter upon Induction of Somatic Embryogenesis in *Arabidopsis*

To evaluate the embryogenic nature of the growth and proliferation observed in the cotyledon adaxial proximal region and the shoot apical meristem, we induced somatic embryogenesis from IZEs of an *Arabidopsis WUS*-reporter line. As a control, we also cultured IZEs in hormone-free medium, which was unable to induce somatic embryogenesis. In five-day-old control IZEs, *WUS*-reporter expression was confined to the central zone of the shoot apical meristem, as expected (Fig. 4A–C). In IZEs cultured in inductive medium (with 2,4-D), *WUS*-reporter expression at day 5 was observed only in cells of the cotyledon nodes, immediately after their initial swelling to form protrusions (Fig. 4D–F), confirming the induction of embryogenesis in these cells.

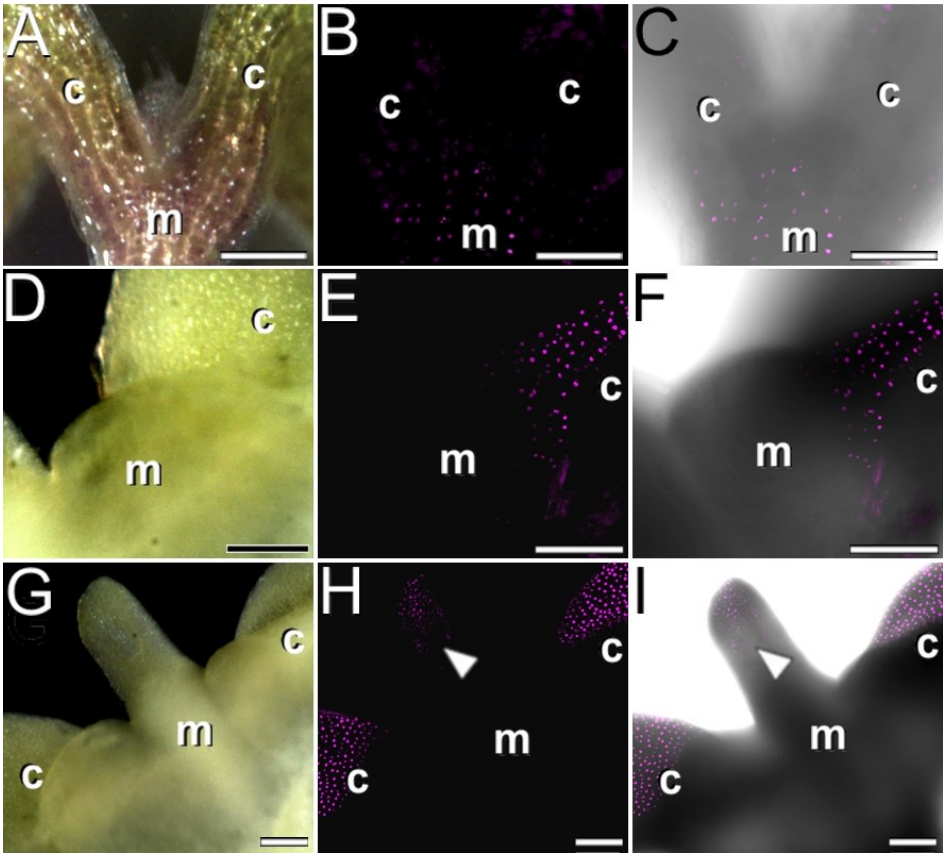

Fig. 4. Induction of somatic embryogenesis in IZEs of an *Arabidopsis* line expressing a *WUS*-reporter. Each row of images shows the same field imaged in the binocular microscope by bright field (**left**), fluorescence (**center**), and merge of both signals (**right**). (**A**–**C**) Control IZE cultured in non-embryogenic conditions. Note that the *WUS* signal is limited to the central zone of the shoot apical meristem (m). (**D**–**F**) 5-day-old IZE cultured in somatic embryogenesis medium showing WUS expression only at the swollen adaxial proximal region of the cotyledon (c). (**G**–**I**) 7-day-old IZE showing *WUS* expression at the enlarged appendix (arrowhead) of the shoot apical meristem (m) and the protrusions emerged from the adaxial proximal regions of both cotyledons (c). Bars: 100 μm.

At this stage we also observed a parallel silencing of *WUS*-reporter expression in the central cells of the shoot apical meristem. In IZEs at day 7, a finger-like appendix emerged from the shoot apical meristem region (Fig. 4G), *WUS*- reporter expression was also found in cells of the tip of the finger-like appendix (arrowhead in Fig. 4H,I), in addition to the mesophyll cells of the

protrusions at the cotyledon nodes. The rest of the explant did not show any detectable *WUS*-reporter expression. Together, these results confirm that, upon induction of somatic embryogenesis, the protodermal and subprotodermal cells of the cotyledon nodes are first reprogrammed to embryogenesis. Later on, and when present, cells from the finger-like appendix of the shoot apical meristem are also reprogrammed to embryogenesis.

3.3.4. Callose Staining during Somatic Embryogenesis in *Arabidopsis*

We used aniline blue to stain cultured IZEs and study callose distribution during the induction of somatic embryogenesis. It was described that during the second week of culture (around day 10), callose was synthesized in the cell walls of cells of the cotyledon protrusions as they grow and switch towards embryogenesis (Godel-Jedrychowska et al. 2020). In our IZE cultures, we also observed a similar increase in callose deposition at the cells of cotyledonary protrusions, as revealed by aniline blue staining. However, in our samples, such an increase was observed around day 5 of culture (Fig. 5A–C), indicating that, at least in our IZE culture system, somatic embryogenesis seems to proceed faster. In addition, in some IZEs we also observed a clear aniline blue staining at the shoot apical meristem region, before the appearance of the finger-like appendix, and during the first stages of appendix elongation (Fig. 5D–F). However, in growing embryos emerged from the appendix, aniline blue staining was notably reduced (Fig. 5G–I). Together, these results confirm that callose accumulates in the cells undergoing the embryogenic switch in the two cotyledonary protrusions, and in the shoot apical meristem region as it transforms into a finger-like embryogenic appendix. We also evaluated the role of callose during the process by inhibiting callose synthesis with 2-deoxy-D-glucose (Fig. 5J) and found that, for all concentrations and durations tested, inhibition of callose synthesis was seriously detrimental for embryo production, being almost null for 5 mM. The percentage of embryogenic IZEs was similar for 7-day and continuous 2-deoxy-D-glucose exposures, indicating that the role of callose on embryogenesis induction is exerted during the first week of culture, having no relevant effect after the first week. Together, these results show that callose deposition during the first week of culture is essential for a successful induction of somatic embryogenesis, being abundantly deposited at embryogenic regions prior to the development of somatic embryos.

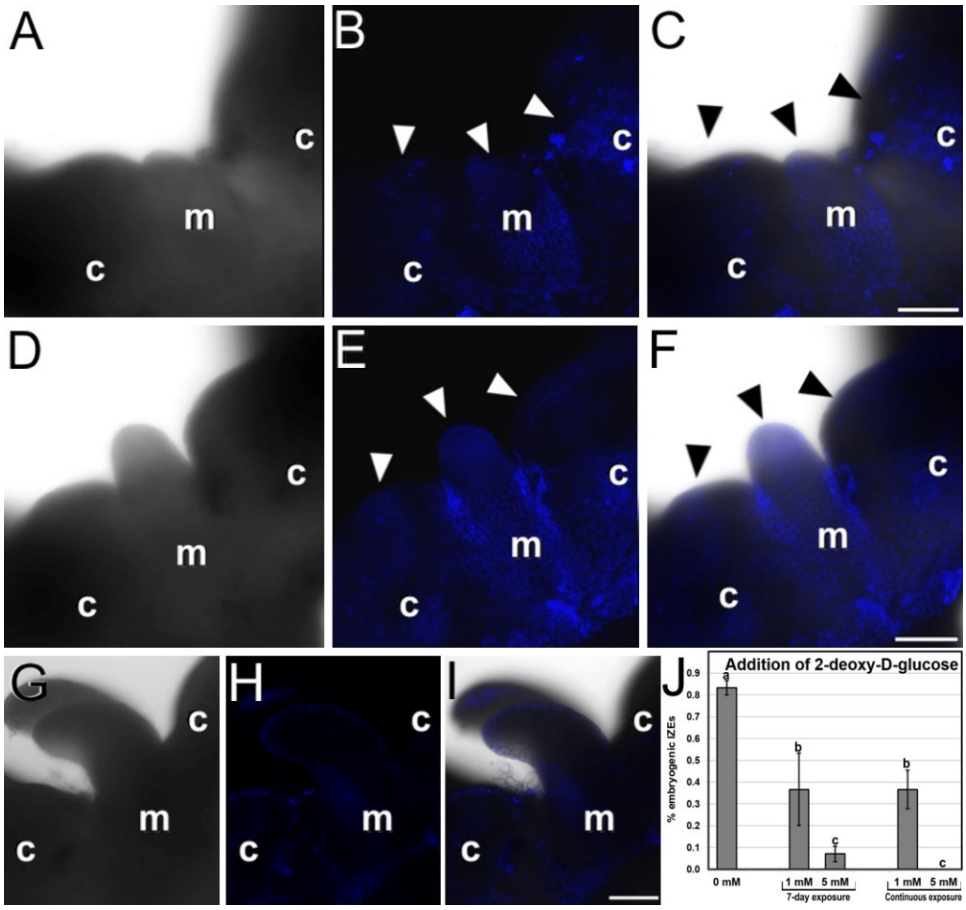

Fig. 5. Callose staining with aniline blue cultured IZEs. Each row of images shows the same field of aniline blue-stained samples imaged by bright field (**left**), fluorescence (**center**), and merge of both signals (**right**). (**A**–**C**) Five-day-old IZE with aniline blue staining (arrowheads) in the cotyledon nodes (c) and in the shoot apical meristem region (m). (**D**–**F**) IZE with aniline blue staining (arrowheads) in the cotyledon nodes (c) and in the shoot apical meristem region (m) where the finger-like appendix is also stained. (**G**–**I**) IZE with a somatic embryo growing from the finger-like appendix with almost no aniline blue staining in the cotyledon nodes (c) nor in the shoot apical meristem region (m). (**J**) Effect of 2-deoxy-D-glucose (applied during the first 7 days and continuously) in the percentage of embryogenic IZEs produced (% embryogenic IZEs) out of the total of embryos cultured. Different letters represent significant differences according to the LSD test. Bars: 100 µm.

3.3.5. FRET Imaging of Ca^{2+} Distribution during Somatic Embryogenesis in *Arabidopsis*

We performed a FRET study to track the dynamics of Ca^{2+} during the process of induction of somatic embryogenesis in our *Arabidopsis cameleon* lines (Fig. 6 and Supplementary Fig. S2). The first sign of change in the Ca^{2+} levels after the onset of in vitro culture was an increase in the protodermal cell layer of the shoot apical meristem region and the cotyledon nodes (arrowheads in Fig. 6A), outlining the regions where embryogenic cell proliferation will take place. Then, the Ca^{2+} signal persisted in the protoderm and increased in the inner cells of the cotyledon node region (Fig. 6B), while the rest of the IZE did not show relevant changes in Ca^{2+} signal. Once the protrusions were evident at the surface of the adaxial proximal cotyledon region, the Ca^{2+} signal markedly increased in these regions, as well as in the enlarged shoot apical meristem appendix (Fig. 6C). Large protrusions (Fig. 6D) and appendices showed the highest levels of Ca^{2+}, which were much higher than in any other IZE region. Ca^{2+} signal in the

protrusions was distributed in a gradient manner (Fig. 6D), with less signal at the periphery of the protrusion and more intense signal at the center of the protrusion, which is the place where new embryogenic structures are being formed (Fig. 2D). In parallel, we cultured IZEs in hormone-free medium, unable to induce somatic embryogenesis, and observed their Ca^{2+} signal in the cotyledons and shoot apical meristem. As seen in Fig. 6E, Ca^{2+} signal of non-induced IZEs was remarkably homogeneous, having cotyledons and shoot apical meristem levels of Ca^{2+} similar to those of the rest of the IZE. Together, these results show that Ca^{2+} levels increase in the cotyledon node and the shoot apical meristem, prior to the occurrence of somatic embryogenesis, with a pattern remarkably similar to that of *WUS*-reporter expression, making Ca^{2+} increase an early marker of somatic embryogenesis. Later on, Ca^{2+} levels increase even more in the protrusions in general and particularly in embryogenic cells, showing that high Ca^{2+} levels are necessary for an efficient transition of somatic cells into somatic embryos.

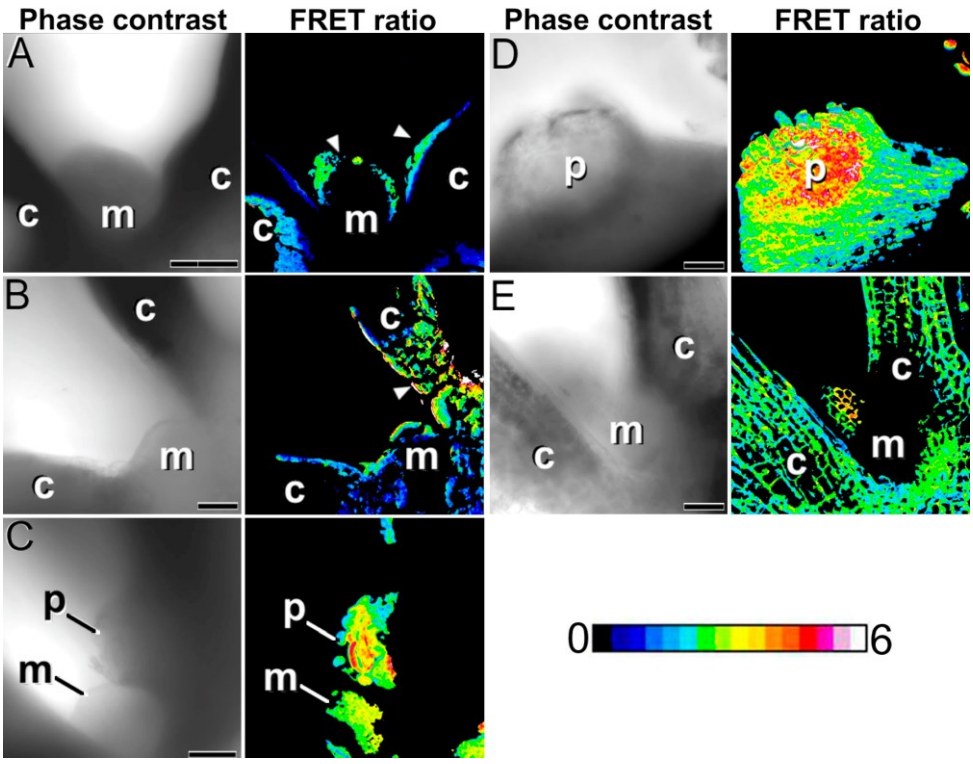

Fig. 6. FRET imaging of Ca2+ signaling during the induction of somatic embryogenesis in YC3.6-Bar *cameleon Arabidopsis* IZEs. Each pair of images show the same field imaged by phase contrast (**left**) and by the FRET (YFP/CFP emissions) ratios. The LUT bar displays the false coloration of FRET ratios. (**A**) Shoot apical meristem (m) and proximal region of the cotyledons (c), showing increased Ca^{2+} levels in the outermost cell layer of the shoot apical meristem and in the epidermis of the adaxial proximal cotyledon region (arrowheads). (**B**) Cells of the mesophyll region (arrowhead) of the cotyledon (c). (**C**) Shoot apical meristem (m) and a protrusion (p) at the adaxial proximal cotyledon region showing high Ca^{2+} levels. (**D**) Large protrusion (p) at the adaxial proximal region of the cotyledon with a radial gradient of Ca2+ levels, being higher at the center of the protrusion, where somatic embryos are being formed. (**E**) Shoot apical meristem (m) and proximal region of the cotyledons (c) of an IZE cultured in non-embryogenic conditions. Note the homogeneous distribution of Ca^{2+} in the regions imaged. Bars: 60 µm.

3.3.6. Modulation of Intracellular Ca^{2+} Levels

We performed a pharmacological study to modulate the intracellular Ca^{2+} levels. We treated embryogenic cultures with different chemicals known to interfere with intracellular Ca^{2+} levels, observed the embryos produced, and calculated the percentage of embryogenic IZEs for each treatment. First, we applied compounds known to increase Ca^{2+} levels in other somatic embryogenesis systems. We added different $CaCl_2$ concentrations (2 and 4 mM) and compared the embryo production with that of control cultures with 1.02 mM $CaCl_2$, the standard $CaCl_2$ concentration of the induction medium (Fig. 7A). $CaCl_2$ addition did not show any positive effect in terms of percentage of embryogenic IZEs produced, not during a 7-day exposure or during continuous exposure. Even with the highest concentration, the morphology of both the IZEs and the somatic embryos produced was similar to controls (Fig. 8A–C). The use of ionophore A23187, a plasma membrane Ca^{2+} channel used to alter intracellular Ca^{2+} gradients (Ge et al. 2007), produced no positive effects at any concentration or duration, but produced negative effects at higher concentrations in terms of reduced percentages of embryogenic IZEs (Fig. 7B) and of proliferation in IZEs of callus masses instead of somatic embryos (Fig. 8D–F). In line with this, the addition of $InsP_3$, known to induce Ca^{2+} efflux from different intracellular stores such as the ER or vacuoles (Winnicki 2020), did not produce any significant change, positive or negative, in the percentage and morphology of embryogenic IZEs, or at any of the concentrations used (0.1, 1, 10 and 100 µM). In summary, none of these compounds were effective for increasing embryogenesis. Instead, the effect was negative in some cases.

To reduce intracellular Ca^{2+} levels we used EGTA, a highly specific Ca^{2+} chelator, which at 1 mM caused a significant inhibition of embryogenesis for both exposure times, inhibiting about 50% when applied for 7 days, and almost completely when applied continuously (Fig. 7C). IZE morphology was also severely affected, being almost totally covered by callus tissue (Fig. 8G–I). We also used chlorpromazine and W-7, two CaM antagonists, to interfere with Ca^{2+}-CaM signaling. The inhibition of CaM with chlorpromazine (Fig. 7D) and W-7 (Fig. 7E) caused a dose-dependent inhibition of embryogenesis for both durations, which was almost complete when chlorpromazine was applied at 100 µM continuously. Consistent with this, the morphology of IZEs was dramatically altered, with almost no signs of somatic embryo growth and the development of callus masses with both chlorpromazine (Fig. 8J–L) and W-7 (Fig. 8M–O). In summary, both reducing the levels of intracellular Ca^{2+} or interfering with Ca^{2+} binding to CaM, negatively affects the induction and growth of somatic embryos, producing very similar patterns of callus growth and reduction of the percentages of embryogenic IZEs.

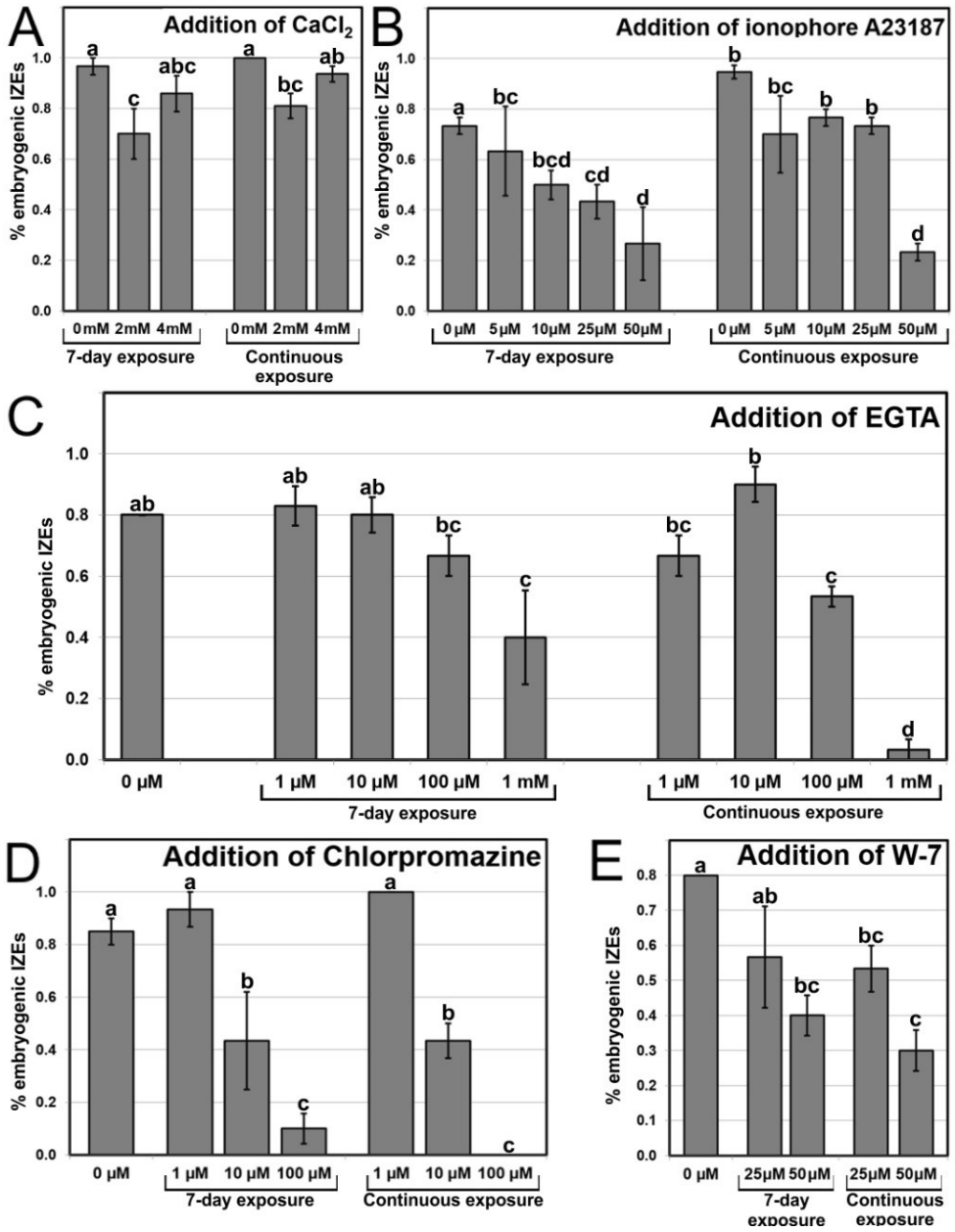

Fig. 7. Modulation of intracellular Ca^{2+} levels with different chemicals: $CaCl_2$ (**A**), ionophore A23187 (**B**), EGTA (**C**), chlorpromazine (**D**), and W-7 (**E**). Chemicals were used at different concentrations and for 7-day and continuous exposures. The effect of each treatment is expressed as the percentage of embryogenic IZEs produced (% embryogenic IZEs) out of the total of embryos cultured. Different letters represent significant differences according to the LSD test.

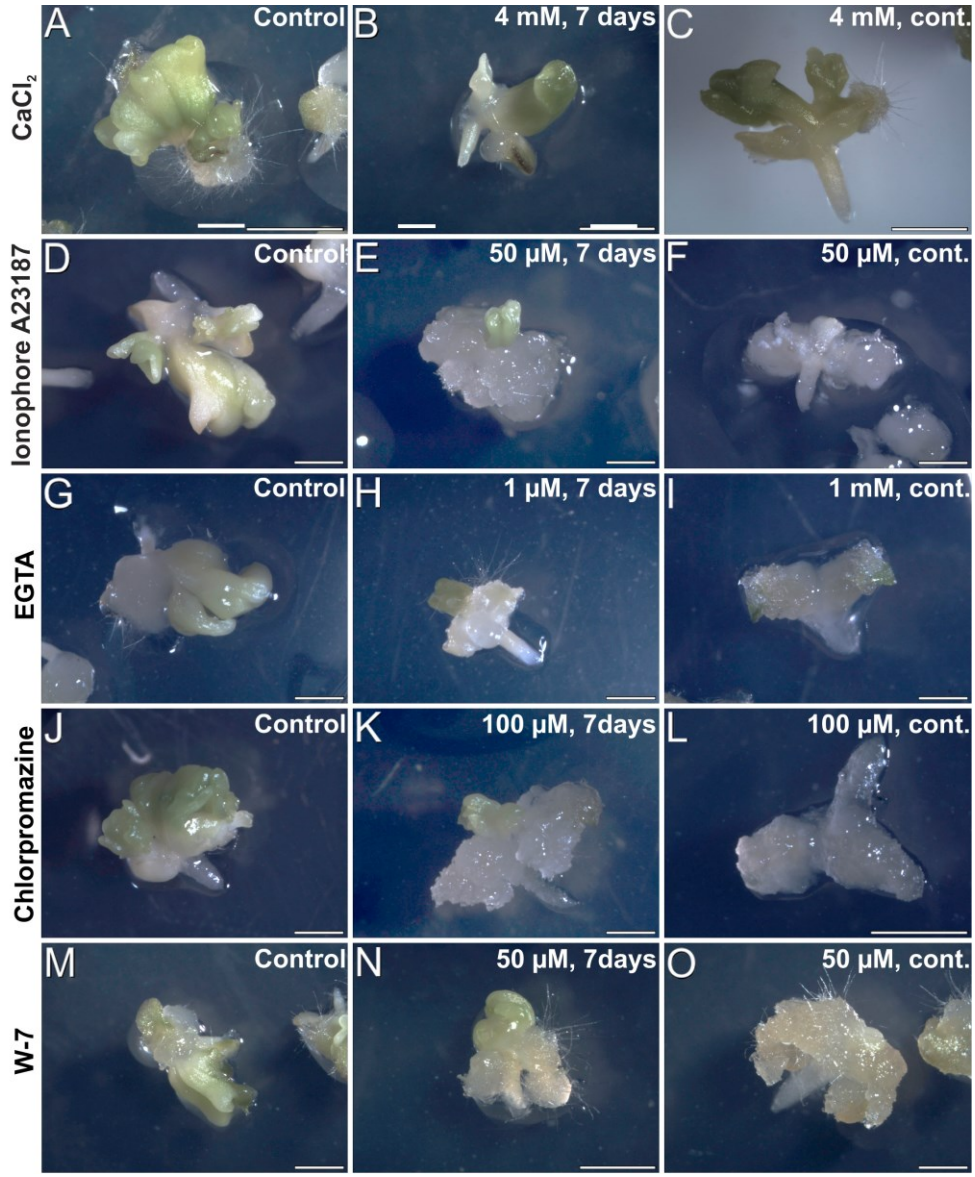

Fig. 8. Somatic embryos produced in cultures with different added chemicals, including $CaCl_2$ (**A**–**C**), ionophore A23187 (**D**–**F**), EGTA (**G**–**I**), chlorpromazine (**J**–**L**), and W-7 (**M**–**O**) at different concentrations and durations, as described in the images. Bars: 1 mm.

3.4.Discussion

3.4.1. The Shoot Apical Meristem of IZEs also Produces Somatic Embryos

Our microscopical analysis of somatic embryogenesis from IZEs showed the direct development of embryos from the cotyledon surface together with the development of inner cell masses that give rise to embryo clusters (Figs. 1 and 2), which is consistent with their reported protodermal and subprotodermal origin (Kurczynska et al. 2007), respectively. We also observed the occasional development of protrusions in the abaxial side of the cotyledons (Fig. 3A), which may possibly come from the same inner cells of the cotyledon node that, for any reason (difficult cotyledon separation, for example), cannot emerge from the adaxial side. This is also in line with the reported formation of a callus-like structure on the cotyledon abaxial side that may indirectly produce somatic

embryos (Kurczynska et al. 2007). However, we also consistently observed that, once established the cotyledon protrusions, some IZEs developed, at the shoot apical meristem region, an appendix that eventually produced somatic embryos (Fig. 3). This is surprising because it was never reported in the previous literature describing this system. Pioneering studies (Wu et al. 1992) did not mention anything about the involvement of the IZE shoot apical meristem in somatic embryogenesis. However, it is interesting to note that in one of their images, different cultured IZEs with finger-like appendices are clearly observed. In other, more recent works, the shoot apical meristem is described as not being involved in somatic embryo formation (Kurczynska et al. 2007; Godel-Jedrychowska et al. 2020). However, it is also interesting to note that in their analysis of IZEs expressing *WOX2:YFP,* an enlarged structure at the shoot apical meristem region showed an intense *WOX2* signal, consistent with the *WUS* expression we hereby show. Thus, our light microscopy and SEM analyses, together with our data on *WUS* expression and calcium dynamics during the establishment of embryo identity in IZE cells, clearly demonstrate that the appendix formed at the shoot apical meristem is also capable of producing somatic embryos. This is not surprising, since induction of somatic embryogenesis was demonstrated to be possible from shoot apex explants excised from 4–5-day-old seedlings (Ikeda-Iwai et al. 2003; Kadokura et al. 2018).

3.4.2. High Ca^{2+} Levels Act as a Trigger of Somatic Embryogenesis, Marking the Onset of the Process

During sexual plant reproduction, zygotic embryogenesis is initiated with two defined Ca^{2+} increases, the so-called Ca^{2+} signature of initiation of embryogenesis (Denninger et al. 2014). First, there is a short cytoplasmic Ca^{2+} transient increase (oscillation) in the egg and central cells, associated with pollen tube burst and the discharge of sperm cells. Then, there is a second, prolonged Ca^{2+} increase exclusive for the egg cell, associated with successful egg fertilization (Denninger et al. 2014). It is assumed that the developmental programs of zygotic and somatic embryogenesis are very similar, if not indistinguishable (Mordhorst et al. 2002). Thus, one can expect that in the somatic cell to be reprogrammed to embryogenesis, a similar Ca^{2+} signature should also be observed as a trigger for embryogenesis initiation. We were not able to identify the first, short Ca^{2+} transient peak at the onset of somatic embryogenesis, most likely due to its short duration, and principally because it is associated to pollen tube discharge (Denninger et al. 2014), which does not apply in this context. However, we observed a prolonged Ca^{2+} increase in the embryogenic regions that initiated in the protoderm and extended to the inner cells of the cotyledon nodes and the shoot apical meristem appendix (Fig. 6), coinciding with regions with cells expressing the *WUS*-reporter (Fig. 4). Thus, Ca^{2+} increase is an early marker of the onset of somatic embryogenesis. Interference with Ca^{2+} signaling by inhibiting CaM with two CaM antagonists, W-7 and chlorpromazine, led to a significant decrease of the percentage of embryogenic IZEs and a dramatic alteration of their morphology (Fig. 7D,E and Fig. 8J–O). The fact that 7-day and continuous treatments with CaM antagonists resulted in a similar reduction of embryo production may indicate that the signaling role of Ca^{2+} is principally exerted during the inductive stage of the embryogenic process, which strengthens the notion of a critical role of Ca^{2+} as a

triggering element for somatic embryogenesis. We therefore postulate that this would be the Ca^{2+} signature in somatic embryogenesis equivalent to the zygotic counterpart.

3.4.3. Ca^{2+} Homeostasis Cannot Be Altered to Induce Somatic Embryogenesis from IZEs

The role for Ca^{2+} in the induction of zygotic embryogenesis has been widely acknowledged (Denninger et al. 2014). In somatic embryogenesis, several reports have documented the need for defined, constant Ca^{2+} levels for this process to occur in different species (Anil and Rao 2000; Malabadi and van Staden 2006; Ramakrishna et al. 2011). Other reports, however, have documented that alteration of the intracellular Ca^{2+} levels has direct consequences in the rate of embryogenesis induction. In some of these cases, increasing Ca^{2+} levels had a positive impact in embryo production and reducing them was detrimental for embryo production (Marimuthu et al. 2019; Rivera-Solís et al. 2018; Etienne et al. 1997; Takeda et al. 2003), whereas in others, a reduction of Ca^{2+} levels was beneficial for somatic embryogenesis (Pullman et al. 2003). In this work, we used different pharmacological approaches to modulate intracellular Ca^{2+} levels. With the addition of $CaCl_2$ to the medium, no positive results were observed in any case (Fig. 7A and 8A–C), which suggests that Ca^{2+} influx is tightly regulated at the plasma membrane level, since increasing the intracellular–extracellular Ca^{2+} gradient had no effect. In turn, alteration of intracellular Ca^{2+} levels with ionophore A23187 produced dramatic, dose-dependent negative effects in IZE morphology in their competence to produce somatic embryos (Fig. 7B and 8D–F). On the other hand, reducing the levels of available Ca^{2+} by EGTA chelation produced similarly negative and dose-dependent results (Fig. 7C and 8G–I).

Together, these results show that influx or efflux of even small amounts of Ca^{2+} have important consequences in the maintenance of Ca^{2+} homeostasis, as expected considering the typically very low cytosolic Ca^{2+} concentrations (50–100 nM; (Pirayesh et al. 2021)). For the particular case of induction of somatic embryogenesis from *Arabidopsis* IZEs, a strict control of Ca^{2+} homeostasis is required, and the efficiency of the process cannot be improved by increasing intracellular Ca^{2+} levels, as occurs in other, more plastic systems described above. It seems that modulation of somatic embryogenesis by altering Ca^{2+} levels is not a common feature for all somatic embryogenesis systems. It is possible in some systems, like *Musa* (Marimuthu et al. 2019), *Cocos nucifera* (Rivera-Solís et al. 2018), *Hevea brasiliensis* (Etienne et al. 1997), or *Daucus carota* (Takeda et al. 2003), but not in others like *Santalum album* (Anil and Rao 2000), *Pinus patula* (Malabadi and van Staden 2006), *Coffea canephora* (Ramakrishna et al. 2011), and *Arabidopsis*, as we hereby show. However, the reason why different species behave differently remains to be elucidated.

3.4.4. Somatic Cells Transition to Embryogenesis First at the Cotyledon Protrusions and then at the Tip of the Shoot Apical Meristem Appendix

WUS is a transcription factor defined as a master regulator in plant growth signaling due to its key role in the regulation of both embryogenic and meristematic stem cells (Jha et al. 2020). In *Arabidopsis* plants and zygotic embryos, *WUS* is typically expressed in the central zone of the shoot apical meristem (Mayer et al. 1998). Upon induction of somatic embryogenesis, *WUS* is also expressed in the newly induced embryogenic cells even before they transform into embryos (Jha et al. 2020; Su et al. 2009), which makes *WUS* an early marker of the developmental transition from vegetative to embryogenic development. We used *Arabidopsis WUS* lines to check for the induction of primary somatic embryos from IZEs. Early *WUS* expression in the protrusion-producing protodermal and subprotodermal cells of the cotyledon node (Fig. 4D–F) was accompanied by deposition of callose (Fig. 5A–C) and increased calcium levels (Fig. 6B) in these cells, which confirms the embryogenic nature of the cells of these protrusions and the involvement of calcium and callose at the onset of this process. Previously, callose deposition was shown as essential to isolate the embryogenic domains from the rest of the explant (Godel-Jedrychowska et al. 2020), and Ca^{2+} increases could be related with both triggering of embryogenesis and the activation of callose synthesis by Ca^{2+}-dependent callose synthases, as reported for other in vitro embryogenesis systems (Rivas-Sendra et al. 2019). However, deposition of callose and increased calcium levels were not paralleled by *WUS* expression at the shoot apical meristem region, which is consistent with the absence of somatic embryos directly produced from cells of the shoot apical meristem. This suggests that the role of Ca^{2+} and callose in this region would not be related with triggering of somatic embryogenesis. Instead, it could be speculated that Ca^{2+}-mediated callose deposition at the shoot apical meristem would be needed to isolate these cells not for the establishment of embryo identity, but for the elimination of the stem cell identity of shoot meristem cells in order to allow for their growth. Indeed, successful induction of somatic embryogenesis in IZEs from different *Arabidopsis* mutants lacking embryonic shoot apical meristems demonstrated that a functional shoot meristem is not necessary for the induction of somatic embryos (Mordhorst et al. 2002). At later culture stages, when cotyledonary protrusions are clearly visible and a large, finger-like appendix emerges at the shoot apical meristem region, cells of the tip of this appendix begin to express *WUS,* as revealed by the expression of the *WUS*-reporter (Fig. 4G–I) with a pattern similar to that described for *WOX2* (Godel-Jedrychowska et al. 2020), and somatic embryos are produced from these cells. Thus, the transition to embryogenesis in IZEs would take place in two steps: first in protodermal and subprotodermal cells of the cotyledon nodes, which is accompanied by a loss of stem cell identity in the shoot apical meristem, and then in the tip of the finger-like appendix developed from the shoot apical meristem.

3.4.5. Concluding remarks

In this work, we studied the process of induction of somatic embryogenesis from *Arabidopsis* IZEs. Some of the results presented here, including the changes undergone by the cotyledonary nodes to become embryogenic regions, are in line

with those previously shown by other authors (Wu et al. 1992; Godel-Jedrychowska et al. 2020). However, there are some others that, to the best of our knowledge, have not been reported before and may be relevant for a better knowledge and understanding of the system. First, we observed that, at least in our hands, this system develops faster than reported in other cases, as the events associated with callose deposition previously described around day 10 (Godel-Jedrychowska et al. 2020) were observed in our cultures around day 5. This was confirmed by our light microscopy and SEM observations, and by the 2-deoxy-D-glucose experiments (Fig. 5J), which confirmed that callose deposition during the first week of culture is essential for successful embryo induction. We also showed that, in addition to the transformation of the cotyledon nodes into embryogenic regions where somatic embryos emerged from, a finger-like appendix develops from the shoot apical meristem region, and somatic embryos are, to a lesser extent, also generated from this appendix. We demonstrated that, as opposed to other somatic embryogenesis systems, Ca^{2+} homeostasis in *Arabidopsis* IZEs is strictly maintained and cannot be altered. Finally, we showed the dynamics of Ca^{2+} in the embryogenic regions, assigning putative roles in the activation of callose deposition and the induction of somatic embryogenesis. Together, these results contribute to a better understanding of this fascinating morphogenic process.

Acknowledgements

We thank the Electron Microscopy Service of Universitat Politècnica de València and to Marisol Gascón (IBMCP Microscopy Service) for their excellent technical help. Thanks are also due to Prof. Jörg Kudla from the University of Münster, Germany, for providing the Arabidopsis *cameleon* lines used in this study, and to Dr. Cristina Ferrandiz (IBMCP, Spain) for providing the Arabidopsis *WUS* lines.

References

Anil VS, Rao KS (2000) Calcium-mediated signaling during sandalwood somatic embryogenesis. Role for exogenous calcium as second messenger. Plant Physiol 123 (4):1301-1312

Camacho-Fernández C, Hervás D, Rivas-Sendra A, Marín MP, Seguí-Simarro JM (2018) Comparison of six different methods to calculate cell densities. Plant Methods 14 (1):30. doi:10.1186/s13007-018-0297-4

de Silva KK, Dunwell JM, Wickramasuriya AM (2022) Weighted Gene Correlation Network Analysis (WGCNA) of Arabidopsis Somatic Embryogenesis (SE) and Identification of Key Gene Modules to Uncover SE-Associated Hub Genes. International Journal of Genomics 4 (7471063)

Denninger P, Bleckmann A, Lausser A, Vogler F, Ott T, Ehrhardt DW, Frommer WB, Sprunck S, Dresselhaus T, Grossmann G (2014) Male-female communication triggers calcium signatures during fertilization in *Arabidopsis*. Nature Communications 5:4645. doi:10.1038/ncomms5645

Elhiti M, Stasolla C (2022) Transduction of Signals during Somatic Embryogenesis. Plants 11 (2):178

Etienne H, Lartaud M, Carron MP, Michaux-Ferriere N (1997) Use of calcium to optimize long-term proliferation of friable embryogenic calluses and plant regeneration in *Hevea brasiliensis* (Mull Arg). J Exp Bot 48 (306):129-137. doi:10.1093/jxb/48.1.129

Gaj MD (2011) Somatic Embryogenesis and Plant Regeneration in the Culture of *Arabidopsis thaliana* (L.) Heynh. Immature Zygotic Embryos. In: Thorpe TA, Yeung EC (eds) Plant

Embryo Culture: Methods and Protocols. Humana Press, Totowa, NJ, pp 257-265. doi:10.1007/978-1-61737-988-8_18

Gamborg OL, Miller RA, Ojima K (1968) Nutrient requirements of suspension cultures of soybean root cells. Exp Cell Res 50 (1):151-158. doi:http://dx.doi.org/10.1016/0014-4827(68)90403-5

Ge LL, Tian HQ, Russell SD (2007) Calcium function and distribution during fertilization in angiosperms. Am J Bot 94 (6):1046-1060. doi:10.3732/ajb.94.6.1046

Godel-Jedrychowska K, Kulinska-Lukaszek K, Horstman A, Soriano M, Li M, Malota K, Boutilier K, Kurczynska EU (2020) Symplasmic isolation marks cell fate changes during somatic embryogenesis. J Exp Bot 71 (9):2612-2628. doi:10.1093/jxb/eraa041

Horstman A, Bemer M, Boutilier K (2017) A transcriptional view on somatic embryogenesis. Regeneration 4 (4):201-216

Ikeda-Iwai M, Umehara M, Satoh S, Kamada H (2003) Stress-induced somatic embryogenesis in vegetative tissues of Arabidopsis thaliana. Plant J 34 (1):107-114

Jha P, Ochatt SJ, Kumar V (2020) *WUSCHEL*: a master regulator in plant growth signaling. Plant Cell Rep 39 (4):431-444. doi:10.1007/s00299-020-02511-5

Kadokura S, Sugimoto K, Tarr P, Suzuki S, Matsunaga S (2018) Characterization of somatic embryogenesis initiated from the *Arabidopsis* shoot apex. Developmental Biology 442 (1):13-27. doi:https://doi.org/10.1016/j.ydbio.2018.04.023

Kobayashi T, Nagayama Y, Higashi K, Kobayashi M (2010) Establishment of a tissue culture system for somatic embryogenesis from germinating embryos of *Arabidopsis* thaliana. Plant Biotechnol 27 (4):359-364

Krebs M, Held K, Binder A, Hashimoto K, Den Herder G, Parniske M, Kudla J, Schumacher K (2012) FRET-based genetically encoded sensors allow high-resolution live cell imaging of Ca^{2+} dynamics. Plant J 69 (1):181-192. doi:10.1111/j.1365-313X.2011.04780.x

Kulinska-Lukaszek K, Tobojka M, Adamiok A, Kurczynska EU (2012) Expression of the BBM gene during somatic embryogenesis of Arabidopsis thaliana. Biol Plant 56 (2):389-394. doi:10.1007/s10535-012-0105-3

Kurczynska EU, Gaj MD, Ujczak A, Mazur E (2007) Histological analysis of direct somatic embryogenesis in *Arabidopsis thaliana* (L.) Heynh. Planta 226 (3):619-628

Loyola-Vargas VM, Ochoa-Alejo N (2016) Somatic Embryogenesis. An Overview. In: Loyola-Vargas VM, Ochoa-Alejo N (eds) Somatic Embryogenesis: Fundamental Aspects and Applications. Springer International Publishing, Cham, pp 1-8. doi:10.1007/978-3-319-33705-0_1

Mahdavi-Darvari F, Noor NM, Ismanizan I (2015) Epigenetic regulation and gene markers as signals of early somatic embryogenesis. Plant Cell Tissue Organ Cult 120 (2):407-422. doi:10.1007/s11240-014-0615-0

Malabadi RB, van Staden J (2006) Cold-enhanced somatic embryogenesis in *Pinus patula* is mediated by calcium. South African Journal of Botany 72 (4):613-618. doi:10.1016/j.sajb.2006.04.001

Marimuthu K, Subbaraya U, Suthanthiram B, Marimuthu SS (2019) Molecular analysis of somatic embryogenesis through proteomic approach and optimization of protocol in recalcitrant *Musa* spp. Physiol Plant 167 (3):282-301. doi:10.1111/ppl.12966

Mayer KFX, Schoof H, Haecker A, Lenhard M, Jurgens G, Laux T (1998) Role of WUSCHEL in regulating stem cell fate in the Arabidopsis shoot meristem. Cell 95 (6):805-815

Mohanta TK, Yadav D, Khan AL, Hashem A, Abd_Allah EF, Al-Harrasi A (2019) Molecular Players of EF-hand Containing Calcium Signaling Event in Plants. International Journal of Molecular Sciences 20 (6):1476

Mordhorst AP, Hartog MV, El Tamer MK, Laux T, de Vries SC (2002) Somatic embryogenesis from *Arabidopsis* shoot apical meristem mutants. Planta 214 (6):829-836. doi:10.1007/s00425-001-0700-6

Murashige T, Skoog F (1962) A revised medium for rapid growth and bioassays with tobacco tissue cultures. Physiol Plant 15:473-479

O'Neill CM, Mathias RJ (1995) Regeneration of Plants from Protoplasts of *Arabidopsis thaliana* CV. Columbia L. (C24), Via Direct Embryogenesis. In: Terzi M, Cella R, Falavigna A

(eds) Current Issues in Plant Molecular and Cellular Biology: Proceedings of the VIIIth International Congress on Plant Tissue and Cell Culture, Florence, Italy, 12–17 June, 1994. Springer Netherlands, Dordrecht, pp 377-382. doi:10.1007/978-94-011-0307-7_52

Overvoorde PJ, Grimes HD (1994) The role of calcium and calmodulin in carrot somatic embryogenesis. Plant Cell Physiol 35 (2):135-144

Pirayesh N, Giridhar M, Ben Khedher A, Vothknecht UC, Chigri F (2021) Organellar calcium signaling in plants: An update. Biochimica et Biophysica Acta (BBA) - Molecular Cell Research 1868 (4):118948. doi:https://doi.org/10.1016/j.bbamcr.2021.118948

Pullman GS, Montello P, Cairney J, Xu NF, Feng XR (2003) Loblolly pine (*Pinus taeda* L.) somatic embryogenesis: maturation improvements by metal analyses of zygotic and somatic embryos. Plant Sci 164 (6):955-969. doi:10.1016/s0168-9452(03)00079-7

Ramakrishna A, Giridhar P, Ravishankar GA (2011) Calcium and calcium ionophore A23187 induce high-frequency somatic embryogenesis in cultured tissues of *Coffea canephora* P ex Fr. In Vitro Cell Dev Biol -Pl 47 (6):667-673. doi:10.1007/s11627-011-9372-5

Reinert J (1958) Morphogenese und ihre Kontrolle an Gewebekulturen aus Carotten. Naturwissenschaften 45:344-345

Rivas-Sendra A, Corral-Martínez P, Porcel R, Camacho-Fernández C, Calabuig-Serna A, Seguí-Simarro JM (2019) Embryogenic competence of microspores is associated with their ability to form a callosic, osmoprotective subintinal layer. J Exp Bot 70 (4):1267–1281. doi:10.1093/jxb/ery458

Rivera-Solís G, Sáenz-Carbonell L, Narváez M, Rodríguez G, Oropeza C (2018) Addition of ionophore A23187 increases the efficiency of *Cocos nucifera* somatic embryogenesis. 3 Biotech 8 (8):366. doi:10.1007/s13205-018-1392-y

Rizza A, Walia A, Tang B, Jones AM (2019) Visualizing cellular gibberellin levels using the nlsGPS1 Förster resonance energy transfer (FRET) biosensor. JoVE (Journal of Visualized Experiments) 143:e58739. doi:10.3791/58739

Satpute G, Long H, Seguí-Simarro JM, Risueño MC, Testillano PS (2005) Cell architecture during gametophytic and embryogenic microspore development in *Brassica napus*. Acta Physiol Plant 27 (4B):665-674. doi:10.1007/s11738-005-0070-y

Schindelin J, Arganda-Carreras I, Frise E, Kaynig V, Longair M, Pietzsch T, Preibisch S, Rueden C, Saalfeld S, Schmid B, Tinevez JY, White DJ, Hartenstein V, Eliceiri K, Tomancak P, Cardona A (2012) Fiji: an open-source platform for biological-image analysis. Nature methods 9 (7):676-682. doi:10.1038/nmeth.2019

Schmidt ED, Guzzo F, Toonen MA, de Vries SC (1997) A leucine-rich repeat containing receptor-like kinase marks somatic plant cells competent to form embryos. Development 124 (10):2049-2062. doi:10.1242/dev.124.10.2049

Seguí-Simarro JM, Jacquier NMA, Widiez T (2021) Overview of i*n vitro* and *in vivo* doubled haploid technologies. In: Seguí-Simarro JM (ed) Doubled Haploid Technology, vol 1: General Topics, Alliaceae, Cereals. Methods in Molecular Biology, vol 2287, 1st edn. Springer Science+Business Media, LLC, New York, USA, pp 3-22. doi:10.1007/978-1-0716-1315-3_1

Stael S, Wurzinger B, Mair A, Mehlmer N, Vothknecht UC, Teige M (2011) Plant organellar calcium signalling: an emerging field. J Exp Bot 63 (4):1525-1542. doi:10.1093/jxb/err394

Steward FC, Mapes MO, Mears K (1958) Growth and organized development of cultured cells. II. Organization in cultures grown from freely suspended cells. Am J Bot 45 (10):705-708

Su YH, Zhao XY, Liu YB, Zhang CL, O'Neill SD, Zhang XS (2009) Auxin-induced WUS expression is essential for embryonic stem cell renewal during somatic embryogenesis in Arabidopsis. Plant J 59 (3):448-460. doi:10.1111/j.1365-313X.2009.03880.x

Takeda T, Inose H, Matsuoka H (2003) Stimulation of somatic embryogenesis in carrot cells by the addition of calcium. Biochem Eng J 14 (2):143-148. doi:http://dx.doi.org/10.1016/S1369-703X(02)00186-9

Tian W, Wang C, Gao Q, Li L, Luan S (2020) Calcium spikes, waves and oscillations in plant development and biotic interactions. Nature Plants 6 (7):750-759. doi:10.1038/s41477-020-0667-6

Winnicki K (2020) The Winner Takes It All: Auxin-The Main Player during Plant Embryogenesis. Cells 9 (3). doi:10.3390/cells9030606

Wu Y, Haberland G, Zhou C, Koop H-U (1992) Somatic embryogenesis, formation of morphogenetic callus and normal development in zygotic embryos of *Arabidopsis thaliana* in vitro. Protoplasma 169:89-96

Zuo J, Niu QW, Frugis G, Chua NH (2002) The *WUSCHEL* gene promotes vegetative-to-embryonic transition in *Arabidopsis*. Plant J 30 (3):349-359

Supplementary materials

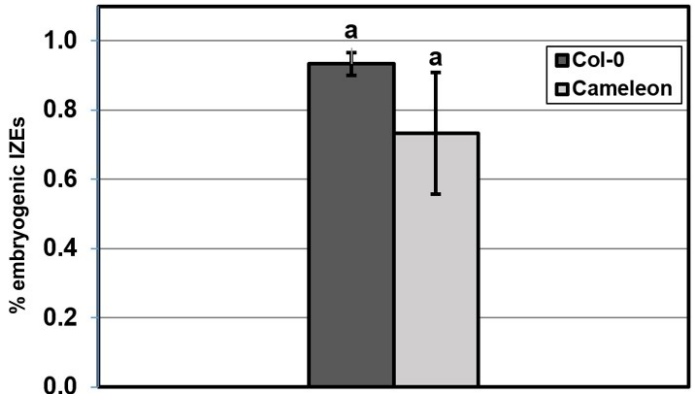

Suppl. Fig. S1. Comparison of the embryogenic response of wild type (Col-0) and *cameleon* lines, expressed as the percentage of embryogenic IZEs produced (% embryogenic IZEs) out of the total of embryos cultured. Same letters represent absence of significant differences according to the LSD test.

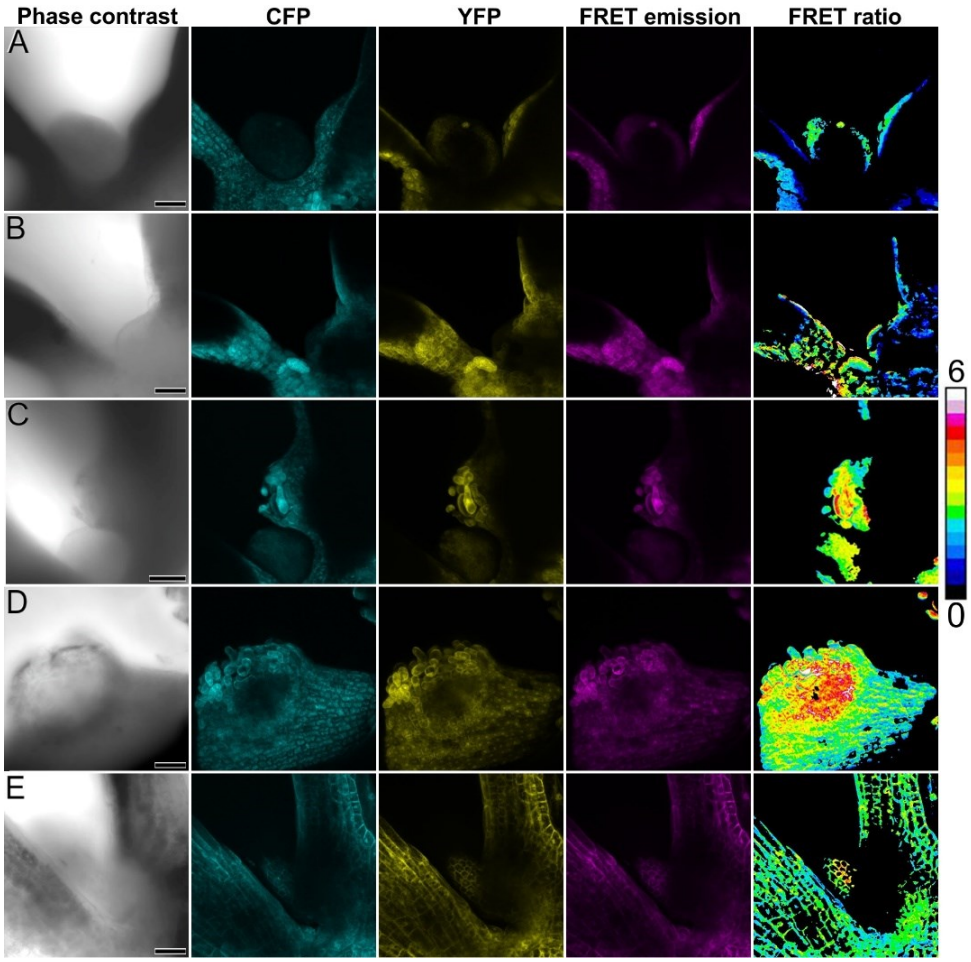

Suppl. Fig. S2. FRET imaging of Ca^{2+} signaling during the induction of somatic embryogenesis in YC3.6-Bar *cameleon* arabidopsis IZEs. Each set of images show the same stages shown in Fig. 4 imaged by phase contrast, CFP, YFP, FRET emission fluorescence and FRET (YFP/CFP emissions) ratio. The LUT bar displays the false coloration of FRET ratios. A: Shoot apical meristem and proximal region of the cotyledons, showing increased Ca^{2+} levels in the outermost cell layer of the shoot apical meristem and in the epidermis of the adaxial proximal cotyledon region. B: Cells of the mesophyll region of the cotyledon. C: Shoot apical meristem and a protrusion at the adaxial proximal cotyledon region. D: Large protrusion at the adaxial proximal region of the cotyledon with a radial gradient of Ca^{2+} levels. E: Shoot apical meristem and proximal region of the cotyledons of an IZE cultured in non-embryogenic conditions showing a homogeneous Ca^{2+} distribution. Bars: 60 µm.

4. Chapter 2: Calcium dynamics and modulation in carrot somatic embryogenesis

Antonio Calabuig-Serna, Ricardo Mir, Paloma Arjona, Jose María Seguí-Simarro.

Cell Biology Group - COMAV Institute, Universitat Politècnica de València, 46022 Valencia, Spain.

Keywords: Callose, *Daucus carota*, EGTA, FRET, *in vitro* culture, ionophore A23187, morphogenesis, W-7.

This article has been published as: Calabuig-Serna A, Mir R, Arjona P and Seguí-Simarro JM (2023) Calcium dynamics and modulation in carrot somatic embryogenesis. *Front. Plant Sci*. 14:1150198. doi: 10.3389/fpls.2023.1150198

In this research work, Antonio Calabuig-Serna contributed in the processes of investigation, methodology, data curation, formal analysis, and writing, reviewing and editing the draft.

Abstract

Free calcium (Ca^{2+}) is a pivotal player in different *in vivo* and *in vitro* morphogenic processes. In the induction of somatic embryogenesis, its role has been demonstrated in different species. In carrot, however, this role has been more controversial. In this work, we developed carrot lines expressing *cameleon* Ca^{2+} sensors. With them, Ca^{2+} levels and distribution in the different embryogenic structures formed during the induction and development of somatic embryos were analyzed by FRET. We also used different chemicals to modulate intracellular Ca^{2+} levels ($CaCl_2$, ionophore A23187, EGTA), to inhibit calmodulin (W-7) and to inhibit callose synthesis (2-deoxy-D-glucose) at different times, principally during the first stages of embryo induction. Our results showed that high Ca^{2+} levels and the development of a callose layer are markers of cells induced to embryogenesis, which are the precursors of somatic embryos. Disorganized calli and embryogenic masses have different Ca^{2+} patterns associated to their embryogenic competence, with higher levels in embryogenic cells than in callus cells. The efficiency of somatic embryogenesis in carrot can be effectively modulated by allowing, within a range, more Ca^{2+} to enter the cell to act as a second messenger to trigger embryogenesis induction. Once induced, Ca^{2+}-calmodulin signaling seems related with the transcriptional remodeling needed for embryo progression, and alterations of Ca^{2+} or calmodulin levels negatively affect the efficiency of the process.

4.1.Introduction

Free calcium (Ca^{2+}) has many different structural, metabolic and regulatory functions. One of the most important is its role as signaling molecule in both plant and animal cells (Permyakov and Kretsinger 2009). Ca^{2+} is typically kept at very low concentrations in the cytoplasm (50-100 nM), being stored principally at the endoplasmic reticulum, nucleus, cell wall and vacuoles (Pirayesh et al. 2021). Thus, Ca^{2+} signaling relies on transient Ca^{2+} releases that change cytosolic Ca^{2+} concentrations in order to trigger regulation of gene expression and physiological responses (White and Broadley 2003; Demidchik et al. 2018). Plants use Ca^{2+} to regulate and control, among others, the responses to biotic and abiotic stresses as well as different aspects of plant reproduction including pollen tube growth, double fertilization, embryo development and seed yield (White and Broadley 2003; Tian et al. 2020; Tang and Luan 2017; Denninger et al. 2014; Ge et al. 2007; Antoine et al. 2000). However, there is still limited information about Ca^{2+} dynamics during *in vivo* development of the plant zygotic embryo, probably due to the difficulties imposed by the surrounding maternal tissues. As alternatives, microspore-derived embryos (Rivas-Sendra et al. 2017; Rivas-Sendra et al. 2019) and principally somatic embryos have been used to study Ca^{2+} dynamics during early embryo development (Anil and Rao 2000; Mahalakshmi et al. 2007). Somatic embryogenesis is an *in vitro* biotechnological process whereby plant somatic cells dedifferentiate from their original identity and start developing as embryos (Yang and Zhang 2010). Somatic embryogenesis systems have been widely used to develop efficient micropropagation protocols as well as to study embryogenic development in several species including carrot (*Daucus carota*), where the first embryogenic suspension cultures were reported more than six decades ago (Reinert 1958; Steward et al. 1958). Typically, the carrot somatic

embryogenesis system is based on the generation of hypocotyl-derived calli, which are then disaggregated in auxin-containing medium into a suspension of cell clumps, from which embryogenic masses are formed. Upon hormone removal, embryos start developing from the embryogenic masses (de Vries et al. 1988). Carrot somatic embryos strongly resemble zygotic embryos with the exception of the suspensor (Halperin 1964), which makes this system a useful model to study different aspects of plant embryogenesis, including Ca^{2+} dynamics. Besides, understanding the role of Ca^{2+} in the *in vitro* induction of embryogenesis may open new ways to improve the efficiency of this biotechnological tool of wide interest in applied plant breeding.

The role of Ca^{2+} in the induction of somatic embryogenesis has been demonstrated in species such as sandalwood (Anil and Rao 2000), *Pinus patula* (Malabadi and van Staden 2006), coffee (Ramakrishna et al. 2011) or *Arabidopsis* (Calabuig-Serna et al. 2023). In carrot, however, this role has been somehow controversial. Some reports proposed that increased intracellular Ca^{2+} levels, induced through the addition of $CaCl_2$ to the culture medium or by facilitating the diffusion of Ca^{2+} across the plasma membrane by adding ionophore A23187, could increase somatic embryogenesis in carrot (Takeda et al. 2003; Jansen et al. 1990), as shown in other species like coconut (Rivera-Solís et al. 2018). Instead, other studies showed that maintenance of Ca^{2+} homeostasis was essential to induce carrot somatic embryos, since increasing Ca^{2+} levels by adding $CaCl_2$ or ionophore A23187 had no beneficial effect on embryo yield (Overvoorde and Grimes 1994), concluding that a strict maintenance of Ca^{2+} homeostasis was a requisite for carrot somatic embryogenesis. In turn, addition of exogenous Ca^{2+} was found beneficial in other species such as *Hevea brasiliensis* to increase both the rate of induction of somatic embryos and to increase the capacity of regeneration and germination of the induced embryos (Etienne et al. 1997). In carrot, however, Ca^{2+} was suggested to allow for a more efficient progression of the embryos already induced, rather than for the induction of more embryos (Mizukami et al. 2008).

Most of these works were developed at least 20 years ago, using biochemical analyses and the fluorescence imaging technologies available at that time, including staining with Ca^{2+}-binding fluorescent dyes such as chlorotetracycline (Timmers et al. 1989; Overvoorde and Grimes 1994) or Fura2-AM (Anil and Rao 2000; Ramakrishna et al. 2011). Although informative, some of these dyes have limited cell penetration and do not allow for *in vivo* Ca^{2+} observation. These limitations can now be overcome with genetically-encoded Ca^{2+} sensors such as *cameleon* probes (Miyawaki et al. 1997), based on fluorescence resonance energy transfer (FRET) for Ca^{2+} detection. *Cameleon* probes are produced by the tandem expression of a construct including a donor cyan fluorescent protein (CFP), a calmodulin (CaM) residue fused to the specific binding peptide M13, and an acceptor yellow fluorescent protein (YFP). Free Ca^{2+} binds CaM and induces a conformational change that favors the acceptor YPF excitation by the donor CPF emission (Miyawaki et al. 1997). *Cameleons* are also targetable to specific intracellular locations. For example, in Arabidopsis, a collection of *cameleon* constructs adapted for plants and specifically targeted to the cytoplasm, nucleus, or plasma membrane was developed (Krebs et al. 2012). Therefore, plant *cameleons* are nowadays powerful tools to study Ca^{2+} oscillations in plant cells.

In this work, we assayed two different protocols in order to optimize carrot transformation and develop for the first time transgenic lines expressing *cameleon* probes. We produced three carrot lines expressing plasma membrane-targeted *cameleons* and used them, together with their wild type counterparts, to induce somatic embryogenesis, characterize the different stages of the process, study the dynamics of callose deposition, image Ca^{2+} distribution in living cells during embryo induction and development and test the effect of applying different Ca^{2+} chemical modulators at different times, principally during the first stages of embryo induction. Our results show that Ca^{2+} is tightly associated to the embryogenic fate of specific cells. Besides, Ca^{2+} homeostasis can be altered to modulate embryo production. Together, these results help to improve and understand this fascinating *in vitro* process.

4.2.Materials and methods

4.2.1. Plant material

Commercial seeds of carrot (*Daucus carota)* cv. Nantese 5 from Semillas Batlle S.A. were used for transformations, induction of somatic embryogenesis and modulation of Ca^{2+} homeostasis. Transgenic seedlings developed from carrot transformation expressing the PM-YC3.6-LTI6b *cameleon* construct were used for Ca^{2+} visualization by confocal microscopy. Carrot seeds were surface-sterilized in two consecutive cycles of 15 minutes in 70% ethanol + 0.1% triton solution, 15 minutes in 50% bleach solution and three rinses in distilled sterile water. Seeds were kept in solid MS2% medium (Table 1) for 7-10 days at 25 °C in darkness.

4.2.2. Plant transformation and regeneration

Two *cameleon* constructs were used for carrot transformation: YC3.6-Bar and PM-YC3.6-LTI6b, coding for *cameleon* fusion proteins targeted to the cytoplasm and the cytosolic side of the plasma membrane (Krebs et al. 2012). Both *cameleon* plasmids were kindly provided by Dr. Jörg Kudla and described in detail in (Krebs et al. 2012). *Escherichia coli* One Shot™ ccdB Survival™ 2 T1R Competent Cells were transformed with YC3.6-Bar and PM-YC3.6-LTI6b plasmids respectively. The *Agrobacterium tumefaciens* strain LBA4404 carrying the helper *vir* plasmid pAL4404 (ElectroMAX™ *A. tumefaciens* LBA4404 Cells, Invitrogen™) was transformed with the YC3.6-Bar and PM-YC3.6-LTI6b plasmids respectively following provider instructions. Transformed cells were plated in YM solid medium supplemented with 50 mg/L rifampicin and appropriate bacterial selective agents: 50 mg/L kanamycin for YC3.6-Bar and 100 mg/L spectinomycin and 100 mg/L streptomycin for PM-YC3.6-LTI6b.

Two transformation protocols were assayed, namely protocol D (Gonzalez-Calquin and Stange 2020) and protocol E (Hardegger and Sturm 1998). Protocol D started pre-culturing 2 cm-long hypocotyl explants for 3 days at 25 °C in darkness in Co-culture D medium (Table 1). Explants were incubated for 15 min in *Agrobacterium tumefaciens* suspensions prepared in 4.6 g/L MS medium at a final OD_{600} of 0.2. Incubation was performed in petri dishes. During the process, small wounds were performed in the explants with a scalpel to facilitate the penetration of bacteria in the explants. Then, explants were deposited in sterile

paper to remove the excess of bacterial inoculum. Explants were placed in Co-culture D medium and incubated for 3 days at 25 °C in darkness. After that, explants were transferred to MI medium (Table 1) and plates were kept at 25 °C in darkness. Two weeks later, explants were transferred to MII medium (Table 1) and incubated for at least one month, refreshing the medium every two weeks. MII plates were kept at 25 °C in a 16/8 h photoperiod. When developing embryos were visible and detached from the explant, explants were transferred to plates with MIII medium (Table 1) supplemented with 5 mg/L BASTA for explants transformed with YC3.6-Bar and with 50 mg/L kanamycin for explants transformed with PM-YC3.6-LTI6b, and kept at 25 °C and 16/8 h photoperiod. Medium was refreshed monthly.

For protocol E, 2 cm hypocotyl explants were obtained from 7-10 day-old seedlings. Inoculation was assayed under two different conditions: dipping the explants for few minutes in the suspension preparation or applying three cycles of vacuum (5 minutes each) to the explants. In both cases, after inoculation, explants were incubated in Co-culture E medium (Table 2) for 3 days in darkness at 25 °C. Excess of bacteria was washed with liquid basic GB5 medium and explants were incubated in Selection 1 medium (Table 2) for two weeks at 25 °C and 16/8 h photoperiod. Then, explants were transferred to Selection 2 medium (Table 2) and incubated for six weeks at 25 °C and 16/8 h photoperiod. Medium was refreshed every two weeks. For plant regeneration, an adaptation of the (Overvoorde and Grimes 1994) protocol was followed. Greenish calli were transferred to Embryogenesis Induction Selective Medium (EISM; Table 2) and kept for at least eight weeks at 25 °C and 16/8 h photoperiod, refreshing plates every two weeks. Portions of approximately 0.2 g of resistant calli were transferred to 100 mL flasks containing 50 mL of liquid EISM (excluding plant agar), and kept for one week in a rotary shaker (140 rpm) at 25 °C in darkness. Then, liquid cultures were filtered through a 41 μm nylon filter. Cells were recovered with 50 mL of liquid MS2% medium (Table 1) supplemented with 500 mg/L carbenicilin and transferred to 100 mL flasks. Flasks were kept in a rotary shaker at 25 °C in darkness for at least one week. 1 mL aliquots of cultures were transferred to plates with solid MS2% medium (Table 1) and incubated at 25 °C and 16/8 h photoperiod. When embryos germinated into seedlings, a portion of cotyledon was used for genotyping with the primers pUBQ 5’ttcaccgccttagctttctcg (forward) and CFP5’ 5’gcacgacttcttcaagtccgc (reverse).

Table 1. Composition of the seed germination and plant *in vitro* culture media used for the carrot transformation protocol D. MS: Murashige and Skoog basal medium + vitamins (Murashige and Skoog 1962). All basal media and other medium components were purchased from Duchefa (Netherlands).

	Solid MS2%	**Liquid MS2%**	**Co-culture D**	**MI**	**MII**	**MIII**	**Immobilization**
MS (g/L)	4.6	4.6	4.6	4.6	4.6	4.6	9.2
Sucrose (%)	2	2	2				4
Myo-inositol (%)			0.05				
2,4-D (mg/L)			1	0.5	0.25		
Carbenicilin (mg/L)				500	500	500	
Plant agar (%)	0.8		0.8	0.8	0.8	0.8	
pH	5.8	5.8	5.8	5.8	5.8	5.8	5.8

4.2.3. Somatic embryogenesis

Induction of carrot somatic embryogenesis was performed as previously described (Overvoorde and Grimes 1994), with some modifications. Two-cm hypocotyl explants, directly taken from *in vitro*-growing transgenic seedlings, were cultured in solid Embryogenesis Induction Medium (EIM; Table 2), for at least 40 days at 25 °C in darkness, until abundant calli were clearly developed from the explants. Then, 0.2 g of the developed calli were disaggregated in 100 mL flasks containing 50 mL of liquid EIM (excluding plant agar) and kept in a rotary shaker for 7 days at 140 rpm, 25 °C in darkness. Then, cell cultures were filtered through 41 µm nylon filters and the filters were transferred to sterile glass flasks. Retained cells were washed with 50 mL liquid MS2% medium (Table 1), transferred to a new flask and incubated for 7 days in agitation in a rotary shaker at 140 rpm, 25 °C in darkness. Aliquots of 1 mL of embryogenic cell cultures were transferred to 3-cm sterile culture dishes and kept at 25 °C in darkness and no agitation for 30 days. In immobilized carrot cultures, aliquots of 200 µL of immobilization medium (Table 1) were mixed with 200 µL of embryogenic cell cultures in 3 cm culture dishes. Then, 200 µL of autoclaved 1.5% liquid low melting point agarose (SeaPlaque, Duchefa), pre-warmed at 60 °C, were gently pipetted into the dishes. Open dishes were incubated on ice for 5 min until the culture medium gelified, covered with the lid, sealed and kept upside down (immobilized cells up) to avoid condensation on immobilized cells. Dishes were kept at 25 °C either in darkness or in a 16/8 h photoperiod. For all carrot cultures, the proportion of embryos was calculated 30 days after culture initiation by counting the number of embryos (considered as bipolar structures with a clear heart-shaped, torpedo or cotyledonary morphology) and dividing it by the total

number of structures (non-growing clumps, calli and embryos) counted. For both embryo and total counts, the field counting method was used (Camacho-Fernández et al. 2018). At least 200 structures per dish were counted.

Table 2. Composition of the plant *in vitro* culture media used for transformation protocol E and for induction of somatic embryogenesis. GB5: Gamborg B5 basal medium + vitamins (Gamborg et al. 1968). EIM: Embryogenesis Induction Medium. EISM: Embryogenesis Induction Selective Medium. BAP: 6-benzylaminopurine. NAA: naphthaleneacetic acid. Geneticin is a kanamycin derivative. All basal media and other medium components were purchased from Duchefa (Netherlands).

	Co-culture E	**Selection 1**	**Selection 2**	**EIM**	**EISM**
GB5 (g/L)	3.2	3.2	3.2	3.2	3.2
Sucrose (%)	3			3	
2,4-D (mg/L)				0.2	0.1
Carbenicilin (mg/L)		500	500		500
Geneticin (mg/L)			10		10
NAA (mg/L)	1	1	1		
BAP.(mg/L)	0.5	0.5	0.5		
Plant agar (%)	0.8	0.8	0.8	0.8	0.8
pH	5.8	5.8	5.8	5.8	5.8

4.2.4. Chemical treatments

For the chemical treatments, stocks of $CaCl_2$, ionophore A23187, ethylene glycol-bis(β-aminoethyl ether)-N,N,N′,N′-tetraacetic acid (EGTA) and N-(6-Aminohexyl)-5-chloro-1-naphthalenesulfonamide hydrochloride (W-7) were prepared following the guidelines provided by the manufacturer. Embryogenic cell cultures from liquid MS2% flasks, containing mostly proembryogenic masses and cell clumps, were inoculated into 3-cm culture dishes. To allow for comparisons among stages and concentrations for each chemical, equal aliquots (1 mL) of the same embryogenic cell culture were inoculated, so the initial amounts of proembryogenic masses/cell clumps were the same in all cases. Then the different chemicals, at different concentration (as described in Results), were applied during the first three days, during the first seven days, or continuously (for 30 days). Control plates were prepared with the proper concentrations of the solvent used to dilute the corresponding compound. At least three different repeats were performed for each chemical, concentration and exposure time applied. In all cases, plates were kept at 25 °C in darkness and no agitation. For the cultures with three and seven days of exposure, experimental plates with the chemical (and their corresponding control) were centrifuged (800 rpm, 4 min, 25 °C in a refrigerated Eppendorf Centrifuge 5804R with A-4-44 rotor) to wash the

compound. The proportion of embryos was calculated 30 days after culture initiation as described for somatic embryogenesis cultures.

4.2.5. 2-deoxy-D-glucose and callose staining

To inhibit callose deposition, we applied 2-deoxy-D-glucose to two different types of cultures, wild-type carrot calli disaggregated in liquid EIM, where predominantly cell clumps can be found, and one-week-old liquid EIM cultures filtered and resuspended in liquid MS2%, where proembryogenic masses can predominantly be found. One mL aliquots of each culture were poured in 3-cm sterile culture dishes and cultured for a week without (controls) and with 2-deoxy-D-glucose at 0.1, 1 and 5 mM. Incubations were performed in a rotary shaker at low speed and at room temperature. At least three different repeats were performed for each 2-deoxy-D-glucose concentration and exposure time applied. The proportion of embryos was calculated 30 days after culture initiation as described for somatic embryogenesis cultures. For visualization in the confocal microscope, control and 2-deoxy-D-glucose samples were collected in tubes, centrifuged (2 min, 8,000 rpm) and stained with 1% aniline blue for 10 min. Then, samples were washed three times with PBS 1x. Approximately 20 µL of sample were mounted in a glass slide, covered with a coverslip and observed in the confocal microscope.

4.2.6. Confocal microscopy

Carrot samples stained with aniline blue were observed in a Zeiss 780 Axio Observer confocal laser scanning microscope at an excitation wavelength of 405 nm. Emission was recorded at 450 nm. Cell cultures from PCR-positive carrot plants were imaged using a Zeiss LSM880 laser scanning confocal microscope. Samples were excited at 440 nm (for CFP excitation) and 514 nm (for YFP excitation) and emission was recorded between 400 and 600 nm.

For FRET imaging of embryogenic cultures from carrot transgenic lines, embryogenic structures were mounted in a petri dish using half-strength MS medium (pH 5.7) supplemented with 0.3% agarose. Mounted samples were covered with liquid half-strength MS medium (pH 5.7) and observed in a Leica SP8-FLIMan confocal laser scanning microscope using an immersion objective. CFP was excited at 448 nm and emission was recorded between 460 and 493 nm, YFP was excited at 514 nm and recorded between 525 and 560 nm. FRET imaging was performed exciting at 448 nm and recording the emission between 525 and 560 nm. For imaging, the FRET ratio was defined as the ratio between YFP and CFP emissions (480/535 nm). Image treatment and calculation of fluorescence emission ratios were performed as previously described (Rizza et al. 2019; Rowe et al. 2022). For all cases, Ca^{2+} levels were defined as very low, low, moderate, high or very high according to the colorimetric scale based on the FRET ratio images. Very low Ca^{2+} levels corresponded to dark blue colors, low levels to light blue, moderate to green-yellow, high to orange-red and very high levels to purple-white colors. Image analysis was performed using the FIJI software (Schindelin et al. 2012).

4.2.7. Statistical analysis

Data were analyzed using the ANOVA test. Groups of significance were established according to the least significant difference (LSD) test ($p \leq 0.05$). All the analyses were performed with the Statgraphics software.

4.3.Results

4.3.1. Development of *cameleon* carrot lines

To produce *cameleon* carrot lines, we first tested two carrot transformation protocols, namely D (Gonzalez-Calquin and Stange 2020) and E, which is a combination of previously reported transformation (Hardegger and Sturm 1998) and regeneration protocols (Overvoorde and Grimes 1994). For protocol D (Suppl. Fig. S1), we inoculated an average of 184±69 hypocotyl explants per assay transformed with the YC3.6-Bar construct, and 163.5±28 explants per assay transformed with the PM-YC3.6-LTI6b construct. YC3.6-Bar explants did not produce any embryo, and PM-YC3.6-LTI6b produced embryos that eventually died upon transference to media with kanamycin as selective agent. Kanamycin has been reported to inhibit cell growth and prevent embryo formation in some carrot cultivars (Hardegger and Sturm 1998). Since this seemed to be our case, we focused on protocol E for transformation of explants with the PM-YC3.6-LTI6b construct using geneticin, a kanamycin derivative, as selective agent. An average of 196.67±33.3 explants per assay were inoculated. After two weeks in Selection 1 medium, most of the explants developed greenish calli on their surface and/or at their ends (Fig. 1A). After one month in Selection 2 medium (Fig. 1B), clear differences were observed between calli resistant (green) and sensitive to the selective agents (whitish or brown). Green calli were transferred to EIM supplemented with selective agents and along four rounds of medium refreshment during two months, some turned brown and arrested growth while others kept green and growing (Fig. 1C). Green and growing, potentially transformed calli were cultured in liquid EIM and, upon transference to MS medium, they eventually produced fully developed embryos (Fig. 1D). Finally, eight full seedlings from four resistant embryo-producing calli were regenerated and all of them tested positive for the construct by PCR analysis (Fig. 1E). Cell cultures from one PCR-positive plant per line (four plants in total) were imaged at the confocal microscope to check for FRET performance (Suppl. Fig. S2), confirming the successful production of three different PM-YC3.6-LTI6b *cameleon* lines using protocol E. Two of them showed an equivalent and stronger signal for both CFP and YFP. We focused on the use of these two lines for all FRET experiments.

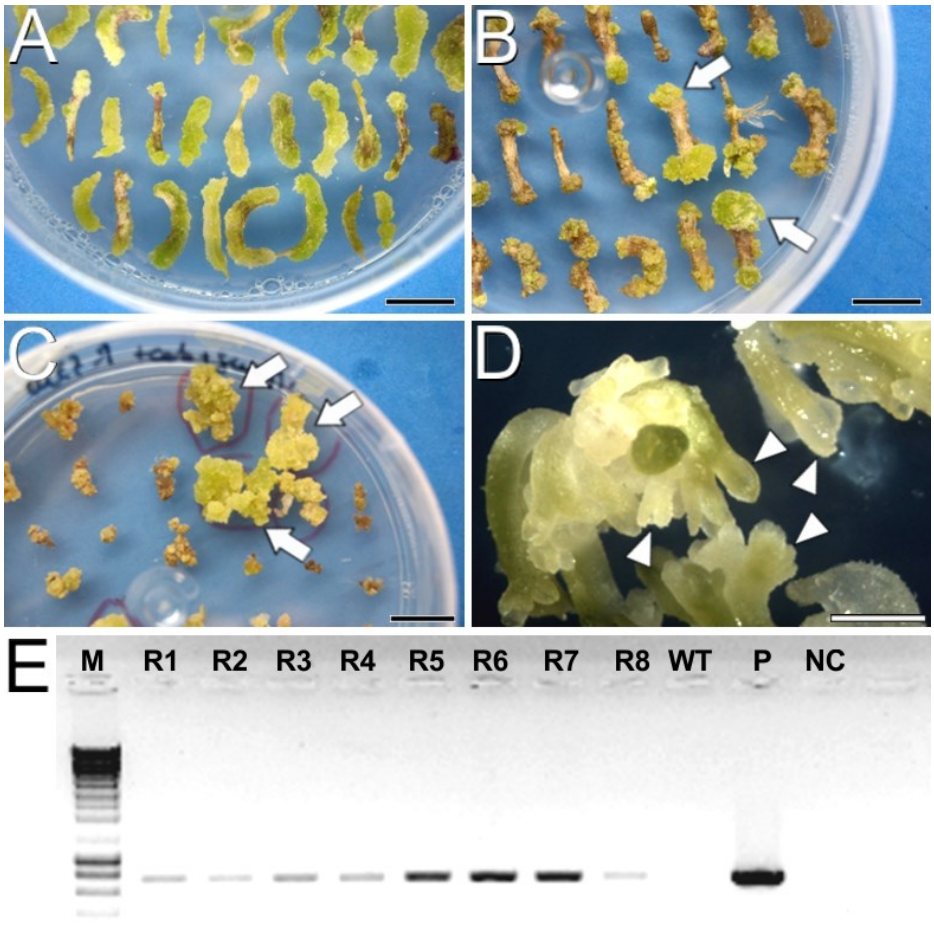

Fig. 1. **Carrot transformation and regeneration using protocol E.** A: Hypocotyl explants after 15 days in Selection 1 medium. B: Hypocotyl explants after one month in Selection 2 medium. Arrows point to green, growing calli resistant to the selective agents. C: Calli after one month in EIM with selective agents. D: Full embryos developed in solid MS2% medium. Arrowheads point to developing somatic embryos. E: Agarose electrophoresis gel showing PCR amplification of the transgene. From left to right, M: DNA molecular weight marker; R1-R8: Eight plantlets regenerated from the four resistant calli; WT: Wild type plant; P: PM-YC3.6-LTI6b plasmid; NC: PCR negative control. Bars: A-C: 1 cm; D: 1 mm.

4.3.2. Somatic embryogenesis

Once developed the *cameleon* carrot lines, we induced somatic embryogenesis using both liquid and immobilized cultures to track changes during the process. After 40 days of culture in solid EIM, carrot hypocotyls developed calli that were disaggregated in liquid EIM under agitation, producing isolated cell clumps, defined as irregularly shaped cell clusters with weak cell adhesion (Fig. 2A). Upon culture in liquid MS2% medium with agitation, some cell clumps proliferated as embryogenic masses, defined as compact cell aggregates with higher structural order, showing the first signs of differentiation into early (globular) embryo-like structures (Fig. 2B). In immobilized cultures, we tracked the progression from globular-like to torpedo embryos in one month (Figs. 2C-F). Time-lapse imaging also revealed the developmental asynchrony of the different structures, since from an initial population enriched in embryogenic masses (Fig. 2C), embryos at all possible developmental stages were observed after one month (Fig. 2F, arrowheads), together with irregularly shaped,

disorganized callus-like masses (Fig. 2F, arrow) coming from some of the initial masses.

In order to optimize the process, we evaluated the possibility of reducing the stage of culture with agitation from two to just one week and directly moving the cell clumps to liquid MS2% medium without agitation or to solid, immobilization medium. In all cases, the second week of agitation was found essential to increase and accelerate the production of embryogenic masses and to reduce the formation of disorganized callus masses (Suppl. Fig. S3). Embryo progression was higher and faster in liquid cultures, where mature, cotyledonary embryos ready to germinate (Fig. 2G) were produced in just three weeks of culture. Irrespective of the culture method used, embryos germinated when transferred to solid MS2% (Fig. 2H) and became entire, adult plants upon acclimatization and transference to soil (Fig. 2I). In conclusion, both liquid and immobilized cultures are useful to produce carrot somatic embryos. Immobilized cultures are convenient for experiments where embryos must develop in fixed positions, but liquid culture is faster and more efficient. In both cases, somatic embryos and callus masses are formed, and the second week in agitation is essential for a proper cell clump-to-embryo conversion.

4.3.3. Distribution of Ca^{2+} during carrot somatic embryogenesis

Next, we used our *cameleon* carrot lines to study, using FRET imaging, how Ca^{2+} distributes in the different structures formed during the process of somatic embryo induction and development (Fig. 3; Suppl. Fig. S4). During the first week of culture, just induced cell clumps (Fig. 3A) presented irregular morphologies, with loosely attached cells and in general low-moderate Ca^{2+} levels in the plasma membranes of all their cells. However, there were defined regions, generally at one end of the structure, that presented higher Ca^{2+} levels (Fig. 3A, arrowhead). These regions developed into compact, globular embryogenic cell masses that maintained high Ca^{2+} levels (Fig. 3B). After two weeks of culture, compact, globular embryos increased their size and their Ca^{2+} levels increased to high or very high. The distribution, however, was not uniform, concentrating towards one pole of the embryo (Fig. 3C). At this stage, non-embryogenic callus masses clearly differed from globular embryos in their Ca^{2+} levels, which were typically low-moderate for most of their cells, with few, exceptional cells with higher levels (Fig. 3D), in a pattern similar to that of cell clumps. In three-week-old cultures, differentiation of globular embryos into heart-shaped somatic embryos coincided with a non-uniform distribution of Ca^{2+}, which concentrated at the periphery of the embryo, coinciding with the protodermal layer, and especially in the apical regions (shoot apical meristem and cotyledons, Fig. 3E). In elongating torpedo embryos, Ca^{2+} clearly concentrated in the actively growing cotyledons and the shoot apical meristem, which presented high Ca^{2+} levels all along their inner regions (Fig. 3F). The root meristem region, however, presented low Ca^{2+} levels. In developed cotyledonary embryos, moderate-high Ca^{2+} levels principally concentrated in the inner mesophyll region of the cotyledons (Fig. 3G) and the root meristem (Fig. 3H), being low or very low in all other regions of the embryo. Together, these results show that Ca^{2+} levels are highly dynamic during the different stages of somatic embryogenesis, concentrating in the proliferating cells and embryogenic structures, and in the actively growing

regions of the developing somatic embryo. These results point to a role of Ca^{2+} in the induction of somatic embryogenesis and the development of somatic embryos.

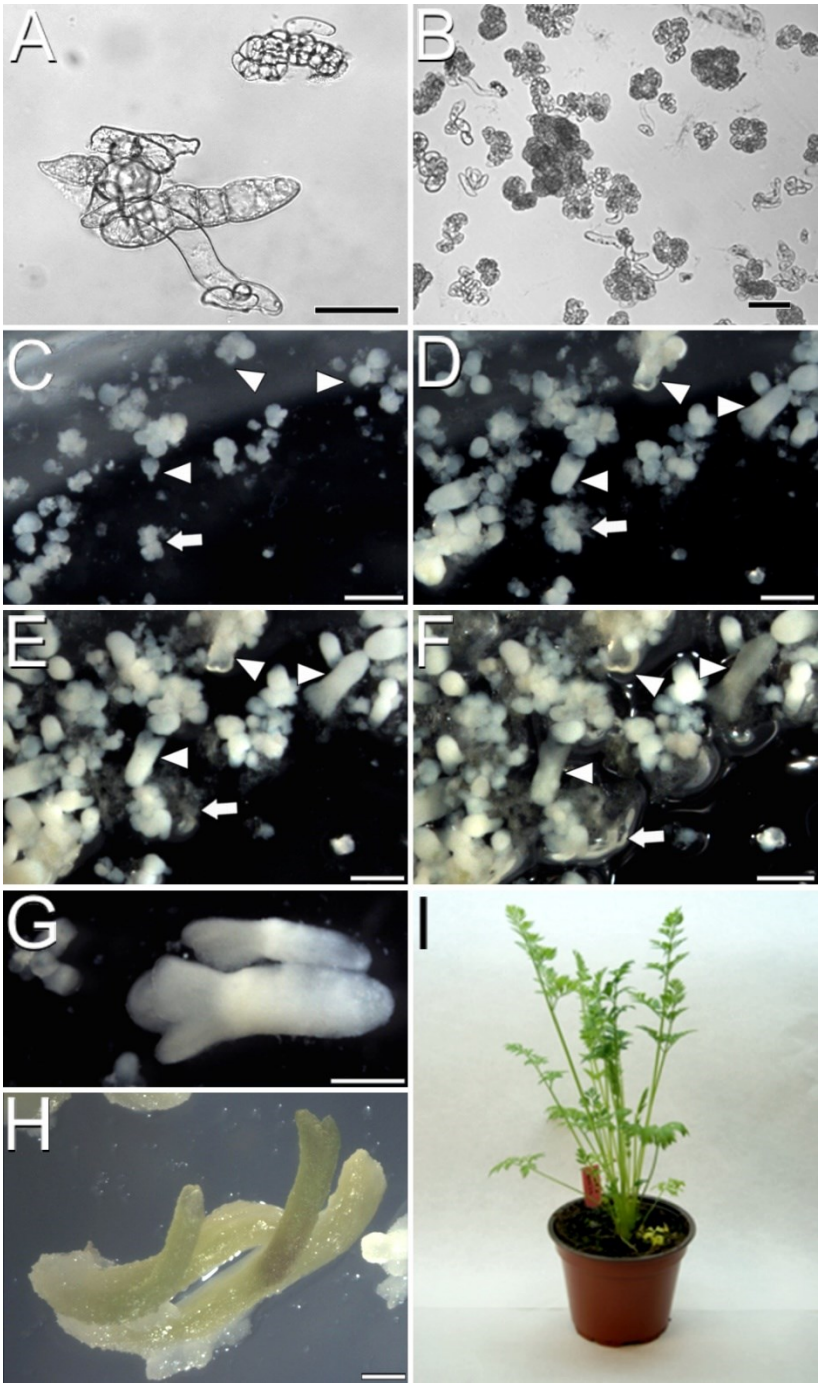

Fig. 2. Carrot somatic embryogenesis. A: Cell clumps after one week in liquid EIM. B: Compact embryogenic masses after one week in liquid MS2%. C-F: Time-lapse images of an immobilized culture one week (C), two weeks (D), three weeks (E) and one month after immobilization (F). Arrowheads point to individual developing embryos progressing through different developmental stages. Arrows point to an individual proliferating callus mass. G: Fully developed embryo after three weeks in liquid MS2%. H: Embryos germinated in solid MS2%. I: Acclimatized adult carrot plant regenerated from somatic embryos. Bars: A, B: 50 µm; C-H: 500 µm.

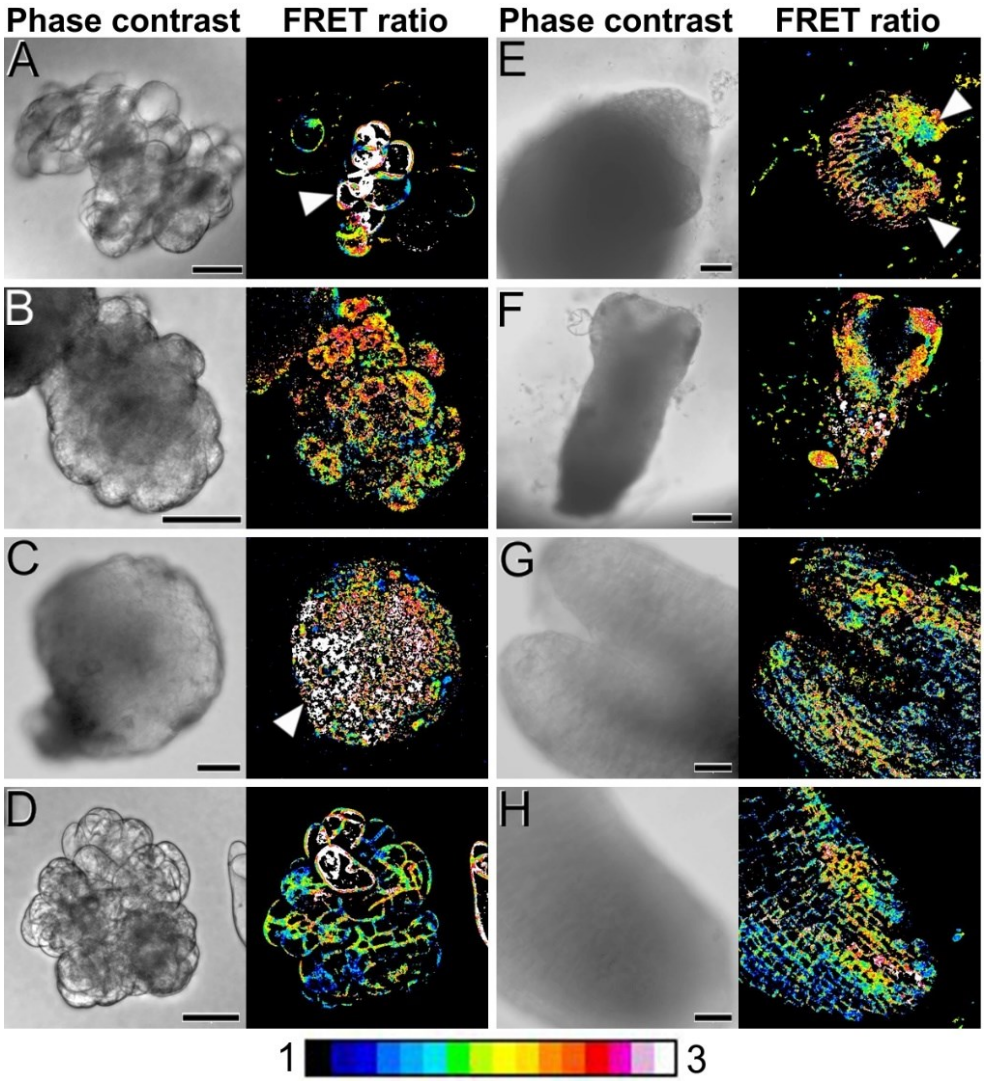

Fig. 3. FRET imaging of Ca^{2+} levels during carrot somatic embryogenesis in PM-YC3.6-LTI6b *cameleon* lines. Each pair of images shows the same field imaged by phase contrast (left) and FRET ratio (YFP/CFP emissions; right). The LUT bar displays the false coloration of FRET ratios. A: One-week-old cell clumps. Note the higher Ca^{2+} levels of the cells at the left side (arrowheads). B: Cell clump transforming into an embryogenic mass. Note the higher Ca^{2+} levels of the cell mass at the left side (arrowhead). C, D: Two-weeks-old compact, globular embryo (C) and callus mass (D). Arrowhead in C points to a pole with higher Ca^{2+} levels. E: Three-weeks-old heart-shaped embryo. Arrowheads point to the cotyledon primordia. F: Torpedo embryo. G, H: Shoot (G) and root (H) apical regions of a cotyledonary embryo. Bars: A-E, G, H: 40 µm; F: 100 µm.

4.3.4. Distribution of callose during carrot somatic embryogenesis

We stained embryogenic cultures with aniline blue to study the pattern of callose deposition. Abundant callose accumulation at the cell wall region was found surrounding particular cells in the form of a continuous layer, generally in cells at one end of small clumps of loosely connected cells (Fig. 4A). This pattern of permanent callose deposition in a layer surrounding the cell does not correspond with its conventional, transient role during plant cytokinesis (Thiele et al. 2009). Thus, callose deposition must be related to embryogenesis induction. The shape, position and size of the aniline blue-positive cells and the cells with high Ca^{2+} levels (Fig. 3A) was similar, indicating a relationship between increased Ca^{2+} levels and callose deposition. Similar callose-positive cells were

found at specific regions of small proembryogenic masses, before embryo differentiation (Fig. 4B). In callus-like masses, where Ca^{2+} levels were mostly low or moderate (Fig. 3D), the levels of callose staining were much lower, almost negligible (Fig. 4C). These results showed that during the very first stages of induction of somatic embryogenesis, cultured embryogenic carrot cells develop a callose layer around them, while non-embryogenic callus-like masses do not develop such layer.

In order to elucidate the role of callose in the initial stages of the process, we added 2-deoxy-D-glucose, an inhibitor of callose biosynthesis, at different concentrations in the culture medium during the first 3 and 7 days of culture, as well as during all the culture time. With 1 mM and principally with 5 mM 2-deoxy-D-glucose, we observed that cells of both cell clumps (Fig. 4D) and small proembryogenic masses (Fig. 4E) showed almost no aniline blue staining, indicating a lack of callose deposition in their cell walls. In order to study the relevance of the absence of callose in cell walls of these structures, we quantified the somatic embryogenesis response of explants treated with different concentrations and application times of 2-deoxy-D-glucose. The observed lack of callose correlated with the quantification of the embryos produced (Fig. 4F), which had a significant negative effect when applied at 5 mM during both the first 7 days and continuously, where embryo production was almost null. In conclusion, in addition to calcium, callose deposition in the cell walls during the stages of embryo induction and differentiation has a critical role in carrot somatic embryogenesis.

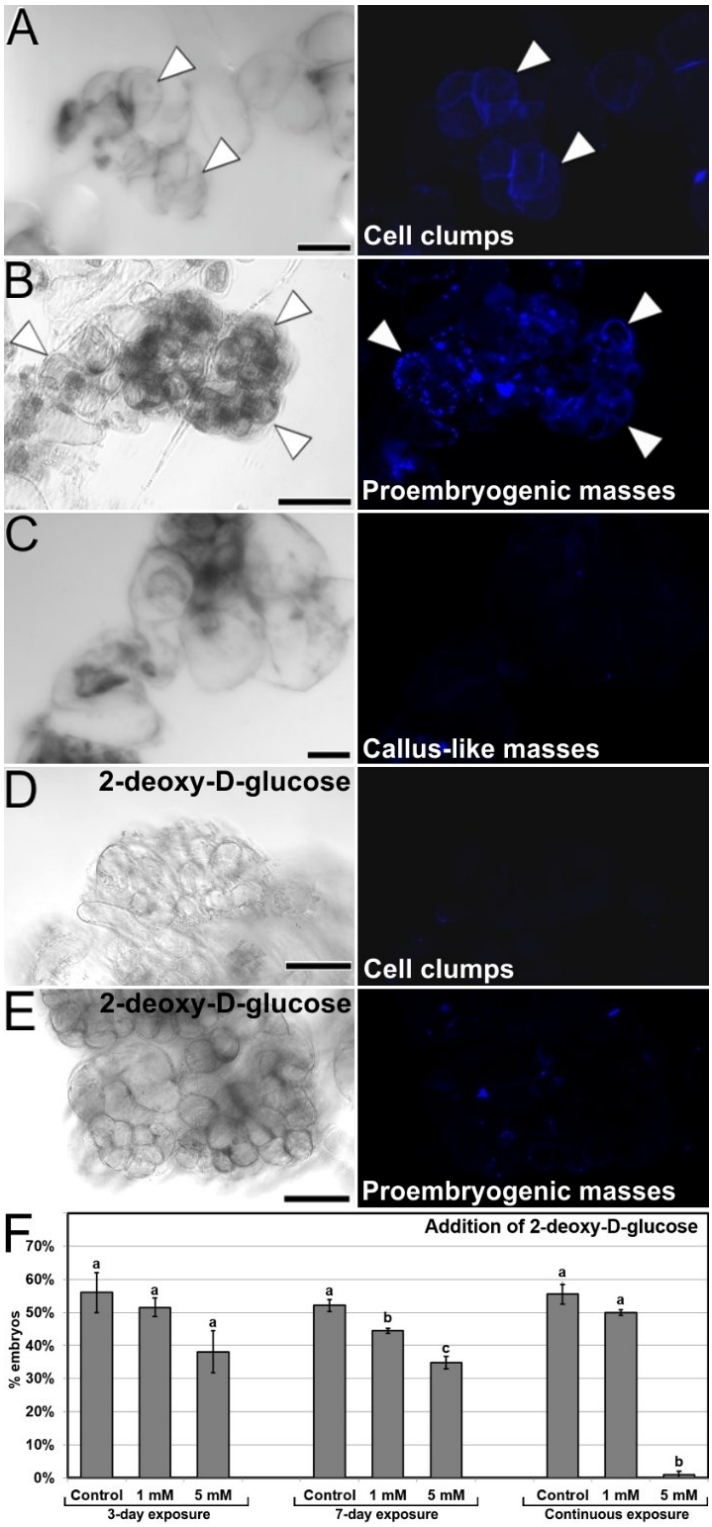

Fig. 4. **Callose deposition in cultured embryogenic structures.** Each pair of A-E images shows the same field of aniline blue-stained samples imaged by phase contrast (left) and fluorescence (right). **A, B:** Small clusters of callose-positive cells in cell clumps (A) and proembryogenic masses (B). Note the intense aniline blue staining in the cell wall region of specific cells (arrowheads). **C:** Irregular callus mass with loosely connected cells. **D, E:** Small cell clump (D) and proembryogenic mass (E) from cultures with 5 mM 2-deoxy-D-glucose. **F:** Modulation of callose deposition by the addition of 2-deoxy-D-glucose at different concentrations and 3-day, 7-day and continuous exposures. The effects of the treatments are expressed as percentages of embryos produced (% embryos). Letters represent significant differences with respect to their respective controls according to the LSD test. Bars: A, B, D, E: 40 µm; C: 80 µm.

4.3.5. Modulation of Ca^{2+} homeostasis

Once established the relationship between increased Ca^{2+} levels and induction of somatic embryogenesis, we performed a pharmacological study to modulate the intracellular Ca^{2+} levels. We treated embryogenic liquid carrot cultures with different chemicals known to interfere with intracellular Ca^{2+} levels and calculated the percentage of embryos produced by each treatment after 30 days of culture. First, we increased the levels of available Ca^{2+} by adding increased $CaCl_2$ concentrations (2, 3 and 4 mM) to the culture medium (Fig. 5A), and compared embryo production with that of control cultures. When applied during the first 3 days of culture, +4 mM $CaCl_2$ produced significantly more embryos (3-fold) than the control. In these conditions, addition of increased $CaCl_2$ levels also reduced the occurrence of disorganized calli and accelerated embryo growth, producing larger and elongated embryos (Figs. 6A-C). A 7-day and a continuous exposure during all culture stages to increased $CaCl_2$ levels did not produce any significant change in embryo production (Fig. 5A). Together, these observations indicate that Ca^{2+} modulation is effective to increase embryo induction and growth during the first stages of the process. Next, we applied ionophore A23187, a plasma membrane-intercalating channel that allows Ca^{2+} to freely cross it, increasing Ca^{2+} influx and thereby altering intracellular gradients (Ge et al. 2007). The application of 1 and 5 µM ionophore A23187 during the first three days of culture significantly increased the production of somatic embryos (Fig. 5B). As for the addition of $CaCl_2$, the conditions that produced more embryos also promoted an accelerated embryo growth, producing larger and more mature, sometimes germinating embryos (Figs. 6D-F). Applications during the first 7 days or continuously did not show significant differences with respect to controls without the chemical. Together, these results confirmed the role of Ca^{2+} during the first stages of somatic embryo induction and, most importantly, showed that an increase of Ca^{2+} levels can be beneficial for embryo induction and development.

Next, we studied the effect of reducing intracellular Ca^{2+} levels with EGTA, a highly specific Ca^{2+} chelator capable of freely diffusing through the plasma membrane. With the range of EGTA concentrations used (Fig. 5C), we observed a significant reduction of embryo production, which was completely inhibited at the highest concentration (10 mM). These effects were similar for the 3-day, 7-day and continuous EGTA application. The reduction was accompanied by a dose-dependent delay in embryo growth and the increased occurrence of disorganized callus masses, which were the only morphogenic structures observed at the highest EGTA concentration (Figs. 6G-I). Thus, Ca^{2+} chelation dramatically affects somatic embryogenesis, reducing the proportion of somatic embryos induced and their further development. Finally, we applied W-7, a CaM antagonist (Fig. 5D). For all the concentrations tested, inhibition of CaM by W-7 significantly reduced the production of somatic embryos. The extent of the reduction was dependent on the dose used and the duration of the treatment. In addition, embryos exposed to W-7 were less developed than control embryos of the same age, suggesting that W-7 delays embryo development (Figs. 6J-L). W-7 also promoted the conversion of embryos into large, disorganized calli. Thus, interference of Ca^{2+}-CaM binding by W-7 negatively affects embryo production and development, producing an effect very similar to that observed with the Ca^{2+}

chelator. In summary, altering Ca^{2+} signaling by reducing their levels or by interfering with CaM has a significantly negative impact on embryogenesis induction.

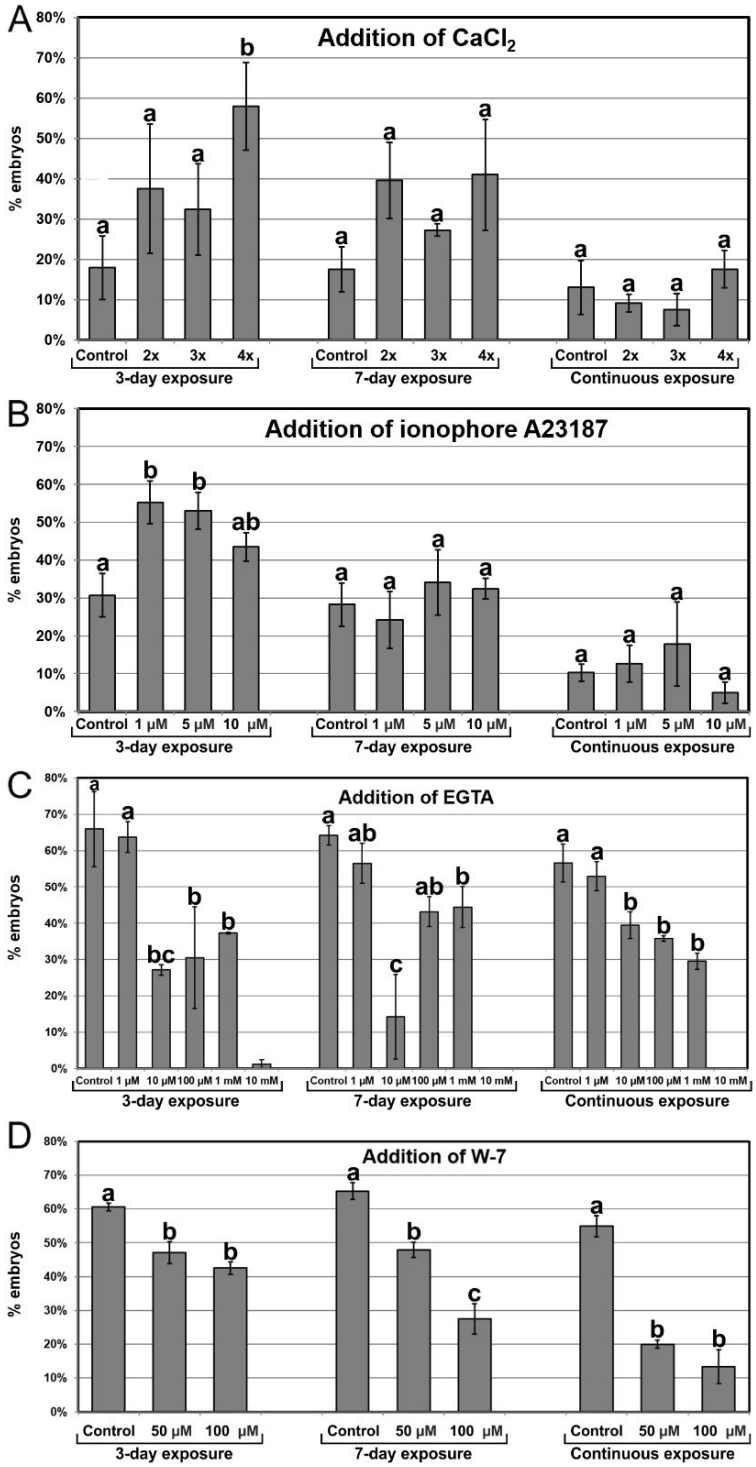

Fig. 5. Modulation of intracellular Ca^{2+} homeostasis by the addition of $CaCl_2$ (**A**), the Ca^{2+} channel ionophore A23187 (**B**), EGTA, a Ca^{2+} chelator (**C**), and W-7, a CaM antagonist (**D**) at different concentrations and 3-day, 7-day and continuous exposures. The effects of the treatments are expressed as percentages of embryos produced (% embryos) ± standard error. At least three different repeats were performed for each chemical, concentration and exposure time applied. Data were analyzed using the ANOVA test and groups of significance were established according to the least significant difference (LSD) test ($p \leq 0.05$). Different letters represent significant differences with respect to their respective controls according to the LSD test.

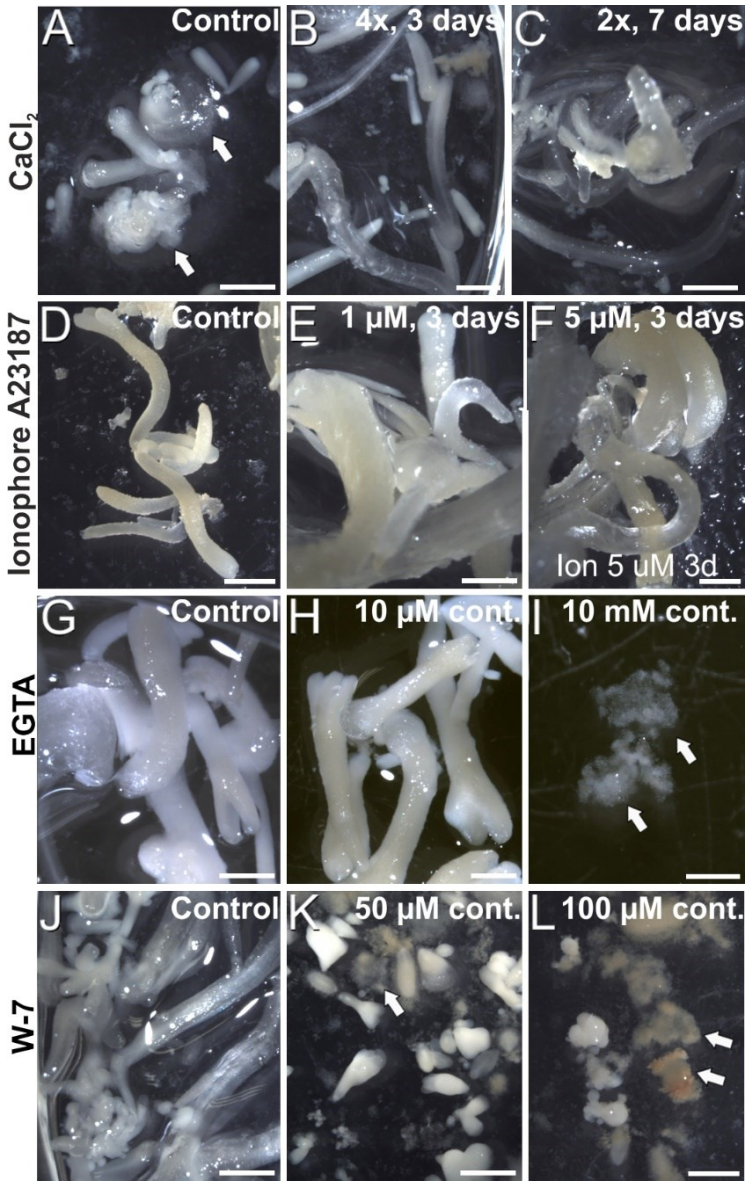

Fig. 6. Carrot somatic embryos produced in cultures with added $CaCl_2$ (**A-C**), ionophore A23187 (**D-F**), EGTA (**G-I**) and (**J-L**) at different concentrations and durations, as described in the images. Arrows point to disorganized callus masses. Bars: 1 mm.

4.4.Discussion

Artificial, *in vitro* embryogenesis systems and, in particular, somatic embryogenesis systems such as the one we present here are very useful tools first in plant biotechnology, and second in basic plant biology to study different aspects of embryo development. The *in vitro* development of "naked" embryos facilitates their visualization and study, which is very difficult during zygotic embryogenesis due to the different tissue layers that surround the minute embryo during the first stages of its development and preclude its correct visualization and/or isolation. We report on the generation of three functional *cameleon* carrot lines. This is, to the best of our knowledge, the first work to develop *cameleon*-expressing carrot lines. These lines open the way to study the role of Ca^{2+} in living carrot cells in many different *in vivo* and *in vitro* processes. We used them here to study the role of Ca^{2+} during this process, as described next.

4.4.1. Mechanical stress is beneficial for carrot somatic embryogenesis

Different protocols for carrot somatic embryogenesis implement a step of culture in liquid medium under an agitation regime (Timmers et al. 1989; Overvoorde and Grimes 1994). In an attempt to optimize the process, we reduced such step to one week. As a result, the occurrence of embryos was significantly reduced and callus formation was increased. We hypothesize that, in addition to a better access to medium components, culture agitation provides cells with a mild and prolonged mechanical stress that would be beneficial for induction of *in vitro* embryogenesis. In another morphogenic process of *in vitro*-induced embryogenesis such as microspore embryogenesis, high-speed centrifugation for 30 min was able to induce tobacco microspores towards embryogenesis (Tanaka 1973). Even shorter and milder centrifugations were effective for chickpea microspores to increase embryo yield and reduce callus occurrence (Grewal et al. 2009). We observed a similar effect in carrot somatic cell cultures with agitation, which can be considered a milder and prolonged form of centrifugal stress. Additional evidence for this comes from the fact that, for all the chemicals used to modulate Ca^{2+} levels (Fig. 5), the controls of the three and seven-day exposure to the chemical, which include a centrifugation step to wash the medium, always showed higher percentages of embryo production than the control of continuous exposure to the compound, without centrifugation. It was postulated that centrifugation would alter the auxin-to-cytokinin ratio, thereby facilitating embryo induction (Tanaka 1973). Instead, we believe that, for both microspore and somatic embryogenesis, mechanical stress (centrifugal in this case) would be a source of abiotic stress that, alone or combined with others, may trigger the induction of *in vitro* embryogenesis. This is a well known effect in microspore embryogenesis systems (Seguí-Simarro et al. 2021), where the combination of different stresses has increased beneficial effects in embryo production and callus avoidance (Grewal et al. 2009).

4.4.2. High Ca^{2+} levels are markers of embryogenic induction and embryo patterning

Carrot embryogenic cultures typically include cell clumps that become either disorganized callus masses or embryo-producing, proembryogenic masses. FRET imaging in living cultures revealed that cell clumps show in general low or moderate Ca^{2+} levels, except for some discrete cells where Ca^{2+} levels are higher. Similar results were previously observed using fluorescent probes (Timmers et al. 1989). These regions are then transformed into proembryogenic masses that seem not to be just disorganized structures but organized embryo precursors, since high Ca^{2+} levels are typically found in cells of discrete regions at fixed positions. This is also supported by the polarized localization of CaM in particular regions of these masses (Timmers et al. 1989) and by the similarities between the protein patterns and gene expression programs of carrot somatic embryos and their precursors, the proembryogenic masses (Wilde et al. 1988; Sung and Okimoto 1981). In turn, cells of undifferentiated callus masses keep in general low or moderate Ca^{2+} levels and never produce embryos. Thus, each structure has different Ca^{2+} patterns that seem associated to their embryogenic competence from their very beginning, with high levels in the cells of

embryogenic nodes that will become embryos. This is in agreement with Ca^{2+} dynamics in other *in vitro* embryogenesis systems. In *Brassica napus,* microspores ready for embryogenesis induction and immediately after induction show high levels of intracellular Ca^{2+} (Rivas-Sendra et al. 2019; Rivas-Sendra et al. 2017). Indeed, Ca^{2+} levels were related to the embryogenic competence of microspores of different species (Rivas-Sendra et al. 2019; Rivas-Sendra et al. 2017). Therefore, Ca^{2+} would be an early marker of embryogenic fate not only for carrot somatic embryogenesis, but in general for *in vitro* embryogenesis processes.

In our living carrot cultures, Ca^{2+} gradients were observed during the development of carrot somatic embryos from the globular stage (Fig. 3C). Upon transitioning from radial to bilateral symmetry in heart-shaped and torpedo embryos, high Ca^{2+} levels delineated the differentiating protoderm first (Fig. 3E) and then the shoot apical meristem and cotyledons (Fig. 3F). In mature, cotyledonary embryos, high Ca^{2+} levels marked the differentiating root meristem and the inner, mesophyll region of the cotyledons of newly formed somatic embryos (Figs. 3G-H). An RNA-seq comparative study between the transcriptomes of somatic embryo and callus cells in Arabidopsis revealed that embryogenic cells are transcriptionally rather than metabolically active (Magnani et al. 2017). These changes involved rearrangements at the subcellular level and chromatin remodeling, repression of root meristem genes, and activation of pathways involved in shoot patterning and polarized cell growth (Magnani et al. 2017). It is interesting to note that the spatial pattern of gene expression depicted by this transcriptomic study matches with the spatial distribution of Ca^{2+} we observed during the development of carrot somatic embryos. This pattern is also similar to the reported distribution of CaM, polarized in the early somatic embryo and highly increased at the cotyledons of maturing embryos (Timmers et al. 1989). We also showed the direct relationship between somatic embryogenesis and CaM with the use of W-7, a CaM antagonist that consistently produced a dose and time-dependent decrease of embryo percentages (Fig. 5D), and a delay and disorganization of embryo development, which in some cases reverted to calli (Figs. 6J-L). Together, these results make reasonable to propose a direct relationship between Ca^{2+}-CaM signaling and embryogenesis induction and activation of the large transcriptional remodeling undergone by somatic cells to become embryos.

4.4.3. Embryogenic cells are defined by the development of a callose layer that is essential for embryo induction

We showed that a callose layer is created around specific cells of cell clumps and small proembryogenic masses which share a number of features with the embryo-precursor cells that present high Ca^{2+} levels. Although we were not able to co-localize callose staining and *cameleon* signal in our samples due to technical difficulties (overlapping of the aniline blue and CFP emission wavelengths), the shapes, sizes and positions of callose-positive (Figs. 4A, B) and Ca^{2+}-positive cells (Fig. 3A) are the same, which makes us deduce a clear relationship between these two features. In carrot somatic embryogenesis it was already postulated that high Ca^{2+} levels could stimulate callose deposition to isolate embryogenic cells (Timmers et al. 1996). In line with this, we showed that

callose must be deposited in the cell wall at these stages for a successful induction of embryogenesis in these cells, since callose inhibition with 2-deoxy-D-glucose inhibits the deposition of callose and reduces the percentage of embryo production. In Arabidopsis somatic embryogenesis from cotyledon nodes, it was demonstrated that callose symplasmically isolate cells of the proembryogenic domain from the surrounding tissue, in order to create a different chemical environment to establish cell totipotency and develop as somatic embryos (Godel-Jedrychowska et al. 2020). In *Brassica napus* microspore embryogenesis, the embryogenic competence of microspores was shown associated to their high Ca^{2+} levels and their parallel ability to form an osmoprotective, isolating callose layer through the activation of Ca^{2+}-dependent callose synthases (Rivas-Sendra et al. 2019). Together, these findings clearly establish a link between Ca^{2+} levels and callose deposition, needed to isolate different cell types in different species as a previous requisite to reprogram them towards *in vitro* embryogenesis.

4.4.4. Ca^{2+} homeostasis during the induction of somatic embryogenesis from carrot cells is plastic

The role of Ca^{2+} in both zygotic and somatic embryogenesis is widely acknowledged (Calabuig-Serna et al. 2023; Ge et al. 2007; Antoine et al. 2000), but in the case of carrot somatic embryogenesis, there have been a number of controversial reports regarding the importance of keeping Ca^{2+} homeostasis during the process. While some reports proposed that Ca^{2+} levels can be altered to increase the embryo induction rate (Takeda et al. 2003; Jansen et al. 1990), other studies suggested that such alterations would not be beneficial for embryo induction (Overvoorde and Grimes 1994). To gain further insight into the role of Ca^{2+} in this process, we used different approaches to modulate intracellular Ca^{2+} levels. Increasing cytoplasmic Ca^{2+} availability during the first days of culture by adding extra $CaCl_2$ to the culture medium or by using ionophore A23187 to open plasma membrane channels where through extracellular Ca^{2+} can enter the cytoplasm, led to higher percentages of embryo induction, accelerated embryo growth and lower callus occurrence. However, there seemed to be a limit for the direct relationship between Ca^{2+} and induction of embryogenesis, since a continuous increase of Ca^{2+} levels did not make any significant difference. This is in line with previous reports suggesting that excessive Ca^{2+} influx may have detrimental consequences on somatic embryogenesis (Takeda et al. 2003). Conversely, when the intracellular Ca^{2+} levels were reduced by chelating Ca^{2+} with EGTA, the percentage of embryos decreased in a dose-dependent manner. Thus, there is a range of Ca^{2+} concentrations where somatic embryogenesis can be modulated by altering Ca^{2+} homeostasis. A possible explanation for this could be that increased extracellular Ca^{2+} levels would create an even higher Ca^{2+} gradient (the cytoplasmic resting Ca^{2+} concentration revolves around 100 nM; (Hepler 2005; Pirayesh et al. 2021) that would boost Ca^{2+} influx in more cells, thereby triggering the *embryogenic Ca^{2+} signature* in more cells. An alternative explanation would be that higher extracellular Ca^{2+} levels would make the plasma membrane less permeable. Although counterintuitive in principle, this effect has been documented for some cell types (Hepler 2005). A calcium-induced impermeabilization of the plasma membrane would add to the cell isolation imparted by the callose layer, thereby increasing the probabilities for isolated carrot cells to become embryos. However, the positive effect observed with the

addition of $CaCl_2$ was similar to that of ionophore A23187, a Ca^{2+} channel that increases Ca^{2+} influx (Ge et al. 2007). Thus, it seems that, at least in carrot, adding increased Ca^{2+} concentrations to the culture medium increases Ca^{2+} influx in more cells, which in turn increases somatic embryogenesis.

It is interesting to note that increasing Ca^{2+} levels by adding both $CaCl_2$ and ionophore A23187 had positive effects only when applied during the first days of culture, when cell clumps are converting into proembryogenic masses and early embryos. The application of increased Ca^{2+} levels for longer times or continuously did not have any significant effect in embryo yield, which implies that the observed positive effect of increased Ca^{2+} levels during the first stages is compensated by a detrimental effect during later stages of embryo development in order to produce no significant final changes. In turn, a reduction of intracellular Ca^{2+} by chelation with EGTA produced similarly detrimental effects when applied during 3 days, 7 days or continuously, which indicates that the detrimental effect seems to be exerted principally during the first stage of embryo induction. Thus, increasing the intracellular Ca^{2+} levels during the inductive stage, when the first embryogenic cells differentiate from cell clumps/proembryogenic masses, increases the percentage of cells effectively induced to embryogenesis, and decreasing the levels has the opposite effect. However, once embryos are induced, during the embryo development stages, any alteration of Ca^{2+} homeostasis would have detrimental effects on embryo production. This is indicating that Ca^{2+} has a key role during the induction of somatic embryogenesis from carrot cells, and that Ca^{2+} homeostasis at this stage is plastic and can be altered to modulate the induction rate, but only during this stage. Once embryos are induced, Ca^{2+} homeostasis must be strictly maintained in order to allow for an efficient embryo maturation, since fully functional, differentiated embryos are able to autonomously regulate their Ca^{2+} levels in their different organs and any external interference may be detrimental.

Acknowledgements

We thank Marisol Gascón (IBMCP-CSIC Microscopy Service) for her excellent technical help. Thanks are also due to Prof. Jörg Kudla from the University of Münster, Germany, for providing the *cameleon* plasmids used un this study, to Dr. Jongho Sun, Prof. Giles Oldroyd, and the rest of members of the Oldroyd laboratory at the Crop Science Centre of the University of Cambridge, UK, for kindly hosting and helping ACS during his stay, and to Dr. Annalisa Rizza and Dr. Colleen Drapek from the Sainsbury Laboratory Cambridge University (SLCU) for their technical advice and support.

References

Anil VS, Rao KS (2000) Calcium-mediated signaling during sandalwood somatic embryogenesis. Role for exogenous calcium as second messenger. Plant Physiol 123 (4):1301-1312

Antoine AF, Faure J-E, Cordeiro S, Dumas C, Rougier M, Feijó JA (2000) A calcium influx is triggered and propagates in the zygote as a wavefront during *in vitro* fertilization of flowering plants. Proceedings of the National Academy of Sciences 97 (19):10643-10648. doi:10.1073/pnas.180243697

Calabuig-Serna A, Mir R, Seguí-Simarro JM (2023) Calcium Dynamics, *WUSCHEL* Expression and Callose Deposition during Somatic Embryogenesis in *Arabidopsis thaliana* Immature Zygotic Embryos. Plants 12 (5):1021

Camacho-Fernández C, Hervás D, Rivas-Sendra A, Marín MP, Seguí-Simarro JM (2018) Comparison of six different methods to calculate cell densities. Plant Methods 14 (1):30. doi:10.1186/s13007-018-0297-4

de Vries SC, Booij H, Meyerink P, Huisman G, Wilde HD, Thomas TL, Van Kammen A (1988) Acquisition of embryogenic potential in carrot cell-suspension cultures. Planta 176 (2):196-204

Demidchik V, Shabala S, Isayenkov S, Cuin TA, Pottosin I (2018) Calcium transport across plant membranes: mechanisms and functions. New Phytol 220 (1):49-69

Denninger P, Bleckmann A, Lausser A, Vogler F, Ott T, Ehrhardt DW, Frommer WB, Sprunck S, Dresselhaus T, Grossmann G (2014) Male-female communication triggers calcium signatures during fertilization in *Arabidopsis*. Nature Communications 5:4645. doi:10.1038/ncomms5645

Etienne H, Lartaud M, Carron MP, Michaux-Ferriere N (1997) Use of calcium to optimize long-term proliferation of friable embryogenic calluses and plant regeneration in *Hevea brasiliensis* (Mull Arg). J Exp Bot 48 (306):129-137. doi:10.1093/jxb/48.1.129

Gamborg OL, Miller RA, Ojima K (1968) Nutrient requirements of suspension cultures of soybean root cells. Exp Cell Res 50 (1):151-158. doi:http://dx.doi.org/10.1016/0014-4827(68)90403-5

Ge LL, Tian HQ, Russell SD (2007) Calcium function and distribution during fertilization in angiosperms. Am J Bot 94 (6):1046-1060. doi:10.3732/ajb.94.6.1046

Godel-Jedrychowska K, Kulinska-Lukaszek K, Horstman A, Soriano M, Li M, Malota K, Boutilier K, Kurczynska EU (2020) Symplasmic isolation marks cell fate changes during somatic embryogenesis. J Exp Bot 71 (9):2612-2628. doi:10.1093/jxb/eraa041

Gonzalez-Calquin C, Stange C (2020) *Agrobacterium tumefacien*s-mediated stable transformation of *Daucus carota*. In: Rodríguez-Concepción M, Welsch R (eds) Plant and Food Carotenoids: Methods and Protocols. Methods in Molecular Biology, vol 2083. Springer Science+Business Media, New York, USA, pp 313-320. doi:10.1007/978-1-4939-9952-1_24

Grewal RK, Lulsdorf M, Croser J, Ochatt S, Vandenberg A, Warkentin TD (2009) Doubled-haploid production in chickpea (*Cicer arietinum* L.): role of stress treatments. Plant Cell Rep 28 (8):1289-1299. doi:10.1007/s00299-009-0731-1

Halperin W (1964) Morphogenetic studies with partially synchronized cultures of carrot embryos. Science 146 (3642):408-410

Hardegger M, Sturm A (1998) Transformation and regeneration of carrot (*Daucus carota* L.). Mol Breed 4 (2):119-127

Hepler PK (2005) Calcium: a central regulator of plant growth and development. Plant Cell 17 (8):2142-2155. doi:10.1105/tpc.105.032508

Jansen MA, Booij H, Schel JH, de Vries SC (1990) Calcium increases the yield of somatic embryos in carrot embryogenic suspension cultures. Plant Cell Rep 9 (4):221-223

Krebs M, Held K, Binder A, Hashimoto K, Den Herder G, Parniske M, Kudla J, Schumacher K (2012) FRET-based genetically encoded sensors allow high-resolution live cell imaging of Ca^{2+} dynamics. Plant J 69 (1):181-192. doi:10.1111/j.1365-313X.2011.04780.x

Magnani E, Jimenez-Gomez JM, Soubigou-Taconnat L, Lepiniec L, Fiume E (2017) Profiling the onset of somatic embryogenesis in *Arabidopsis*. BMC Genomics 18 (1):998. doi:10.1186/s12864-017-4391-1

Mahalakshmi A, Singla B, Khurana JP, Khurana P (2007) Role of calcium–calmodulin in auxin-induced somatic embryogenesis in leaf base cultures of wheat (*Triticum aestivum* var. HD 2329). Plant Cell Tissue Organ Cult 88 (2):167-174

Malabadi RB, van Staden J (2006) Cold-enhanced somatic embryogenesis in *Pinus patula* is mediated by calcium. South African Journal of Botany 72 (4):613-618. doi:10.1016/j.sajb.2006.04.001

Miyawaki A, Llopis J, Heim R, McCaffery JM, Adams JA, Ikura M, Tsien RY (1997) Fluorescent indicators for Ca^{2+} based on green fluorescent proteins and calmodulin. Nature 388 (6645):882-887

Mizukami M, Takeda T, Satonaka H, Matsuoka H (2008) Improvement of propagation frequency with two-step direct somatic embryogenesis from carrot hypocotyls. Biochem Eng J 38 (1):55-60. doi:10.1016/j.bej.2007.06.004

Murashige T, Skoog F (1962) A revised medium for rapid growth and bioassays with tobacco tissue cultures. Physiol Plant 15:473-479

Overvoorde PJ, Grimes HD (1994) The role of calcium and calmodulin in carrot somatic embryogenesis. Plant Cell Physiol 35 (2):135-144

Permyakov EA, Kretsinger RH (2009) Cell signaling, beyond cytosolic calcium in eukaryotes. Journal of Inorganic Biochemistry 103 (1):77-86

Pirayesh N, Giridhar M, Ben Khedher A, Vothknecht UC, Chigri F (2021) Organellar calcium signaling in plants: An update. Biochimica et Biophysica Acta (BBA) - Molecular Cell Research 1868 (4):118948. doi:https://doi.org/10.1016/j.bbamcr.2021.118948

Ramakrishna A, Giridhar P, Ravishankar GA (2011) Calcium and calcium ionophore A23187 induce high-frequency somatic embryogenesis in cultured tissues of *Coffea canephora* P ex Fr. In Vitro Cell Dev Biol -Pl 47 (6):667-673. doi:10.1007/s11627-011-9372-5

Reinert J (1958) Morphogenese und ihre Kontrolle an Gewebekulturen aus Carotten. Naturwissenschaften 45:344-345

Rivas-Sendra A, Calabuig-Serna A, Seguí-Simarro JM (2017) Dynamics of calcium during *in vitro* microspore embryogenesis and *in vivo* microspore development in *Brassica napus* and *Solanum melongena*. Front Plant Sci 8:1177. doi:10.3389/fpls.2017.01177

Rivas-Sendra A, Corral-Martínez P, Porcel R, Camacho-Fernández C, Calabuig-Serna A, Seguí-Simarro JM (2019) Embryogenic competence of microspores is associated with their ability to form a callosic, osmoprotective subintinal layer. J Exp Bot 70 (4):1267–1281. doi:10.1093/jxb/ery458

Rivera-Solís G, Sáenz-Carbonell L, Narváez M, Rodríguez G, Oropeza C (2018) Addition of ionophore A23187 increases the efficiency of *Cocos nucifera* somatic embryogenesis. 3 Biotech 8 (8):366. doi:10.1007/s13205-018-1392-y

Rizza A, Walia A, Tang B, Jones AM (2019) Visualizing cellular gibberellin levels using the nlsGPS1 Förster resonance energy transfer (FRET) biosensor. JoVE (Journal of Visualized Experiments) 143:e58739. doi:10.3791/58739

Rowe JH, Rizza A, Jones AM (2022) Quantifying phytohormones i*n vivo* with FRET biosensors and the FRETENATOR analysis toolset. In: Duque P, Szakonyi D (eds) Environmental Responses in Plants: Methods and Protocols, vol 2494. Methods in Molecular Biology. Springer Science+Business Media, LLC, New York, pp 239-253. doi:10.1007/978-1-0716-2297-1_17

Schindelin J, Arganda-Carreras I, Frise E, Kaynig V, Longair M, Pietzsch T, Preibisch S, Rueden C, Saalfeld S, Schmid B, Tinevez JY, White DJ, Hartenstein V, Eliceiri K, Tomancak P, Cardona A (2012) Fiji: an open-source platform for biological-image analysis. Nature methods 9 (7):676-682. doi:10.1038/nmeth.2019

Seguí-Simarro JM, Jacquier NMA, Widiez T (2021) Overview of i*n vitro* and *in vivo* doubled haploid technologies. In: Seguí-Simarro JM (ed) Doubled Haploid Technology, vol 1: General Topics, Alliaceae, Cereals. Methods in Molecular Biology, vol 2287, 1st edn. Springer Science+Business Media, LLC, New York, USA, pp 3-22. doi:10.1007/978-1-0716-1315-3_1

Steward FC, Mapes MO, Mears K (1958) Growth and organized development of cultured cells. II. Organization in cultures grown from freely suspended cells. Am J Bot 45 (10):705-708

Sung ZR, Okimoto R (1981) Embryonic proteins in somatic embryos of carrot. Proc Natl Acad Sci USA 78 (6):3683-3687. doi:doi:10.1073/pnas.78.6.3683

Takeda T, Inose H, Matsuoka H (2003) Stimulation of somatic embryogenesis in carrot cells by the addition of calcium. Biochem Eng J 14 (2):143-148. doi:http://dx.doi.org/10.1016/S1369-703X(02)00186-9

Tanaka M (1973) The effect of centrifugal treatment on the emergence of plantlet from cultured anther of tobacco. Japan J Breed 23 (4):171-174. doi:10.1270/jsbbs1951.23.171

Tang R-J, Luan S (2017) Regulation of calcium and magnesium homeostasis in plants: from transporters to signaling network. Curr Opin Plant Biol 39:97-105. doi:https://doi.org/10.1016/j.pbi.2017.06.009

Thiele K, Wanner G, Kindzierski V, Jürgens G, Mayer U, Pachl F, Assaad FF (2009) The timely deposition of callose is essential for cytokinesis in Arabidopsis. Plant J 58 (1):13-26. doi:10.1111/j.1365-313X.2008.03760.x

Tian W, Wang C, Gao Q, Li L, Luan S (2020) Calcium spikes, waves and oscillations in plant development and biotic interactions. Nature Plants 6 (7):750-759. doi:10.1038/s41477-020-0667-6

Timmers A, De Vries S, Schel J (1989) Distribution of membrane-bound calcium and activated calmodulin during somatic embryogenesis of carrot (*Daucus carota* L.). Protoplasma 153 (1):24-29

Timmers ACJ, Reiss H-D, Bohsung J, Traxel K, Schel JHN (1996) Localization of calcium during somatic embryogenesis of carrot (*Daucus carota* L.). Protoplasma 190 (1):107-118. doi:10.1007/bf01281199

White PJ, Broadley MR (2003) Calcium in plants. Ann Bot 92 (4):487-511

Wilde HD, Nelson WS, Booij H, de Vries SC, Thomas TL (1988) Gene-expression programs in embryogenic and non-embryogenic carrot cultures. Planta 176 (2):205-211. doi:10.1007/BF00392446

Yang X, Zhang X (2010) Regulation of somatic embryogenesis in higher plants. Critical Reviews in Plant Science 29 (1):36-57

Supplementary materials

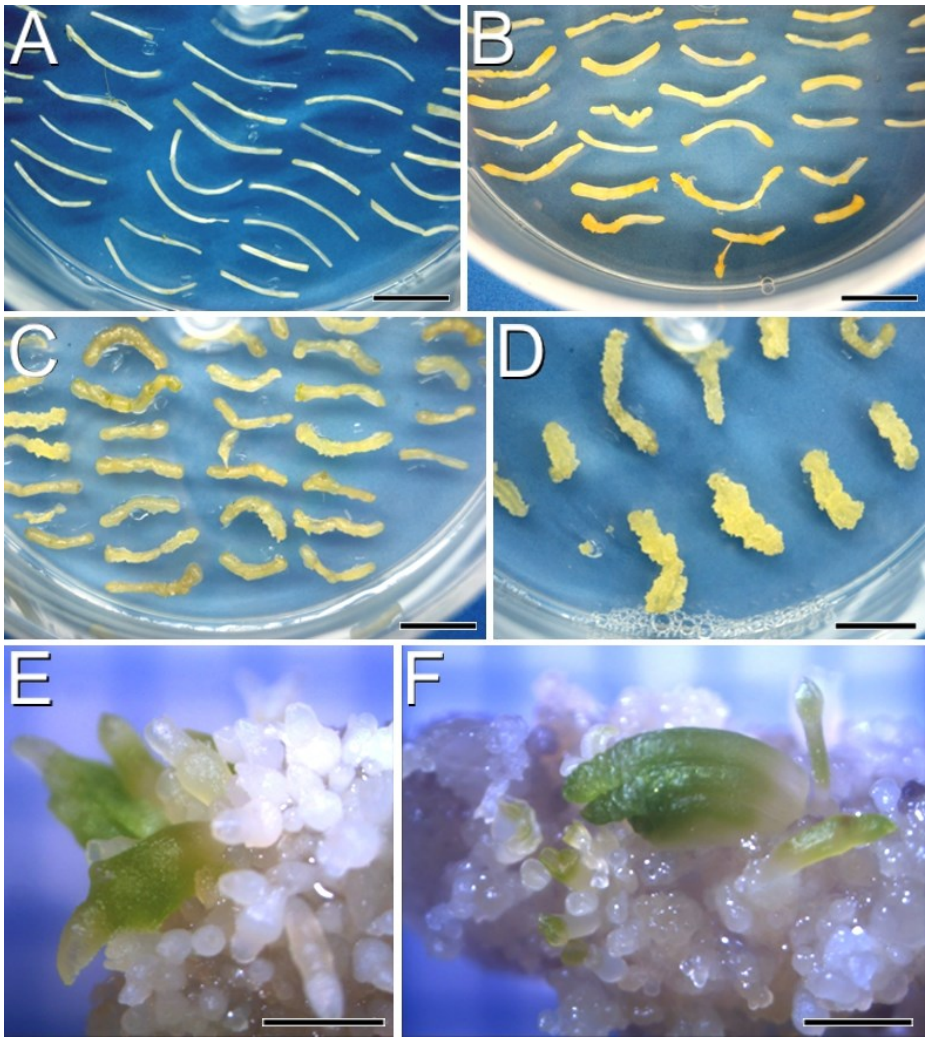

Suppl. Fig. S1. Carrot transformation and regeneration using protocol D. A: Fresh hypocotyl explants just transferred to MI medium. B: Hypocotyl explants after 15 days in MI medium. Note their color change from whitish to greenish and their swelling as a consequence of callus growth. C: Explants after 15 days in MII medium, swollen and covered by callus tissue. D: Explants transformed with the PM-YC3.6-LTI6b construct after one month in MII medium, where embryogenic structures developed on the surface of calli. E: Emerging embryogenic structures. F: Embryos from explants transformed with the PM-YC3.6-LTI6b construct at different developmental stages. Bars: A-D: 1 cm; E, F: 1 mm

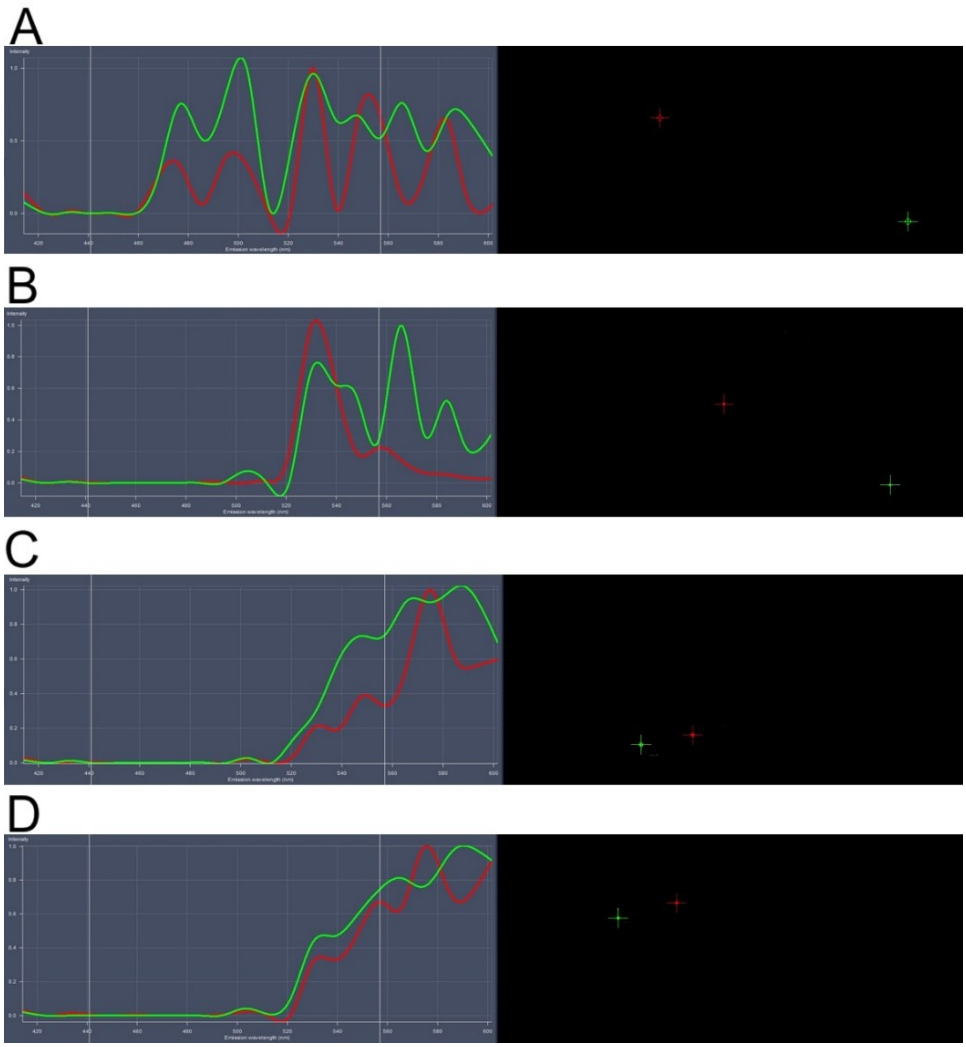

Suppl. Fig. S2. **Emission spectrum and confocal images of *D. carota* cell cultures**. **A**: Signal of a transformed cell irradiated at 440 nm, the excitation wavelength of CFP. Transformed cell cultures presented a double emission peak at 470 and 500 nm, corresponding to the emission spectrum of CFP, and another peak at 530 nm, corresponding to the emission of YFP resulting from FRET. **B:** Signal of a transformed cell irradiated at 514 nm, the excitation wavelength of YFP. Transformed cultures showed an emission peak at 530 nm, corresponding to the maximum emission peak of YFP. The red and green crosses in the right column images indicate two different plasma membrane regions from two different cells analyzed. When transformed cells are excited at 440 nm (A), three specific peaks are recorded: two at 475 and 500 nm, corresponding to the emission of CFP, and a third at 530 nm corresponding to the emission of the YFP excited by the CFP emission (resonance energy transfer). When transformed cells are excited at 514 nm (B), a specific peak at 530 nm, corresponding to the emission of YFP, is recorded. **C, D**: Signal of non-transformed (control) cells irradiated at 440 nm, the excitation wavelength of CFP (C), and at 514 nm, the excitation wavelength of YFP (D**)**. Note that only unspecific autofluorescence is detected, and no sharp emission corresponding to the specific peaks of CFP and YFP emission described above are observed in these cells.

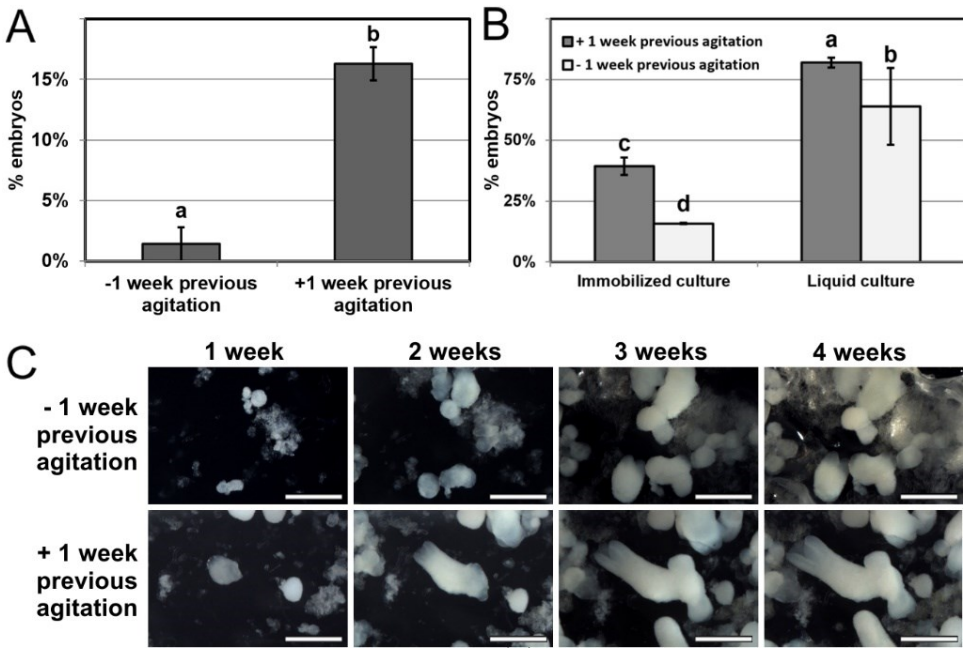

Suppl. Fig. S3. Development of carrot somatic embryos with different culture protocols. A: Comparison of the efficiency of somatic embryogenesis, expressed in percentage of embryos produced (% embryos), either including or excluding a step of one-week culture in liquid medium with agitation prior to transference to the final liquid culture medium. **B**: Comparison of the efficiency of somatic embryogenesis between immobilized cultures and conventional culture in liquid medium, either including or excluding a step of one-week culture in liquid medium with agitation prior to transference to the final immobilized or conventional liquid culture medium. **C**: Time-lapse images taken at one-week intervals of the progression of immobilized cultures either including or excluding a step of one-week culture in liquid medium with agitation prior to transference to the final immobilized medium. Bars: 500 µm.

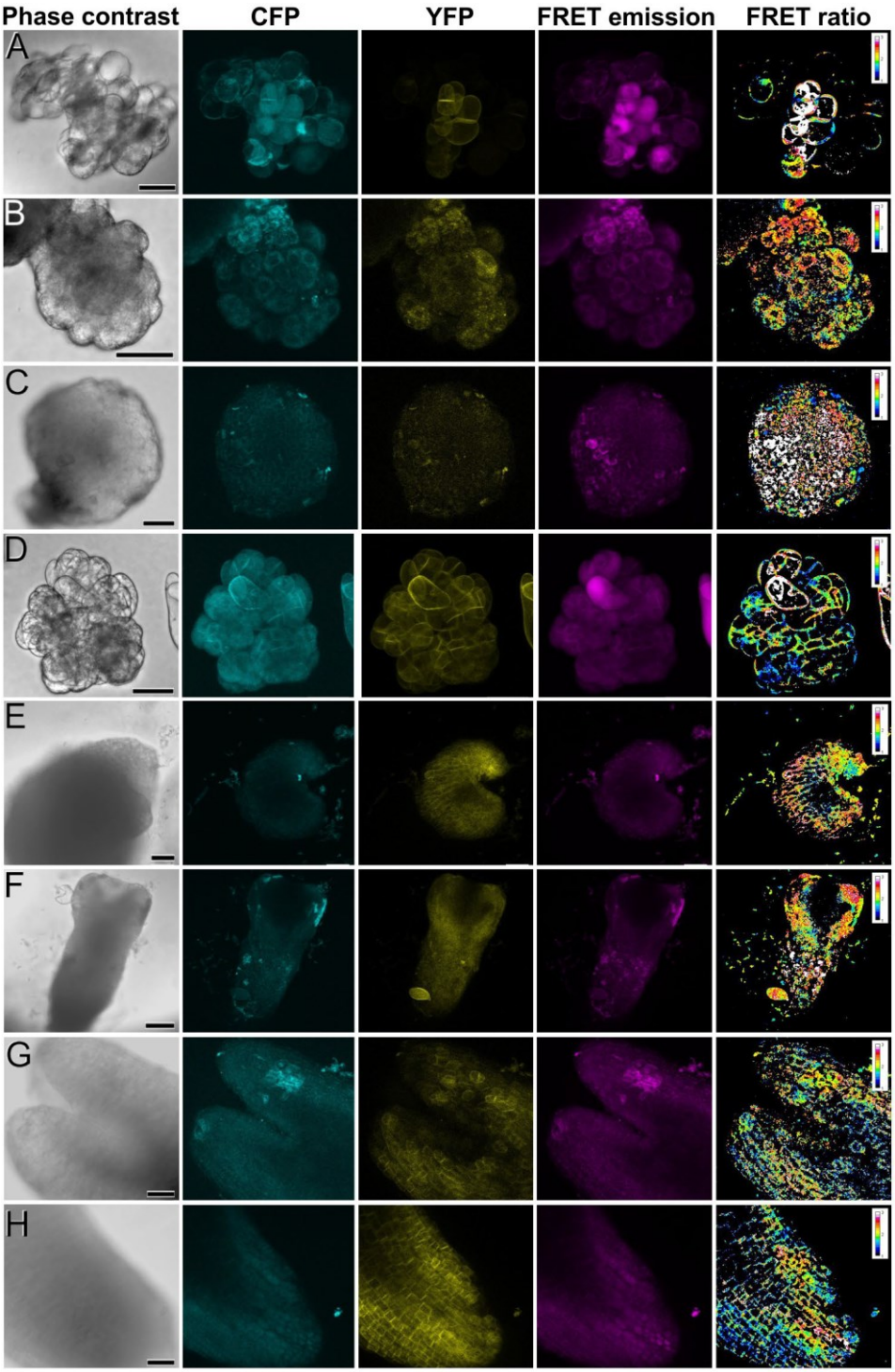

Suppl. Fig. S4. FRET imaging of Ca^{2+} levels during carrot somatic embryogenesis in *cameleon* lines. Each set of images show the same stages shown in Fig. 3 imaged by phase contrast, CFP, YFP, FRET emission fluorescence and FRET (YFP/CFP emissions) ratio. The LUT bar displays the false coloration of FRET ratios. **A**: One-week-old cell clumps. **B:** Cell clump transforming into an embryogenic mass. **C, D**: Two-weeks-old compact, globular embryo (C) and callus mass (D). **E**: Three-weeks-old heart-shaped embryo. **F**: Torpedo embryo. **G, H**: Shoot apical (G) and root (H) regions of a cotyledonary embryo. Bars: A-E, G, H: 40 µm; F: 100 µm.

5. Chapter 3: Dynamics of nuclear calcium during somatic embryogenesis in tobacco *(Nicotiana tabacum)*

Antonio Calabuig-Serna, Ricardo Mir, Consuelo Sabater, Jose María Seguí-Simarro.

Cell Biology Group - COMAV Institute, Universitat Politècnica de València, 46022 Valencia, Spain.

Keywords: *Nicotiana tabacum*, tobacco, Ca^{2+}, cameleon, FRET, *in vitro* culture.

In this research work, Antonio Calabuig-Serna contributed in the processes of investigation, methodology, data curation, formal analysis, and writing, reviewing and editing the draft.

Abstract

Somatic embryogenesis is the process whereby differentiated cells change their identity and start developing as embryogenic structures. Despite the advantages of this system as a model to study zygotic embryogenesis, and as a biotechnological tool to clonally propagate plant material, the cellular and molecular basis of induction of somatic embryogenesis in tobacco (*Nicotiana tabacum* L.) are still unraveled. In this work, we studied nuclear calcium (Ca^{2+}) dynamics during the different stages of somatic embryogenesis, including induction and development of the somatic embryo, using tobacco leaf explants from a transgenic, nucleus-targeted *cameleon* reporter line. We show that an increase in nuclear Ca^{2+} levels precedes the induction of somatic embryos, marking the onset of this process, and that nuclear Ca^{2+} distribution varies through embryo development, suggesting a prominent role of Ca^{2+} in regulating and signaling somatic embryogenesis in tobacco.

5.1.Introduction

Somatic embryogenesis is the process whereby differentiated somatic cells change their identity and start developing as embryogenic structures (Elhiti and Stasolla 2022). In basic research, somatic embryogenesis has been used as a model to study zygotic embryogenesis due to the similarities shared by the two systems (Méndez-Hernández et al. 2019). Besides, somatic embryogenesis is a powerful tool in plant breeding, principally because of its direct application in the development of micropropagation protocols (Egertsdotter et al. 2019). Multiple molecular and cellular processes and signaling events accompany embryogenesis, and calcium (Ca^{2+}) is one of the most important effectors (Winnicki 2020).

Ca^{2+} is thought to take part in multiple signal transduction processes in plant cells. In fact, Ca^{2+} signals may happen not only in the cytosol but also in cell organelles such as chloroplasts, mitochondria, the endoplasmic reticulum, or the nucleus. In this sense, numerous Ca^{2+} signals in nuclei have been observed in response to a wide range of stimuli, such as abiotic and biotic stresses, or the application of exogenous plant growth regulators (Pirayesh et al. 2021). Nuclear Ca^{2+} signatures are involved in transcriptional regulation either directly, through the activation of Ca^{2+}-binding and calmodulin-binding transcription factors, or indirectly, via Ca^{2+} and Ca^{2+}-calmodulin dependent kinases and other Ca^{2+} binding proteins (Charpentier 2018). During somatic embryogenesis in *Arabidopsis thaliana*, Calmodulin-binding Transcription factors (CAMTAs) are overrepresented at the first stages of the process (Wang et al. 2020), and modulation of Ca^{2+} homeostasis and calmodulin inhibition during the inductive stage greatly affected embryo yield (Calabuig-Serna et al. 2023a), thus confirming the involvement of Ca^{2+} in somatic embryo development. Previously, Ca^{2+} has been reported to be pivotal in other somatic embryogenesis systems such as carrot (Jansen et al. 1990), sandalwood (Anil and Rao 2000), *Pinus patula* (Malabadi and van Staden 2006) or *Coffea canephora* (Ramakrishna et al. 2012).

Tobacco (*Nicotiana tabacum* L.) is a solanaceous crop traditionally used for recreational and pharmacological purposes (Dewey and Xie 2013). In 2021, circa

6 million tonnes of tobacco were produced and more than 3 million ha were harvested worldwide (FAOSTAT 2022). In basic research, tobacco has been used as a model system to study different *in vitro* biotechnological processes including plant transformation (Niedbała et al. 2021), microspore embryogenesis (Seguí-Simarro et al. 2021), and somatic embryogenesis, which was first reported in tobacco by Stolarz et al. (1991). In this pioneering work, embryos were induced in MS medium supplemented with benzylaminopurine (BAP) and 1-naphthaleneacetic acid (NAA). Since then, several protocols have been successfully ideated using other hormones such as thidiazuron (TDZ) (Gill and Saxena 1993) and different concentrations of auxin and cytokinin (Pathi et al. 2013; Heidari Japelaghi et al. 2018; Kaya et al. 2021; Shahbazi et al. 2022).

Somatic embryogenesis is a highly regulated process at the transcriptome and signal transduction levels (Elhiti and Stasolla 2022). In particular, the overexpression in tobacco of *LEAFY COTYLEDON* (*LEC*) and *WUSCHEL related homebox* (*WOX*) genes, as well as the transcription factor *BABY BOOM* (*BBM*) Ap2/ERF, promote somatic embryogenesis (Rashid et al. 2007; Guo et al. 2013; Kyo et al. 2018), therefore suggesting the involvement of a complex genetic network in the embryogenic process. Although these findings shed some light on the genetic regulation of tobacco somatic embryogenesis, the initial signals that trigger gene activation are still unraveled. Indeed, the application of exogenous Ca^{2+} in the form of $CaCl_2$ on tobacco pith explants enhanced the organogenic response when cultured in hormone-free culture medium (Capitani and Altamura 2004), whereas other works pointed to calreticulin, a Ca^{2+}-binding protein involved in Ca^{2+} cellular homeostasis, as involved in the organogenic response (Jin et al. 2005). Although these findings suggest that Ca^{2+} may play a significant role in the induction of tobacco somatic embryogenesis, to our knowledge no work has deepened specifically into Ca^{2+} signaling in this process in tobacco.

Traditionally, Ca^{2+} signaling in plant cells has usually been studied by fluorescent stains (Rivas-Sendra et al. 2017; Zhao et al. 2002). However, the last decade has witnessed the discovery of *cameleon* sensors and their application to the study of Ca^{2+} in plant systems (Krebs et al. 2012). *Cameleons* are genetically-encoded Ca^{2+} sensors based on the energy transfer that occurs between two fluorophores when they become spatially close due to the interaction of Ca^{2+} with a calmodulin molecule separating both fluorophores (Miyawaki et al. 1997). At present, this approach is preferred, as it allows for *in vivo* Ca^{2+} visualization and quantification without interfering with cell functions and physiology. In this work, we studied nuclear Ca^{2+} dynamics during somatic embryogenesis induction and embryogenic development using leaf explants from a transgenic tobacco line expressing a nuclear-targeted *cameleon* reporter. We show that an increase in nuclear Ca^{2+} levels precedes the embryogenic initiation and that Ca^{2+} distribution varies through embryo development, confirming the prominent role of Ca^{2+} in regulating and signaling somatic embryogenesis in tobacco.

5.2.Materials and methods

5.2.1. Plant material

We used Petite Havana transgenic lines expressing the NLS-YC3.6 *cameleon* construct (pL2B-pNOS-BASTA-p35S), carrying a signal for nuclear targeting, kindly provided by Dr. Jongho Sun and Prof. Giles Oldroyd, University of Cambridge, UK (unpublished material). Seeds of these lines were sterilized for 5 min in 70% ethanol + 0.1% Triton and 15 min in a 4 g/L bleach solution, followed by three rinses in sterile water. Seeds were incubated 3 days at 4 °C and then germinated in solid Murashige and Skoog (MS) medium supplemented with 1% sucrose and 0.8% plant agar. Plates were kept for 21 days at 25 °C in 16/8 h photoperiod.

5.2.2. Somatic embryogenesis in tobacco

Induction of tobacco somatic embryogenesis from leaf explants was performed as described by (Pathi et al. 2013). Tobacco seeds were surface sterilized and germinated in MS solid medium supplemented with 1% sucrose. The first two true leaves from one-month-old seedlings were cut in square pieces and placed in tobacco induction medium with the abaxial surface contacting the medium until embryo production. Tobacco induction medium consisted of 4.4 g/L Murashige and Skoog basal medium + B5 vitamins (Murashige and Skoog 1962; Gamborg et al. 1968), 2% sucrose, 0.2 mg/L IAA, 2.5 mg/L BAP and 0.03% Phytagel. pH was adjusted to 5.8 and medium was autoclaved for 20 min at 121ºC. Basal medium and medium components were purchased from Duchefa (Netherlands). Explants were incubated at 25 °C in 16/8 h photoperiod until somatic embryo occurrence.

5.2.3. Confocal microscopy and FRET in tobacco

Explants were observed through confocal microscopy at day 4 and day 8. Developing embryos were monitored in 14-day cultured explants. For FRET visualization, tobacco embryogenic explants were mounted on a petri dish and immobilized with double-adhesive tape. Mounted samples were covered with liquid half-strength MS medium (pH 5.7) and observed in a Leica SP8-FLIMan confocal laser scanning microscope using an immersion objective. FRET imaging was performed by exciting at 448 nm and recording the emission between 525-560 nm. CFP was excited at 448 nm and emission was recorded between 460-493 nm. YFP was excited at 514 nm and recorded between 525-560 nm. FRET emission ratios were calculated as [acceptor emission/donor emission after donor excitation] using the FRETENATOR analysis toolset and following the protocol developed by Rowe et al. (2022). Briefly, FRETENATOR automatically detected nuclei and calculated their respective FRET emission ratios. Besides, it generated artificially colored images based on the calculated FRET ratios.

For all cases, Ca^{2+} levels were defined as very low, low, moderate, high or very high according to the colorimetric scale based on the FRET ratio images. Very low Ca^{2+} levels corresponded to dark blue colors, low levels to light blue, moderate to green-yellow, high to orange-red and very high levels to white color.

Image analysis was performed using the FIJI software (Schindelin et al. 2012). Quantitative differences in FRET ratios of tobacco somatic embryogenesis were detected by the non-parametric Kluskal-Wallis test ($p \leq 0.05$). Comparisons between groups were performed by Bonferroni's procedure ($p \leq 0.05$). For all statistical analysis, StatGraphics software was used.

5.3.Results

5.3.1. Induction of somatic embryogenesis from leaf explants of tobacco *cameleon* lines

We established a system for induction of somatic embryogenesis from leaf explants of the tobacco cameleon line expressing nucleus-targeted cameleon sensors (Fig. 1A). In all cases, explants included a leaf vein (delineated by arrowheads in Fig. 1A). Four days after culture initiation, some cells began to proliferate forming embryogenic nodules (Fig. 1B).

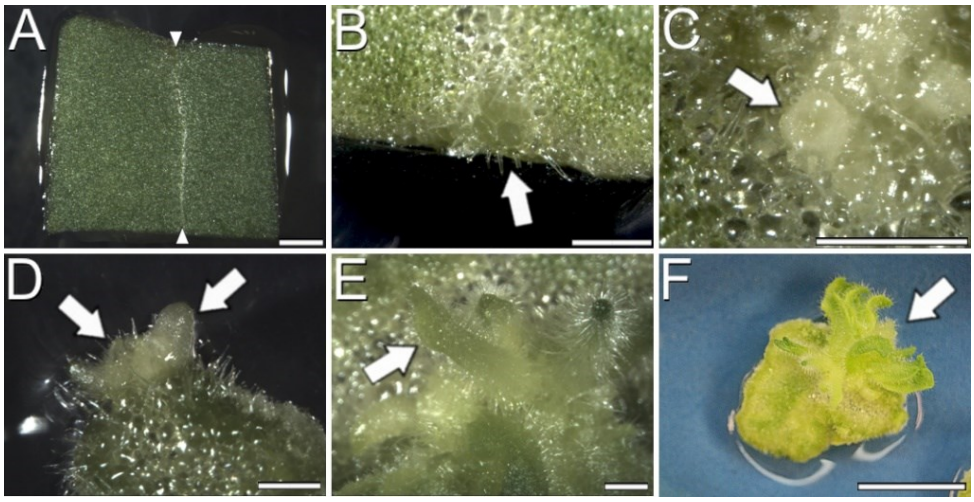

Fig. 1. **Induction of somatic embryogenesis from NLS-YC3.6 *cameleon* tobacco leaf explants.** A: Freshly excised leaf explant including a leaf vein (arrowheads). B: Formation of embryogenic nodules (arrow) after four days in culture. C: Cluster of embryogenic structures at day 8 of culture where a heart-shaped embryo (arrow) can be observed. D: Torpedo-like embryo where both cotyledons (arrows) are clearly visible. E: Elongated, mature embryo at day 14 of culture. F: Shoot-forming, germinating embryo on the surface of the leaf explant. Bars: A-E: 1 mm; F: 1 cm.

These structures progressed to become heart-shaped embryos (Fig. 1C) and, after 14 days of culture, clusters of embryos at different developmental stages were observed, including torpedo-like (Fig. 1D) and elongated, cotyledonary-like embryos (Fig. 1E). In almost all the explants, embryos were found to arise from the edge of the wound made in leaf veins (Figs. 1B, C), although they were also occasionally observed to be produced from the leaf mesophyll wounds (Fig. 1D). Irrespective of their origin, embryos eventually germinated and produced in vitro shoots, ready for rooting (Fig. 1F). Thus, nuclear cameleon lines of tobacco responded to the protocol of induction of somatic embryogenesis, which makes them useful tools to study the role of calcium during this experimental process.

5.3.2. FRET imaging of Ca^{2+} distribution during somatic embryogenesis in leaf tobacco explants

Next, we studied Ca^{2+} levels and distribution during tobacco somatic embryogenesis by observing FRET signal of the *cameleon* lines at the confocal microscope (Fig. 2 and Suppl. Fig. 1). Even before the formation of the first embryogenic nodules, the FRET ratio increased notably in particular regions of the leaf margin (Fig. 2A), potentially predicting the future site of nodule formation (Fig. 2B).

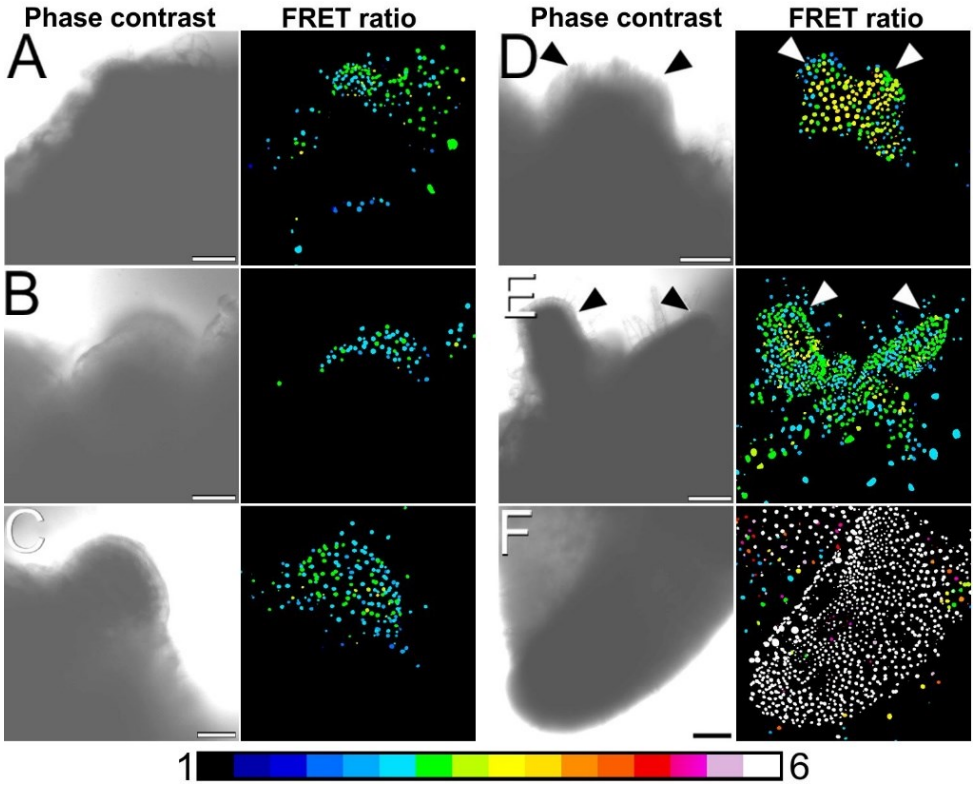

Fig. 2. FRET imaging of Ca^{2+} signaling during the induction of somatic embryogenesis in NLS-YC3.6 *cameleon* tobacco leaf explants. Each pair of images show the same field imaged by phase contrast (left) and by the FRET (YFP/CFP emissions) ratios. The LUT bar displays the false coloration of FRET ratios. A: Region of the leaf margin. B: Embryogenic nodule. C: Globular-like structure. D: Embryo-like structure with two emerging cotyledon primordia (arrowheads). E, F: Shoot (E) and root (F) tips of an elongating, cotyledonary embryo. Note in E the moderate Ca^{2+} levels (green and yellow nuclei) at the shoot tip and cotyledons (arrowheads) and in F the highest levels (white nuclei) at the root tip. Bars: 100 µm.

Then, clear globular-like structures emerging from the leaf surface showed Ca^{2+} levels higher than those of the surrounding tissues (Fig. 2C). Growth and transformation of globular-like into embryo-like structures was paralleled by an increase in their Ca^{2+} levels, especially at the central region, while two separate lobes, corresponding to the cotyledon primordia, differentiated at the distal end of the structure (arrowheads in Fig. 2D). At the differentiating cotyledon primordia, nuclei showed low Ca^{2+} levels, below the levels of the meristem region. Fifteen days after culture initiation, elongating torpedo and cotyledonar embryos kept moderate levels of FRET ratio at the shoot tip, including the apical meristem and the cotyledons (Fig. 2E), while it was the highest at the root tip (Fig. 2F). In summary, induction of somatic embryogenesis was accompanied by dynamic changes of Ca^{2+} levels, increasing in the embryogenic region and also

in the growing embryos with respect to the surrounding tissue, and being in general moderate at the shoot apical meristem region, low in cotyledons and high at the root tip region of the developing embryo.

5.3.3. Quantification of FRET signal

These qualitative observations tightly matched with the quantitative analysis of the FRET signal. We cultured leaf explants in somatic embryogenesis-inducing medium, measured the average FRET ratio at days 4 and 8, and compared them with the corresponding ratios of leaf explants cultured under non-inductive conditions (Fig. 3). We compiled data for at least three hundred nuclei for each treatment and compared their FRET ratios through non-parametric statistic tests.

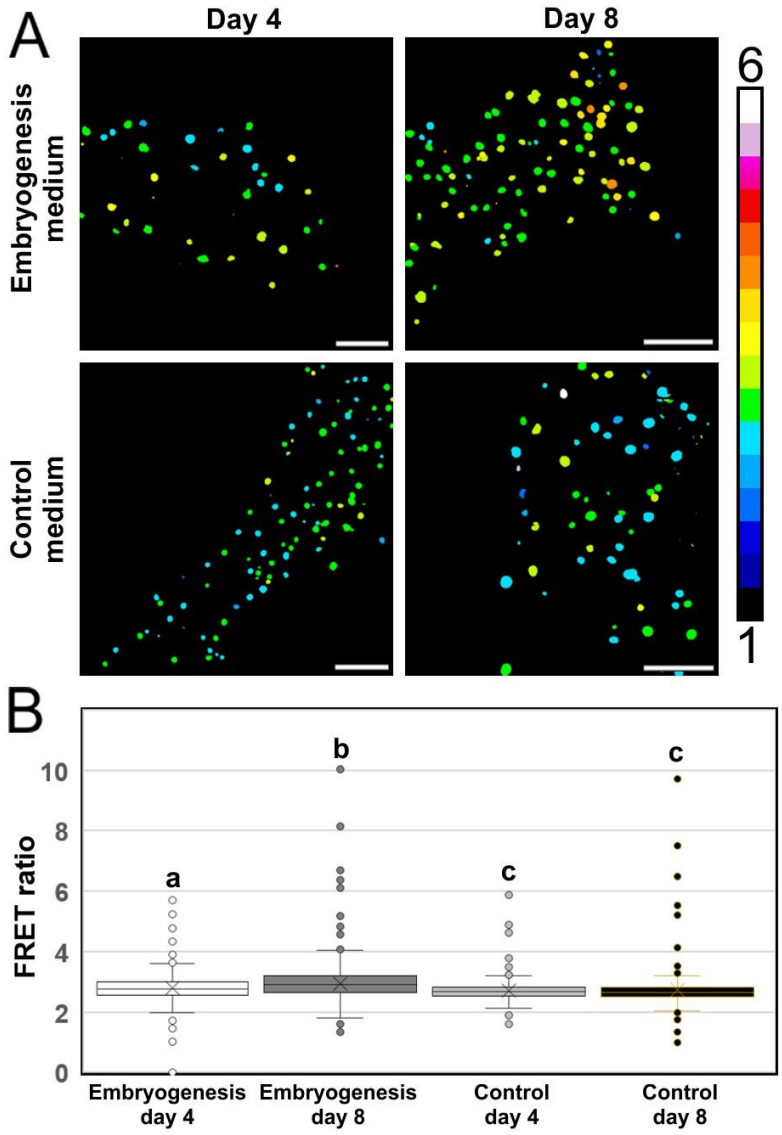

Fig. 3. Quantitative analysis of FRET/CFP ratio during the induction of somatic embryogenesis in NLS-YC3.6 *cameleon* tobacco leaf explants. A: Leaf explants cultured in somatic embryogenesis-inducing and in non somatic embryogenesis-inducing (control) conditions, both imaged at days 4 and 8. B: Graphical representation of the FRET ratio of the four stages described in A. Different letters indicate statistically significant differences for a Kluskal-Wallis test ($p<0.05$).

The FRET ratio of non-induced explants was similar at days 4 and 8, and significantly lower than the ratio of embryogenic explants at days 4 and 8, which is the stage where the highest FRET ratio was observed (Fig. 3B). Furthermore, differences between induced explants at days 4 and 8 were also detected, being FRET ratio higher at day 8. This quantitative analysis was confirmed with qualitative visualization of the cultured tissues, which reported a higher proportion of nuclei showing increased Ca^{2+} levels in embryogenic media-cultured explants (Fig. 3A). Again, this proportion of nuclei with higher FRET ratios increased in 8-day cultured explants with respect to 4-day explants. In summary, these results confirmed that increased levels of Ca^{2+} are also associated to the induction of somatic embryogenesis and the development of the somatic embryo from tobacco leaf explants, thus pointing to a key and dynamic role of Ca^{2+} during this process.

5.4.Discussion

We report for the first time on the description of nuclear Ca^{2+} dynamics during *in vitro* induction of somatic embryogenesis and the development of somatic embryos in tobacco. For this purpose, we used a transgenic tobacco line expressing a nuclear-targeted *cameleon* Ca^{2+} sensor. To our knowledge, this line was never used before to produce somatic embryos. We showed that somatic embryos were produced principally at the region surrounding the wound of leaf veins. The occurrence of embryos at the perivascular region has been widely described (Rose et al. 2010; Guzzo et al. 1994; de Almeida et al. 2012). It was proposed that the origin of embryogenic cells is the procambial cells of the pericycle surrounding the vascular tissue (Fehér 2019). Using Ca^{2+}-sensitive fluorescent probes in other somatic embryogenesis systems it was shown that, although Ca^{2+} levels are dynamic, Ca^{2+} can be detected in all cell compartments of embryogenic cells (Rivas-Sendra et al. 2019; Rivas-Sendra et al. 2017) but, at least in carrot somatic embryos, the most intense signal comes from the nucleus (Timmers et al. 1996). Therefore, using a nuclear Ca^{2+} sensor, as we hereby show, to analyze nuclear FRET ratios as indicators of Ca^{2+} levels in the nuclei of embryogenic cells may be a useful tool to study Ca^{2+} dynamics during *in vitro* somatic embryogenesis, and opens the way to study the role of Ca^{2+} in living tobacco cells in many different *in vivo* and *in vitro* processes.

Somatic embryogenesis from tobacco leaf explants starts in the explant margins with the reprogramming of cells, which start developing as embryogenic nodules and eventually evolve into mature embryos (Fig. 1). FRET imaging showed that, upon culture in inductive medium and even prior to becoming proliferating embryos, the nuclei of these cells presented higher Ca^{2+} levels than nuclei from cells cultured in non-inductive medium (Fig. 3). Furthermore, our analysis showed that cells from the embryogenic nodules exhibited higher nuclear FRET ratios than the surrounding cells of the same explant (Figs. 2A, B). Similar Ca^{2+} distribution patterns have been reported in other systems of somatic embryogenesis. For example, in *Arabidopsis thaliana*, where somatic embryogenesis is induced from immature zygotic embryos (IZEs), an increase in Ca^{2+} signal is observed in the IZE regions transforming into embryogenic nodes (Calabuig-Serna et al. 2023a). In *Daucus carota*, a model species for the study of somatic embryogenesis, Ca^{2+} accumulation precedes the development of

embryogenic structures from somatic cell clumps (Timmers et al. 1989; Calabuig-Serna et al. 2023b). In other *in vitro* embryogenesis systems such as *Brassica napus* microspore embryogenesis, increased cytosolic and also nuclear Ca^{2+} levels were reported after embryogenesis induction (Rivas-Sendra et al. 2017; Rivas-Sendra et al. 2019). Furthermore, transcriptome analysis during maize somatic embryogenesis showed that several Ca^{2+}-transporter ATPases are downregulated 24 hours after culture initiation (Salvo et al. 2014), suggesting that Ca^{2+} may accumulate in still somatic cells as a consequence of embryogenesis induction. Together, all these direct and indirect evidences point to the notion that increased Ca^{2+} levels in the cell nucleus, as part of a general increase of the cellular Ca^{2+} levels, are premature markers of induction of *in vitro* embryogenesis.

In addition to marking the onset of embryogenesis induction, the dynamics of Ca^{2+} during the development of tobacco somatic embryos can also be used as indicative of a proper embryo development. While Ca^{2+} levels at the cotyledons are kept moderate-low during all embryo development, the transition from globular-like (Fig. 2C) to cotyledon-bearing embryos implies the differentiation of a shoot apical meristem region with increased Ca^{2+} levels (Fig. 2D), and the accumulation of very high Ca^{2+} levels at the root apical region of the mature embryo (Fig. 2F). This pattern of Ca^{2+} distribution resembles the described in somatic embryos from *cameleon*-transformed carrot lines, where Ca^{2+} levels increased in the differentiating shoot apical meristem and cotyledons during embryo development, and in cotyledonary embryos, Ca^{2+} levels in the root apical region were also higher than in the shoot apical region (Calabuig-Serna et al. 2023b). Similar patterns were also observed by fluorescent detection of activated Ca^{2+}-calmodulin complexes during carrot somatic embryogenesis, where signal was polarized during the development of the somatic embryo and in mature embryos, it concentrated at the shoot and root meristem regions (Timmers et al. 1989).

In conclusion, in this work we used a nuclear-targeted *cameleon* line to study Ca^{2+} dynamics during tobacco somatic embryogenesis, and showed that an increase in nuclear Ca^{2+} levels mark the onset of embryogenesis induction and that nuclear Ca^{2+} levels are dynamic, changing in different embryo regions and throughout the different stages of the process. Given the widely known signaling role of Ca^{2+} in regulation of gene expression by activation of calmodulin-binding transcription factors and nucleus-localized proteins such as Ca^{2+}-dependent kinases (Charpentier 2018; Pirayesh et al. 2021), it is reasonable to speculate that one of the roles of Ca^{2+} in the induction of somatic embryogenesis could be related with the activation of embryo identity genes and the subsequent reprogramming towards embryogenesis.

Acknowledgements

We thank Dr. Jongho Sun, Prof. Giles Oldroyd, and the rest of members of the Oldroyd laboratory at the Crop Science Centre of the University of Cambridge, UK, for providing the *cameleon* tobacco lines and for kindly hosting and helping ACS during his stay. Thanks are also due to Dr. Annalisa Rizza and

Dr. Colleen Drapek from Sainsbury Laboratory Cambridge University (SLCU) for their technical advice and support.

References

Anil VS, Rao KS (2000) Calcium-mediated signaling during sandalwood somatic embryogenesis. Role for exogenous calcium as second messenger. Plant Physiol 123 (4):1301-1312

Calabuig-Serna A, Mir R, Seguí-Simarro JM (2023a) Calcium Dynamics, *WUSCHEL* Expression and Callose Deposition during Somatic Embryogenesis in *Arabidopsis thaliana* Immature Zygotic Embryos. Plants 12 (5):1021

Calabuig-Serna A, Mir R, Arjona P, Seguí-Simarro JM (2023b) Calcium dynamics and modulation in carrot somatic embryogenesis. Front Plant Sci 14:1150198. doi:10.3389/fpls.2023.1150198

Capitani F, Altamura MM (2004) Exogenous calcium enhances the formation of vegetative buds, flowers and roots in tobacco pith explants cultured in the absence of exogenous hormones. Plant Cell Tissue Organ Cult 77 (1):1-10

Charpentier M (2018) Calcium signals in the plant nucleus: origin and function. J Exp Bot 69 (17):4165-4173

de Almeida M, de Almeida CV, Graner EM, Brondani GE, de Abreu-Tarazi MF (2012) Pre-procambial cells are niches for pluripotent and totipotent stem-like cells for organogenesis and somatic embryogenesis in the peach palm: a histological study. Plant Cell Rep 31 (8):1495-1515. doi:10.1007/s00299-012-1264-6

Dewey RE, Xie J (2013) Molecular genetics of alkaloid biosynthesis in Nicotiana tabacum. Phytochemistry 94:10-27

Egertsdotter U, Ahmad I, Clapham D (2019) Automation and scale up of somatic embryogenesis for commercial plant production, with emphasis on conifers. Front Plant Sci 10:109

Elhiti M, Stasolla C (2022) Transduction of Signals during Somatic Embryogenesis. Plants 11 (2):178

FAOSTAT (2022) http://www.fao.org/faostat. Accessed February 2022

Fehér A (2019) Callus, Dedifferentiation, Totipotency, Somatic Embryogenesis: What These Terms Mean in the Era of Molecular Plant Biology? Front Plant Sci 10. doi:10.3389/fpls.2019.00536

Gamborg OL, Miller RA, Ojima K (1968) Nutrient requirements of suspension cultures of soybean root cells. Exp Cell Res 50 (1):151-158. doi:http://dx.doi.org/10.1016/0014-4827(68)90403-5

Gill R, Saxena PK (1993) Somatic embryogenesis in Nicotiana tabacum L.: induction by thidiazuron of direct embryo differentiation from cultured leaf discs. Plant Cell Rep 12 (3):154-159

Guo F, Liu C, Xia H, Bi Y, Zhao C, Zhao S, Hou L, Li F, Wang X (2013) Induced expression of AtLEC1 and AtLEC2 differentially promotes somatic embryogenesis in transgenic tobacco plants. PLoS ONE 8 (8):e71714

Guzzo F, Baldan B, Mariani P, Schiavo FL, Terzi M (1994) Studies on the origin of totipotent cells in explants of *Daucus carota* L. J Exp Bot 45 (10):1427-1432. doi:10.1093/jxb/45.10.1427

Heidari Japelaghi R, Haddad R, Valizadeh M, Dorani Uliaie E, Jalali Javaran M (2018) High-efficiency Agrobacterium-mediated transformation of tobacco (Nicotiana tabacum). Journal of Plant Molecular Breeding 6 (2):38-50

Jansen MA, Booij H, Schel JH, de Vries SC (1990) Calcium increases the yield of somatic embryos in carrot embryogenic suspension cultures. Plant Cell Rep 9 (4):221-223

Jin Z-L, Hong JK, Yang K, Koo JC, Choi YJ, Chung WS, Yun D-J, Lee SY, Cho MJ, Lim CO (2005) Over-expression of Chinese cabbage calreticulin 1, BrCRT1, enhances shoot and root regeneration, but retards plant growth in transgenic tobacco. Transgenic Res 14 (5):619-626

Kaya Y, Mohammed KT, Javed MA, Huyop F (2021) Plant tissue culture of Nicotiana tabacum cv. TAPM 26 and its minimum inhibition against herbicide-Dalapon.

Krebs M, Held K, Binder A, Hashimoto K, Den Herder G, Parniske M, Kudla J, Schumacher K (2012) FRET-based genetically encoded sensors allow high-resolution live cell imaging of Ca^{2+} dynamics. Plant J 69 (1):181-192. doi:10.1111/j.1365-313X.2011.04780.x

Kyo M, Maida K, Nishioka Y, Matsui K (2018) Coexpression of WUSCHEL related homeobox (WOX) 2 with WOX8 or WOX9 promotes regeneration from leaf segments and free cells in Nicotiana tabacum L. Plant Biotechnol:18.0126 a

Malabadi RB, van Staden J (2006) Cold-enhanced somatic embryogenesis in *Pinus patula* is mediated by calcium. South African Journal of Botany 72 (4):613-618. doi:10.1016/j.sajb.2006.04.001

Méndez-Hernández HA, Ledezma-Rodríguez M, Avilez-Montalvo RN, Juárez-Gómez YL, Skeete A, Avilez-Montalvo J, De-la-Peña C, Loyola-Vargas VM (2019) Signaling overview of plant somatic embryogenesis. Front Plant Sci 10:77

Miyawaki A, Llopis J, Heim R, McCaffery JM, Adams JA, Ikura M, Tsien RY (1997) Fluorescent indicators for Ca^{2+} based on green fluorescent proteins and calmodulin. Nature 388 (6645):882-887

Murashige T, Skoog F (1962) A revised medium for rapid growth and bioassays with tobacco tissue cultures. Physiol Plant 15:473-479

Niedbała G, Niazian M, Sabbatini P (2021) Modeling agrobacterium-mediated gene transformation of tobacco (Nicotiana tabacum)—a model plant for gene transformation studies. Front Plant Sci 12:695110

Pathi KM, Tula S, Tuteja N (2013) High frequency regeneration via direct somatic embryogenesis and efficient Agrobacterium-mediated genetic transformation of tobacco. Plant Signaling & Behavior 8 (6):e24354

Pirayesh N, Giridhar M, Ben Khedher A, Vothknecht UC, Chigri F (2021) Organellar calcium signaling in plants: An update. Biochimica et Biophysica Acta (BBA) - Molecular Cell Research 1868 (4):118948. doi:https://doi.org/10.1016/j.bbamcr.2021.118948

Ramakrishna A, Giridhar P, Jobin M, Paulose CS, Ravishankar GA (2012) Indoleamines and calcium enhance somatic embryogenesis in *Coffea canephora* P ex Fr. Plant Cell Tissue Organ Cult 108 (2):267-278. doi:10.1007/s11240-011-0039-z

Rashid SZ, Yamaji N, Kyo M (2007) Shoot formation from root tip region: a developmental alteration by WUS in transgenic tobacco. Plant Cell Rep 26 (9):1449-1455

Rivas-Sendra A, Calabuig-Serna A, Seguí-Simarro JM (2017) Dynamics of calcium during *in vitro* microspore embryogenesis and *in vivo* microspore development in *Brassica napus* and *Solanum melongena*. Front Plant Sci 8:1177. doi:10.3389/fpls.2017.01177

Rivas-Sendra A, Corral-Martínez P, Porcel R, Camacho-Fernández C, Calabuig-Serna A, Seguí-Simarro JM (2019) Embryogenic competence of microspores is associated with their ability to form a callosic, osmoprotective subintinal layer. J Exp Bot 70 (4):1267–1281. doi:10.1093/jxb/ery458

Rose R, Mantiri F, Kurdyukov S, Chen S, Wang X, Nolan K, Sheahan M (2010) Developmental biology of somatic embryogenesis. In: Pua E-C, Davey MR (eds) Plant developmental biology - Biotechnological perspectives, vol 2. Springer Verlag, Heidelberg, Germany, pp 3-26. doi:10.1007/978-3-642-04670-4

Rowe JH, Rizza A, Jones AM (2022) Quantifying phytohormones i*n vivo* with FRET biosensors and the FRETENATOR analysis toolset. In: Duque P, Szakonyi D (eds) Environmental Responses in Plants: Methods and Protocols, vol 2494. Methods in Molecular Biology. Springer Science+Business Media, LLC, New York, pp 239-253. doi:10.1007/978-1-0716-2297-1_17

Salvo SA, Hirsch CN, Buell CR, Kaeppler SM, Kaeppler HF (2014) Whole transcriptome profiling of maize during early somatic embryogenesis reveals altered expression of stress factors and embryogenesis-related genes. PLoS ONE 9 (10):e111407

Schindelin J, Arganda-Carreras I, Frise E, Kaynig V, Longair M, Pietzsch T, Preibisch S, Rueden C, Saalfeld S, Schmid B, Tinevez JY, White DJ, Hartenstein V, Eliceiri K, Tomancak P, Cardona A (2012) Fiji: an open-source platform for biological-image analysis. Nature methods 9 (7):676-682. doi:10.1038/nmeth.2019

Seguí-Simarro JM, Jacquier NMA, Widiez T (2021) Overview of i*n vitro* and *in vivo* doubled haploid technologies. In: Seguí-Simarro JM (ed) Doubled Haploid Technology, vol 1: General Topics, Alliaceae, Cereals. Methods in Molecular Biology, vol 2287, 1st edn. Springer Science+Business Media, LLC, New York, USA, pp 3-22. doi:10.1007/978-1-0716-1315-3_1

Shahbazi M, Tohidfar M, Aliniaeifard S, Yazdanpanah F, Bosacchi M (2022) Transgenic tobacco co-expressing flavodoxin and betaine aldehyde dehydrogenase confers cadmium tolerance through boosting antioxidant capacity. Protoplasma 259 (4):965-979

Stolarz A, Macewicz J, Lörz H (1991) Direct somatic embryogenesis and plant regeneration from leaf explants of Nicotiana tabacum L. J Plant Physiol 137 (3):347-357

Timmers A, De Vries S, Schel J (1989) Distribution of membrane-bound calcium and activated calmodulin during somatic embryogenesis of carrot (*Daucus carota* L.). Protoplasma 153 (1):24-29

Timmers ACJ, Reiss H-D, Bohsung J, Traxel K, Schel JHN (1996) Localization of calcium during somatic embryogenesis of carrot (*Daucus carota* L.). Protoplasma 190 (1):107-118. doi:10.1007/bf01281199

Wang F-X, Shang G-D, Wu L-Y, Xu Z-G, Zhao X-Y, Wang J-W (2020) Chromatin accessibility dynamics and a hierarchical transcriptional regulatory network structure for plant somatic embryogenesis. Dev Cell 54 (6):742-757. e748

Winnicki K (2020) The Winner Takes It All: Auxin-The Main Player during Plant Embryogenesis. Cells 9 (3). doi:10.3390/cells9030606

Zhao J, Yu F, Liang S, Zhou C, Yang H (2002) Changes of calcium distribution in egg cells, zygotes and two-celled proembryos of rice (Oryza sativa L.). Sex Plant Reprod 14 (6):331-337. doi:10.1007/s00497-002-0127-7

Supplementary materials

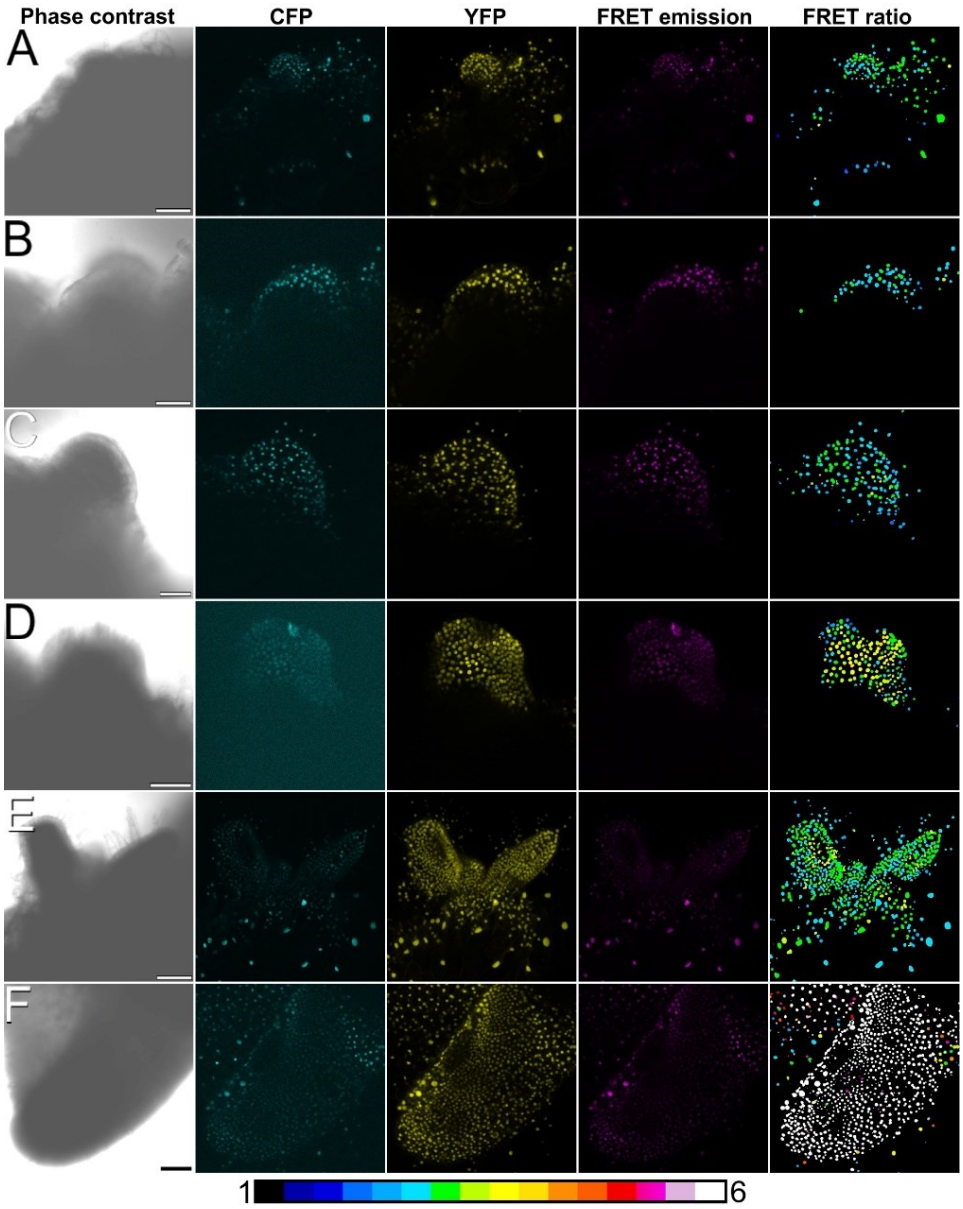

Suppl. Fig. S1. FRET imaging of Ca^{2+} signaling during the induction of somatic embryogenesis in NLS-YC3.6 *cameleon* tobacco leaf explants. Each set of images show the same stages shown in Fig. 2 imaged by phase contrast, CFP, YFP, FRET emission fluorescence and FRET (YFP/CFP emissions) ratio. The LUT bar displays the false coloration of FRET ratios. A: Increased Ca^{2+} levels in specific regions of the leaf margins. B: Embryogenic nodule with increased Ca^{2+} levels at the peripheral cell layers. C: Globular-like structure emerging from the leaf surface. D: Embryo-like structure. E, F: Shoot (E) and root (F) tips of an elongating, cotyledonary embryo. Bars: 100 µm.

6. Chapter 4: The highly embryogenic *Brassica napus* DH4079 line is recalcitrant to *Agrobacterium*-mediated genetic transformation

Antonio Calabuig-Serna, Ricardo Mir, Rosa Porcel, Jose María Seguí-Simarro.

Cell Biology Group - COMAV Institute, Universitat Politècnica de València, 46022 Valencia, Spain.

Keywords: *Agrobacterium rhizogenes, Agrobacterium tumefaciens,* canola, DH12075*, in vitro* culture, oilseed rape, rapeseed, transgenic

This article has been published as: Calabuig-Serna A, Mir R, Porcel R and Seguí-Simarro JM (2023) The highly embryogenic *Brassica napus* DH4079 line is recalcitrant to *Agrobacterium*-mediated genetic transformation. *Plants, 12 (10): 2008. doi: 10.3390/plants12102008.*

In this research work, Antonio Calabuig-Serna contributed in the processes of investigation, methodology, data curation, formal analysis, and writing, reviewing and editing the draft.

Abstract

Brassica napus is a species of high agronomic interest, and is used as a model for the study of different biological and biotechnological processes, including microspore embryogenesis. The DH4079 and DH12075 lines show a high and low embryogenic response, respectively, which makes them ideal to study the basic mechanisms controlling embryogenesis induction. Therefore, the availability of protocols for genetic transformation of this species, and especially of these two backgrounds, would help to generate tools to better study and understand this process. There are some reports in the literature demonstrating that it is possible to transform the DH12075 line, but the DH4079 line is believed to be somehow recalcitrant to *Agrobacterium*-mediated transformation. However, no studies confirming such recalcitrance has been reported to date. In this work, we aimed to obtain transformed DH4079 plants. As a reference to compare with, we used the same protocols to transform DH12075. We used three different protocols previously reported as successful for *B. napus* stable transformation and one protocol for transient transformation. We analyzed the response of plants to stable transformation with *Agrobacterium tumefaciens* and transient transformation with *A. rhizogenes*. Whereas DH12075 plants responded to both types of bacterial genetic transformation, DH4079 plants were completely recalcitrant, not producing any single regenerant out of the 1,784 explants transformed and cultured. Therefore, we propose that the DH4079 line is extremely recalcitrant to *Agrobacterium*-mediated transformation.

6.1.Introduction

Genetic transformation consists on the introduction of a foreign DNA molecule into a genome, generating a genetically modified organism. The first reports on plant genetic transformation date from 1983 and used *Agrobacterium tumefaciens* as a transformation vector to introduce foreign DNA into the genomes of different plant species (van Montagu 2011). Among the different technologies available for plant genetic transformation, *Agrobacterium*-mediated transformation is nowadays the most used approach. The use of genetically modified crops has increased both plant productivity and farmer profits, while reducing the use of pesticides, among other advantages (Klümper and Qaim 2014). Indeed, a total of 438 plant genetically modified events have been approved worldwide (ISAAA 2022). More recently, the impact of biotechnology on agriculture has been enhanced by different genome editing techniques, such as zinc-finger nucleases, transcription activator-like effector nucleases (TALENs), and CRISPR/Cas9-based genome editing, which most of the times implies the previous generation of genetically modified plants (Hua et al. 2019). On the other hand, the use of genetic transformation to generate gain and loss-of-function lines in different model and crop species, has helped us to understand gene function and constitutes a powerful biotechnological tool for basic and applied plant genetic and molecular research (Hopp et al. 2022). Therefore, the availability of efficient plant transformation protocols for different crops and plant species is crucial for the improvement of crop performance for agriculture as well as for the generation of new biotechnological research tools.

Microspore embryogenesis is a process whereby the male gametophyte deviates from its original developmental pathway and is induced to develop as a haploid embryo whose genome can then be doubled to become a doubled haploid (DH), fully homozygous individual (Seguí-Simarro et al. 2021). This process constitutes a powerful biotechnological tool for both basic research (Jouannic et al. 2001; Satpute et al. 2005) and applied plant breeding (Weyen 2021). *Brassica napus* is a model species for the study of this experimental process (Custers et al. 2001; Ferrie and Möllers 2011) due to the high potential of the microspores of some genotypes, such as the DH4079 line, to become induced to embryogenesis, whereas other lines, such as the DH12075 line, consistently show a low response to the same embryogenesis-inductive conditions (Corral-Martínez et al. 2021). Thus, *B. napus* is an interesting target species to combine transformation and microspore embryogenesis protocols in order to develop DH individuals from haploid transformed microspores, thereby fixing the transgene in homozygosis and avoiding the occurrence of hemizygous regenerants (Ferrie and Möllers 2011). The development of successful transformation protocols for *B. napus* lines with different embryogenic competence would greatly help to develop biotechnological tools to study the cellular and molecular basis of this morphogenic process.

The type of explant tissue, the selection marker used and the genotype have been reported among the main factors affecting the efficiency of stable *B. napus* transformation (Dai et al. 2020; Bhalla and Singh 2008). Some of the first attempts to transform *B. napus* were based on the use of cotyledon petioles as explants (Moloney et al. 1989). Afterwards, other effective protocols have been developed, also based on the use of cotyledons (Sparrow et al. 2006) or other explants such as stem portions (Fry et al. 1987), protoplasts (Wang et al. 2005) or hypocotyl sections (Maheshwari et al. 2011). Among the different selection markers available, kanamycin has been commonly used as an effective selection agent in *B. napus* transformation, whereas the use of BASTA has been less frequent (Gocal 2021). The third major factor is the genotype. In other members of the brassicaceae family such as *B. oleracea*, there are protocols to stably transform with agrobacterium different genotypes of crops such as cauliflower and broccoli, among others, with low genotype dependence (Sheng et al. 2022). However, different *B. napus* genotypes show different responses to *Agrobacterium*-mediated transformation (Maheshwari et al. 2011). Several works reported the successful transformation of the low embryogenesis-responsive lines Westar (Fry et al. 1987; Moloney et al. 1989) and DH12075 (Wu et al. 2011; Wang et al. 2009), whereas to our knowledge no transgenic lines have been described so far for the highly embryogenic DH4079 line. Whether DH4079 is recalcitrant to *Agrobacterium*-mediated transformation, or simply no transformed DH4079 lines have been reported yet is unknown. However, due to the enormous importance of this line as a model experimental system for the study of microspore embryogenesis (Custers et al. 2001), we can reasonably assume that transformation of this line has been previously and repeatedly attempted, and the lack of positive reports on DH4079 transgenic lines is indicative of a lack of success.

In this work, we aimed to determine an optimal protocol for *Agrobacterium*-mediated stable transformation of the *B. napus* DH4079 line using different

conditions, including different plant explants, plasmids, agrobacterium strains and incubation times. As references to compared with, we also attempted stable transformation of the DH12075 line with the same protocols and analyzed transient transformation mediated by *Agrobacterium rhizogenes* in DH4079 and DH12075 seedlings. Our results point to a genetic recalcitrance of the DH4079 line but not of the DH12075 line, which was possible to transform with both agrobacterium species. These results make these *B. napus* lines convenient models to study the mechanisms of recalcitrance to agrobacterium-mediated transformation in plants.

6.2.Materials and Methods

6.2.1. Plant material

Seedlings from two different *B. napus* DH lines were used as donors of explants: the DH4079 line, derived from cv. Topas (Ferrie and Möllers 2011), and the DH12075 line, derived from a cross between cvs. Westar × Cresor.

6.2.2. Constructs

Three plasmids were used in this experiment (Fig 1A). On the one hand, we used YC3.6-Bar and PM-YC3.6-LTI6b, two *cameleon* calcium sensor constructs that confer BASTA and kanamycin resistance, respectively, kindly provided by Dr. Jörg Kudla (Krebs et al. 2012). On the other hand, we used pCRISPR, a Golden Braid-based construction for CRISPR/Cas9 genome editing (Vazquez-Vilar et al. 2016) containing a CaMV 35S promoter, Cas9 CDS, and Nos Terminator cassette, assembled in the pDGB3-alpha1 binary plasmid containing a cassette for kanamycin for plant selection.

6.2.3. Management and transformation of Escherichia coli, Agrobacterium tumefaciens and Agrobacterium rhizogenes strains

Chemically competent *Escherichia coli* One Shot™ ccdB Survival™ 2 T1R cells were prepared from cells growing under agitation and 37 ºC in 50 ml Psi medium (Table 1) until the DO_{600} reached 0.4-0.5. Bacterial culture was cooled down and centrifuged (5 min, 5000 g, 4 °C). The pellet was resuspended in 20 mL of cold Transformation Buffer I (TBI; Table 1) and incubated on ice for 15 min. Next, the bacterial suspension was centrifuged (10 min, 2000 g, 4ºC) and the resulting pellet was resuspended in 2 mL of Transformation Buffer II (TBII; Table 1) and incubated in ice for 15 min. Finally, 50 µL aliquots were kept at -80 °C. For transformation, aliquots were thawed and 5 µL (~ 1 µg) of DNA was added. Tubes were incubated 60 min on ice, 30 s at 42 °C and then on ice for 2 min. Next, 250 µL of autoclaved SOC medium (Table 1) were added and tubes were incubated at 37 °C for 1 h in a shaker at 225 rpm. From each tube, 25-100 µL were plated in commercial LB-Agar Miller medium (VWR Life Science) plates supplemented with the corresponding bacterial selective agents (Table 2) and incubated at 37 °C. Saturated *E. coli* liquid LB cultures were used to perform plasmid extractions with NZYMiniprep kit (NZYtech).

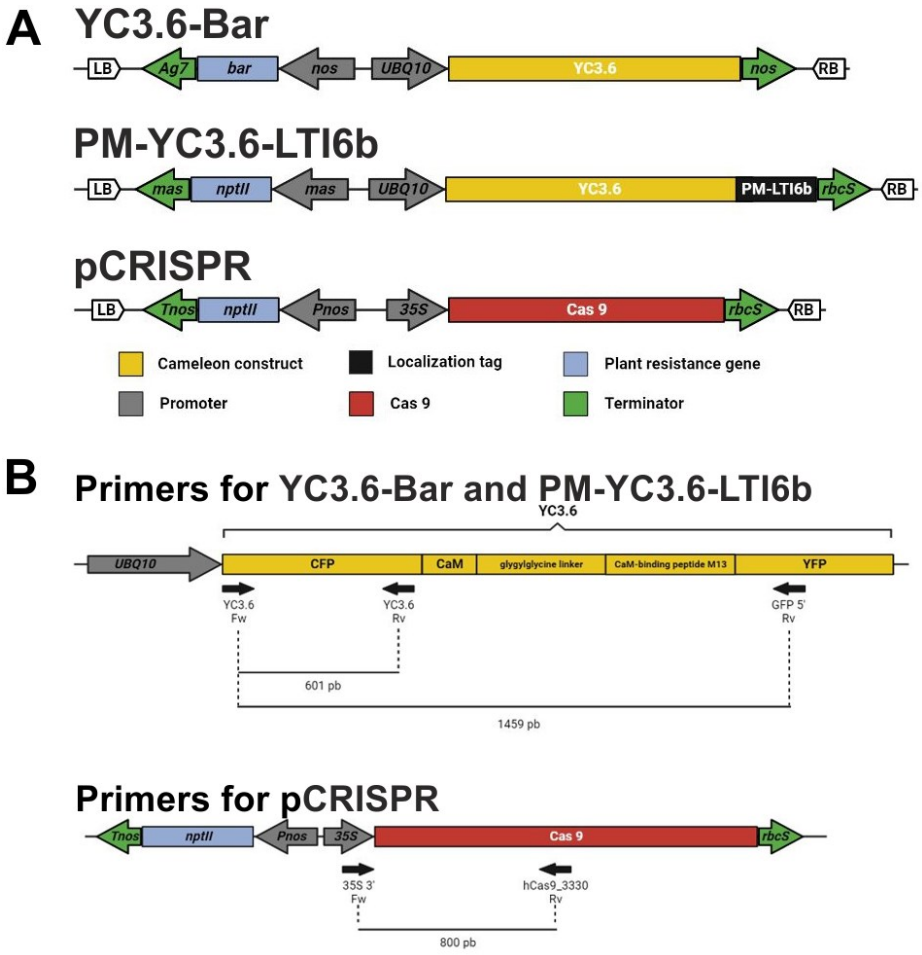

Fig 1. Diagrams of the vectors and primers used for *B. napus* transformation. A. Vectors used for the optimization of *Brassica napus* transformation protocol: YC3.6-Bar, PM-YC3.6-LTI6b and CRISPR/Cas9 recombinant plasmid (pCRISPR). LB: Left Border; RB: Right Border; *Ag7*: *gene7*; *mas*: mannopine synthase; *UBQ10: UBIQUITIN10; nos:* nopalin synthase; *rbcS*: *ribulose bisphosphate carboxylase oxygenase small subunit*. B. Scheme of the primers (black arrows) used to genotype the regenerated plants and their amplification products. The first scheme shows the primer combinations used for *cameleon* constructs (YC3.6-Bar and PM-YC3.6-LTI6b), and the second scheme shows the primers used for CRISPR/Cas9 constructs.

Agrobacterium tumefaciens strain LBA4404 carrying the helper *vir* plasmid pAL4404 (ElectroMAX™ *A. tumefaciens* LBA4404 Cells, Invitrogen™) was used for plant transformations. Electrocompetent *A. tumefaciens* cells were prepared by culturing a single colony in liquid YM medium (Table 1) for 2 days at 28-30 °C. One mL of culture was diluted 1:100 in liquid YM medium. The dilution was incubated at 28-30 °C in agitation until DO_{600} ranged 0.5-0.7. The *Agrobacterium* culture was centrifuged (15 min, 4 °C, 6000 g) and the pellet was washed with 30 mL of cold sterile MilliQ water. Centrifugation (same conditions) and washing was repeated twice. Finally, cells were resuspended in 1 mL of cold 10% (v/v) glycerol and 20 µL aliquots were stored at -80 °C. For transformation of *A. tumefaciens* LBA4404 competent cells, each aliquot was thawed, 1 µL (~200 ng) of plasmid was added and the mixture was pipetted into the electroporation cuvette. The mixture was electroporated at 2.0 kV, 200 Ω y 25 µF using a BTX Electroporation Electro Cell Manipulator 600 from LabX. After electroporation, 1 mL of autoclaved liquid YM medium was added to the micro tube. The content was transferred to a 15 mL tube and incubated at 225 rpm and

28°C for 3 h. Then, 50-100 µL were plated in solid YM (Table 1) medium with the corresponding plasmid-specific selective agents (Table 2). Plates were incubated at 28 °C for 2-3 days until colonies were observed.

Table 1. Composition of the different culture media used for management and transformation of bacterial strains. TBI: Transformation Buffer I; TBII: Transformation Buffer II.

	Psi	**TBI**	**TBII**	**SOC**	**Liquid YM**	**Solid YM**	**MGL**
Potassium acetate (mM)		30					
$RbCl_2$ (mM)		100	10				
$CaCl_2 \cdot 2H_2O$ (mM)		10	75				
$MnCl_2 \cdot 4\ H_2O$ (mM)		50					
MOPS (mM)			10				
$MgCl_2$ (mM)	52.63			10			
NaCl (mM)				10	1.7	1.7	85.5
KCl (mM)				2.5			
$MgSO_4$ (mM)				10			
$MgSO_4 \cdot 7H_2O$ (mM)					0.8	0.8	0.4
Glucose (mM)				20			
$K_2HPO_4 \cdot 3H_2O$ (mM)					2.2	2.2	1.4
Tryptone (%)	2			2			0.5
Yeast extract (%)	0.5			0.5	0.04	0.04	0.25
Mannitol (%)					1	1	0.5
Glycerol (% v/v)		15	15				
L-glutamic acid (g/L)							1
Biotin (mg/L)							1
Bacteriological agar (%)						1	
Rifampicin (mg/L)						50	
pH	7.6	5.8	6.5	7	7	7	7

Table 2. Plasmid selection agents used for bacterial transformation.

	YC3.6-Bar	CRISPRp	PM-YC3.6-LTI6b
Kanamycin	50 mg/L	50 mg/L	
Spectinomycin			100 mg/L
Streptomycin			100 mg/L

Preparation of *Agrobacterium rhizogenes* strain 15834 competent cells and transformation with pCRISPR by electroporation was performed as described above for *A. tumefaciens,* but using MGL liquid medium (Table 1).

6.2.4. Explant transformation and plant regeneration

Three transformation protocols were assayed (Fig 2), two (B and A) based on (Maheshwari et al. 2011) and one (protocol Z) based on (Sparrow et al. 2006). For all protocols, bacterial inoculums were prepared by centrifuging (5975 g, 10 h, 4º C) liquid cultures grown at 28 °C in liquid YM medium (Table 1) supplemented with 50 mg/L rifampicin and appropriate bacterial selective agents (Table 2) until reaching an approximate OD_{600}=1.0. The bacterial pellets were resuspended in liquid MS medium with 1% sucrose until reaching a OD_{600} ranging 0.15-0.2, and 100 µM acetosyringone was added. To produce the explant-donor seedlings, *B. napus* seeds of the DH4079 and DH12075 lines were surface sterilized 15 min in a 70% ethanol + 0.1% Triton X-100 solution, followed by 15 min in 10% bleach solution and three rinses with distilled water. Seeds were then germinated in Germination Medium (GM; Table 3).

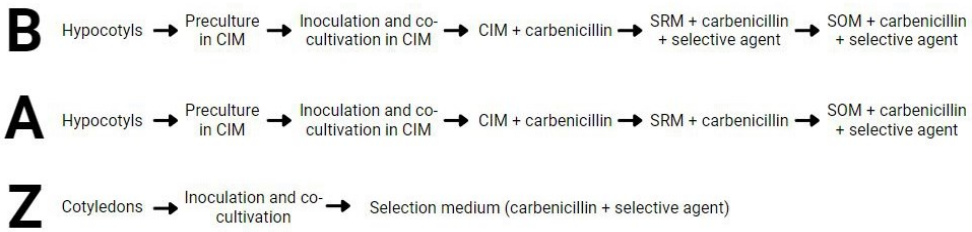

Fig 2. **Scheme of the different steps of the three transformation protocols (B, A and Z) used in this work.** See text for further details.

Table 3. Composition of the different culture media used for explant transformation and plant regeneration. 2,4-D: 2,4-dichlorophenoxyacetic acid; BAP: 6-benzylaminopurine; CCM: Co-Cultivation Medium; CIM: Callus Induction Medium; GM: germination medium; MS+V: Murashige and Skoog basal medium including vitamins (Duchefa Biochemie); RRM: Root Regeneration Medium; SM: Selection medium; SOM: Shoot Outgrowth Medium; SRM: Shoot Regeneration Medium.

	GM	CIM	SRM	SOM	RRM	CCM	SM	RM
MS+V (g/L)	4.6	4.6	4.6	4.6	2.3	4.6	4.6	2.3
MES (g/L)		2.5	2.5	2.5	2.5			
Myo-inositol (g/L)		1	1	1	1			
$AgNO_3$ (mg/L)		5	5					
2,4-D (mg/L)		1						
BAP (mg/L)			5	0.05		2	2	
Sucrose (g/L)	20	30	30	30	10	30	30	10
Plant agar (g/L)	8	8	8	8	8	8	8	8
Carbenicillin (mg/L)			500	500	100		500	500
pH	5.8	5.8	5.8	5.8	5.8	5.8	5.8	5.8

In protocols A and B, 0.5-1 cm hypocotyl explants were excised from 7 day-old seedlings and pre-cultured in Callus Induction Medium (CIM; Table 3) for 5 days. After 3-5 days, explants were inoculated with the corresponding *A. tumefaciens* culture. Pre-cultured explants were submerged in the bacterial suspension, blotted on sterile paper and transferred to CIM medium for 72 h at 25 °C under reduced light conditions by covering the culture with a piece of white paper to reduce light intensity to dim light. After co-cultivation with *A. tumefaciens,* explants were transferred to CIM medium supplemented with 500 mg/L carbenicillin and cultured for 2 weeks at 25 °C under dim light. Regenerated calli were cut into pieces and cultured for 4-6 weeks in Shoot Regeneration Medium (SRM; Table 3) for protocol A, and for protocol B in SRM medium supplemented with 50 mg/L kanamycin as plant selection agent for PM-YC3.6-LTI6b transformation and 10 mg/L BASTA (amonium glufosinate) for YC3.6-Bar. Developing shoot buds were transferred to Shoot Outgrowth Medium (SOM; Table 3) supplemented with plant selection agents as described above. Shoots longer than 2 cm were transferred to Root Regeneration Medium (RRM; Table 3) supplemented with plant selection agents as described above.

For protocol Z, cotyledon explants were obtained by cutting the petiole base from 5-7 day-old seedlings. Excised cotyledons were inoculated by dipping for 3-5 s the petiole base in liquid MS+V medium + 1% sucrose and the *A. tumefaciens* preparation (OD_{600}=0.2 supplemented with 100 µM acetosyringone). Then, explants were inoculated by inserting 1-2 mm of the petiole base in solid Co-Cultivation Medium (CCM; Table 3). Plates were kept at 25 °C for 72 h under dim light. Then, explants were transferred to Selection Medium (SM; Table 3) supplemented with plant selection agents (15 mg/L kanamycin for PM-YC3.6-

LTI6b and CRISPRp transformations and 5 mg/L BASTA for YC3.6-Bar) for at least four weeks, subculturing them to fresh SM every week. The regenerating shoots produced were transferred to Rooting Medium (RM; Table 3) supplemented with plant selection agents as described above.

For genotyping regenerated plants, when potential T1 plants developed 2-3 true leaves, 1 cm^2 pieces of leaf tissue were excised and DNA was extracted on TNES extraction buffer (100 mM Tris Buffer, 100 mM EDTA, 250 mM NaCl, pH 8) and precipitated with 1 volume of isopropanol at room temperature for 2 min. The pellet was resuspended in 50 µL MilliQ water. The primer pairs used to genotype regenerated plants from transformations with PM-YC3.6-LTI6b, YC3.6-Bar and pCRISPR are shown in Fig 1B, and their respective sequences in Table 4. All PCRs were performed adding 1 µM primers to the Mix MZY Taq II 2x Green Master Mix (NZYtech), with annealing temperature of 59 °C and extension time of 40 s.

Table 4. List of oligonucleotides used as primers (Fw: forward primer; Rv: Reverse primer).

Oligonucleotide	Sequence (5' to 3')
35S 3' Fw	GATGACGCACAATCCCACTATCC
hCas9_3330 Rv	GCAGAATGGCGTCTGACAGG
YC3.6 Fw	TAAACGGCCACAGGTTCAGC
YC3.6 Rv	CGATCACATGGTCCTGCTGGA
GFP5' Rv	GCGACGTAAACGGCCACAAGTTCAG

For transient hairy root transformation of *B. napus* with *Agrobacterium rhizogenes,* the protocol was adapted from Ron et al. (Ron et al. 2014). Briefly, 3 mL of saturated *A. rhizogenes* culture on MGL liquid medium supplemented with kanamycin (50 mg/mL) was centrifuged at 5000 g, 4 ºC for 15 min, and the obtained pellet was resuspended in 200 µL of fresh MGL liquid medium. The resulting concentrated bacterial suspension was used to infect 10-day-old *B. napus* seedlings sowed and grown as described above, and cultured on solid MS media (0.8% plant agar) under sterile conditions. For *A. rhizogenes* infection, a sterile needle tip was impregnated with the concentrated bacterial suspension, and two soft, little wounds were made along the stem of each seedling. Plantlets were then cultured *in vitro* for 3-4 additional weeks under the same conditions, and the numbers of roots produced were then registered.

6.2.5. Statistical analysis

Plant regeneration data were analyzed using the StatGraphics software. The Kruskal-Wallis test with $p \leq 0.05$ was used to detect statistically significant differences in plant regeneration and transformation rates.

6.3.Results and discussion

In this work we used three transformation and regeneration protocols (namely B, Z and A) previously described for *B. napus* with some modifications (Sparrow et al. 2006; Maheshwari et al. 2011). These protocols were assayed using the YC3.6-Bar, PM-YC3.6-LTI6b and pCRISPR plasmids. Hypocotyl and cotyledon explants were excised from *B. napus* donor plants (Table 5). In total, we excised and cultured 1,784 explants of the DH4079 line and 1,077 explants of the DH12075 line, which was used as a reference (control) of a previously transformed *B. napus* line (Wu et al. 2011; Wang et al. 2009). Each protocol was tested in the two *B. napus* lines, transforming them with different plasmids depending on the case. We first assessed the efficiency of plant regeneration of the three protocols used in this study (Table 5, "Plants/explant"), and then the number of regenerated explants successfully transformed (Table 5, "Positive plants/explant"). We found that the genotype and the plasmid type had no significant effect on the rate of plant regeneration, since no or very few regenerants were obtained from both lines and transformation events with protocols B and Z, but all lines and transformation events produced regenerants with protocol A. Protocol A was found to be significantly better than protocol B in terms of plant regeneration, estimated as the number of regenerated plants per explant (Table 6). The reasons for such better performance are discussed next.

Table 5. **Summary of the results of DH4079 and SH12075 *B. napus* transformation with the B, Z and A protocols.**

Genotype	Protocol	Plasmid	Resistance	Explants	Plants/explant	Percentage of positive plants
4079	B	YC3.6-Bar	BASTA	296	0.00	0%
4079	B	PM-YC3.6-LTI6b	Kanamycin	266	0.00	0%
12075	B	YC3.6-Bar	BASTA	285	0.00	0%
12075	B	PM-YC3.6-LTI6b	Kanamycin	403	0.00	0%
4079	Z	YC3.6-Bar	BASTA	138	0.00	0%
4079	Z	PM-YC3.6-LTI6b	Kanamycin	143	0.02	0%
12075	Z	YC3.6-Bar	BASTA	98	0.00	0%
12075	Z	PM-YC3.6-LTI6b	Kanamycin	138	0.46	0%
4079	A	YC3.6-Bar	BASTA	358	2.48	0%
4079	A	PM-YC3.6-LTI6b	Kanamycin	361	0.64	0%
4079	A	CRISPR	Kanamycin	222	0.12	0%
12075	A	CRISPR	Kanamycin	153	0.19	3.4%

Table 6. **Effect of the protocol in the regeneration capacity of plants.** Different letters indicate statistically significant differences according to LSD test ($p \leq 0.05$).

Protocol	Plants/Explant
B	0.00 ± 0.00 b
Z	0.12 ± 0.06 ab
A	1.10 ± 0.12 a

6.3.1. The selective agents have a critical role in plant regeneration

Protocol B was the only protocol that did not produce any plant (either transformed or not) per explant, while protocols Z and A were able to regenerate plants from both DH4079 and DH12075 lines (Table 5). Regeneration was, therefore, seriously compromised with protocol B. Interestingly, the only difference between protocols B and A is the time point of the addition of the selective agent to the culture medium (Fig 2). In protocol A, the selective agent was added to SOM medium, whereas in protocol B it was added earlier, to SRM medium, and this appeared to be crucial for the final fate of explants. We used a kanamycin concentration of 50 mg/L since it was previously described to combine moderate rates of escapes and regeneration for successful *B. napus* transformation (Fry et al. 1987). When 50 mg/L kanamycin was used in SRM medium (for explants transformed with the PM-YC3.6-LTI6b plasmid), few adventitious roots and leaves were produced from calli after one month of culture. After two months, all the calli from both DH4079 and DH12075 lines turned creamy or brown and arrested their growth, showing clear signs of necrosis in some cases (Figs 3A, B). No developed shoots were observed in any case. When SRM medium was supplemented with 10 mg/L BASTA (for explants transformed with the YC3.6-bar plasmid), the regeneration capacity of calli was completely inhibited. Neither adventitious organs nor shoots emerged from DH4079 or DH12075 calli and after two months of culture, all callus tissue was dead (Figs 3C, D). Thus, the use of selective agents in these conditions prevented shoot regeneration before callus death.

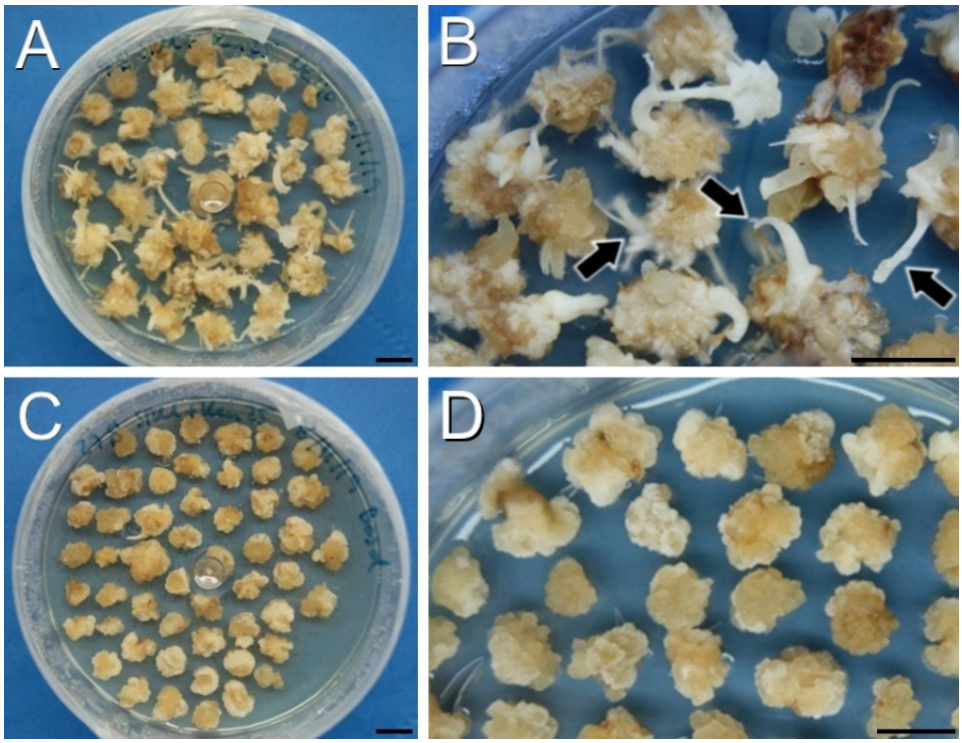

Fig 3. Callus production and growth using protocol B after one month. A, B: DH4079 calli in SRM supplemented with 50 mg/L kanamycin. Note the presence of adventitious organs (arrowheads in B) sin some of these calli. C, D: DH12075 calli in SRM supplemented with 10 mg/L BASTA. D: amplified image where the absence of regeneration is clear. Bars: 1 cm.

In protocol Z, cotyledons of the DH4079 and DH12075 lines were used as explants. With this protocol, callus formation and growth was more limited than with protocol B, but clear differences in terms of regeneration were observed between explants exposed to different selective agents. After one month growing in selection medium with 50 mg/L kanamycin, explants from PM-YC3.6-LTI6b transformation developed the first shoots (Fig 4A) and after two months, resistant (green) and susceptible (purple) shoots were observed (Fig 4B). However, explants grown on selection medium supplemented with 5 mg/L BASTA (for YC3.6-bar explants) did not develop any shoot. After one month of culture visible signs of necrosis appeared in the explants (Fig 4C) and after two months, all cotyledon explants died (Fig 4D). Thus, the use of kanamycin allowed for plant regeneration from explants whereas BASTA promoted their death.

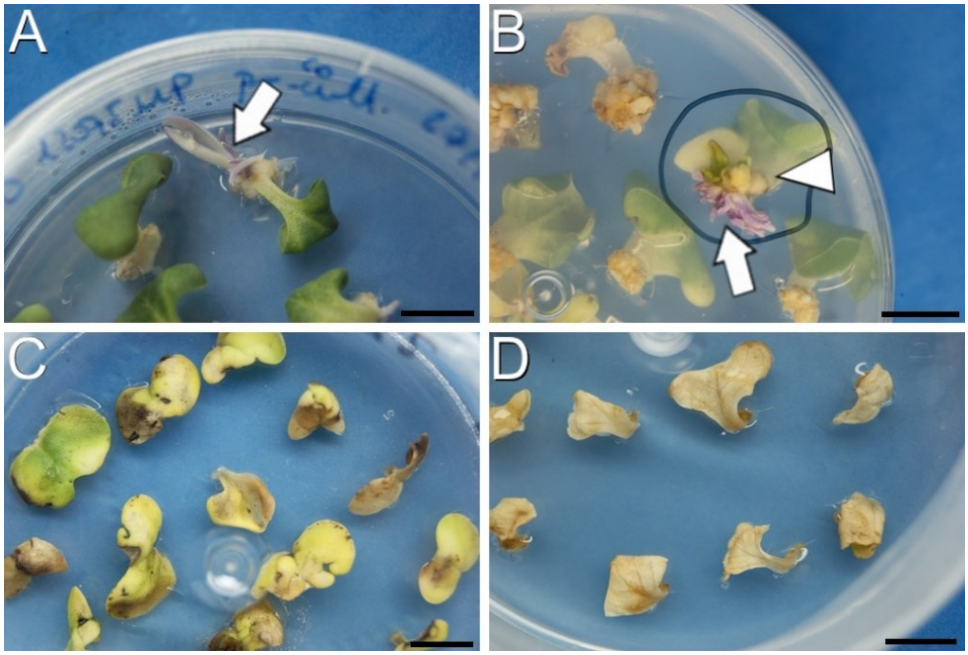

Fig 4. Callus production and growth using protocol Z. A: Cotyledons after one month in selection medium (50 mg/L kanamycin) showing a susceptible, purple shoot (arrow). B: Cotyledons after two months in selection medium (50 mg/L kanamycin) showing resistant, green shoots (arrowhead) and susceptible, purple shoots (arrow). C, D: Cotyledons after one (C) and two months (D) in selection medium with 5 mg/L BASTA. Bars: 1 cm.

The conditions of use of the selective agent in culture media has been reported as one of the main factors affecting transformation efficiency (Bhalla and Singh 2008). Indeed, in the *B. napus* cv. Westar, an increase in selection conditions from 50 to 100 mg/L kanamycin resulted in a reduction of non-transformed regenerated shoots (escape shoots), but the regeneration rate dropped down from 19% to 13% (Fry et al. 1987). However, kanamycin concentration seemed not to be a problem in our case, since for protocol A, regenerants were obtained with this concentration in both protocols B and Z. Instead, the problem in protocol B seemed the timepoint of addition of the selective agent. A similar effect of kanamycin in plant regeneration has already been described in other species as grapevine (Colby and Meredith 1990), carrot (Hardegger and Sturm 1998) and cotton (Zhang et al. 2001). A similar scenario appears to occur with the use of BASTA in protocol B. However, BASTA was toxic in protocol Z. In general, herbicides have not been commonly used as selective agents as much as

antibiotics due to the difficulty to establish efficient concentrations which permit tissue regeneration and transformed plant selection (Khuong et al. 2013), as it appears to occur in our *B. napus* explant transformations using BASTA in the selective medium. Such inhibitory effect of BASTA in plant regeneration has also been described at even lower concentrations in watermelon (Ganasan and Huyop 2010) and peach (Ricci et al. 2020). Therefore, the addition of the selective agent (either kanamycin or BASTA) in early steps of the protocol, when organogenesis is not yet initiated, results in an arrest of growth and organogenic differentiation, as well as the use of BASTA at both 5 (protocol Z) and 10 mg/L (protocol B).

6.3.2. The DH12075 line, but not DH4079, can be genetically transformed using protocol A

The protocol showing the highest plant regeneration ratio was protocol A (Tables 5, 6), where inoculation consisted in submersion of hypocotyl explants in the *Agrobacterium* suspension. With protocol A, calli were produced at the cuttings of hypocotyl explants after two weeks of culture (Fig 5A). Upon individualization of calli, the first evidences of shoot formation were visible after approximately four weeks of culture (Fig 5B, arrowheads) and, after six weeks, clearly visible, well formed shoots were visible (Fig 5C, arrowheads). Plants were produced from both DH4079 and DH12075 lines transformed with YC3.6-Bar, PM-YC3.6-LTI6b and pCRISPR. As opposed to the other protocols used, no differences were observed in terms of regeneration efficiency between the use of kanamycin and BASTA. After three weeks in SOM medium supplemented with carbenicillin and the corresponding selective agent, some plants turned whitish and stopped growing (Fig 5D, arrows), indicating sensitivity to the selective agent. Others were able to survive in the presence of the selective agent and kept growing green and vigorous, regenerating plantlets (Fig 5D, arrowheads). These results confirmed that it is possible to regenerate plantlets from *B. napus* DH4079 and DH12075 lines using protocol A, whose regeneration ability did not depend on the explant genotype or the type of selective agent used.

To assess whether regenerated green, growing plantlets incorporated the plasmid, they were genotyped by PCR with different primer pair combinations (Fig 1B). None of the regenerated plantlets from the DH4079 line tested positive for PCR (Fig 5E), whereas few plantlets regenerated from DH12075-excised explants were genotyped as positive (Fig 5F), being able to grow to fully regenerated transgenic plants (Figs 5G, H), which resulted in a calculated efficiency of 0.65% in terms of PCR-positive plants regenerated per explant. In all the transformation and regeneration events performed, there was a difference between the number of total and PCR-positive plants per explant, revealing the presence of *escapes* (Table 5), defined as plants resistant to selective agents but not transformed with the corresponding construct. This was particularly high in the case of the YC3.6-Bar experiments (2.48 plants per explant, but not a single PCR-positive plant). We speculate that this high occurrence of escapes could be due to not sufficiently restrictive concentrations of the corresponding selective agent, as also reported in other backgrounds (Fry et al. 1987). Notwithstanding this, we were unable to identify any single transformed DH4079 regenerant, which confirms the extreme recalcitrance of this DH line. Together, these results show that the *B. napus* DH lines DH12075 and DH4079 exhibit a remarkably low

transformation efficiency. In particular, the DH4079 line is recalcitrant to *Agrobacterium*-mediated transformation using the protocols described so far, including the modifications presented in this work.

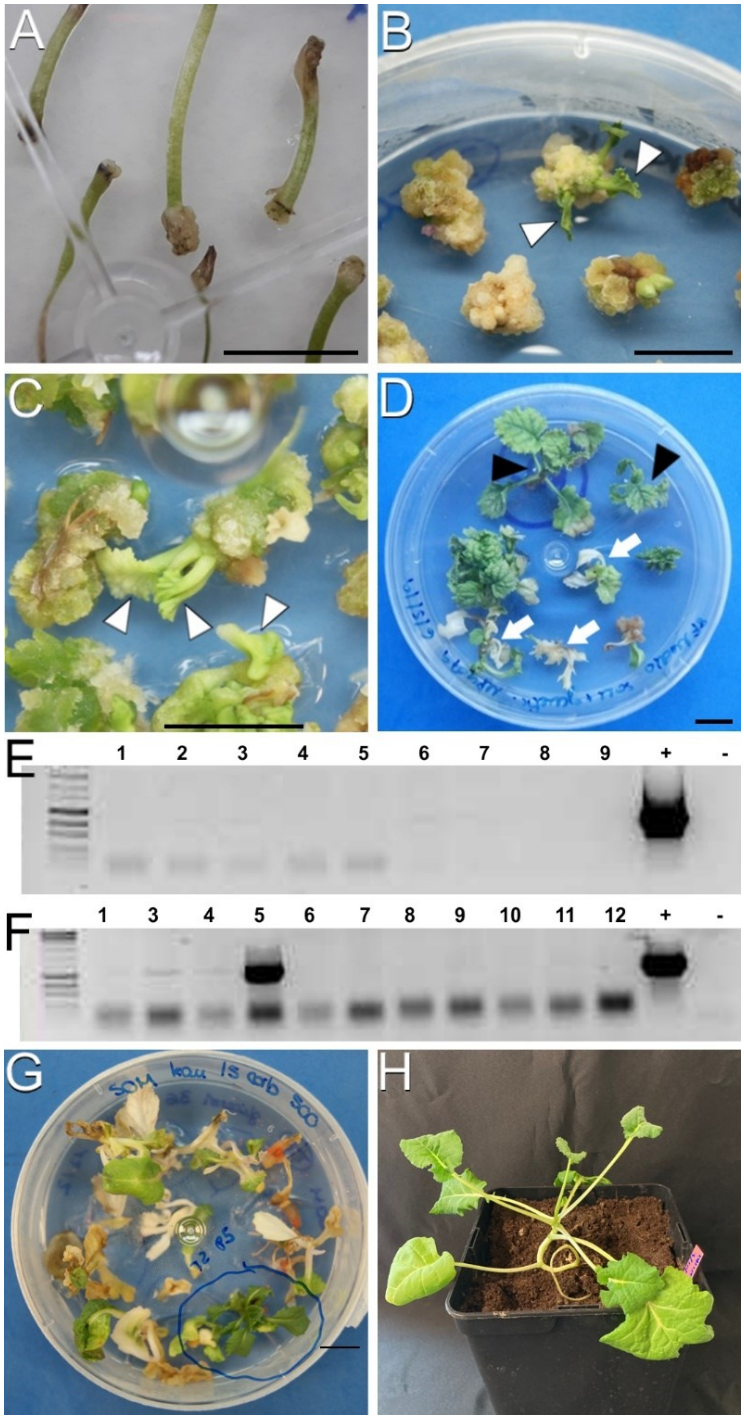

Fig 5. Callus production and plant regeneration using protocol A. A: Explants after 2 weeks in CIM + carbenicillin. B: Calli after 4 weeks in SRM + carbenicillin. Note the occurrence of some green shoots on the callus surface (arrowheads). C: Shoots (arrowheads) emerging from calli after 6 weeks in SRM + carbenicillin. D: Green, regenerated plantlets resistant to the selective agent (black arrowheads) and white, arrested shoots sensitive to the selective agent (white arrows) after three weeks in SOM + carbenicillin + kanamycin. E, F: PCR genotyping of green, transformed plants of the DH4079 (E) and DH12075 lines (F), using YC3.6 Fw and GFP 5' Rv primers. Plasmid DNA was used as PCR positive control (+) and water was used as negative control (-). Note the presence of a PCR-positive DNA sample in F, lane 5. G, H: Green regenerated transgenic *in vitro* (G) and acclimated (H) plant of the DH12075 line. Bars: 1 cm.

Traditionally, the DH4079 background has been considered as recalcitrant for transformation (Maheshwari et al. 2011). Indeed, despite the enormous practical applicability that the development of DH4079 lines transformed with different genetic markers would have for the study of microspore embryogenesis, no DH4079 transgenic lines have been reported up to date. Out of the 1,784 explants excised from DH4079 plants and transformed, we were not able to identify any single transgenic plant. This contrasts with the 13.4% of transformation efficiency previously reported for 62 DH4079 explants transformed and regenerated using the same protocol (Maheshwari et al. 2011). The reasons for such discrepancy are difficult to elucidate. Possible explanations could be the use of somehow different DH4079 plant material, or the residual presence of *A. tumefaciens* in the plant material used to analyze the efficiency of transformation. To avoid these potential problems, on the one hand, we are confident to be using the highly embryogenic *B. napus* DH4079 line, since we routinely perform microspore cultures with microspores isolated from plants of this line (Camacho-Fernández et al. 2021) and confirm their high embryogenic response. Moreover, plant samples for PCR where excised from leaves of regenerated plants at the 2-3 true leaf stage upon plant acclimation, avoiding possible *Agrobacterium* dragging within the sample. We used the same protocol previously published by Maheshwari et al. (Maheshwari et al. 2011) adapted to our experimental conditions, and obtained similar regeneration rates. Overall we obtained with such protocol a transformation efficiency for the DH12075 line similar to that previously described for the same line (Kazan et al. 1997). Therefore, we strongly believe that our data (both the successful transformation of DH12075 and the unsuccessful transformation of DH4079) are robust and consistent. The remarkably different amounts of DH4079 explants transformed, cultured and analyzed in both cases (1,784 in this work vs. 62 in Maheshwari et al. (Maheshwari et al. 2011)) support this notion. Therefore, we postulate that the DH4079 line of *B. napus* is recalcitrant to *A. tumefaciens*-mediated genetic transformation.

6.3.3. The *B. napus* DH4079 line is also recalcitrant to transient *A. rizhogenes* transformation

Different methods of transient plant transformation have been tried in *B. napus*, including for example *A. tumefaciens* transformation of microspore-derived embryos (Dubas et al. 2014) or microprojectile bombardment of isolated microspores combined with *A. tumefaciens* incubation (Abdollahi et al. 2009), but not infection with *Agrobacterium rhizogenes*. *A. rhizogenes,* a gram-negative, soil-borne bacterium, naturally harbors large Ri plasmids that contain genes that favor infection of plant tissues and transference of their DNA into host plant cells (Moore et al. 1979). However, as opposed to Ti plasmids from *A. tumefaciens*, Ri plasmids from *A. rhizogenes* induce the formation of hairy roots in the infected plant tissue (Moore et al. 1979). Thus, genetic manipulation of these plasmids has allowed to establish protocols for transient plant transformation in different species, including *B. napus* (Christey and Sinclair 1992). We used this method to evaluate whether our *B. napus* lines show a response similar or different from that of *A. tumefaciens* transformation. We infected with *A. rhizogenes* hypocotyls of one-week-old entire plants of both DH12075 and DH4079 lines, and analyzed the occurrence of morphogenic processes as a consequence of infection after 3-4

weeks. In DH12075 we found plants with no specific response to infection, plants producing a callus at the site of wounding for infection, and plants developing large hairy roots at the site of infection, whereas DH4079 only presented plants with no specific response or with callus production (Fig 6A).

Fig 6. Response of *B. napus* DH12075 and DH4079 to transient *A. rhizogenes* infection. A: The infected DH12075 plants (left) show in some cases no specific response, and in others callus formation (arrowhead) or formation of adventitious roots (arrow). In contrast, DH4079 plants (right) only show either no specific response in some plants or just callus formation (arrowhead) in others. B: Comparison of the percentages of root and callus formation in DH12075 and DH4079. Bar: 1 cm.

The percentage of plants producing calli was similar for both lines, ranging between ~10-15% (Fig 6B), what may indicate a plant response to wound rather than to bacterial infection. However, there was a remarkable difference in root production upon infection, which revolved around 50% for DH12075, but was null for DH4079 (Fig 6B). These results confirmed the recalcitrance of DH4079 to agrobacterium transformation, not only with *A. tumefaciens* but also with *A. rhizogenes*. A recent work reported the formation of hairy roots from both DH12075 and DH4079 when infected with a modified *A. tumefaciens* strain carrying a Ri hairy-root-inducing plasmid (Jedličková et al. 2022). Hairy roots developed from 97% and 42% of the infected DH12075 and DH4079 seedlings, respectively, but transgenic plants were only possible to regenerate from transformed and cultured DH12075 roots (Jedličková et al. 2022). This transformation approach using engineered *A. tumefaciens* with Ri plasmid is essentially different from the protocols used in the present work and may open an alternative approach to produce transgenic *B. napus* lines upon plant regeneration from transformed roots in different genotypes, including DH12075. However, it also failed in achieving stable transformation of DH4079. These observations, together with the work presented in this manuscript, support the

notion that the DH4079 line is extremely recalcitrant to *Agrobacterium* transformation.

6.3.4. A possible relationship between genetic transformation and doubled haploidy?

Within the *Brassica* genus, efficiencies of stable transformation are quite variable, ranging between 0.59-1.56% for wucai (*B. campestris)* (Chen et al. 2019), 2.2-10.83% for Chinese cabbage (*B. rapa* ssp. *Pekinensis)* (Park et al. 2005; Li et al. 2021), 2.7-6.4% for broccoli (*B. oleracea* var. *italica)* (Chen et al. 2001), ~7% for *B. juncea* (Naeem et al. 2020), 7-13.6% for *B. oleraceae* var *Botrytis* (Bhalla and Smith 1998; Chakrabarty et al. 2002) and as high as 32.5-45% for cabbage (*B. oleracea* subsp. *capitata*), depending on the explant type (shoot tips and hypocotyls, respectively) (Rafat et al. 2010). As to *B. napus*, the efficiency reported by different works was highly dependent on the genetic background used. In commercial cultivars such as Oscar and RK7, an efficiency of up to 67% was reported (Zhang et al. 2005). In cv. Westar, a range of transformation efficiency of 7-33%, depending on *in vitro* conditions, was reported (Fry et al. 1987; Zhang et al. 2005). Interestingly, when fully homozygous, DH plants derived from Westar were used in similar experimental conditions, the transformation efficiency dropped down to 0.3-3% (Kazan et al. 1997). Whether these differences are due to different specific experimental conditions, or to allele fixation derived from the process of chromosome doubling inherent to DH production (Seguí-Simarro et al. 2021), is not known. However, the transformation efficiency reported in our work for DH12075, a Westar-derived DH line, was 0.65%, which fits within the range of efficiencies reported for DH backgrounds (Kazan et al. 1997). This supports the hypothesis that recalcitrance to transformation could be influenced by the degree of gene fixation in a partially allogamous species such as *B. napus*.

Finally, it is also worth to mention that DH4079, in addition to being recalcitrant to transformation, is one of the backgrounds most responsive to induction of microspore embryogenesis for DH production (Ferrie and Möllers 2011). In parallel, some of the *B. napus* backgrounds where genetic transformation has been proven efficient or at least possible, such as Westar and DH12075, are also known to show a very low or null response to induction of microspore embryogenesis (Malik et al. 2008; Corral-Martinez et al. 2020). Interestingly, it is also known that *Arabidopsis thaliana*, a model species for genetic studies where genetic transformation is very well developed and widely used for decades, is extremely recalcitrant to microspore embryogenesis, with no successful reports of induction of such morphogenic process published to date. The scenario in tomato, another plant model species, is similar: transformation has been successfully achieved, but its extreme recalcitrance to microspore embryogenesis is widely acknowledged. Thus, there seems to be an inverse relationship between the ability for genetic transformation and the response to induction of microspore embryogenesis. This could be an interesting hypothesis to elucidate in future research.

References

Abdollahi MR, Corral-Martinez P, Mousavi A, Salmanian AH, Moieni A, Seguí-Simarro JM (2009) An efficient method for transformation of pre-androgenic, isolated *Brassica napus* microspores involving microprojectile bombardment and *Agrobacterium*-mediated transformation. Acta Physiol Plant 31 (6):1313-1317. doi:10.1007/s11738-009-0365-5

Bhalla PL, Singh MB (2008) *Agrobacterium*-mediated transformation of *Brassica napus* and *Brassica oleracea*. Nature Protocols 3 (2):181-189

Bhalla PL, Smith N (1998) *Agrobacterium tumefaciens*-mediated transformation of cauliflower, *Brassica oleracea* var. botrytis. Mol Breed 4 (6):531-541. doi:10.1023/a:1009658614579

Camacho-Fernández C, Seguí-Simarro JM, Mir R, Boutilier K, Corral-Martínez P (2021) Cell Wall Composition and Structure Define the Developmental Fate of Embryogenic Microspores in *Brassica napus*. Front Plant Sci 12 (2260). doi:10.3389/fpls.2021.737139

Colby SM, Meredith CP (1990) Kanamycin sensitivity of cultured tissues of *Vitis*. Plant Cell Rep 9 (5):237-240

Corral-Martínez P, Camacho-Fernández C, Mir R, Seguí-Simarro JM (2021) Doubled haploid production in high- and low-response genotypes of rapeseed (*Brassica napus*) through isolated microspore culture. In: Seguí-Simarro JM (ed) Doubled Haploid Technology, vol 2: Hot Topics, Apiaceae, Brassicaceae, Solanaceae. Methods in Molecular Biology, vol 2288, 1st edn. Springer Science+Business Media, LLC, New York, USA, pp 129-144. doi:10.1007/978-1-0716-1335-1_8

Corral-Martinez P, Siemons C, Horstman A, Angenent GC, de Ruijter N, Boutilier K (2020) Live Imaging of embryogenic structures in *Brassica napus* microspore embryo cultures highlights the developmental plasticity of induced totipotent cells. Plant Reprod 33 (3-4):143-158. doi:10.1007/s00497-020-00391-z

Custers JBM, Cordewener JHG, Fiers MA, Maassen BTH, van Lookeren-Campagne MM, Liu CM (2001) Androgenesis in *Brassica*: a model system to study the initiation of plant embryogenesis. In: Bhojwani SS, Soh WY (eds) Current trends in the embryology of angiosperm. Kluwer Academic Publishers, Dordrecht, The Netherlands, pp 451-470

Chakrabarty R, Viswakarma N, Bhat S, Kirti P, Singh B, Chopra V (2002) *Agrobacterium*-mediated transformation of cauliflower: optimization of protocol and development of Bt-transgenic cauliflower. Journal of Biosciences 27 (5):495-502

Chen G, Zeng F, Wang J, Ye X, Zhu S, Yuan L, Hou J, Wang C (2019) Transgenic Wucai (*Brassica campestris* L.) produced via *Agrobacterium*-mediated anther transformation in planta. Plant Cell Rep 38 (5):577-586

Chen L-FO, Hwang J-Y, Charng Y-Y, Sun C-W, Yang S-F (2001) Transformation of broccoli (*Brassica oleracea* var. italica) with isopentenyltransferase gene via *Agrobacterium tumefaciens* for post-harvest yellowing retardation. Mol Breed 7 (3):243-257

Christey MC, Sinclair BK (1992) Regeneration of transgenic kale (*Brassica oleracea* var. acephala), rape (*B. napus*) and turnip (*B. campestris* var. rapifera) plants via *Agrobacterium rhizogenes* mediated transformation. Plant Sci 87 (2):161-169. doi:https://doi.org/10.1016/0168-9452(92)90147-E

Dai C, Li Y, Li L, Du Z, Lin S, Tian X, Li S, Yang B, Yao W, Wang J (2020) An efficient *Agrobacterium*-mediated transformation method using hypocotyl as explants for *Brassica napus*. Mol Breed 40 (10):1-13

Dubas E, Moravčíková J, Libantová J, Matušíková I, Benková E, Żur I, Krzewska M (2014) The influence of heat stress on auxin distribution in transgenic *B. napus* microspores and microspore-derived embryos. Protoplasma:1-11. doi:10.1007/s00709-014-0616-1

Ferrie A, Möllers C (2011) Haploids and doubled haploids in *Brassica* spp. for genetic and genomic research. Plant Cell Tissue Organ Cult 104 (3):375-386. doi:10.1007/s11240-010-9831-4

Fry J, Barnason A, Horsch RB (1987) Transformation of *Brassica napus* with *Agrobacterium tumefaciens* based vectors. Plant Cell Rep 6 (5):321-325

Ganasan K, Huyop F (2010) The sensitivity of plant tissue culture and plant cell of *Citrullus lanatus* cv. Round dragon against BASTA. Int J Agr Res 5:11-18

Gocal GF (2021) Gene editing in *Brassica napus* for basic research and trait development. In Vitro Cellular & Developmental Biology-Plant 57 (4):731-748

Hardegger M, Sturm A (1998) Transformation and regeneration of carrot (*Daucus carota* L.). Mol Breed 4 (2):119-127

Hopp HE, Spangenberg G, Herrera-Estrella L (2022) Editorial: Plant Transformation. Front Plant Sci 13. doi:10.3389/fpls.2022.876671

Hua K, Zhang J, Botella JR, Ma C, Kong F, Liu B, Zhu J-K (2019) Perspectives on the Application of Genome-Editing Technologies in Crop Breeding. Mol Plant 12 (8):1047-1059. doi:https://doi.org/10.1016/j.molp.2019.06.009

GM Approval Database [last accessed May 23rd 2022] (2022).

Jedličková V, Mácová K, Štefková M, Butula J, Staveníková J, Sedláček M, Robert HS (2022) Hairy root transformation system as a tool for CRISPR/Cas9-directed genome editing in oilseed rape (*Brassica napus*). Front Plant Sci 13:919290. doi:10.3389/fpls.2022.919290

Jouannic S, Champion A, Seguí-Simarro JM, Salimova E, Picaud A, Tregear J, Testillano P, Risueno MC, Simanis V, Kreis M, Henry Y (2001) The protein kinases AtMAP3Kε1 and BnMAP3Kε1 are functional homologues of *S. pombe* cdc7p and may be involved in cell division. Plant J 26 (6):637-649

Kazan K, Curtis MD, Goulter KC, Manners JM (1997) *Agrobacterium tumefaciens*-mediated transformation of double haploid canola (*Brassica napus*) lines. Functional Plant Biology 24 (1):97-102. doi:https://doi.org/10.1071/PP96024

Khuong TTH, Crété P, Robaglia C, Caffarri S (2013) Optimisation of tomato Micro-tom regeneration and selection on glufosinate/Basta and dependency of gene silencing on transgene copy number. Plant Cell Rep 32 (9):1441-1454

Klümper W, Qaim M (2014) A Meta-Analysis of the Impacts of Genetically Modified Crops. PLoS ONE 9 (11):e111629. doi:10.1371/journal.pone.0111629

Krebs M, Held K, Binder A, Hashimoto K, Den Herder G, Parniske M, Kudla J, Schumacher K (2012) FRET-based genetically encoded sensors allow high-resolution live cell imaging of Ca^{2+} dynamics. Plant J 69 (1):181-192. doi:10.1111/j.1365-313X.2011.04780.x

Li X, Li H, Zhao Y, Zong P, Zhan Z, Piao Z (2021) Establishment of a simple and efficient *Agrobacterium*-mediated genetic transformation system to Chinese Cabbage (*Brassica rapa* L. ssp. pekinensis). Horticultural Plant Journal 7 (2):117-128

Maheshwari P, Selvaraj G, Kovalchuk I (2011) Optimization of *Brassica napus* (canola) explant regeneration for genetic transformation. New Biotechnol

Malik MR, Wang F, Dirpaul J, Zhou N, Hammerlindl J, Keller W, Abrams SR, Ferrie AMR, Krochko JE (2008) Isolation of an embryogenic line from non-embryogenic *Brassica napus* cv. Westar through microspore embryogenesis. J Exp Bot 59 (10):2857-2873. doi:10.1093/jxb/ern 149

Moloney MM, Walker JM, Sharma KK (1989) High efficiency transformation of *Brassica napus* using *Agrobacterium* vectors. Plant Cell Rep 8:238-242

Moore L, Warren G, Strobel G (1979) Involvement of a plasmid in the hairy root disease of plants caused by *Agrobacterium rhizogenes*. Plasmid 2 (4):617-626. doi:https://doi.org/10.1016/0147-619X(79)90059-3

Naeem I, Munir I, Durrett TP, Iqbal A, Aulakh KS, Ahmad MA, Khan H, Khan IA, Hussain F, Shuaib M (2020) Feasible regeneration and agro bacterium-mediated transformation of *Brassica juncea* with *Euonymus alatus* diacylglycerol acetyltransferase (EaDAcT) gene. Saudi journal of biological sciences 27 (5):1324-1332

Park B-J, Liu Z, Kanno A, Kameya T (2005) Genetic improvement of Chinese cabbage for salt and drought tolerance by constitutive expression of a *B. napus* LEA gene. Plant Sci 169 (3):553-558

Rafat A, Abd Aziz M, Abd Rashid A, Abdullah SNA, Kamaladini H, Sirchi MT, Javadi M (2010) Optimization of *Agrobacterium tumefaciens*-mediated transformation and shoot regeneration after co-cultivation of cabbage (*Brassica oleracea* subsp. capitata) cv. KY Cross with AtHSP101 gene. Sci Hort 124 (1):1-8

Ricci A, Sabbadini S, Prieto H, Padilla IM, Dardick C, Li Z, Scorza R, Limera C, Mezzetti B, Perez-Jimenez M (2020) Genetic transformation in peach (*Prunus persica* L.): challenges and ways forward. Plants 9 (8):971

Ron M, Kajala K, Pauluzzi G, Wang D, Reynoso MA, Zumstein K, Garcha J, Winte S, Masson H, Inagaki S, Federici F, Sinha N, Deal RB, Bailey-Serres J, Brady SM (2014) Hairy root transformation using *Agrobacterium rhizogenes* as a tool for exploring cell type-specific gene expression and function using tomato as a model. Plant Physiol 166 (2):455-469. doi:10.1104/pp.114.239392

Satpute G, Long H, Seguí-Simarro JM, Risueño MC, Testillano PS (2005) Cell architecture during gametophytic and embryogenic microspore development in *Brassica napus*. Acta Physiol Plant 27 (4B):665-674. doi:10.1007/s11738-005-0070-y

Seguí-Simarro JM, Jacquier NMA, Widiez T (2021) Overview of i*n vitro* and *in vivo* doubled haploid technologies. In: Seguí-Simarro JM (ed) Doubled Haploid Technology, vol 1: General Topics, Alliaceae, Cereals. Methods in Molecular Biology, vol 2287, 1st edn. Springer Science+Business Media, LLC, New York, USA, pp 3-22. doi:10.1007/978-1-0716-1315-3_1

Sheng X, Yu H, Wang J, Shen Y, Gu H (2022) Establishment of a stable, effective and universal genetic transformation technique in the diverse species of *Brassica oleracea*. Front Plant Sci 13. doi:10.3389/fpls.2022.1021669

Sparrow PAC, Dale PJ, Irwin JA (2006) *Brassica oleracea*. In: Wang K (ed) *Agrobacterium* Protocols. Humana Press, Totowa, NJ, pp 417-426. doi:10.1385/1-59745-130-4:417

van Montagu M (2011) It Is a Long Way to GM Agriculture. Ann Rev Plant Biol 62 (1):1-23. doi:doi:10.1146/annurev-arplant-042110-103906

Vazquez-Vilar M, Bernabé-Orts JM, Fernandez-Del-Carmen A, Ziarsolo P, Blanca J, Granell A, Orzaez D (2016) A modular toolbox for gRNA-Cas9 genome engineering in plants based on the GoldenBraid standard. Plant Methods 12:10-10. doi:10.1186/s13007-016-0101-2

Wang Y, Beaith M, Chalifoux M, Ying J, Uchacz T, Sarvas C, Griffiths R, Kuzma M, Wan J, Huang Y (2009) Shoot-specific down-regulation of protein farnesyltransferase (α-subunit) for yield protection against drought in canola. Mol Plant 2 (1):191-200

Wang Y, Sonntag K, Rudloff E, Han J (2005) Production of fertile transgenic *Brassica napus* by *Agrobacterium*-mediated transformation of protoplasts. Plant Breed 124 (1):1-4

Weyen J (2021) Applications of doubled haploids in plant breeding and applied research. In: Seguí-Simarro JM (ed) Doubled Haploid Technology, vol 1: General Topics, Alliaceae, Cereals. Methods in Molecular Biology, vol 2287, 1st edn. Humana Press, New York, USA, pp 23-39. doi:10.1007/978-1-0716-1315-3_2

Wu L, El-Mezawy A, Shah S (2011) A seed coat outer integument-specific promoter for *Brassica napus*. Plant Cell Rep 30 (1):75-80

Zhang B-H, Liu F, Liu Z-H, Wang H-M, Yao C-B (2001) Effects of kanamycin on tissue culture and somatic embryogenesis in cotton. Plant Growth Regul 33 (2):137-149

Zhang Y, Singh MB, Swoboda I, Bhalla PL (2005) *Agrobacterium*-mediated transformation and generation of male sterile lines of Australian canola. Australian Journal of Agricultural Research 56 (4):353-361. doi:https://doi.org/10.1071/AR04175

7. Chapter 5: Modulation of Ca^{2+} in *Brassica napus* microspore embryogenesis

Antonio Calabuig-Serna, Ricardo Mir, Paloma Arjona, Rosa Porcel, Jose María Seguí-Simarro.

Cell Biology Group - COMAV Institute, Universitat Politècnica de València, 46022 Valencia, Spain.

Keywords: Androgenesis, calcium*, in vitro* culture, *in vitro* embryogenesis, morphogenesis, rapeseed.

In this research work, Antonio Calabuig-Serna contributed in the processes of investigation, methodology, data curation, formal analysis, and writing, reviewing and editing the draft.

Abstract

Calcium (Ca^{2+}) is a universal signaling cation with a prominent role as second messenger in many different plant processes, including sexual reproduction. However, there is much less knowledge about the involvement of Ca^{2+} during *in vitro* embryogenesis processes. In this work we performed a study of Ca^{2+} levels during the different stages of microspore embryogenesis in *Brassica napus*, with especial attention to the different embryogenic structures with different embryogenic potential formed after induction and how Ca^{2+} can influence their occurrence. We also performed a pharmacological study to modulate Ca^{2+} homeostasis during different stages of the process using a series of Ca^{2+}-altering chemicals (BAPTA-AM, chlorpromazine, cyclopiazonic acid, EGTA, inositol 1,4,5-trisphosphate, ionophore A23187, W-7). This study shows that Ca^{2+} increase can be considered as an early marker of induction to microspore embryogenesis. Besides, Ca^{2+} levels are highly dynamic and flexible during microspore embryogenesis, determining the final embryo yield. Increase of either extracellular or intracellular Ca^{2+} level is sufficient to improve embryo yield by increasing the amount of microspores reaching the minimum Ca^{2+} level required to be induced to embryogenesis. Cultured microspores would react to increases in extracellular Ca^{2+} levels by increasing Ca^{2+} influx. Accordingly, inhibition of Ca^{2+} uptake or signalling results in reduced embryogenic response. This can be used to modulate embryo yield within a functional lower and upper Ca^{2+} threshold beyond which, embryo yield is reduced. There seems to be a clear positive link of Ca^{2+} with embryo differentiation, more than with undifferentiated cell proliferation.

7.1.Introduction

Hybrid seed, which is by far the most used worldwide, is produced by crossing two homozygous (pure) parental lines. Pure lines can be generated by multiple self-crossing generations, which may last up to 7-10 years depending on the species and the desired homozygosity degree. Alternatively, *in vitro* culture of immature gametophytes produces haploid embryos that, either naturally or in an induced manner, can develop doubled haploid (DH), fully homozygous individuals in a single generation (Seguí-Simarro et al. 2021a). Up to date, protocols to produce haploids or DHs have been reported for nearly 400 species (Seguí-Simarro et al. 2021b). One of the androgenic pathways for DH production is microspore embryogenesis, whereby vacuolated microspores or young pollen grains deviate from their natural gametophytic fate towards embryogenesis (Seguí-Simarro 2010). Factors such as the developmental stage of isolated microspores/pollen, the growth conditions of donor plants or their genotype, are key to determine the embryogenic response of microspores (Rivas-Sendra et al. 2020; Seguí-Simarro 2010). Indeed, not all genotypes are prone to induction. Whereas some species such as *Brassica napus* or tobacco are highly embryogenic (Camacho-Fernández et al. 2021; Seguí-Simarro 2016; Nitsch and Nitsch 1969), the response of other species such as eggplant or pepper is still limited or null, as in tomato (Mir et al. 2021; Seguí-Simarro 2016). Even within the same species, there are enormous differences among genotypes, as is the case in *B. napus* for the highly responding DH4079 line and the low-response DH12075 line (Corral-Martínez et al. 2021). The *in vitro* culture conditions, including the type of

inductive treatment applied and the composition of the culture medium, are also key factors. As seen, there are many different intervening factors whose elucidation would help to improve the efficiency of the process, principally in recalcitrant backgrounds. However, the nature of the triggering signal that transform microspores into embryos remains elusive.

Calcium in its cationic form (Ca^{2+}) is a fast and universal signaling element acting as a second messenger in multiple plant processes, including stress response, cell division and growth, pollen development, and embryogenesis and establishment of embryo polarity (Hause et al. 1994; Tian et al. 2020). Signaling is mediated by binding principally to calmodulin (CaM), a Ca^{2+}-dependent protein that regulates the activity of a diverse array of enzymes, ion channels, and other proteins with many diverse roles in cell function. Ca^{2+} signaling is involved on the induction of *in vitro* somatic embryogenesis (Overvoorde and Grimes 1994; Mahalakshmi et al. 2007; Calabuig-Serna et al. 2023b). Indeed, addition of Ca^{2+} to the induction medium enhances somatic embryo yield (Calabuig-Serna et al. 2023a; Jansen et al. 1990; Ramakrishna et al. 2012). As to microspore embryogenesis, induction in most species involves the application of a heat stress. The first perception of heat stress occurs through changes in plasma membrane fluidity which, together with the activation of stress-specific Ca^{2+} permeable channels, causes a transient increase in cytoplasmic Ca^{2+} levels, which leads to increased Ca^{2+}-CaM binding and the expression of several heat shock (HS) genes (Liu et al. 2005). In wheat, Reynolds (2000) deduced that external Ca^{2+} is required for embryogenic commitment, where it plays a role in signal transduction, since both reduced Ca^{2+} concentrations in the medium and CaM inhibition suppressed embryogenesis induction. Similarly, Ca^{2+} was associated to enhanced induction frequency and improved embryo structure in *Solanum carolinense* (Reynolds 1990), *Hordeum vulgare* (Hoekstra et al. 1997) or *Triticum aestivum* (Cho and Kasha 1995).

Traditionally, the dynamics of Ca^{2+} levels in plant embryogenesis has been studied using three principal approaches: Ca^{2+} modulators to alter Ca^{2+} levels, CaM-interacting chemicals to interfere with Ca^{2+} binding to CaM, and Ca^{2+} probes and sensors to track changes in Ca^{2+} levels. For example, to study the role of Ca^{2+} during somatic embryogenesis, the ionophore A23187 has been used to increase Ca^{2+} permeability of the plasma membrane, BAPTA and EGTA for Ca^{2+} chelation, or W-7 as CaM antagonist (Jansen et al. 1990; Takeda et al. 2003; Rivera-Solís et al. 2018; Calabuig-Serna et al. 2023b; Overvoorde and Grimes 1994). Ca^{2+} sensors such as the genetically-encoded *cameleon* construct are FRET-based tools very convenient for the detection of small and transient Ca^{2+} changes (Krebs et al. 2012), and have been previously used to detect calcium dynamics during somatic embryogenesis in arabidopsis and carrot (Krebs et al. 2012; Calabuig-Serna et al. 2023b; Calabuig-Serna et al. 2023a). However, this technology relies on the availability of efficient protocols for genetic transformation, which is not the case for the DH4079 *B. napus* line.

As to Ca^{2+} probes, Ca^{2+}-binding fluorescent stains such as chlortetracycline, Indo-1, Fura2, or their acetoxymethyl ester (AM) forms that allow for a free passive passage through the plasma membrane, have been used for decades for visualization and quantification of intracellular Ca^{2+} (Ramakrishna et al. 2011;

Overvoorde and Grimes 1994; Bush and Jones 1987). Although informative, some of these dyes have limited cell penetration and preclude *in vivo* Ca^{2+} observation. Alternatively, FluoForte is an AM, Ca^{2+}-binding fluorescent probe that solves some of the problems of previous probes and has proven useful to detect Ca^{2+} changes at specific time points. Using FluoForte to study microspore embryogenesis, it was shown in the *B. napus* DH4079 line that Ca^{2+} levels at the stages most sensitive to embryogenesis induction are higher than at earlier or later stages, and just during the HS, Ca^{2+} levels increase even more, and then decrease (Rivas-Sendra et al. 2017). It was also observed that in microspores issolated from low-responsive materials like eggplant or the *B. napus* DH12075 line, Ca^{2+} levels were lower than those of the high response DH4079 line (Rivas-Sendra et al. 2019). Thus, there is a clear relationship between Ca^{2+} levels and embryogenic competence.

More recently, time-lapse imaging experiments revealed that few days after induction, DH12075 microspores form four types of embryogenic structures (Corral-Martinez et al. 2020): (1) the exine-enclosed (EE) structures, which are abundant, globular and compact cell structures fully surrounded by exine; (2) loose bicelular structures (LBS), which are less frequent embryogenic structures formed by two usually asymmetrically divided structures, sometimes with loosely connected cells and exine breaks, which soon differentiate into suspensor-bearing embryos (SUS); (3) compact callus (CC), abundant irregular cell masses with the exine broken and sometimes detached; and (4) loose callus (LC), scarce callus masses characterized by their very irregular morphology, low intercellular adhesion and extended areas devoid of exine. Irrespective of their frequency, each structure has different potential to become embryo, being EE and LBS/SUS considered highly embryogenic as many of them transform into viable embryos, whereas CC and LC are considered barely embryogenic because they never or very rarely, respectively, become embryos (Corral-Martinez et al. 2020). Later on, these four types of structures were also described in the high-response DH4079 line, and specific cell wall features were found associated to their different embryogenic competences (Camacho-Fernández et al. 2021). Despite the clear relationship between Ca^{2+} and embryogenic competence, there are no clues about a possible involvement of Ca^{2+} in the occurrence of these different structures, in their different embryogenic potential, or in the modulation of the final embryo yield.

In this work, we performed an exhaustive study of Ca^{2+} dynamics using FluoForte staining during different stages of microspore embryogenesis in the DH4079 *B. napus* line, paying especial attention to the stages when the different embryogenic structures are formed, and how Ca^{2+} is distributed in their different cell domains. We also performed a pharmacological study to analyze the effect of different modulators of Ca^{2+} homeostasis during different stages of the process. We added to the culture medium different chemicals to increase and to reduce intracellular and extracellular Ca^{2+} levels, to block ER Ca^{2+} pumps, and to interfere with Ca^{2+}-CaM binding. Altogether, these results show that Ca^{2+} levels are highly dynamic during microspore embryogenesis and determine the final embryo yield.

7.2.Materials and Methods

7.2.1. Plant material

DH4079, a high-response doubled haploid line selected from the *B. napus* Topas cultivar was used for all the experiments. Plants were grown in a growth chamber at 23°C during their vegetative growth period. Upon blooming, plants were transferred to chambers at 15 °C. Flower buds were collected at least one week after transference to 15 °C.

7.2.2. Microspore culture

Microspore cultures were performed according to Corral-Martínez et al. (2021). Flower buds were collected from donor plants, measured and separated by size in three different ranges: 3.0-3.1, 3.2-3.3 and 3.4-3.5 mm. Microspores of the three ranges were processed and cultured in parallel, and only results from the best responding range were considered. Flower buds were transferred to tea sieves and surface-sterilized in the laminar flow hood by submerging them in 70% ethanol for 30 s and 10% bleach solution for 10 min. Then floral buds were rinsed three times in sterile distilled water and transferred to three sterile 50 ml glass beakers. Filtered NLN-13, consisting of NLN salts and vitamins (Nitsch and Nitsch 1967), (Duchefa, Netherlands) supplemented with 130 g/L sucrose, pH 5.8, was used to isolate microspores. Buds were crushed with a sterile syringe piston to release microspores in NLN-13. The resulting microspore suspension was then filtered through a 41 μm nylon filter, and washed two times with 10 ml of NLN-13 medium. For this purpose, tubes containing microspore suspensions were centrifuged at 800 rpm for 4 minutes at 4 °C in a refrigerated Eppendorf Centrifuge 5804R equipped with A-4-44 rotor. Finally, pelleted microspores were resuspended in 1 ml NLN-13 medium and the microspore density was estimated using a Improved Neubauer chamber as described (Camacho-Fernández et al. 2018). The final volume was adjusted by adding NLN-13 medium until reaching a density of 20.000 microspores/ml, and 500 μl of suspension were plated in each well of 24-well sterile plates. The induction treatment consisted of a 32 °C heat shock for 3 days, after which plates were transferred to 25 °C. Microspores were kept under darkness conditions along the whole in vitro culture process. Embryo yield was measured by counting the total number of embryos in each well after one month in culture.

7.2.3. Fluorescence and confocal microscopy

FluoForte (Enzo Life Sciences, ENZ-52015) staining was used to observe Ca^{2+} in microspores following Rivas-Sendra et al. (2019) indications. Briefly, microspores were centrifuged 4 minutes at 200 g at room temperature, resuspended in PBS and centrifuged again. Precipitated microspores were resuspended in equal volumes of PBS and 0.2 g/l FluoForte solution. Samples were incubated 30 minutes in darkness, washed with PBS and centrifuged 2 minutes at 200 g. Microspores were mounted with microscope slides with Mowiol anti-fading mounting solution (17% Mowiol 4–88 from Sigma-Aldrich +33% glycerol, v/v, in PBS). Samples were observed in a Zeiss 780 Axio Observer confocal microscope using an excitation wavelength of 488 nm and recording emission at 516 nm, and in a Nikon E1000 Fluorescence Microscope.

7.2.4. Quantification of size and fluorescence intensity

Quantification of area and FluoForte-specific fluorescence intensity was performed using the FIJI software (Schindelin et al. 2012). For each studied structure, paired bright field and fluorescence images were taken. The perimeter, excluding the exine coat, was delineated in the bright field image, generating a Region of Interest (ROI) that was transferred to the fluorescence image, where area and signal intensity were estimated using the *Area* and *Mean gray value* tools. Day 3 microspores were discriminated by size using a threshold of 720 μm^2, which is the area of the largest microspore measured at day 0, prior to induction. Thus, day 3 microspores with an area lower than 720 μm^2 were considered as not growing, since after 3 days they did not exceed the size of the largest day-0 microspore, whereas those with an area higher than 720 μm^2 were considered as growing. The Kruskal-Wallis non-parametric test ($p \leq 0.05$) was used to determine differences between medians. Paired comparisons among samples waere performed using the Bonferroni procedure ($p<0.05$). All fluorescence intensity measurements were made under identical experimental conditions.

7.2.5. Chemical treatments

$Ca(NO_3)_2$ was used as an additional source of Ca^{2+}. Ionophore A23187 was used as a Ca^{2+} channel to alter Ca^{2+} gradients. To release intracellular Ca^{2+}, inositol 1,4,5-trisphosphate ($InsP_3$) was used. 1,2-Bis(2-aminophenoxy)ethane-N,N,N',N'-tetraacetic acid tetrakis acetoxymethyl ester (BAPTA-AM) and ethylene glycol-bis(β-aminoethyl ether)-N,N,N′,N′-tetraacetic acid (EGTA) were used as Ca^{2+}-selective chelators (Calabuig-Serna et al. 2023b; Calabuig-Serna et al. 2023a). N-(6-Aminohexyl)-5-chloro-1-naphthalenesulfonamide hydrochloride (W-7) and Chlorpromazine hydrochloride (CPZ) were used as calmodulin inhibitors. Cyclopiazonic acid (CPA) was used as a inhibitor of ER Ca^{2+} pumps. All chemicals were purchased from Sigma-Aldrich except for BAPTA-AM (Abcam). Stocks were prepared according to product specifications, dissolved in water ($Ca(NO_3)_2$, CPZ, EGTA, and $InsP_3$) or DMSO 2.6% (ionophore A23187), 1% (BAPTA-AM), 10% (W-7) or 100% (CPA). They were added to microspore cultures in appropriate volumes of the stock solutions for the final concentrations described in Results. Controls were prepared adding the corresponding solvent concentrations. All compounds were added at culture initiation (day 0) and removed after 3 days, 7 days or one month, when cultures were finished and embryos counted (continuous exposure). At least three biological replicates were performed for each experiment. One-way ANOVA test ($p \leq 0.05$) was performed to determine statistical differences among culture conditions. Then, significant groups were established through the Least Significance Difference (LSD) method. To estimate the percentages of the different embryogenic structures (EE, LBS/SUS, CC and LC), experiments were repeated using the optimal concentration of each chemical, defined for chemicals with positive effects as the concentration producing the highest embryo yield, and the maximum concentration with a non-null effect for chemicals with negative effects. For both cases, a minimum of 200 structures were counted at day 6 of culture.

7.3.Results

7.3.1. Occurrence of different types of embryogenic structures in *Brassica napus* microspore culture

Microspore culture starts with the isolation of vacuolated microspores and young pollen grains and their inoculation in the culture medium (Fig. 1A) for application of the 3-day-long heat-shock treatment. After this time, some microspores/pollen were not sensitive to the induction treatment and developed into pollen-like structures (Fig. 1B) whereas others became induced, as evidenced by their enlargement and the occurrence of the first equatorial divisions (Fig. 1C). At this culture time, no clear morphological differences among embryogenic structures could be detected.

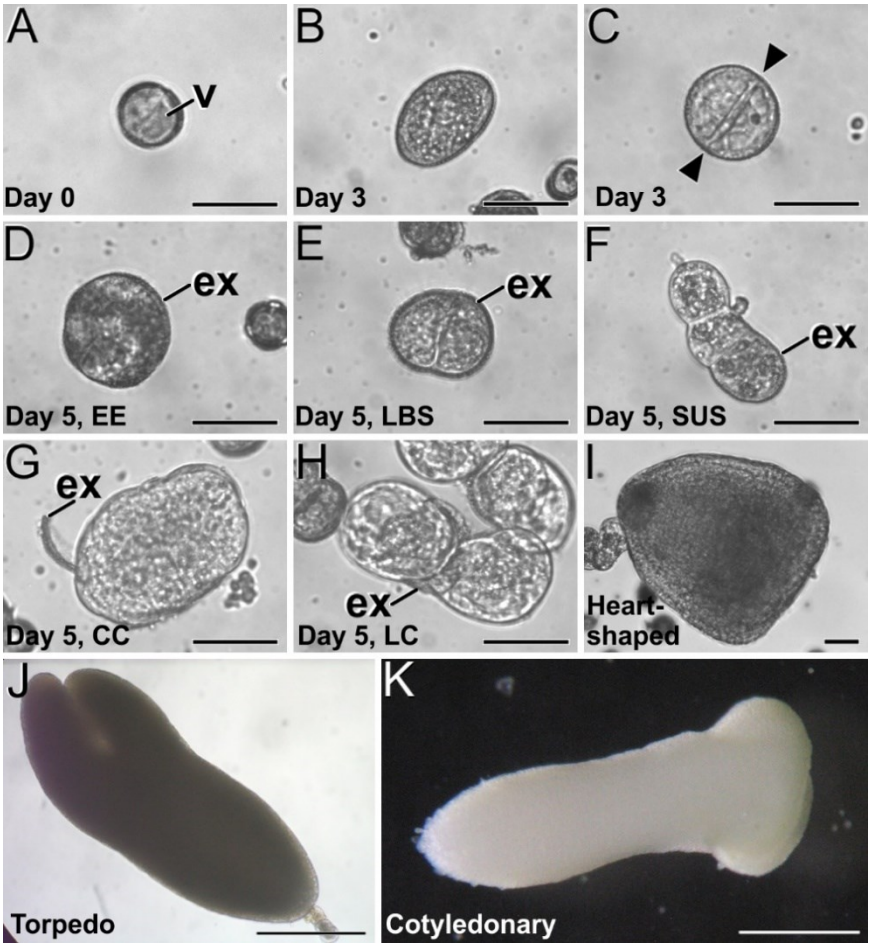

Fig 1. *B. napus* microspore culture. A: Freshly isolated vacuolated microspore before induction. B, C: Three-day-old cultures, just after induction, showing a non-induced, pollen-like structure (B) and an induced, embryogenic structure (C) where a equatorial division is clearly observed (arrowheads). D-H: Five-day-old cultures where four distinct embryogenic structures can be distinguished, including an EE structure (D), an LBS still mostly covered by exine (E) and transformed into an early suspensor (SUS) embryo (F), a CC (G) and a LC structure (H). I: Two-week-old suspensorless heart-shaped embryo. J: Three-week-old suspensor-bearing torpedo embryo. K: One-month-old cotyledonary embryo. ex: exine; v: vacuole. Bars: A-I: 50 µm; J, K: 200 µm.

Five days after culture initiation, however, the differentiation of four distinct embryogenic structures was evident. As previously described in Camacho-Fernández et al. (2021), we observed compact EE structures (Fig. 1D), LBS (Fig. 1E) which developed into SUS embryos (Fig. 1F), disorganized CC structures

with exine detached from the structure (Fig. 1G) and LC structures, with loosely connected cells almost devoid of exine (Fig. 1H). From day 8 on, both globular embryo and callus structures kept growing and heart-shaped (Fig. 1I), torpedo (Fig. 1J) and cotyledonar embryos (Fig. 1K) were observed, most likely coming from LBS/SUS structures (for suspensor-bearing embryos; Fig. 1J) and principally from EE (for suspensorless embryos; Fig. 1K), as previously described (Corral-Martinez et al. 2020). This experimental system was used in all the studies presented next.

7.3.2. Ca^{2+} distribution in the different microspore-derived embryogenic structures

The We studied Ca^{2+} levels and distribution through the different stages of microspore culture by FluoForte staining and observation at the fluorescence microscope, paying special attention to the different embryogenic structures developed from induced microspores. We also performed a quantitative study of fluorescence intensity (Fig. 3) and size of the different structures observed at each stage (Suppl. Fig. S2). In freshly isolated microspores (Fig. 2A), FluoForte staining was high in vacuolated microspores and young pollen grains, as previously described (Rivas-Sendra et al. 2017), whereas in other, younger stages, the FluoForte signal was negligible. One day after induction (Fig. 2B), FluoForte staining was intense in the cytoplasm, nucleus and vacuoles of enlarged, growing microspores whereas in other microspores with no visible signs of growth, the FluoForte signal was much lower or even absent. Three days after induction (Fig. 2C), most microspores showed very low or no signal, but some of them still presented fluorescence with variable intensities, ranging from similar to that of day 0 to much higher in other cases. Due to this variability, we discriminated day-3 microspores in two size-based categories, considering those with an area lower than 720 μm^2 as not growing, and those larger than 720 μm^2 as growing, and therefore possibly embryogenic but not yet differentiated into embryogenic structures, as described in Materials and methods. Fluorescence intensity of >720 μm^2 microspores doubled that of <720 μm^2 microspores (Fig. 3A), thereby confirming the tight relationship between Ca^{2+} accumulation and embryogenic cell growth at early stages. At days 5 (Figs. 2D-H, 3B) and 6 of culture (Fig. 3C), when the four types of embryogenic structures were easily identifiable, all of them showed an increased FluoForte signal intensity, being 2-3 times higher than the measured for isolated microspores. There were not significant differences in intensity among the different types of structures (Figs. 2D-F, 3B, C). However, signal in LBS/SUS structures was consistently observed higher in one of the two cells of the LBS, that was much brighter than the other (Fig. 2E). In slightly more advanced structures, when LBS transform into SUS embryos (Fig. 2F), the cells of the suspensor presented levels of FluoForte signal much higher than cells of the embryo proper, suggesting a link between Ca^{2+} accumulation and suspensor cell identity. In 6-day-old cultures, the different embryogenic structures were slightly larger, but the pattern of FluoForte staining was almost identical to that described for day 5. There was, however, an unusually high standard error for LBS structures (Fig. 3C). This, together with the observation of different signal intensities in cells of LBS structures (Fig. 2E), led us to calculate separately the fluorescence intensities of each cell, confirming that one LBS cell has approximately twice the intensity of the other (Fig. 3D).

From day 8 on (Fig. 3E; Suppl. Fig. S1), the different embryogenic structures produced from highly embryogenic structures, namely suspensorless and suspensor-bearing globular embryos, presented in general low or moderate levels of FluoForte staining, much lower than their precursors, comparable to that of freshly isolated microspores, and mostly located at the vacuoles of the peripheral cells that conform the protoderm. Callus-like structures also presented low levels of FluoForte staining, mostly concentrating in the vacuoles of their enlarged cells.

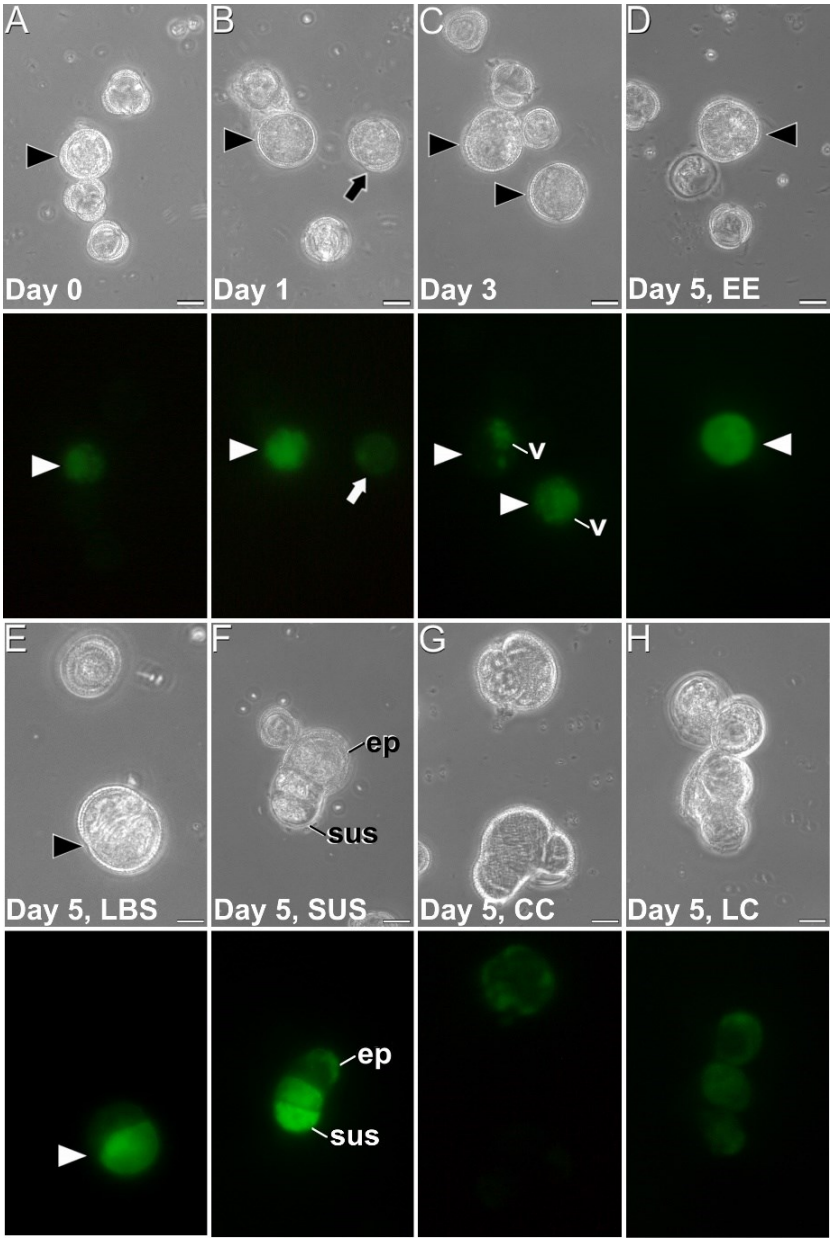

Fig 2. Ca^{2+} detection with FluoForte in *B. napus* microspore cultures. Paired images of the same microscopic field imaged by phase contrast optics (top image) and fluorescence (bottom image). A: Freshly isolated, vacuolated microspore (arrowhead). B: One-day-old culture showing an enlarged, growing microspore (arrowhead) with an intense FluoForte signal, and a non-growing microspore (arrow) with a less intense signal. C: Three-day-old induced structures with visible Fluoforte signal concentrated in vacuoles (v). D-H: Images of five-day-old cultures showing an EE structure (arrowhead in D), an LBS still mostly covered by exine (arrowhead in E) and transformed into an early suspensor (SUS) embryo (F), a CC (G) and a LC structure (H). Note the difference in FluoForte intensity of the two cells of the LBS in E and the suspensor cells in F. Bars: 20 μm.

In conclusion, both qualitative and quantitative analysis of Ca^{2+} dynamics with FluoForte revealed that induction of embryogenesis is associated to a progressive increase in Ca^{2+} levels from day 1, just after heat-shock application, to day 5, when embryogenic microspores differentiate into four types of embryogenic structures without differences in Ca^{2+} levels among them. At day 6, signs of decrease are first seen, at least in some embryogenic structures, reaching the initial, day 0 levels in 8-day calli and embryos.

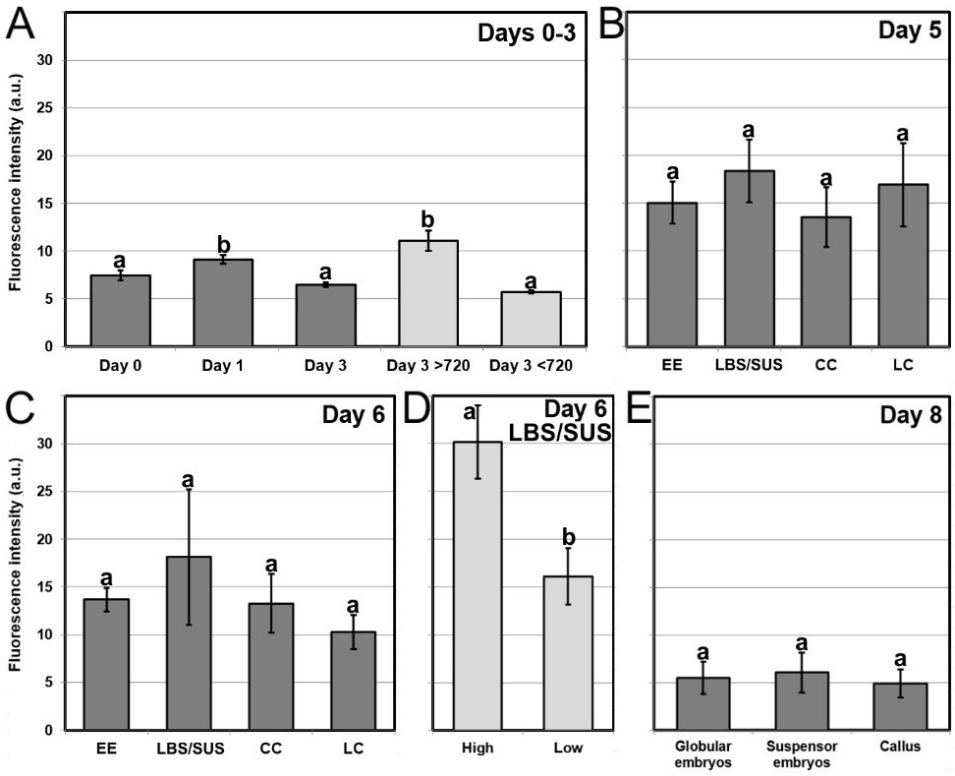

Fig. 3. Quantification of FluoForte-signal in *B. napus* microspore cultures. Fluorescent signal intensity is expressed in arbitrary units (a.u.) ± standard error (error bars). A: Quantification of FluoForte signal in microspores of day 1, day 2 and day 3 cultures. Light grey bars represent a segregation of total day 3 structures in two categories: structures smaller and larger than 720 μm^2 (see text for further details). B, C: Quantification of FluoForte signal in the different embryogenic structures (EE, LBS/SUS, CC and LC) identified in five (B) and six-day-old cultures (C). D: Quantification of FluoForte signal in each of the two cells (one with higher and one with lower signal) of the LBS structures observed at day six. E: Quantification of FluoForte signal in the different suspensorless globular embryos, suspensor-bearing embryos and calli observed in eight-day-old cultures. All fluorescence intensity measurements were made under identical experimental conditions and are represented using the same scale. For each chart, different letters indicate significant differences according to the Kruskal-Wallis test ($p \leq 0.05$).

7.3.3. Effects of increasing Ca^{2+} availability

Once established the relationship between Ca^{2+} levels and microspore embryogenesis, we performed a pharmacological study to modulate the intracellular Ca^{2+} levels with different chemicals known to interfere with Ca^{2+} levels and signaling. Chemicals were applied at different concentrations and exposure times, and their effects were evaluated by counting the number of embryos produced by each treatment after 30 days of culture. First, we attempted to increase the levels of available Ca^{2+} by using three different approaches:

addition of ionophore A23187, a plasma membrane-intercalating Ca^{2+} channel, addition of increased $Ca(NO_3)_2$ concentrations to the culture medium, and addition of $InsP_3$, to release Ca^{2+} from intracellular stores. With the addition of ionophore A23187, embryo yield was drastically reduced or null, at all the exposure times and concentrations used (Suppl. Fig. S3), suggesting that interfering with the intracellular-extracellular Ca^{2+} gradient is extremely harmful for embryo induction and progression. Next, we added $Ca(NO_3)_2$ to the culture medium at concentrations corresponding to 2, 3 and 4-fold the concentration in control cultures with the standard $Ca(NO_3)_2$ concentration of the NLN medium (Fig. 4A). When applied during the first 3 days of culture, 2x and 3x Ca^{2+} concentrations significantly increased embryo production. No differences were found with any Ca^{2+} concentration at 7-day application, but for continuous exposure, there were significant and dose-dependent increases in embryo yield, almost doubling that of control cultures (Fig. 4A). Addition of $InsP_3$ (Fig. 4B) resulted in a similar pattern in terms of embryo yield. The number of embryos was higher than in controls using 0.1, 1 and 10 µM $InsP_3$ when applied during the first 3 days of culture, and almost doubled when applied continuously at 1 and 10 µM (Fig. 4B). No significant differences were observed when $InsP_3$ was applied for 7 days. Thus, it seems that increasing Ca^{2+} availability by increasing either extracellular or intracellular Ca^{2+} levels during the first 3 days or continuously favors embryo production, but increasing it during the days 4-7 may prevent embryogenic diferentiation, since it compensates the positive results of the first 3 days for a net result of no significant differences. Due to the positive effects in embryo yield of specific concentration-time combinations of $Ca(NO_3)_2$ and $InsP_3$, we explored possible synergistic effects with the combined application of $Ca(NO_3)_2$ and $InsP_3$ at 3x and 10 µM, the respective concentrations where they showed the highest embryo yields, but no positive results were observed (Fig. 4C). Instead, application during 3 days of culture and continous application resulted in no significant differences with respect to control conditions. Interestingly, when applied for 7 days, embryo yield decreased versus control conditions. Thus, the positive effects of separately adding $Ca(NO_3)_2$ and $InsP_3$ during the first three days and continuously disappeared when added together, being even negative when applied during 7 days.

In parallel to calculating the final embryo yield, we took 6-day-old samples of each treatment and calculated the percentages of each type of embryogenic structure produced by each treatment (Fig. 4D). The addition of 3x $Ca(NO_3)_2$ led to a reduction of 18% in the percentage of highly embryogenic structures (EE+LBS/SUS), due principally to a 38% reduction in the percentage of LBS/SUS, whereas the addition of 10 µM $InsP_3$ caused a reduction of 27% in the percentage of highly embryogenic structures (EE+LBS/SUS), due principally to a 31% reduction in the percentage of EE (Fig. 4D). However, the combined application of $InsP_3$ and $Ca(NO_3)_2$, which had negative effects in embryo yield, produced very limited reductions of the percentages of highly embryogenic structures (9% EE and 9% LBS/SUS). Thus, the increases in embryo yield observed with the independent use of $Ca(NO_3)_2$ and $InsP_3$ were not correlated with an increase in the proportion of highly embryogenic structures present in early culture stages. This indicates that changes in Ca^{2+} levels affect embryo production, but not the proportion of highly embryogenic structures formed.

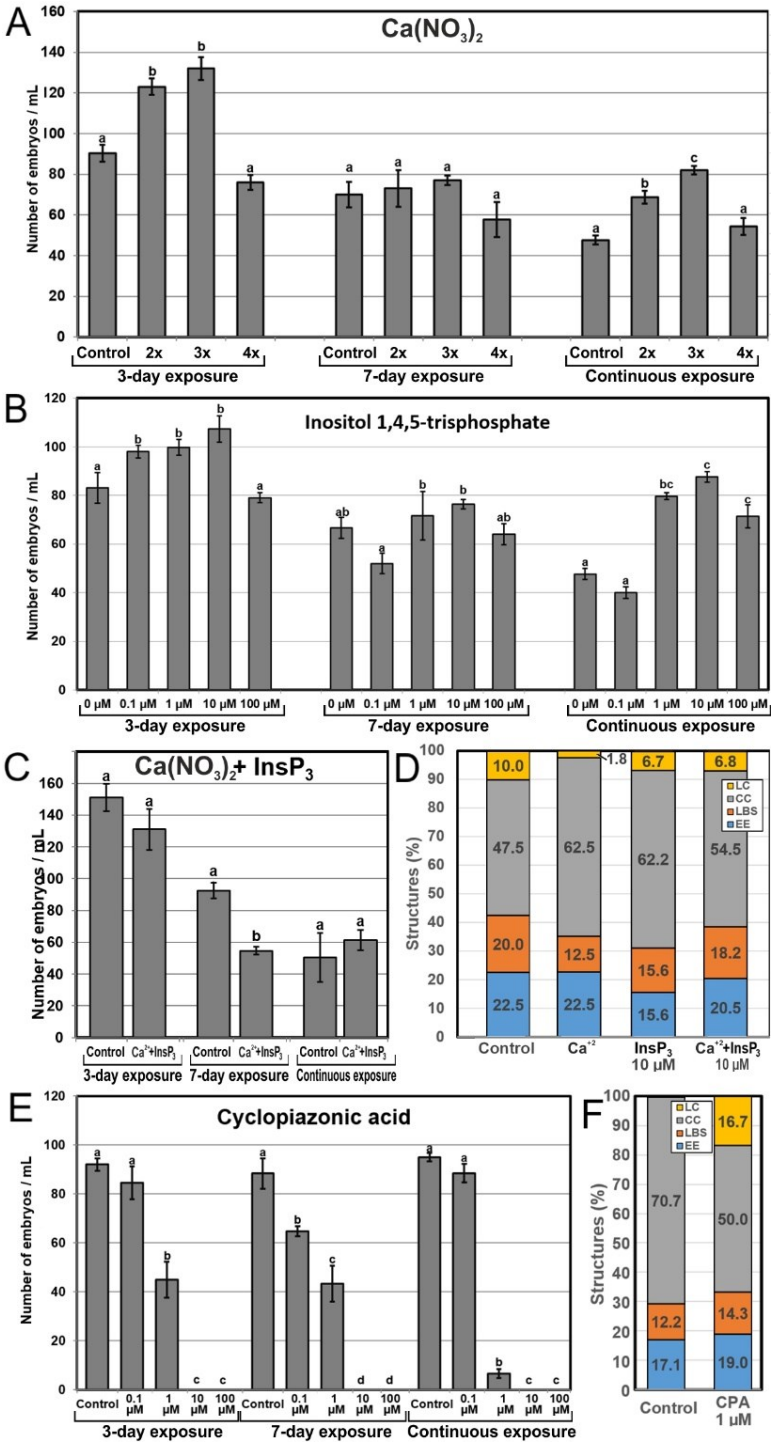

Fig 4. Effects of increasing Ca^{2+} availability. Ca^{2+} availability was increased with the independent addition to the culture medium of different concentrations of $Ca(NO_3)_2$ (A), $InsP_3$ (B), a combination of 3x $Ca(NO_3)_2$ and 10 µM $InsP_3$ (C). The different chemicals and concentrations were applied during the first three days of culture, during seven days, and continuously, and effects are expressed as number of embryos produced per mL of culture medium. D: Changes in the percentages of embryogenic structures produced with the independent addition during 6 days of 3x $Ca(NO_3)_2$ (A), 10 µM $InsP_3$ (B), and a combination of 3x $Ca(NO_3)_2$ and 10 µM $InsP_3$. E, F: Changes in the number of embryos (E) and the percentage of embryogenic structures (F) produced with the addition of cyclopiazonic acid (CPA) in the same conditions described above. Different letters indicate significant differences according to the LSD test ($p \leq 0.05$).

7.3.4. Effects of blocking ER Ca^{2+} pumps

We used CPA to block ER Ca^{2+} pumps, precluding the return of intracellular Ca^{2+} levels to those previous to Ca^{2+} release. In general, the effects of CPA in terms of embryo yield (Fig. 4E) were negative at all exposure times and dose-dependent, being slightly reduced at low concentrations, largely reduced at mid range concentrations, and null at the highest concentrations. The percentages of highly embryogenic structures were similar to those of controls (Fig. 4F), with little individual differences between EE and LBS/SUS. The overall percentages of barely embryogenic structures were also similar to control, but a remarkable transition from CC to LC structures was evidenced. Thus, a blockage of Ca^{2+} translocation back to the ER did not increase embryo production, but reduced it in a dose-dependent (but not time-dependent) manner. However, the effects in the percentage of embryogenic structures were almost negligible, insufficient to explain the negative effect in the final embryo yield. The only relevant change was a notable increase in the percentage of LC, but the overall percentage of barely embryogenic structures (CC and LC) remained similar. These results demonstrate that a proper recovery after Ca^{2+} release is essential for proper embryo development.

7.3.5. Effects of reducing Ca^{2+} availability

Next, we assessed the effects of reducing Ca^{2+} availability with the use of two Ca^{2+} chelators, BAPTA-AM and EGTA. Application of BAPTA-AM (Fig. 5A) during the first three days of culture had only a negative effect in embryo production at 50 μM, the highest concentration (~50% reduction vs control). Application for seven days evidenced negative effects even with lower concentrations, and the effects with higher concentrations were more severe (~67% reduction *vs* control for 50 μM). Continuous application completely inhibited embryo production at all concentrations. These time and dose-dependent negative effects of BAPTA-AM were not anticipated by a dramatic alteration of the percentages of the different embryogenic structures formed at day 6 of culture, that were remarkably similar to those found in controls (Fig. 5B). Exposure to EGTA had similar dose-dependent effects, being slightly negative at low concentrations, severely negative at mid range concentrations, and completely inhibiting embryo production at the highest concentration tested (Fig. 5C). Mid range concentrations showed also a time-dependent effect. For example, the reduction of embryo yield *vs* control caused by 100 μM EGTA was ~33% for 3-day, ~70% for 7-day and ~85% for continuous exposure. As with BAPTA-AM, EGTA did not alter the percentages of the different embryogenic structures at day 6, which were similar to those of controls except for LC structures, which nearly doubled (Fig. 5D). This, however, did not represent a relevant change in the percentage of barely embryogenic structures. Together, these results confirm that chelation had a time and dose-dependent negative effect in embryo yield. The effects of BAPTA-AM were more severe than those of EGTA, possibly due to the chelating effect of BAPTA-AM not only on Ca^{2+}, but also on Mg^{2+}. However, as for the experiments to increase Ca^{2+} availability, changes in Ca^{2+} levels have no effect in the proportion of highly embryogenic structures formed.

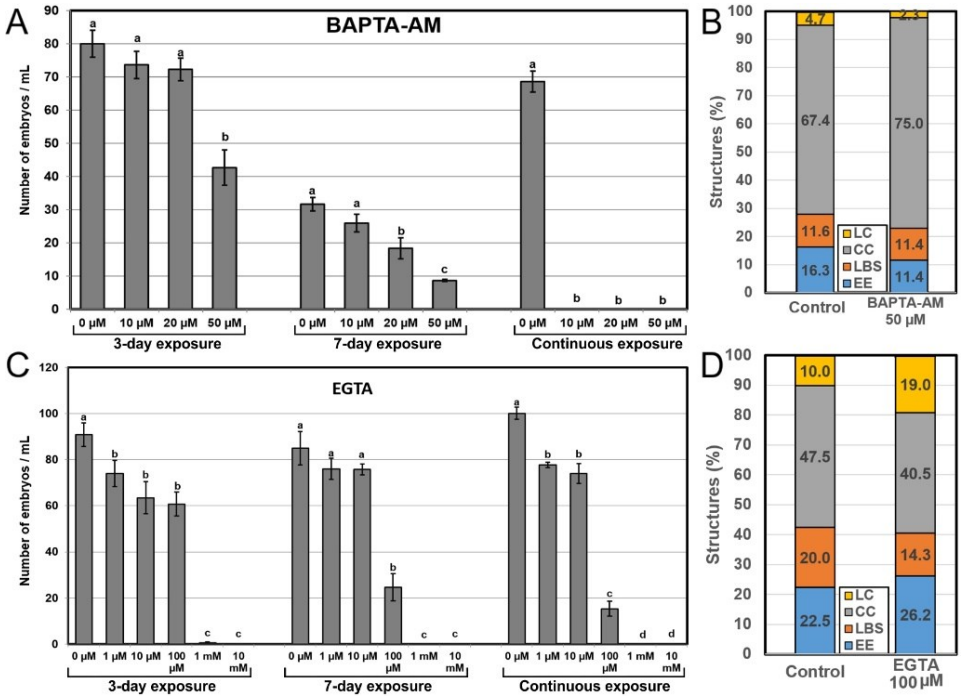

Fig. 5. Effects of reducing Ca^{2+} availability. Ca^{2+} availability was reduced with the independent addition to the culture medium of different concentrations of BAPTA-AM (A, B) and EGTA (C, D). For A and C, the different chemicals and concentrations were applied during the first three days of culture, during seven days, and continuously, and effects are expressed as number of embryos produced per mL of culture medium. Different letters indicate significant differences according to the LSD test ($p \leq 0.05$). For B and D, the concentration used was applied during 6 days and the different embryogenic structures produced were counted and expressed as percentages.

7.3.6. Effects of inhibiting CaM

Our next goal was to evaluate the effect of chemically inhibiting CaM. We used W-7, a CaM antagonist, and CPZ, a CaM inhibitor. Upon application of W-7 to the culture medium (Fig. 6A), embryo yield was severely affected at 50 µM and almost completely inhibited at 100 µM. The effects seemed similar for 3 and 7-day applications, and more severe for continuous application, which led to a complete inhibition of embryo production at any concentration. Thus, we focused on CPZ (Fig. 6B), which had in general a clear dose-dependent negative effect. Low and high concentrations behaved similarly for the three exposure times, but as described for Ca^{2+} chelators, intermediate concentrations showed time-dependent effects. For example, the reduction of embryo yield *vs* control caused by 10 µM CPZ was ~45% for 3-day treatment, ~63% for 7-day treatment and ~80% for continuous exposure. This negative effect was also reflected in the percentages of the different embryogenic structures formed at day 6 with 10 µM CPZ (Fig. 6C). Although the overall percentage of highly embryogenic structures was not far from that of control (38.1% vs 42.5%, ~10% reduction), the percentage of EE structures, where the vast majority of embryos come from (Corral-Martinez et al. 2020), was reduced to ~50%, which is in between the percentages of embryo yield reduction observed for 3 and 7-day exposures to 10 µM CPZ. Thus, it seemed that CaM inhibition affected the differentiation of EE structures, which in turn reduced embryo yield.

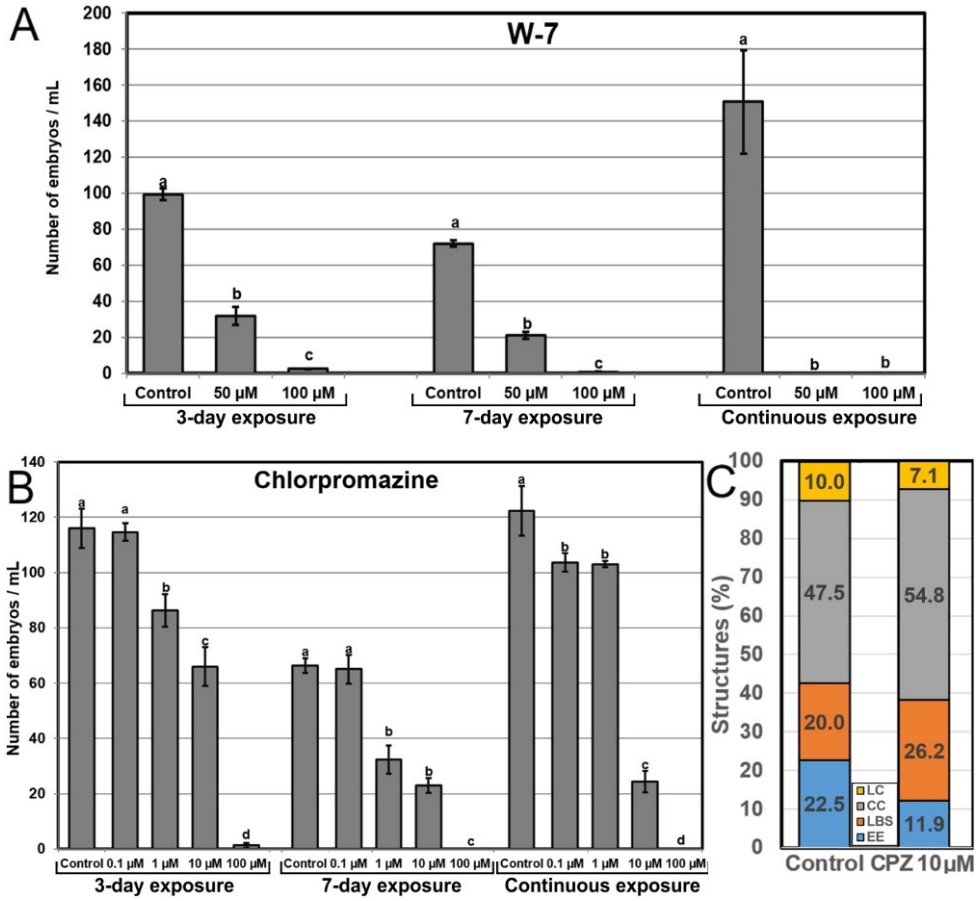

Fig. 6. Effects of inhibiting CaM. CaM was inhibited with the independent addition to the culture medium of different concentrations of W-7 (A) and CPZ (B, C). For A and B, the different chemicals and concentrations were applied during the first three days of culture, during seven days, and continuously, and effects are expressed as number of embryos produced per mL of culture medium. Different letters indicate significant differences according to the LSD test ($p \leq 0.05$). For C, the concentration used was applied during 6 days and the different embryogenic structures produced were counted and expressed as percentages.

7.4.Discussion

We showed that in the DH4079 line of *B. napus*, it is possible to induce the formation of embryogenic microspores from which, upon cessation of the HS, different types of embryogenic structures with different embryogenic potential (highly embryogenic EE and LBS/SUS and barely embryogenic CC and LC), are formed after 5 days of culture. This contrasts with previous reports showing the occurrence of these same embryogenic structures after just 3 culture days in both the highly responding DH4079 and the low response DH12075 lines (Camacho-Fernández et al. 2021; Corral-Martinez et al. 2020; Li et al. 2014). This apparent discrepancy relies on the fact that in these reports, an incubation of microspores at 32-33 ºC during just one day was sufficient to induce a sufficient number of embryos. Although we have routinely been using the 1 day-32 ºC conditions (Camacho-Fernández et al. 2021; Corral-Martínez et al. 2019; Rivas-Sendra et al. 2019; Rivas-Sendra et al. 2017; Parra-Vega et al. 2015b, a; Corral-Martínez et al. 2013), we have observed that, in some cases, 1 day is not enough to induce a high response, and the HS has been extended for up to 3 days at 32 ºC to obtain similar results (Rivas-Sendra et al. 2017; Satpute et al. 2005; Jouannic et al. 2001). Even in some cases, 14 days at 30 ºC have successfully been used

(Abdollahi et al. 2012). Temperature is key to determine the developmental fate of *B. napus* cultured microspores (Custers et al. 1994). Indeed, there is a clear correlation between HS duration and developmental speed of the embryos produced (Corral-Martínez et al. 2021). In this work, a 3-day-long HS was applied and this delayed the growth of the different embryogenic structures with respect to previous reports, although their anatomy, developmental features and FluoForte staining patterns were not affected, and were therefore comparable to those of previous works, as described next.

7.4.1. Ca^{2+} increase is sufficient to improve embryo yield by increasing the number of embryogenic microspores

We used higher $Ca(NO_3)_2$ and $InsP_3$ concentrations to increase the available extracellular and intracellular Ca^{2+} levels, respectively. $InsP_3$ is a signal transduction intermediate that triggers the release of Ca^{2+} from intracellular stores, principally (but not only) the vacuole (Im et al. 2010), thereby activating the corresponding Ca^{2+}-mediated signaling cascades (Berridge 1993). In particular, $InsP_3$ stimulates Ca^{2+} release for activation of the embryo sac central cells (Han et al. 2002), similar to sperm cell-mediated activation of Ca^{2+} release in plant and animal egg cells (Ge et al. 2007). With both $Ca(NO_3)_2$ and $InsP_3$, we obtained very similar results: three-day applications significantly increased embryo production (Fig. 4), which confirms that Ca^{2+} increases during heat shock are sufficient to improve embryo yield. Such improvement might come from (1) an increase of the total number of induced microspores, (2) an increase of the percentage of the highly embryogenic structures, which are responsible for most of the embryos produced, or (3) all of the above. Our results with the different Ca^{2+}-interfering chemicals clearly points to the first option, as no relevant increases in the percentages of highly embryogenic structures (i.e. EE and LBS/SUS), were observed. Thus, raised Ca^{2+} levels would increase the number of embryogenesis-activated microspores by increasing the amount of microspores reaching the minimum Ca^{2+} level required to be activated.

7.4.2. Microspore embryogenesis can be modulated by altering Ca^{2+} levels within a functional range

This study and others showed that Ca^{2+} can be considered as an early marker of induction to *in vitro* embryogenesis (Calabuig-Serna et al. 2023b; Rivas-Sendra et al. 2019; Rivas-Sendra et al. 2017; Calabuig-Serna et al. 2023a). Ca^{2+} demands during microspore embryogenesis are dynamic and flexible, which allows for modulation of embryo yield by altering Ca^{2+} levels. Such plasticity, however, must have some limits, as revealed by CPA experiments. CPA is a mycotoxin known to inhibit ER Ca^{2+} pumps, responsible for translocating Ca^{2+} from the cytoplasm back to the ER to return to the levels previous to Ca^{2+} release, thereby affecting the role of Ca^{2+} as an intracellular signaling molecule. We showed that disrupting ER Ca^{2+} pumps precludes embryogenesis. In line with this, the rupture of the intracellular-extracellular Ca^{2+} gradient induced by ionophore A23187 was markedly negative for embryo induction and progression, as also shown for *Arabidopsis* somatic embryogenesis (Calabuig-Serna et al. 2023b) and bread wheat anther culture (Reynolds 2000). Moreover, the combination of intracellular and extracellular Ca^{2+} levels increased by $InsP_3$ and

$Ca(NO_3)_2$, respectively, was excessive, since no beneficial effects, but even a negative effect for 7-day application, were observed. This fact points to the existence of an upper threshold above which intracellular Ca^{2+} would become toxic. We used BAPTA-AM and EGTA as Ca^{2+} chelators to reduce the available free Ca^{2+} levels, and W-7 and CPZ as CaM inhibitors whose main physiological effect is to reduce Ca^{2+} signaling without altering Ca^{2+} levels (Liu et al. 2005). The four chemicals produced very similar profiles of embryo yield reduction, which points to a major physiological role for Ca^{2+} in cell signaling upon binding with CaM. These results are similar to those found in other *in vitro* embryogenesis systems, including bread wheat microspore embryogenesis and carrot and Arabidopsis somatic embryogenesis (Reynolds 2000; Calabuig-Serna et al. 2023a; Calabuig-Serna et al. 2023b). In our system, the observed negative effect in embryo yield was heavily dose-dependent, producing almost no embryos at the highest concentrations (Figs. 5, 6). Exposure time also affected embryo yield, principally at intermediate concentrations. These results are reasonable considering that Ca^{2+}-CaM signaling is widely acknowledged to act in a wealth of physiological and cellular processes along embryo development (Tian et al. 2020). However, it is interesting to note that the profiles of embryo yield observed with Ca^{2+}-increasing chemicals were not time-dependent. The profiles observed with the three application times were similar, indicating that the main role of Ca^{2+} in the increase of embryo yield takes place during the first three days. Thus, during all the process of embryo induction and development, there is a minimum, physiological threshold (possibly the 50-100 nM concentration described for free cytoplasmic Ca^{2+} (Pirayesh et al. 2021)) below which cell signaling and function is compromised. A moderate reduction of Ca^{2+} levels would not affect embryo production as long as this lower threshold is not trespassed. In conclusion, despite the plasticity of Ca^{2+} homeostasis, efficient microspore embryogenesis requires active mechanisms to control Ca^{2+} influx and translocation to intracellular stores in order to keep Ca^{2+} levels between a lower and an upper threshold. As long as Ca^{2+} levels are kept between both thresholds, Ca^{2+} can be used to modulate microspore embryogenesis as it increases the amount of embryogenic microspores.

7.4.3. High Ca^{2+} levels are associated to differentiation stages

We consistently observed that freshly isolated microspores and young pollen grains, the stages more sensitive to embryogenesis induction, present Ca^{2+} levels higher than other *in vivo* developmental stages, which led to the notion that Ca^{2+} facilitates embryogenesis induction (Rivas-Sendra et al. 2019; Rivas-Sendra et al. 2017). In our *B. napus* system, induction of microspore embryogenesis is achieved with the application of a 3-day-long HS treatment. Upon application of the HS, there was a progressive increase of Ca^{2+} levels in induced microspores (Figs. 2, 3). It could be argued that Ca^{2+} increases during days 1-3 would be related to the HS response, as Ca^{2+} is also involved on HS signaling by activating the expression of HS genes (Liu et al. 2005). However, clear differences were found from the very first moment between induced and non-induced microspores, both exposed to the same HS conditions (Rivas-Sendra et al. 2017). We also described that, at day 3, when all microspores are still under HS conditions, Ca^{2+} levels in growing, induced microspores nearly doubled that of non-growing microspores, whose levels were similar to those of freshly isolated microspores,

before induction. Thus, it is likely that the Ca^{2+} changes due to HS signaling are masked by the general increase associated to embryogenesis induction. This is supported by the fact that after day 3, once microspores are released from the HS, Ca^{2+} levels kept increasing, peaking at day 5 where Ca^{2+} levels nearly doubled those of freshly isolated microspores. The initial stages (days 1-5), which are equivalent to days 1-3 of the protocols using 1-day-long HS, are the stages where microspores are induced to embryogenesis and differentiate into embryogenic structures, pointing to a role for Ca^{2+} in cell differentiation, and being this role similar for the four types of structures, as no significant differences in Ca^{2+} levels were found among them.

A 7-day application of Ca^{2+}-increasing chemicals had no significant effects in embryo yield (Fig. 4). This means that between days 4 and 6, the stages with higher endogenous Ca^{2+} levels (Figs. 3B, C), increased Ca^{2+} availability promotes a distortion that negatively affects embryo yield, but is compensated by the positive effect during the first 3 days for a final non-significant net change in embryo yield. The reductions observed in the percentages of highly embryogenic structures with the use of Ca^{2+}-increasing chemicals (Fig. 4D) explain the negative effects of increased Ca^{2+} for 7 days, as this would be detrimental for the growth of the already differentiated highly and barely embryogenic structures, and their progression to globular embryos and calli, respectively, with no remarkable differentiation events. An exception of this would be the establishment of suspensor cell identity in LBS/SUS, which accumulated very high Ca^{2+} levels in their suspensors. The preferential accumulation of Ca^{2+} in the differentiating suspensor reinforces the proposed relationship between Ca^{2+} and polarized cell growth (Tian et al. 2020).

We also observed that CaM inhibition with CPZ promoted a dramatic reduction of the percentage of EE structures down to ~50% (Fig. 6C). EE structures have the highest rate of conversion into embryos (Corral-Martinez et al. 2020) so, despite the increase in the percentage of LBS/SUS, which have a markedly lower rate of conversion into embryos (Corral-Martinez et al. 2020), we can conclude that CaM inhibition affects embryo yield by reducing the percentage of EE structures, the main embryo-producing type. However, reduction of Ca^{2+} levels by chelation had not consistent negative effects in the percentage of highly embryogenic structures (Figs. 5B, D), indicating that a reduction of Ca^{2+} availability at this stage does not interfere with the proliferative growth of highly embryogenic structures into globular embryos. Indeed, Ca^{2+} levels began to decrease at day 6 and by day 8, Ca^{2+} levels in embryos and calli (Fig. 3E) were similar among them and also to those of isolated microspores. Thus, the day 6-7 stage, principally proliferative, does not need the high Ca^{2+} levels required between days 1-5 for embryogenesis induction and differentiation of the different structures.

There also was a clearly positive effect for continuous exposures to Ca^{2+}-increasing chemicals, which indicates that higher Ca^{2+} availability is also beneficial at embryogenic stages later than day 7, and that these effects are even more positive than for 3-day exposures, since they compensate for the negative effects of 7-day application to produce a net positive result that in some cases (3x $Ca(NO_3)_2$ and 10 μM $InsP_3$) nearly doubles control values (Figs. 4A, B). These

are the stages when globular embryos begin to differentiate into heart-shaped embryos and beyond, when activated CaM shows a polarized distribution (Hause et al. 1994), and when the main differentiation events during embryo development take place (Dresselhaus and Jürgens 2021). Thus, there seems to be a clear positive link of Ca^{2+} with embryo differentiation, more than with undifferentiated cell proliferation.

7.4.4. The embryogenic microspore as an experimentally Ca^{2+}-activatable haploid zygote-like cell

It seems that Ca^{2+} increase (up to a certain limit) is necessary to activate the embryogenic development of microspores. This is not surprising if we consider the scenario of zygotic embryogenesis, where in animal, algal and flowering plant models, Ca^{2+} increase is necessary for egg cell activation, blockage of polyspermy and induction of zygote development (Chen et al. 2015; Ge et al. 2007). Interestingly, prior to induction, the embryogenesis-inducible stages (vacuolated microspores/young pollen grains) have increased Ca^{2+} levels compared to the other gametophytic stages (Fig. 2A) (Rivas-Sendra et al. 2019; Rivas-Sendra et al. 2017). Following *in vitro* egg cell fertilization, there is a long-lasting increase of intracellular Ca^{2+} levels that, in turn, promote an increased influx of extracellular free Ca^{2+} (Digonnet et al. 1997; Antoine et al. 2000). Ca^{2+} increases in somatic cells reprogrammed to embryogenesis have also been described in other *in vitro*-inducible systems such as Arabidopsis and carrot (Calabuig-Serna et al. 2023a; Calabuig-Serna et al. 2023b). Assuming that induced, embryogenic microspores behave as a sort of experimentally-activatable haploid zygote-like cells, this would explain why increased levels of both extracellular and intracellular free Ca^{2+} are positive to induce microspore embryogenesis. As in sexual zygotes, cultured microspores would react to increases in extracellular Ca^{2+} levels by increasing Ca^{2+} influx.

Furthermore, Ca^{2+} peaking during double fertilization is thought to induce the reorganization of the cytoskeleton and fragmentation of the vacuole needed to establish zygote polarization (Chen et al. 2015). It is to no surprise that cytoskeletal reorganization and fragmentation of the large vacuole of the microspore are among the first cellular changes undergone by embryogenic microspores (Zaki and Dickinson 1990; Hause et al. 1993). These could well be targets for Ca^{2+}-mediated signaling during the first moments of embryogenesis induction. One of the first events shown to occur upon egg cell fertilization is the formation of a cell wall. During maize *in vitro* fertilization studies, the formation of cell wall material was identified as soon as 30 s after gamete fusion (Kranz et al. 1995). Experimenting with Ca^{2+} in unfertilized maize egg cells, Antoine et al. (2000) found that the artificial activation of Ca^{2+} influx was sufficient to produce a new cell wall 40 min after Ca^{2+} influx activation with no need for interaction with sperm cells. This was proposed to be one of the first events of very early embryogenesis initiation, as a mechanism to block polyspermy (Antoine et al. 2000; Chen et al. 2015). In microspores, induction of embryogenesis implies profound cell wall remodeling(Camacho-Fernández et al. 2021; Corral-Martínez et al. 2019), including the formation of a callose-rich, isolating subintinal layer (Parra-Vega et al. 2015b; Rivas-Sendra et al. 2019). Thus, it is reasonable to

speculate that the early cellular changes undergone by induced microspores could well be a reflection of the early changes undergone by activated egg cells.

Acknowledgements

We thank Marisol Gascón (IBMCP-CSIC Microscopy Service) for her excellent technical help.

References

Abdollahi MR, Ghazanfari P, Corral-Martínez P, Moieni A, Seguí-Simarro JM (2012) Enhancing secondary embryogenesis in *Brassica napus* by selecting hypocotyl-derived embryos and using plant-derived smoke extract in culture medium. Plant Cell Tissue Organ Cult 110 (2):307-315. doi:10.1007/s11240-012-0152-7

Antoine AF, Faure J-E, Cordeiro S, Dumas C, Rougier M, Feijó JA (2000) A calcium influx is triggered and propagates in the zygote as a wavefront during *in vitro* fertilization of flowering plants. Proceedings of the National Academy of Sciences 97 (19):10643-10648. doi:10.1073/pnas.180243697

Berridge MJ (1993) Inositol trisphosphate and calcium signalling. Nature 361 (6410):315-325. doi:10.1038/361315a0

Bush DS, Jones RL (1987) Measurement of cytoplasmic calcium in aleurone protoplasts using indo-1 and fura-2. Cell Calcium 8 (6):455-472. doi:http://dx.doi.org/10.1016/0143-4160(87)90029-7

Calabuig-Serna A, Mir R, Arjona P, Seguí-Simarro JM (2023a) Calcium dynamics and modulation in carrot somatic embryogenesis. Front Plant Sci 14:1150198. doi:10.3389/fpls.2023.1150198

Calabuig-Serna A, Mir R, Seguí-Simarro JM (2023b) Calcium Dynamics, *WUSCHEL* Expression and Callose Deposition during Somatic Embryogenesis in *Arabidopsis thaliana* Immature Zygotic Embryos. Plants 12 (5):1021. doi:10.3390/plants12051021

Camacho-Fernández C, Hervás D, Rivas-Sendra A, Marín MP, Seguí-Simarro JM (2018) Comparison of six different methods to calculate cell densities. Plant Methods 14 (1):30. doi:10.1186/s13007-018-0297-4

Camacho-Fernández C, Seguí-Simarro JM, Mir R, Boutilier K, Corral-Martínez P (2021) Cell Wall Composition and Structure Define the Developmental Fate of Embryogenic Microspores in *Brassica napus*. Front Plant Sci 12 (2260). doi:10.3389/fpls.2021.737139

Corral-Martínez P, Camacho-Fernández C, Mir R, Seguí-Simarro JM (2021) Doubled haploid production in high- and low-response genotypes of rapeseed (*Brassica napus*) through isolated microspore culture. In: Seguí-Simarro JM (ed) Doubled Haploid Technology, vol 2: Hot Topics, Apiaceae, Brassicaceae, Solanaceae. Methods in Molecular Biology, vol 2288, 1st edn. Springer Science+Business Media, LLC, New York, USA, pp 129-144. doi:10.1007/978-1-0716-1335-1_8

Corral-Martínez P, Driouich A, Seguí-Simarro JM (2019) Dynamic changes in arabinogalactan-protein, pectin, xyloglucan and xylan composition of the cell wall during microspore embryogenesis in *Brassica napus*. Front Plant Sci 10:332. doi:10.3389/fpls.2019.00332

Corral-Martínez P, Parra-Vega V, Seguí-Simarro JM (2013) Novel features of *Brassica napus* embryogenic microspores revealed by high pressure freezing and freeze substitution: evidence for massive autophagy and excretion-based cytoplasmic cleaning. J Exp Bot 64 (10):3061-3075. doi:10.1093/jxb/ert151

Corral-Martinez P, Siemons C, Horstman A, Angenent GC, de Ruijter N, Boutilier K (2020) Live Imaging of embryogenic structures in *Brassica napus* microspore embryo cultures highlights the developmental plasticity of induced totipotent cells. Plant Reprod 33 (3-4):143-158. doi:10.1007/s00497-020-00391-z

Custers JBM, Cordewener JHG, Nöllen Y, Dons JJ, van Lookeren-Campagne MM (1994) Temperature controls both gametophytic and sporophytic development in microspore cultures of *Brassica napus*. Plant Cell Rep 13:267-271

Chen J, Gutjahr C, Bleckmann A, Dresselhaus T (2015) Calcium Signaling during Reproduction and Biotrophic Fungal Interactions in Plants. Mol Plant 8 (4):595-611. doi:https://doi.org/10.1016/j.molp.2015.01.023

Cho UH, Kasha KJ (1995) The effect of calcium on ethylene production and microspore-derived embryogenesis in barley (*Hordeum vulgare* L.) and wheat (*Triticum aestivum* L.) anther cultures. J Plant Physiol 146 (5-6):677-680

Digonnet C, Aldon D, Leduc N, Dumas C, Rougier M (1997) First evidence of a calcium transient in flowering plants at fertilization. Development 124 (15):2867-2874. doi:10.1242/dev.124.15.2867

Dresselhaus T, Jürgens G (2021) Comparative Embryogenesis in Angiosperms: Activation and Patterning of Embryonic Cell Lineages. Ann Rev Plant Biol 72 (1):null. doi:10.1146/annurev-arplant-082520-094112

Ge LL, Tian HQ, Russell SD (2007) Calcium function and distribution during fertilization in angiosperms. Am J Bot 94 (6):1046-1060. doi:10.3732/ajb.94.6.1046

Han Y-Z, Huang B-Q, Guo F-L, Zee S-Y, Gu H-K (2002) Sperm extract and inositol 1,4,5-triphosphate induce cytosolic calcium rise in the central cell of *Torenia fournieri*. Sex Plant Reprod 15 (4):187-193. doi:10.1007/s00497-002-0154-4

Hause B, Hause G, Pechan P, van Lammeren AAM (1993) Cytoskeletal changes and induction of embryogenesis in microspore and pollen cultures of *Brassica napus* L. Cell Biol Int 17:153-168

Hause B, van Veenendaal WLH, Hause G, van Lammeren AAM (1994) Expression of polarity during early development of microspore-derived and zygotic embryos of *Brassica napus* L cv. Topas. Botanica Acta 107 (6):407-415

Hoekstra S, van Bergen S, van Brouwershaven IR, Schilperoort RA, Wang M (1997) Androgenesis in *Hordeum vulgare* L.: Effects of mannitol, calcium and abscisic acid on anther pretreatment. Plant Sci 126 (2):211-218. doi:http://dx.doi.org/10.1016/S0168-9452(97)00096-4

Im YJ, Phillippy BQ, Perera IY (2010) $InsP_3$ in Plant Cells. In: Munnik T (ed) Lipid Signaling in Plants. Springer Berlin Heidelberg, Berlin, Heidelberg, pp 145-160. doi:10.1007/978-3-642-03873-0_10

Jansen MA, Booij H, Schel JH, de Vries SC (1990) Calcium increases the yield of somatic embryos in carrot embryogenic suspension cultures. Plant Cell Rep 9 (4):221-223

Jouannic S, Champion A, Seguí-Simarro JM, Salimova E, Picaud A, Tregear J, Testillano P, Risueno MC, Simanis V, Kreis M, Henry Y (2001) The protein kinases AtMAP3Kε1 and BnMAP3Kε1 are functional homologues of *S. pombe* cdc7p and may be involved in cell division. Plant J 26 (6):637-649

Kranz E, von Wiegen P, Lörz H (1995) Early cytological events after induction of cell division in egg cells and zygote development following in vitro fertilization with angiosperm gametes. Plant J 8 (1):9-23

Krebs M, Held K, Binder A, Hashimoto K, Den Herder G, Parniske M, Kudla J, Schumacher K (2012) FRET-based genetically encoded sensors allow high-resolution live cell imaging of Ca^{2+} dynamics. Plant J 69 (1):181-192. doi:10.1111/j.1365-313X.2011.04780.x

Li H, Soriano M, Cordewener J, Muiño JM, Riksen T, Fukuoka H, Angenent GC, Boutilier K (2014) The histone deacetylase inhibitor Trichostatin A promotes totipotency in the male gametophyte. Plant Cell 26 (1):195-209. doi:10.1105/tpc.113.116491

Liu HT, Sun DY, Zhou RG (2005) Ca^{2+} and *AtCaM3* are involved in the expression of heat shock protein gene in Arabidopsis. Plant Cell Environ 28 (10):1276-1284. doi:10.1111/j.1365-3040.2005.01365.x

Mahalakshmi A, Singla B, Khurana JP, Khurana P (2007) Role of calcium–calmodulin in auxin-induced somatic embryogenesis in leaf base cultures of wheat (*Triticum aestivum* var. HD 2329). Plant Cell Tissue Organ Cult 88 (2):167-174

Mir R, Calabuig-Serna A, Seguí-Simarro JM (2021) Doubled haploids in eggplant. Biology 10 (7):685

Nitsch C, Nitsch JP (1967) Induction of flowering in vitro in stem segments of *Plumbago indica* L. I Production of vegetative buds. Planta 72 (4):355-370. doi:10.1007/bf00390146

Nitsch JP, Nitsch C (1969) Haploid plants from pollen grains. Science 163 (3862):85-87

Overvoorde PJ, Grimes HD (1994) The role of calcium and calmodulin in carrot somatic embryogenesis. Plant Cell Physiol 35 (2):135-144. doi:10.1093/oxfordjournals.pcp.a078577

Parra-Vega V, Corral-Martínez P, Rivas-Sendra A, Seguí-Simarro JM (2015a) Formation and excretion of autophagic plastids (plastolysomes) in *Brassica napus* embryogenic microspores. Front Plant Sci 6 (94). doi:doi: 10.3389/fpls.2015.00094

Parra-Vega V, Corral-Martínez P, Rivas-Sendra A, Seguí-Simarro JM (2015b) Induction of embryogenesis in *Brassica napus* microspores produces a callosic subintinal layer and abnormal cell walls with altered levels of callose and cellulose. Front Plant Sci 6:1018. doi:10.3389/fpls.2015.01018

Pirayesh N, Giridhar M, Ben Khedher A, Vothknecht UC, Chigri F (2021) Organellar calcium signaling in plants: An update. Biochimica et Biophysica Acta (BBA) - Molecular Cell Research 1868 (4):118948. doi:https://doi.org/10.1016/j.bbamcr.2021.118948

Ramakrishna A, Giridhar P, Jobin M, Paulose CS, Ravishankar GA (2012) Indoleamines and calcium enhance somatic embryogenesis in *Coffea canephora* P ex Fr. Plant Cell Tissue Organ Cult 108 (2):267-278. doi:10.1007/s11240-011-0039-z

Ramakrishna A, Giridhar P, Ravishankar GA (2011) Calcium and calcium ionophore A23187 induce high-frequency somatic embryogenesis in cultured tissues of *Coffea canephora* P ex Fr. In Vitro Cell Dev Biol -Pl 47 (6):667-673. doi:10.1007/s11627-011-9372-5

Reynolds TL (1990) Interactions between calcium and auxin during pollen androgenesis in anther cultures of *Solanum carolinense* L. Plant Sci 72 (1):109-114. doi:10.1016/0168-9452(90)90192-q

Reynolds TL (2000) Effects of calcium on embryogenic induction and the accumulation of abscisic acid, and an early cysteine-labeled metallothionein gene in androgenic microspores of *Triticum aestivum*. Plant Sci 150 (2):201-207. doi:http://dx.doi.org/10.1016/S0168-9452(99)00187-9

Rivas-Sendra A, Calabuig-Serna A, Seguí-Simarro JM (2017) Dynamics of calcium during *in vitro* microspore embryogenesis and *in vivo* microspore development in *Brassica napus* and *Solanum melongena*. Front Plant Sci 8:1177. doi:10.3389/fpls.2017.01177

Rivas-Sendra A, Corral-Martínez P, Camacho-Fernández C, Porcel R, Seguí-Simarro JM (2020) Effects of growth conditions of donor plants and in vitro culture environment in the viability and the embryogenic response of microspores of different eggplant genotypes. Euphytica 216 (11):167. doi:10.1007/s10681-020-02709-4

Rivas-Sendra A, Corral-Martínez P, Porcel R, Camacho-Fernández C, Calabuig-Serna A, Seguí-Simarro JM (2019) Embryogenic competence of microspores is associated with their ability to form a callosic, osmoprotective subintinal layer. J Exp Bot 70 (4):1267–1281. doi:10.1093/jxb/ery458

Rivera-Solís G, Sáenz-Carbonell L, Narváez M, Rodríguez G, Oropeza C (2018) Addition of ionophore A23187 increases the efficiency of *Cocos nucifera* somatic embryogenesis. 3 Biotech 8 (8):366. doi:10.1007/s13205-018-1392-y

Satpute G, Long H, Seguí-Simarro JM, Risueño MC, Testillano PS (2005) Cell architecture during gametophytic and embryogenic microspore development in *Brassica napus*. Acta Physiol Plant 27 (4B):665-674. doi:10.1007/s11738-005-0070-y

Schindelin J, Arganda-Carreras I, Frise E, Kaynig V, Longair M, Pietzsch T, Preibisch S, Rueden C, Saalfeld S, Schmid B, Tinevez JY, White DJ, Hartenstein V, Eliceiri K, Tomancak P, Cardona A (2012) Fiji: an open-source platform for biological-image analysis. Nature methods 9 (7):676-682. doi:10.1038/nmeth.2019

Seguí-Simarro JM (2010) Androgenesis revisited. Bot Rev 76 (3):377-404. doi:10.1007/s12229-010-9056-6

Seguí-Simarro JM (2016) Androgenesis in solanaceae. In: Germanà MA, Lambardi M (eds) In vitro embryogenesis, vol 1359. Methods in Molecular Biology. Springer Science + Business Media, New York, pp 209-244. doi:10.1007/978-1-4939-3061-6_9

Seguí-Simarro JM, Jacquier NMA, Widiez T (2021a) Overview of i*n vitro* and *in vivo* doubled haploid technologies. In: Seguí-Simarro JM (ed) Doubled Haploid Technology, vol 1: General Topics, Alliaceae, Cereals. Methods in Molecular Biology, vol 2287, 1st edn. Springer Science+Business Media, LLC, New York, USA, pp 3-22. doi:10.1007/978-1-0716-1315-3_1

Seguí-Simarro JM, Moreno JB, Fernández MG, Mir R (2021b) Species with haploid or doubled haploid protocols. In: Seguí-Simarro JM (ed) Doubled Haploid Technology, vol 1: General Topics, Alliaceae, Cereals. Methods in Molecular Biology, vol 2287, 1st edn. Springer Science+Business Media, LLC, New York, USA, pp 41-103. doi:10.1007/978-1-0716-1315-3_3

Takeda T, Inose H, Matsuoka H (2003) Stimulation of somatic embryogenesis in carrot cells by the addition of calcium. Biochem Eng J 14 (2):143-148. doi:http://dx.doi.org/10.1016/S1369-703X(02)00186-9

Tian W, Wang C, Gao Q, Li L, Luan S (2020) Calcium spikes, waves and oscillations in plant development and biotic interactions. Nature Plants 6 (7):750-759. doi:10.1038/s41477-020-0667-6

Zaki MA, Dickinson HG (1990) Structural changes during the first divisions of embryos resulting from anther and free microspore culture in *Brassica napus*. Protoplasma 156:149-162

Supplementary materials

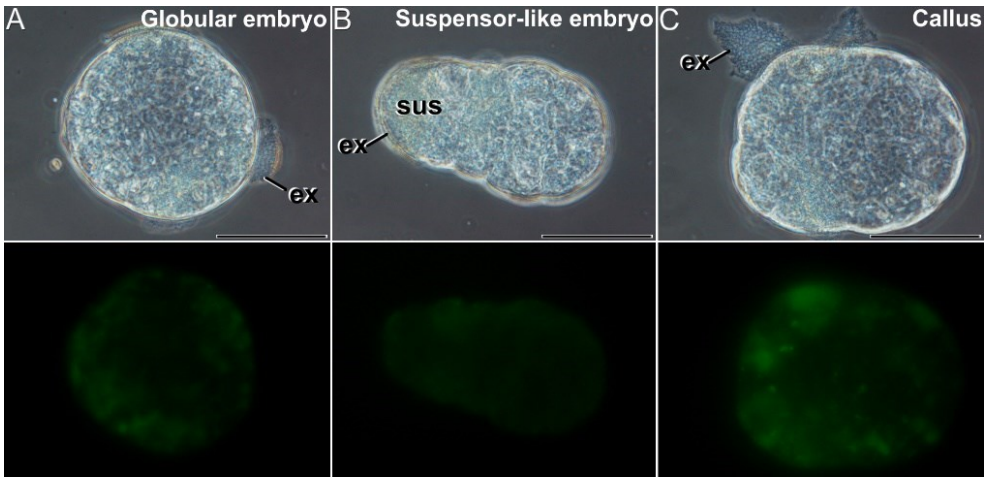

Suppl. Fig. 1. Ca^{2+} detection with FluoForte in 8-day-old *B. napus* microspore cultures. Paired images of the same microscopic field imaged by phase contrast optics (top image) and fluorescence (bottom image). A: Suspensorless globular embryo. B: Suspensor-bearing globular embryo. C: Callus. ex: exine; sus: suspensor. Bars: 50 μm.

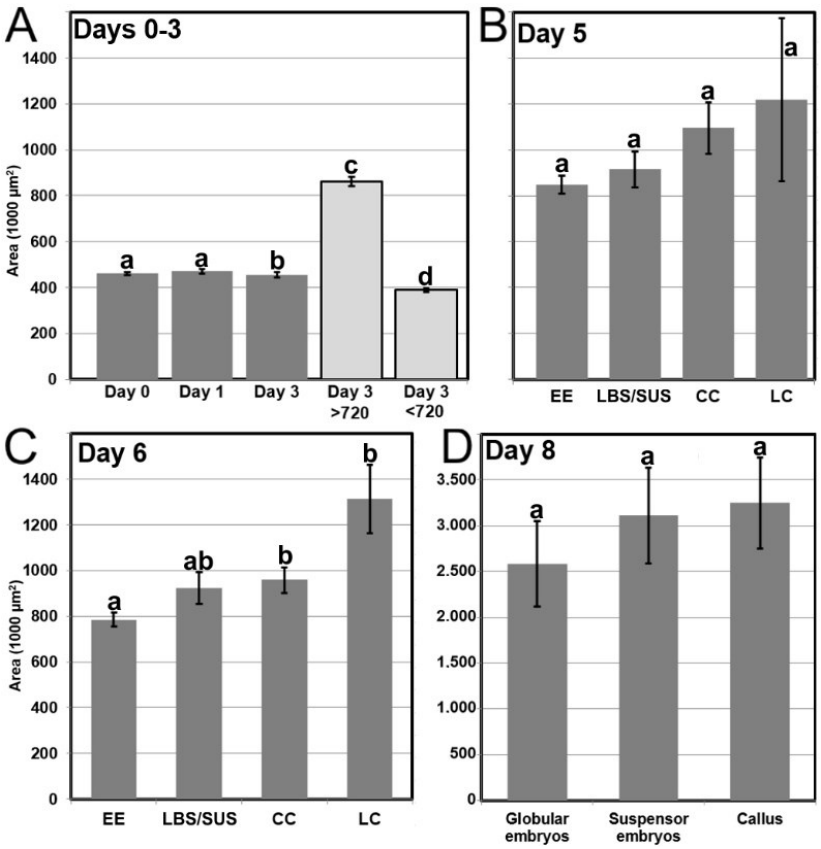

Suppl. Fig. 2. Quantification of the average area of the different structures developed in *B. napus* microspore cultures. Average area is expressed in 1000 µm^2 ± standard error (error bars). A: Average areas in microspores of day 1, day 2 and day 3 cultures. Light grey bars represent a segregation of total day 3 structures in two categories: structures smaller and larger than 720 µm^2 (see text for further details). B, C: Average area of the different embryogenic structures (EE, LBS/SUS, CC and LC) identified in five (B) and six-day-old cultures (C). D: Average area of the different suspensorless globular embryos, suspensor-bearing embryos and calli observed in eight-day-old cultures. All areas were measured under identical experimental conditions and are represented using the same scale, except for day 8 structures. For each chart, different letters indicate significant differences according to the Kruskal-Wallis test ($p \leq 0.05$).

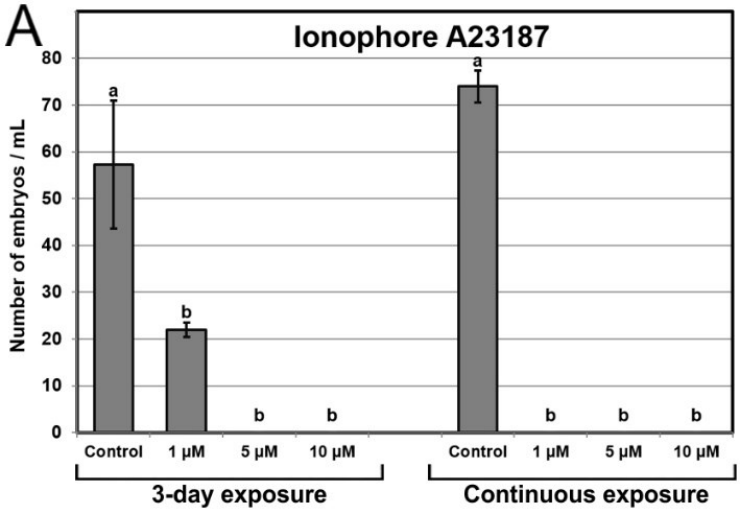

Suppl. Fig. 3. Effects of adding ionophore A23187. Ionophore A23187 was added to the culture medium at 0 (control) 1, 5 and 10 µM and during the first three days of culture and continuously. Effects are expressed as number of embryos produced per mL of culture medium. Different letters indicate significant differences according to the LSD test ($p \leq 0.05$).

8. Discussion

Plant breeding plays a key role in human development. Distinctive circumstances of our time such as climate change and the steady growth in world population are the living demonstrations of the need for developing new plant varieties with improved yields and with capacity to adapt to present-day environmental conditions. During the last decades, biotechnology has provided plant breeding with useful tools that have increased the efficiency in the development of cultivars displaying better performance. In this sense, plant tissue culture has taken a pivotal part mainly through *in vitro* embryogenesis, which has proven to be a very useful tool for both basic studies and agricultural biotechnology. Our main goal was to broaden the knowledge of the cellular and molecular basis underlying plant *in vitro* embryogenesis to improve its efficiency, focusing on the role of Ca^{2+} in this process.

Among all the molecular components and signaling pathways that take part on plant embryogenesis, calcium (Ca^{2+}) is a crucial second messenger. In this doctoral Thesis, the role of Ca^{2+} in plant *in vitro* embryogenesis has been studied in two different systems: somatic embryogenesis (SE, Chapters 1 to 3) and microspore embryogenesis (ME, Chapters 4 and 5). In chapter 1, we explored SE in Arabidopsis, characterizing the process by the analysis of *WUSCHEL* expression, callose deposition and Ca^{2+} distribution through FRET imaging of *cameleon* transgenic lines. In Chapter 2, *cameleon* transgenic lines of *D. carota* were developed and Ca^{2+} dynamics was also imaged by FRET. In Chapter 3 we studied Ca^{2+} distribution in the nuclei of *N. tabacum* during SE using nuclear-targeted *cameleon* transgenic lines. In Chapter 4, in order to study Ca^{2+} dynamics throughout ME, we attempted to develop transgenic lines expressing *cameleon* Ca^{2+} sensors in the *B. napus* ME high-response cultivar DH4079. We observed a complete *Agrobacterium*-mediated transformation recalcitrance in this line, thus we were not able to obtain *B. napus cameleon* lines. Finally, in chapter 5 Ca^{2+} distribution was observed in microspore-derived embryogenic structures through *FluoForte* vital staining. In parallel to this, a pharmacological approach was used to modulate Ca^{2+} levels and to examine their effect on the efficiency of induction of *in vitro* somatic (Chapters 1 and 2) and microspore embryogenesis (Chapter 5). The relevance and implications of our findings are discussed next.

8.1.The challenges of Ca^{2+} observation in plant cells

Genetically-encoded Ca^{2+} sensors are useful tools that enable real-time measure and imaging of Ca^{2+} levels, and *cameleon* FRET-based constructions are among the most popular (Liu et al. 2022). *Cameleon* transgenic lines have been developed in species such as *A. thaliana* (Krebs et al. 2012), *Oryza sativa* (Behera et al. 2015), *Medicago truncatula* (Miwa et al. 2006) or *Solanum lycopersicum* (Wang et al. 2017). We successfully analyzed Ca^{2+} through FRET in *in vitro* embryogenic cultures of *A. thaliana* and *N. tabacum* using previously developed *cameleon* transgenic lines. Since there are no reported *cameleon* lines in carrot and *B. napus*, we attempted their generation. For carrot, we developed the first transgenic lines expressing *cameleon* Ca^{2+} sensor in the plasma membrane, and we used them to visualize Ca^{2+} dynamics during SE. However, we were not able to develop transgenic lines in our model for ME, the *B. napus* high-response cultivar DH4079, while we succeeded to transform the low-response DH12075 line with an efficiency of 0.65%, similar to that reported in previous works

(Kazan et al. 1997). Thus, the first relevant constraint that present the use of genetically-encoded Ca^{2+} sensors is the need of efficient transformation protocols. The genotype stands among the factors to consider, as it strongly determines recalcitrance to transformation. Other factors reported to affect transgene expression are the type of promoters, as some types are reported to silence expression (Sadoine et al. 2021). In our case, this specific aspect was relevant because we intended to visualize Ca^{2+} dynamics in ME, and the 35S-CaMV promoter is silenced during gametophytic development, which precludes its use to study ME early stages (Custers et al. 1999). This is the reason why the *cameleon* constructs we used were controlled by the ubiquitin promoter (*UBQ10*) (Krebs et al. 2012). Therefore, the cell type of interest determines the design of the transgenic construct.

Before the development of genetically-encoded tools, Ca^{2+} levels were observed through staining with fluorescent dyes (Zhao et al. 2002). The main drawback of these approaches was that they do not allow to monitor rapid *in vivo* Ca^{2+} oscillations for a relatively extended period as fluorescence is limited by extinction (Timmers et al. 1989) and eventually the biological tissue will die. Chlortetracycline (CTC) fluorescence was one of the first methods to visualize the Ca^{2+} in plant cells (Reiss and Herth 1978), together with X-ray analysis of calcium antimoniate precipitates (Slocum and Roux 1982). Other fluorescence stains such as *Fluo*-3 were used to visualize free Ca^{2+}, but their use is limited by their low penetration into embryogenic cells, among other plant tissues (Timmers et al. 1991). The use of acetoxymethyl (AM) ester variants, such as and *Fluo-3-AM*, solved this problem and facilitated their passage through the plasma membrane. However, the presence of cell esterases on the extracellular part of the cell wall hydrolyze the AM ester bonds before the compound enters the cell, prematurely releasing the dye. This phenomenon diminishes the staining fluorescence and hampers the measurement of intracellular Ca^{2+}, as observed with quin-2-AM (Cork 1986). This situation imposes technical difficulties when delivering dyes containing AM groups inside the cells, and it makes mandatory the addition of surfactants to the samples, as in the case of *fura-2AM* staining (Anil and Rao 2000), or to vary some conditions such as temperature in order to improve dye permeability (Zhang et al. 1998). As an alternative to genetically-encoded Ca^{2+} sensors, we analyzed Ca^{2+} levels during microspore embryogenesis by staining with *FluoForte*. Although *FluoFlorte* is a Ca^{2+}-sensitive fluorescent stain that also bears an AM ester group, we successfully used this vital staining to determine Ca^{2+} distribution in *B. napus* microspore-derived embryogenic structures, possibly because microspore cell walls do not contain high amounts of cell wall esterases (Solis et al. 2016). To our knowledge, this is one of the very few reports of successful Ca^{2+} visualization in plants using *FluoForte* (Rivas-Sendra et al. 2017; Rivas-Sendra et al. 2019). The coincidences between the results observed in Arabidopsis and carrot SE with *cameleon* sensors and in *B. napus* with *FluoForte* strengthens their validity and confirm that *FluoForte* staining is a useful and convenient alternative to *cameleon* sensors for the study of Ca^{2+} during ME in species recalcitrant to genetic transformation. Besides, Ca^{2+} observation in plant cells does not seem to be trivial at all. On the contrary, the observation method should be carefully chosen attending to the features of the biological process intended to be observed and to the technical requirements involved.

8.2.Understanding Ca^{2+} distribution in plant *in vitro* embryogenesis

Ca^{2+} visualization was performed through *FluoForte* chemical staining in *B. napus* ME, whereas *cameleon* transgenic lines were used for Arabidopsis, carrot and tobacco SE. *FluoForte* stained all the intracellular Ca^{2+} in microspores, while in Arabidopsis, carrot and tobacco, *cameleon* signal was targeted to the cytosol, the plasma membrane and the nucleus, respectively. A common phenomenon observed was that an increase in Ca^{2+} signal accompanied embryogenesis induction in all four systems analyzed. In *B. napus* ME, microspores showed higher fluorescence after one day under heat-shock conditions, indicating an increase in intracellular Ca^{2+} levels. After the 3-day-long heat-shock, enlarged microspores also showed higher signal than non-responsive microspores, as previously reported by Rivas-Sendra et al. (2017). In carrot, embryogenic masses exhibited higher FRET ratios in plasma membranes than disorganized calli while in Arabidopsis, embryogenic protrusions in cotyledons displayed increasing FRET signal in the cytosol. Lastly, tobacco explants nuclei showed increased Ca^{2+} signaling just after 4 days in embryogenesis induction media. Our observations coincided with those previously reported in carrot SE staining with CTC, where Ca^{2+} signal was higher after embryogenic induction (Timmers et al. 1989). Similar Ca^{2+} accumulation was also observed in sandalwood when embryogenic cells were stained with *fura-2AM* (Anil and Rao 2000).

Among its functions as second messenger, Ca^{2+} is involved in transcriptional regulation during diverse biological processes including plant-microbiome interactions (Yuan et al. 2017) and plant response to stress (Noman et al. 2021). This transcriptional regulation is possible thanks to changes in nuclear Ca^{2+} levels, which may have different origins: cytosolic Ca^{2+} incorporated through nuclear pores or released from the nuclear envelope directly to the nucleoplasm, from the nucleoplasmic reticulum or from nuclear microvesicles (Alonso et al. 2006). Hence, it is plausible to propose that Ca^{2+}-mediated transcriptional activation is involved in reprogramming both somatic cells and microspores to start embryogenic development. In this processes, transient Ca^{2+} accumulation would activate calmodulin (CaM) and possibly other Ca^{2+} sensors such as calcineurin B-like proteins, Ca^{2+}-dependent protein kinases and Ca^{2+} and Ca^{2+}/CaM-dependent protein kinases. In turn, these Ca^{2+} sensors would activate or repress Ca^{2+}/CaM-binding transcription factors such as CaM-Binding Transcription Factors (CAMTAs), AtGT-2 (GT-element-binding proteins or GTLs), MYBs, WRKY (zinc-finger-type TF) and CaM-binding NAC protein (CBNAC) or NTL9 (Galon et al. 2010). In fact, previous reports showed that during the early stages of SE in Arabidopsis, CAMTA and WRKY-binding domains are overrepresented, reinforcing the idea of the prominent role that Ca^{2+}/CaM complex plays in embryogenic transcription regulation (Wang et al. 2020; Shang et al. 2022).

Besides the increase in Ca^{2+} levels upon embryogenesis induction, common to somatic and microspore embryogenesis, we also observed that in all the studied systems, Ca^{2+} levels were dynamic and changed during embryo development. In *B. napus* ME, although we were not able to monitor *in vivo* changes in Ca^{2+} signal, the recorded fluorescence in the different embryogenic structures was higher than in induced microspores after heat-shock, indicating that the increase

in Ca^{2+} levels throughout embryo development may be associated to the initial differentiation processes following induction. No significant differences in Ca^{2} levels were observed among the different embryogenic structures differentiated after induction (day 5). However, we distinguished a specific Ca^{2+} accumulation pattern corresponding to suspensor-like (SUS) embryogenic structures. Particularly, we detected a polarization in Ca^{2+} accumulation that occurred in LBS structures, the precursors of SUS embryos, where the basal cell exhibited much higher signal than the apical cell. In Arabidopsis, we monitored the first stages of SE and we observed that FRET ratio increased as embryogenic protrusions developed. Regarding embryo development, we were able to monitor changes in Ca^{2+} signal in carrot and tobacco SE. In both systems, changes in Ca^{2+} levels accompanied embryo growth and signals were different depending on the differentiating tissue and region. In this sense, higher Ca^{2+} signals were observed at shoot apical region and cotyledonary primordia in both tobacco nuclei and carrot plasma membranes. Moreover, embryos at different developmental stages showed distinct Ca^{2+} distribution patterns. Therefore, our observations indicate that embryo development is paralleled by changes in Ca^{2+} dynamics, which agreed with previous reports on carrot SE through staining with CTC and N-phenyl-1-napthylamine (NPN) (Timmers et al. 1991; Overvoorde and Grimes 1994).

Our observations of different Ca^{2+} levels in cells of polarized structures like LBS/SUS are in line with the widely acknowledged role of Ca^{2+} in polarized cell growth in plants. Specifically, it is thought to participate in establishing hallmarks for cell polarity, regulating membrane trafficking, reorganizing cytoskeleton, interacting with small GTPase ROP polarization and coordinating mechanical polarity signals (Yang et al. 2020). Regarding meristematic development, Ca^{2+} is critical to guide auxin transport polarity in plant stem cell niche (Li et al. 2019). As previously discussed, besides establishing polar growth patterns, Ca^{2+} also regulates transcriptional changes and CAMTAs and multiple other CaM-binding transcription factors are involved in plant growth processes (Iqbal et al. 2020). Thus, dynamic changes in Ca^{2+} levels are inherent to embryo development and tissue differentiation, probably linked to cell fate determination.

8.3.Plasticity of embryogenic response to Ca^{2+} depends on the system

In this Thesis, we showed that the exogenous addition of different chemicals is capable to alter Ca^{2+} homeostasis, at least in the studied *in vitro* embryogenic systems. These systems can be classified in two categories: (1) those based on isolated cell suspensions, and (2) explant-based systems. The first group includes carrot SE and *B. napus* ME. The second comprises systems where embryogenesis is induced in some cells of an explant, a piece of tissue excissed from the donor plant and cultured *in vitro* on solid media as such (IZEs in Arabidopsis SE, and leaves in tobacco SE). We observed that the systems where embryogenesis takes place in isolated cells have a more plastic response to modulation of Ca^{2+} levels. However, alteration of embryo yield by Ca^{2+} modulation is more challenging in Arabidopsis, a system where *in vitro* embryogenesis takes place from explants. In the case of carrot and *B. napus* systems, the exogenous addition of Ca^{2+} in the form of $CaCl_2$ and $Ca(NO_3)_2$, respectively, improved the embryogenic response, which is in accordance to previous reports on carrot SE (Jansen et al. 1990). In

sandalwood (*Santalum album*) SE, where the experimental system is also based on cell suspensions, similar results were observed when adding increasing concentrations of Ca^{2+} to culture media (Anil and Rao 2000). However, a positive effect on embryogenesis has also been observed upon exogenous addition of Ca^{2+} in other explant-based systems such as *Pinus patula* SE (Malabadi and van Staden 2006) and *Coffea canephora* (Ramakrishna et al. 2012). Hence, an effect of the genotype and/or the technical particularities of the *in vitro* embryogenesis protocol used in each case might should not be totally excluded. Altogether, these results point to the fact that in cell suspension-based systems, embryogenesis could be enhanced by increasing Ca^{2+} concentration within a functional range, sufficient to improve embryogenic induction but without reaching toxic levels to the cells.

A possible explanation for the observed differences in plasticity among systems would be the different accessibility for Ca^{2+} to enter the cells. In this sense, isolated carrot cells and *B. napus* microspores would have their entire surface in contact with the liquid culture medium with increased Ca^{2+} concentrations, thereby increasing the number of Ca^{2+} channels available for Ca^{2+} uptake. On the other hand, Arabidopsis IZEs are cultured in solid media, and their morphology do not allow the inducible cells (inner cells of the mesophyll at the cotyledon nodes) to be in direct contact with the culture medium. Furthermore, these cotyledon cells remain covered by the IZE protoderm during the initial stages of the embryogenic process. All these factors would likely impose physical barriers that would prevent Ca^{2+} uptake by the inducible somatic cells. Thus, in Arabidopsis SE the addition of Ca^{2+} would have no apparent effect because Ca^{2+} concentration around inducible cells is lower than in carrot SE and *B. napus* ME systems. Nonetheless, a different situation is observed when Ca^{2+} depletion effects are analyzed. We found that treatments with the Ca^{2+} chelators BAPTA and/or EGTA inhibited embryogenesis in *B. napus* ME and also in carrot and Arabidopsis SE systems, indicating that the presence of a basal Ca^{2+} level is necessary to allow embryogenic induction and development independently of the species (Overvoorde and Grimes 1994; Ramakrishna et al. 2012). In Arabidopsis SE, this effect could be explained because the chelating agents would sequester the Ca^{2+} ions present in the culture medium, reducing Ca^{2+} levels below a minimum concentration threshold incompatible with proper IZEs development, thereby compromising their cell viability. This, obviously, would have an impact in the embryogenesis-inducible cells of the IZE cotyledon node, as well as in isolated carrot somatic cells and *B. napus* micropspores.

Regarding the modulation of intracellular Ca^{2+} levels, the ionophore A23187 is a Ca^{2+} carrier that allows the entry of Ca^{2+} through the plasma membrane (Reed and Lardy 1972). We have observed that the effect of the ionophore A23187 varied specifically among systems. In carrot SE, the addition of ionophore A23187 for three days enhanced the embryogenic response. However, the application for extended periods showed no beneficial effect. Our observations agree with previous reports in wheat SE, where transient application of ionophore A23187 also increased embryogenesis (Mahalakshmi et al. 2007). On the other hand, the application of ionophore A23187 to *B. napus* microspore cultures, both continuously and transiently, provoked a decrease in embryogenic response, an effect similar to that observed in sandalwood SE (Anil and Rao 2000). In

Arabidopsis, ionophore A23187 also hampered SE, but this contrasted with its positive effect in other explant-based SE systems such as *Coffea canephora* (Ramakrishna et al. 2012). Altogether, our findings suggest that the effect of a rise in intracellular Ca^{2+} levels as a result of Ca^{2+} ionophore A23187 depends on the embryogenic system and the duration of the treatment. Hence, in carrot somatic cells, short application periods could induce a Ca^{2+} influx that would trigger an increase in the proportion of induced cells towards embryogenesis. Furthermore, in the case of *B. napus* ME it was previously reported that a Ca^{2+} increase occurs upon embryogenesis induction (Rivas-Sendra et al. 2017), thus, this additional Ca^{2+} influx induced by ionophore A23187 would rise Ca^{2+} intracellular concentrations up to toxic levels.

The crucial role that CaM plays in Ca^{2+} transduction signal is well known. In the present PhD Thesis, we confirmed that CaM takes part in the induction of embryogenesis in *B. napus*, carrot and Arabidopsis. In all cases, treatments with CaM antagonists W-7 and/or chlorpromazine resulted in embryogenesis inhibition, in line with previous reports (Overvoorde and Grimes 1994; Anil and Rao 2000). Therefore, independently of the embryogenic system, CaM is pivotal in the *in vitro* embryogenesis induction. This is reasonable due to the high amount of molecular processes in which CaM is involved, including protein kinase activation and transcriptional modifications (Bredow and Monaghan 2022). Comparing the effect of CaM inhibitors and the Ca^{2+} chelators agents, a dose-dependent response is observed in Arabidopsis SE, carrot SE and *B. napus* ME. In the case of EGTA, a concentration of 10 mM was sufficient to inhibit carrot SE and *B. napus* ME, independently of the duration of the application. In Arabidopsis SE, 1 mM EGTA applied continuously practically halted embryogenesis. W-7 treatments reduced embryogenesis response, but they did not inhibit completely carrot and Arabidopsis SE. The fact that, in general, treatments with chelators and CaM antagonists produce similar response patterns would be an indicator of the significant physiological function of Ca^{2+} in cell signaling upon binding with CaM.

8.4.Callose deposition in plant *in vitro* embryogenesis

A common effect in all *in vitro* systems was also observed in treatments with 2-deoxy-D-glucose, where the inhibition of callose biosynthesis resulted in a reduction or even a complete arrest of the embryogenesis response. Callose deposition during Arabidopsis SE was shown to isolate embryogenic cells from the rest of the explant tissue (Godel-Jedrychowska et al. 2020). A similar role was proposed by (Parra-Vega et al. 2015) for the callose-rich subintinal layer that forms upon ME induction in *B. napus*. In Arabidopsis, we also observed an increase in callose deposition in the embryogenic areas of IZEs when SE was induced, and that deposition diminished when treating explants with 2-deoxy-D-glucose. Similarly, we found that in carrot, responding cell clumps and proembryogenic masses also showed a differential callose deposition pattern with respect to non-embryogenic callogenic cells. Again, callose deposition notably decreased with the application of 2-deoxy-D-glucose. Thus, in these embryogenic systems, callose seems to have a critical role mainly during the induction stages. Specifically, callose deposition may be acting as an isolating barrier in reprogramming cells. This isolation would allow the development of

the embryogenic cells independently of the rest of cultured tissues. Furthermore, in both systems callose deposition coincides with an increase in Ca^{2+} levels upon embryogenesis induction. Thus, it is possible that the activity of callose synthases is controlled by Ca^{2+} signals, and they are activated when cells start reprogramming towards the embryogenic route.

8.5.Concluding remarks and future perspectives

Among the different factors involved in *in vitro* embryogenesis, Ca^{2+} signaling is decisive in order to properly induce embryo development. In some of the *in vitro* systems studied in the present work, the embryogenic response can be improved through a pharmacological approach. In other cases, we found that they were not sensitive to chemical modulation or exhibited a negative response. This observation points to a complex regulation of this process by Ca^{2+}, and further investigations are needed to understand the fine-tuned regulation exerted by Ca^{2+}during *in vitro* embryogenesis. Besides these differences between embryogenic systems, a common pattern of transient Ca^{2+} accumulation during induction and differentiation upon embryogenesis induction has been observed in both SE and ME, which suggests the universal involvement of Ca^{2+} in *in vitro* plant embryogenesis. In this sense, more efforts could be done to elucidate the particular role that Ca^{2+} plays in each molecular process in order to increase the efficiency of these *in vitro* systems. Unraveling these molecular bases may be achieved by developing specific mutants for CaM and other proteins involved in transduction signal pathways, and studying their embryogenic performance and their phenotypes. Furthermore, due to the existing link between Ca^{2+} signaling and transcription regulation reported in previous works, it would be interesting to explore how modifications in Ca^{2+} homeostasis would affect gene expression in the different embryogenic systems. This could shed some light on the genetic regulation of embryogenesis induction through the potential identification of embryogenesis-related genes whose expression is under the control of Ca^{2+} signaling pathways. With this PhD Thesis, we contributed to expand the knowledge on plant *in vitro* embryogenesis and to advance towards its optimization.

9. References

Albiñana Palacios M, Seguí-Simarro JM (2021) Anther culture in sweet pepper (*Capsicum annuum* L.). In: Seguí-Simarro JM (ed) Doubled Haploid Technology, vol 2: Hot Topics, Apiaceae, Brassicaceae, Solanaceae. Methods in Molecular Biology, vol 2288, 1st edn. Springer Science+Business Media, LLC, New York, USA, pp 279-291. doi:10.1007/978-1-0716-1335-1_17

Alonso MT, Villalobos C, Chamero P, Alvarez J, García-Sancho J (2006) Calcium microdomains in mitochondria and nucleus. Cell Calcium 40 (5-6):513-525

Anil VS, Rao KS (2000) Calcium-mediated signaling during sandalwood somatic embryogenesis. Role for exogenous calcium as second messenger. Plant Physiol 123 (4):1301-1312

Asadi A, Seguí-Simarro JM (2021) Production of doubled haploid plants in cucumber (*Cucumis sativus* L.) through anther culture. In: Seguí-Simarro JM (ed) Doubled Haploid Technology, vol 3: Emerging Tools, Cucurbits, Trees, Other Species. Methods in Molecular Biology, vol 2289, 1st edn. Springer Science+Business Media, LLC, New York, USA, pp 71-85. doi:10.1007/978-1-0716-1331-3_4

Asif M, Eudes F, Randhawa H, Amundsen E, Spaner D (2014) Induction medium osmolality improves microspore embryogenesis in wheat and triticale. In Vitro Cell Dev Biol -Pl 50 (1):121-126. doi:10.1007/s11627-013-9545-5

Baranski R, Lukasiewicz A (2019) Genetic engineering of carrot. In: The Carrot Genome. Springer, pp 149-186

Behera S, Wang N, Zhang C, Schmitz-Thom I, Strohkamp S, Schültke S, Hashimoto K, Xiong L, Kudla J (2015) Analyses of Ca2+ dynamics using a ubiquitin-10 promoter-driven Yellow *Cameleon* 3.6 indicator reveal reliable transgene expression and differences in cytoplasmic Ca2+ responses in *Arabidopsis* and rice (*Oryza sativa*) roots. New Phytol 206 (2):751-760

Bidabadi SS, Jain SM (2020) Cellular, molecular, and physiological aspects of in vitro plant regeneration. Plants 9 (6):702

Bourke PM, Evers JB, Bijma P, van Apeldoorn DF, Smulders MJ, Kuyper TW, Mommer L, Bonnema G (2021) Breeding beyond monoculture: putting the "intercrop" into crops. Front Plant Sci 12:734167

Boutilier K, Offringa R, Sharma VK, Kieft H, Ouellet T, Zhang L, Hattori J, Liu C-M, van Lammeren AAM, Miki BLA, Custers JBM, van Lookeren Campagne MM (2002) Ectopic expression of BABYBOOM triggers a conversion from vegetative to embryonic growth. Plant Cell 14 (8):1737-1749

Bredow M, Monaghan J (2022) Cross-kingdom regulation of calcium-and/or calmodulin-dependent protein kinases by phospho-switches that relieve autoinhibition. Curr Opin Plant Biol 68:102251

Calabuig-Serna A, Camacho-Fernández C, Mir R, Porcel R, Carrera E, López-Díaz I, Seguí-Simarro JM (2022) Quantitative and qualitative study of endogenous and exogenous growth regulators in eggplant (*Solanum melongena*) microspore cultures. Plant Growth Regul 96 (2):345–355. doi:10.1007/s10725-021-00780-y

Calabuig-Serna A, Porcel R, Corral-Martínez P, Seguí-Simarro JM (2021) Anther and isolated microspore culture in eggplant (*Solanum melongena* L.). In: Seguí-Simarro JM (ed) Doubled Haploid Technology, vol 2: Hot Topics, Apiaceae, Brassicaceae, Solanaceae. Methods in Molecular Biology, vol 2288, 1st edn. Springer Science+Business Media, LLC, New York, USA, pp 235-250. doi:10.1007/978-1-0716-1335-1_14

Camacho-Fernández C, Hervás D, Rivas-Sendra A, Marín MP, Seguí-Simarro JM (2018) Comparison of six different methods to calculate cell densities. Plant Methods 14 (1):30. doi:10.1186/s13007-018-0297-4

Castillo AM, Valero-Rubira I, Burrell M, Allué S, Costar MA, Vallés MP (2020) Trichostatin A Affects Developmental Reprogramming of Bread Wheat Microspores towards an Embryogenic Route. Plants (Basel) 9 (11). doi:10.3390/plants9111442

Cork R (1986) Problems with the application of quin-2-AM to measuring cytoplasmic free calcium in plant cells. Plant, Cell & Environment 9 (2):157-161

Corral-Martínez P, Camacho-Fernández C, Mir R, Seguí-Simarro JM (2021) Doubled haploid production in high- and low-response genotypes of rapeseed (*Brassica napus*) through isolated microspore culture. In: Seguí-Simarro JM (ed) Doubled Haploid Technology, vol 2: Hot Topics, Apiaceae, Brassicaceae, Solanaceae. Methods in Molecular Biology, vol 2288, 1st edn. Springer Science+Business Media, LLC, New York, USA, pp 129-144. doi:10.1007/978-1-0716-1335-1_8

Corral-Martínez P, Camacho-Fernández C, Seguí-Simarro JM (2020) Isolated microspore culture in *Brassica napus*. In: Bayer M (ed) Plant Embryogenesis: Methods and Protocols, vol 2122. Methods in Molecular Biology, vol 2122. Springer Science+Business Media, LLC, New York, NY, pp 269-282. doi:10.1007/978-1-0716-0342-0_19

Corral-Martínez P, Parra-Vega V, Seguí-Simarro JM (2013) Novel features of *Brassica napus* embryogenic microspores revealed by high pressure freezing and freeze substitution: evidence for massive autophagy and excretion-based cytoplasmic cleaning. J Exp Bot 64 (10):3061-3075. doi:10.1093/jxb/ert151

Corral-Martinez P, Siemons C, Horstman A, Angenent GC, de Ruijter N, Boutilier K (2020) Live Imaging of embryogenic structures in *Brassica napus* microspore embryo cultures highlights the developmental plasticity of induced totipotent cells. Plant Reprod 33 (3-4):143-158. doi:10.1007/s00497-020-00391-z

Custers JBM, Cordewener JHG, Fiers MA, Maassen BTH, van Lookeren-Campagne MM, Liu CM (2001) Androgenesis in *Brassica*: a model system to study the initiation of plant embryogenesis. In: Bhojwani SS, Soh WY (eds) Current trends in the embryology of angiosperm. Kluwer Academic Publishers, Dordrecht, The Netherlands, pp 451-470

Custers JBM, Snepvangers S, Jansen HJ, Zhang L, Campagne MMV (1999) The 35S-CaMV promoter is silent during early embryogenesis but activated during nonembryogenic sporophytic development in microspore culture. Protoplasma 208 (1-4):257-264

Digonnet C, Aldon D, Leduc N, Dumas C, Rougier M (1997) First evidence of a calcium transient in flowering plants at fertilization. Development 124 (15):2867-2874

Dresselhaus T, Jürgens G (2021) Comparative Embryogenesis in Angiosperms: Activation and Patterning of Embryonic Cell Lineages. Ann Rev Plant Biol 72 (1):null. doi:10.1146/annurev-arplant-082520-094112

Egertsdotter U, Ahmad I, Clapham D (2019) Automation and scale up of somatic embryogenesis for commercial plant production, with emphasis on conifers. Front Plant Sci 10:109

Elhiti M, Stasolla C (2022) Transduction of Signals during Somatic Embryogenesis. Plants 11 (2):178

Fehér A (2019) Callus, Dedifferentiation, Totipotency, Somatic Embryogenesis: What These Terms Mean in the Era of Molecular Plant Biology? Front Plant Sci 10. doi:10.3389/fpls.2019.00536

Ferrie A, Caswell K (2011) Isolated microspore culture techniques and recent progress for haploid and doubled haploid plant production. Plant Cell Tissue Organ Cult 104 (3):301-309. doi:10.1007/s11240-010-9800-y

Ferrie A, Möllers C (2011) Haploids and doubled haploids in *Brassica* spp. for genetic and genomic research. Plant Cell Tissue Organ Cult 104 (3):375-386. doi:10.1007/s11240-010-9831-4

Fiegert AK, Mix-Wagner G, Vorlop KD (2000) Regeneration of *Solanum tuberosum* L. cv. Tomensa: induction of somatic embryogenesis in liquid culture for the production of "artificial seed". Landbauforschung Völkenrode 50 (3/4):199-202

Frugis G, Mele G, Giannino D, Mariotti D (1999) MsJ1, an alfalfa DnaJ-like gene, is tissue-specific and transcriptionally regulated during cell cycle. Plant Mol Biol 40 (3):397-408

Fujii JA, Slade D, Redenbaugh K (1989) Maturation and greenhouse planting of alfalfa artificial seeds. In Vitro Cellular & Developmental Biology 25 (12):1179-1182. doi:10.1007/bf02621271

Gaj MD (2001) Direct somatic embryogenesis as a rapid and efficient system for in vitro regeneration of Arabidopsis thaliana. Plant Cell Tissue Organ Cult 64:39-46

Gaj MD (2011) Somatic Embryogenesis and Plant Regeneration in the Culture of *Arabidopsis thaliana* (L.) Heynh. Immature Zygotic Embryos. In: Thorpe TA, Yeung EC (eds) Plant Embryo Culture: Methods and Protocols. Humana Press, Totowa, NJ, pp 257-265. doi:10.1007/978-1-61737-988-8_18

Galon Y, Finkler A, Fromm H (2010) Calcium-regulated transcription in plants. Mol Plant 3 (4):653-669

Garcês H, Sinha N (2009) The 'mother of thousands'(Kalanchoë daigremontiana): A plant model for asexual reproduction and CAM studies. Cold Spring Harbor Protocols 2009 (10):pdb. emo133

Ge LL, Tian HQ, Russell SD (2007) Calcium function and distribution during fertilization in angiosperms. Am J Bot 94 (6):1046-1060. doi:10.3732/ajb.94.6.1046

Ghanbarali S, Abdollahi MR, Zolnorian H, Moosavi SS, Seguí-Simarro JM (2016) Optimization of the conditions for production of synthetic seeds by encapsulation of axillary buds derived from minituber sprouts in potato (*Solanum tuberosum*). Plant Cell Tissue Organ Cult 126:449.458. doi:10.1007/s11240-016-1013-6

Godel-Jedrychowska K, Kulinska-Lukaszek K, Horstman A, Soriano M, Li M, Malota K, Boutilier K, Kurczynska EU (2020) Symplasmic isolation marks cell fate changes during somatic embryogenesis. J Exp Bot 71 (9):2612-2628. doi:10.1093/jxb/eraa041

Gonzalez-Calquin C, Stange C (2020) *Agrobacterium tumefacien*s-mediated stable transformation of *Daucus carota*. In: Rodríguez-Concepción M, Welsch R (eds) Plant and Food Carotenoids: Methods and Protocols. Methods in Molecular Biology, vol 2083. Springer Science+Business Media, New York, USA, pp 313-320. doi:10.1007/978-1-4939-9952-1_24

Gresshoff PM, Doy CH (1972) Haploid *Arabidopsis thaliana* callus and plants from anther culture. Australian Journal of Biological Sciences 25 (2):259

Guha S, Maheshwari SC (1964) In vitro production of embryos from anthers of *Datura*. Nature 204:497

Hallauer AR, Darrah LL (1985) Compendium of recurrent selection methods and their application. Crit Rev Plant Sci 3 (1):1-33

Hecht V, Vielle-Calzada J-P, Hartog MV, Schmidt ED, Boutilier K, Grossniklaus U, de Vries SC (2001) The Arabidopsis SOMATIC EMBRYOGENESIS RECEPTOR KINASE 1 gene is expressed in developing ovules and embryos and enhances embryogenic competence in culture. Plant Physiol 127 (3):803-816

Hepler PK (2005) Calcium: a central regulator of plant growth and development. Plant Cell 17 (8):2142-2155. doi:10.1105/tpc.105.032508

Hooghvorst I, Nogués S (2021) Chromosome doubling methods in doubled haploid and haploid inducer-mediated genome-editing systems in major crops. Plant Cell Rep 40 (2):255-270

Iqbal MCM, Mollers C (2019) Towards artificial seeds from microspore derived embryos of Brassica napus. Plant Cell Tissue and Organ Culture 139 (2):207-225. doi:10.1007/s11240-019-01692-6

Iqbal Z, Shariq Iqbal M, Singh SP, Buaboocha T (2020) Ca2+/calmodulin complex triggers CAMTA transcriptional machinery under stress in plants: signaling cascade and molecular regulation. Front Plant Sci 11:598327

Islam SMS, Tuteja N (2012) Enhancement of androgenesis by abiotic stress and other pretreatments in major crop species. Plant Sci 182 (0):134-144. doi:10.1016/j.plantsci.2011.10.001

Iwase A, Mitsuda N, Koyama T, Hiratsu K, Kojima M, Arai T, Inoue Y, Seki M, Sakakibara H, Sugimoto K (2011) The AP2/ERF transcription factor WIND1 controls cell dedifferentiation in Arabidopsis. Curr Biol 21 (6):508-514

Jansen MA, Booij H, Schel JH, de Vries SC (1990) Calcium increases the yield of somatic embryos in carrot embryogenic suspension cultures. Plant Cell Rep 9 (4):221-223

Juzoń-Sikora K, Nowicka A, Plačková L, Doležal K, Żur I (2022) Hormonal homeostasis associated with effective induction of triticale microspore embryogenesis. Plant Cell Tissue Organ Cult:1-22

Kanchiswamy CN, Malnoy M, Occhipinti A, Maffei ME (2014) Calcium imaging perspectives in plants. International Journal of Molecular Sciences 15 (3):3842-3859

Kazan K, Curtis MD, Goulter KC, Manners JM (1997) *Agrobacterium tumefaciens*-mediated transformation of double haploid canola (*Brassica napus*) lines. Functional Plant Biology 24 (1):97-102. doi:https://doi.org/10.1071/PP96024

Kitto SL, Janick J (1982) Polyox as an artificial seed coat for asexual embryos. Hortscience 17:488-488

Krebs M, Held K, Binder A, Hashimoto K, Den Herder G, Parniske M, Kudla J, Schumacher K (2012) FRET-based genetically encoded sensors allow high-resolution live cell imaging of Ca^{2+} dynamics. Plant J 69 (1):181-192. doi:10.1111/j.1365-313X.2011.04780.x

Leitão N, Dangeville P, Carter R, Charpentier M (2019) Nuclear calcium signatures are associated with root development. Nature Communications 10 (1):4865

Li H, Soriano M, Cordewener J, Muiño JM, Riksen T, Fukuoka H, Angenent GC, Boutilier K (2014) The histone deacetylase inhibitor Trichostatin A promotes totipotency in the male gametophyte. Plant Cell 26 (1):195-209. doi:10.1105/tpc.113.116491

Li T, Yan A, Bhatia N, Altinok A, Afik E, Durand-Smet P, Tarr PT, Schroeder JI, Heisler MG, Meyerowitz EM (2019) Calcium signals are necessary to establish auxin transporter polarity in a plant stem cell niche. Nat Commun 10 (1):019-08575

Liu Y, Yuan G, Hassan MM, Abraham PE, Mitchell JC, Jacobson D, Tuskan GA, Khakhar A, Medford J, Zhao C (2022) Biological and Molecular Components for Genetically Engineering Biosensors in Plants. BioDesign Research

Lopez-Hernandez F, Tryfona T, Rizza A, Xiaolan LY, Harris MO, Webb AA, Kotake T, Dupree P (2020) Calcium binding by arabinogalactan polysaccharides is important for normal plant development. Plant Cell 32 (10):3346-3369

Lotan T, Ohto M-a, Yee KM, West MA, Lo R, Kwong RW, Yamagishi K, Fischer RL, Goldberg RB, Harada JJ (1998) Arabidopsis LEAFY COTYLEDON1 is sufficient to induce embryo development in vegetative cells. Cell 93 (7):1195-1205

Mahalakshmi A, Singla B, Khurana JP, Khurana P (2007) Role of calcium–calmodulin in auxin-induced somatic embryogenesis in leaf base cultures of wheat (*Triticum aestivum* var. HD 2329). Plant Cell Tissue Organ Cult 88 (2):167-174

Malabadi RB, van Staden J (2006) Cold-enhanced somatic embryogenesis in *Pinus patula* is mediated by calcium. South African Journal of Botany 72 (4):613-618. doi:10.1016/j.sajb.2006.04.001

Marin-Montes IM, Rodríguez-Pérez JE, Robledo-Paz A, de la Cruz-Torres E, Peña-Lomelí A, Sahagún-Castellanos J (2022) Haploid Induction in Tomato (*Solanum lycopersicum* L.) via Gynogenesis. Plants (Basel) 11 (12):1595. doi:10.3390/plants11121595

Masters BS (2004) Safety of genetically engineered foods: approaches to assessing unintended health effects. Washington, DC: The National Academies of Sciences

Méndez-Hernández HA, Ledezma-Rodríguez M, Avilez-Montalvo RN, Juárez-Gómez YL, Skeete A, Avilez-Montalvo J, De-la-Peña C, Loyola-Vargas VM (2019) Signaling overview of plant somatic embryogenesis. Front Plant Sci 10:77

Miwa H, Sun J, Oldroyd GE, Allan Downie J (2006) Analysis of calcium spiking using a cameleon calcium sensor reveals that nodulation gene expression is regulated by calcium spike number and the developmental status of the cell. Plant J 48 (6):883-894

Miyawaki A, Llopis J, Heim R, McCaffery JM, Adams JA, Ikura M, Tsien RY (1997) Fluorescent indicators for Ca^{2+} based on green fluorescent proteins and calmodulin. Nature 388 (6645):882-887

Moeinizade S, Kusmec A, Hu G, Wang L, Schnable PS (2020) Multi-trait genomic selection methods for crop improvement. Genetics 215 (4):931-945

Niazian M, Shariatpanahi ME (2020) In vitro-based doubled haploid production: recent improvements. Euphytica 216 (5):1-21

Noman M, Aysha J, Ketehouli T, Yang J, Du L, Wang F, Li H (2021) Calmodulin binding transcription activators: An interplay between calcium signalling and plant stress tolerance. J Plant Physiol 256:153327. doi:https://doi.org/10.1016/j.jplph.2020.153327

Overvoorde PJ, Grimes HD (1994) The role of calcium and calmodulin in carrot somatic embryogenesis. Plant Cell Physiol 35 (2):135-144

Parra-Vega V, Corral-Martínez P, Rivas-Sendra A, Seguí-Simarro JM (2015) Induction of embryogenesis in *Brassica napus* microspores produces a callosic subintinal layer and abnormal cell walls with altered levels of callose and cellulose. Front Plant Sci 6:1018. doi:10.3389/fpls.2015.01018

Pathi KM, Tula S, Tuteja N (2013) High frequency regeneration via direct somatic embryogenesis and efficient Agrobacterium-mediated genetic transformation of tobacco. Plant Signaling & Behavior 8 (6):e24354

Phillips GC, Garda M (2019) Plant tissue culture media and practices: an overview. In Vitro Cellular & Developmental Biology-Plant 55 (3):242-257

Pittman JK (2011) Vacuolar Ca2+ uptake. Cell Calcium 50 (2):139-146. doi:http://dx.doi.org/10.1016/j.ceca.2011.01.004

Qaim M (2020) Role of new plant breeding technologies for food security and sustainable agricultural development. Applied Economic Perspectives and Policy 42 (2):129-150

Quiroz-Figueroa F, Fuentes-Cerda C, Rojas-Herrera R, Loyola-Vargas V (2002) Histological studies on the developmental stages and differentiation of two different somatic embryogenesis systems of Coffea arabica. Plant Cell Rep 20:1141-1149

Raghavan V (1986) Embryogenesis in angiosperms. A developmental and experimental study. Cambridge University Press, Cambridge, London

Ramakrishna A, Giridhar P, Jobin M, Paulose CS, Ravishankar GA (2012) Indoleamines and calcium enhance somatic embryogenesis in *Coffea canephora* P ex Fr. Plant Cell Tissue Organ Cult 108 (2):267-278. doi:10.1007/s11240-011-0039-z

Ramakrishna A, Giridhar P, Ravishankar GA (2011) Calcium and calcium ionophore A23187 induce high-frequency somatic embryogenesis in cultured tissues of *Coffea canephora* P ex Fr. In Vitro Cell Dev Biol -Pl 47 (6):667-673. doi:10.1007/s11627-011-9372-5

Reed PW, Lardy HA (1972) A23187: a divalent cation ionophore. J Biol Chem 247 (21):6970-6977

Reinert J (1958) Morphogenese und ihre Kontrolle an Gewebekulturen aus Carotten. Naturwissenschaften 45:344-345

Reinert J, Backs D (1968) Control of totipotency in plant cells growing in vitro. Nature 220 (5174):1340-1341

Reiss H-D, Herth W (1978) Visualization of the Ca 2+-gradient in growing pollen tubes of Lilium longiflorum with chlorotetracycline fluorescence. Protoplasma 97:373-377

Rivas-Sendra A, Calabuig-Serna A, Seguí-Simarro JM (2017) Dynamics of calcium during *in vitro* microspore embryogenesis and *in vivo* microspore development in *Brassica napus* and *Solanum melongena*. Front Plant Sci 8:1177. doi:10.3389/fpls.2017.01177

Rivas-Sendra A, Corral-Martínez P, Camacho-Fernández C, Porcel R, Seguí-Simarro JM (2020) Effects of growth conditions of donor plants and in vitro culture environment in the viability and the embryogenic response of microspores of different eggplant genotypes. Euphytica 216 (11):167. doi:10.1007/s10681-020-02709-4

Rivas-Sendra A, Corral-Martínez P, Porcel R, Camacho-Fernández C, Calabuig-Serna A, Seguí-Simarro JM (2019) Embryogenic competence of microspores is associated with their ability to form a callosic, osmoprotective subintinal layer. J Exp Bot 70 (4):1267–1281. doi:10.1093/jxb/ery458

Sadoine M, Ishikawa Y, Kleist TJ, Wudick MM, Nakamura M, Grossmann G, Frommer WB, Ho C-H (2021) Designs, applications, and limitations of genetically encoded fluorescent sensors to explore plant biology. Plant Physiol 187 (2):485-503

San Noeum LH (1979) In vitro induction of gynogenesis in higher plants. . Paper presented at the Proc. Conf. Broadening Genet., Wageningen: Pudoc,

Seguí-Simarro JM (2010) Androgenesis revisited. Bot Rev 76 (3):377-404. doi:10.1007/s12229-010-9056-6

Seguí-Simarro JM (2016) Androgenesis in solanaceae. In: Germanà MA, Lambardi M (eds) In vitro embryogenesis, vol 1359. Methods in Molecular Biology. Springer Science + Business Media, New York, pp 209-244. doi:10.1007/978-1-4939-3061-6_9

Seguí-Simarro JM (2021) Doubled Haploid Technology, vol 3: Emerging Tools, Cucurbits, Trees, Other Species. Methods in Molecular Biology, vol 2289, 1st edn. Springer Science+Business Media, LLC, New York, USA. doi:10.1007/978-1-0716-1331-3

Seguí-Simarro JM, Jacquier NMA, Widiez T (2021a) Overview of i*n vitro* and *in vivo* doubled haploid technologies. In: Seguí-Simarro JM (ed) Doubled Haploid Technology, vol 1: General Topics, Alliaceae, Cereals. Methods in Molecular Biology, vol 2287, 1st edn. Springer Science+Business Media, LLC, New York, USA, pp 3-22. doi:10.1007/978-1-0716-1315-3_1

Seguí-Simarro JM, Moreno JB, Fernández MG, Mir R (2021b) Species with haploid or doubled haploid protocols. In: Seguí-Simarro JM (ed) Doubled Haploid Technology, vol 1: General Topics, Alliaceae, Cereals. Methods in Molecular Biology, vol 2287, 1st edn. Springer Science+Business Media, LLC, New York, USA, pp 41-103. doi:10.1007/978-1-0716-1315-3_3

Sello S, Moscatiello R, La Rocca N, Baldan B, Navazio L (2017) A Rapid and Efficient Method to Obtain Photosynthetic Cell Suspension Cultures of Arabidopsis thaliana. Front Plant Sci 8 (1444). doi:10.3389/fpls.2017.01444

Shang G-D, Xu Z-G, Wan M-C, Wang F-X, Wang J-W (2022) FindIT2: an R/Bioconductor package to identify influential transcription factor and targets based on multi-omics data. BMC Genomics 23 (1):1-13

Shariatpanahi ME, Bal U, Heberle-Bors E, Touraev A (2006) Stresses applied for the re-programming of plant microspores towards *in vitro* embryogenesis. Physiol Plant 127 (4):519-534

Sivanesan I, Nayeem S, Venkidasamy B, Kuppuraj SP, Samynathan R (2022) Genetic and epigenetic modes of the regulation of somatic embryogenesis: A review. Biologia Futura:1-19

Slocum RD, Roux SJ (1982) An improved method for the subcellular localization of calcium using a modification of the antimonate precipitation technique. Journal of Histochemistry & Cytochemistry 30 (7):617-627. doi:10.1177/30.7.6179981

Snape JW (1989) Doubled haploid breeding: theoretical basis and practical applications. In: Mujeeb-Kazi A, Sitch LA (eds) Review of advances in plant biotechnology, 1985-1988: 2nd International Symposium on Genetic Manipulation in Crops. Mexico y Filipinas: CIMMYT y IRRI, pp 19-30

Solis MT, Berenguer E, Risueño MC, Testillano PS (2016) BnPME is progressively induced after microspore reprogramming to embryogenesis, correlating with pectin de-esterification and cell differentiation in *Brassica napus*. BMC Plant Biol 16 (1):176. doi:10.1186/s12870-016-0863-8

Spinoso-Castillo JL, Bello-Bello JJ (2022) In Vitro Stress-Mediated Somatic Embryogenesis in Plants. In: Somatic Embryogenesis. Springer, pp 223-235

Steward FC, Mapes MO, Mears K (1958) Growth and organized development of cultured cells. II. Organization in cultures grown from freely suspended cells. Am J Bot 45 (10):705-708

Stolarz A, Macewicz J, Lörz H (1991) Direct somatic embryogenesis and plant regeneration from leaf explants of Nicotiana tabacum L. J Plant Physiol 137 (3):347-357

Taheri-Dehkordi A, Naderi R, Martinelli F, Salami SA (2020) A robust workflow for indirect somatic embryogenesis and cormlet production in saffron (Crocus sativus L.) and its wild allies; C. caspius and C. speciosus. Heliyon 6 (12):e05841

Tang R-J, Wang C, Li K, Luan S (2020) The CBL–CIPK calcium signaling network: unified paradigm from 20 years of discoveries. Trends Plant Sci 25 (6):604-617

Thomas E, Herrero S, Eng H, Gomaa N, Gillikin J, Noar R, Beseli A, Daub ME (2020) Engineering Cercospora disease resistance via expression of Cercospora nicotianae

cercosporin-resistance genes and silencing of cercosporin production in tobacco. PLoS ONE 15 (3):e0230362

Thor K (2019) Calcium—nutrient and messenger. Front Plant Sci 10:440

Tian W, Wang C, Gao Q, Li L, Luan S (2020) Calcium spikes, waves and oscillations in plant development and biotic interactions. Nature Plants 6 (7):750-759. doi:10.1038/s41477-020-0667-6

Tichá M, Illésová P, Hrbáčková M, Basheer J, Novák D, Hlaváčková K, Šamajová O, Niehaus K, Ovečka M, Šamaj J (2020) Tissue culture, genetic transformation, interaction with beneficial microbes, and modern bio-imaging techniques in alfalfa research. Critical reviews in biotechnology 40 (8):1265-1280

Timmers A, De Vries S, Schel J (1989) Distribution of membrane-bound calcium and activated calmodulin during somatic embryogenesis of carrot (*Daucus carota* L.). Protoplasma 153 (1):24-29

Timmers A, Reiss H-D, Schel J (1991) Digitonin-aided loading of Fluo-3 into embryogenic plant cells. Cell Calcium 12 (7):515-521

Von Arnold S, Sabala I, Bozhkov P, Dyachok J, Filonova L (2002) Developmental pathways of somatic embryogenesis. Plant Cell Tissue Organ Cult 69 (3):233-249

Wang F-X, Shang G-D, Wu L-Y, Xu Z-G, Zhao X-Y, Wang J-W (2020) Chromatin accessibility dynamics and a hierarchical transcriptional regulatory network structure for plant somatic embryogenesis. Dev Cell 54 (6):742-757. e748

Wang R, Li R, Xu T, Li T (2017) Optimization of the pollen-tube pathway method of plant transformation using the Yellow Cameleon 3.6 calcium sensor in Solanum lycopersicum. Biologia 72 (10):1147-1155

Weyen J (2021) Applications of doubled haploids in plant breeding and applied research. In: Seguí-Simarro JM (ed) Doubled Haploid Technology, vol 1: General Topics, Alliaceae, Cereals. Methods in Molecular Biology, vol 2287, 1st edn. Humana Press, New York, USA, pp 23-39. doi:10.1007/978-1-0716-1315-3_2

Winnicki K (2020) The Winner Takes It All: Auxin-The Main Player during Plant Embryogenesis. Cells 9 (3). doi:10.3390/cells9030606

Wu Y, Haberland G, Zhou C, Koop H-U (1992) Somatic embryogenesis, formation of morphogenetic callus and normal development in zygotic embryos of *Arabidopsis thaliana* in vitro. Protoplasma 169:89-96

Xiong W, Reynolds M, Xu Y (2022) Climate change challenges plant breeding. Curr Opin Plant Biol 70:102308

Yang K, Wang L, Le J, Dong J (2020) Cell polarity: Regulators and mechanisms in plants. J Integr Plant Biol 62 (1):132-147

Yuan P, Jauregui E, Du L, Tanaka K, Poovaiah B (2017) Calcium signatures and signaling events orchestrate plant–microbe interactions. Curr Opin Plant Biol 38:173-183

Zhang L, Zhang Y, Gao Y, Jiang XL, Zhang MD, Wu H, Liu ZY, Feng H (2016) Effects of histone deacetylase inhibitors on microspore embryogenesis and plant regeneration in Pakchoi (*Brassica rapa* ssp chinensis L.). Sci Hort 209:61-66. doi:10.1016/j.scienta.2016.05.001

Zhang M, Wang A, Qin M, Qin X, Yang S, Su S, Sun Y, Zhang L (2021) Direct and indirect somatic embryogenesis induction in Camellia oleifera Abel. Front Plant Sci 12:644389

Zhang WH, Rengel Z, Kuo J (1998) Determination of intracellular Ca2+ in cells of intact wheat roots: loading of acetoxymethyl ester of Fluo-3 under low temperature. Plant J 15 (1):147-151

Zhao J, Yu F, Liang S, Zhou C, Yang H (2002) Changes of calcium distribution in egg cells, zygotes and two-celled proembryos of rice (Oryza sativa L.). Sex Plant Reprod 14 (6):331-337. doi:10.1007/s00497-002-0127-7

10. Conclusions

- *Brassica napus* DH4079 line, but not DH12075, is extremely recalcitrant to *Agrobacterium*-mediated transformation.
- Ca^{2+} increase is an early marker of induction of *in vitro* embryogenesis, common for both somatic and microspore embryogenesis.
- Ca^{2+} levels during *in vitro* embryogenesis are highly dynamic, and Ca^{2+} oscillations might be related to the differentiation processes that take place in the induced cells upon binding to calmodulin.
- The positive effect of Ca^{2+} modulation in the embryogenic response depends on the nature of the system, being more sensitive those using isolated cell suspensions rather than those using tissues as explants.
- Ca^{2+} increase within a defined range has species-specific positive effects in embryo yield.
- Inhibition of callose deposition during somatic embryogenesis prevents embryo development, which suggests a relationship between the formation of a callose barrier and the establishment of embryo identity in somatic cells.